Durham University

Durham E-Theses

A study of the interactions between ylidic phosphorus species and organic acids

Lamb, Sarah

How to cite:

Lamb, Sarah (1998) *A study of the interactions between ylidic phosphorus species and organic acids*, Durham theses, Durham University. Available at Durham E-Theses Online: http://etheses.dur.ac.uk/4850/

Use policy

The full-text may be used and/or reproduced, and given to third parties in any format or medium, without prior permission or charge, for personal research or study, educational, or not-for-profit purposes provided that:

- a full bibliographic reference is made to the original source
- a link is made to the metadata record in Durham E-Theses
- the full-text is not changed in any way

The full-text must not be sold in any format or medium without the formal permission of the copyright holders.

Please consult the full Durham E-Theses policy for further details.

Academic Support Office, The Palatine Centre, Durham University, Stockton Road, Durham, DH1 3LE
e-mail: e-theses.admin@durham.ac.uk Tel: +44 0191 334 6107
http://etheses.dur.ac.uk

A Study of the Interactions between Ylidic Phosphorus Species and Organic Acids

by

Sarah Lamb

St. Mary's College, University of Durham

The copyright of this thesis rests with the author. No quotation from it should be published without the written consent of the author and information derived from it should be acknowledged.

A thesis submitted in part fulfilment of the requirements for the degree of Doctor of Philosophy at the University of Durham.

September 1998

22 JUN 1999

Dedication

I would like to dedicate this thesis
to my Mum and Dad for all their love and support.

Statement of Copyright

The copyright of this thesis rests with the author. No quotation from it should be published without her prior consent and information derived from it should be acknowledged.

Declaration

The work described in this thesis was carried out in the Department of Chemistry at the University of Durham between October 1995 and September 1998. All the work is my own unless stated to the contrary, and it has not been submitted previously for a degree at this or any other University.

Financial Support

The University of Durham is gratefully acknowledged for providing funding in the form of a University studentship.

Contents

Acknowledgements

Firstly, I would like to thank Dr. Matthew Davidson for all his advice, help and numerous pints of Guiness throughout these three years. Also many thanks for letting me be his first PhD student, mad fool that he was - I hope the experience hasn't scarred him for life!

I would also like to thank all those who have had the dubious pleasure of sharing a lab with me. Thanks to, Penny and Iain for making me feel welcome and showing me the ropes when I first arrived. Also to Chris, with whom there was never a dull moment and to Rich and Phil who weren't put off by being our project students, but were gluttons for punishment and came back for the long slog. Thanks for putting up with this 'bird' whilst in the lab, doing crosswords and in the pub! A special big thanks to Rich, cheers for all the help in the lab, especially with computers and during the writing of this thesis, I owe him one.

Thank you to Prof. Judith Howard and Durham University Crystallography group for their invaluable assistance with X-ray data and Dr. Sax Mason at the Institut Laue Langevin for neutron data collection.

Also thank you to Bri for his friendship and the food - I would have starved without you, and in no particular order, to Markus, Marina, Andys aplenty, Ian, Pat, Graham, Nicky, Pete, Tom, Marky, Valli, Paddy, Mel and the Allisons (yes with a double l) for making my time in Durham an enjoyable one!

Finally a big thank you to Elinor and John, my parents Margaret and Tony Lamb and my grandparents Edith New and Miriam and Jim Lamb for being there for me. Last but not least a huge thank you to Si for all his help and support.

Abstract

This thesis describes the synthesis and characterisation of phosphonium aryloxides, amides and phosphides. These compounds have been formed via the deprotonation of organic acids [of the type ROH, and R_2X, where X = NH, PH, R = aryl group] by basic phosphonium ylidic species [R_3PX, X = CH_2, C(Me)H, C(Ph)H, NH] in mixtures of hydrocarbon (toluene) and/or polar (acetonitrile, thf) solvents. All of these compounds contain both acidic CHs and 'naked' anions which promote extensive hydrogen bonding.

Chapter 1 provides an outline of the fields of ylidic chemistry and hydrogen bonding. In Chapter 2, general experimental methods are described. Chapter 3 records all experimental results pertaining to this work. Here preparation of starting materials is documented, followed by an account of the synthesis and characterisation of twenty-three compounds. For all compounds melting point measurements, ^{1}H NMR, ^{31}P NMR, infra-red spectra, and elemental analysis are recorded.

Discussion of these results is documented in Chapters 4 to 7. Where possible, solid-state structures for compounds obtained by single crystal X-ray diffraction (nineteen structures) and single crystal neutron diffraction (two structures) are included. Chapter 4 discusses simple phosphonium aryloxide salts, while Chapter 5 is concerned with related phosphonium amides and phosphides. Chapter 6 deals with an extension of this work involving multifunctional organic acids. Finally, Chapter 7 discusses unexpected results resulting from the work described in Chapter 6.

List of Papers Published

1. Phosphonium ylides as hydrogen-bond acceptors - intermolecular C-H...C interactions in the crystal structure of triphenylphosphonium benzylide.
   A. S. Batsanov, M. G. Davidson, J. A. K. Howard, S. Lamb and C. Lustig, *Chem. Commun.*, 1996, 1791.

2. Synthesis and X-ray structures of N-lithioiminophosphorane-lithium bromide adducts.
   A. S. Batsanov, M. G. Davidson, J. A. K. Howard, S. Lamb, C. Lustig and R. D. Price, *Chem. Commun.*, 1997, 1211.

3. Synthesis and X-ray structures of tetralithium derivatives of tert-butylcalix[4]arene containing unique Li-O cores based on a square-pyramidal geometry.
   M. G. Davidson, J. A. K. Howard, S. Lamb and C. W. Lehmann, *Chem. Commun.*, 1997, 1607.

4. The first structural characterisation of a phosphonium amide: synthesis, isolation and molecular structure of $(Ph_3PEt)^+(NPh_2)^-$.
   M. G. Davidson and S. Lamb, *Polyhedron*, 1997, **16**, 4393.

5. The first synthesis, isolation and X-ray structure of a phosphonium phosphide, $(Ph_3PMe)^+(C_6H_2(CF_3)_3\text{-}2,4,6]_2P)^-$.
   M. G. Davidson, K. B. Dillon, J. A. K. Howard, S. Lamb and M. D. Roden, *J. Organomet. Chem.*, 1998, **550**, 481.

Abbreviations

Ar	aryl
Ar_2PH	$[C_6H_2(CF_3)_3\text{-}2,4,6]_2PH$
Bisphenol	4,4'-methylenebis(2,6-di^{t}butylphenol)
^{t}Bu	tertiary butyl
COSY	correlation spectroscopy
CSD	Cambridge Structural Database
δ	chemical shift
DSC	differential scanning calorimetry
FT	Fourier transform
H_2salen	N,N'-ethylenebis(salicylideneimine)
HMTA	hexamethylenetetramine
IR	infra-red
Kc	cryoscopic constant
LH_4	*p*-tert-butylcalix[4]arene
LUMO	lowest unoccupied molecular orbital
Me	methyl
Mr	relative molecular mass
NMR	nuclear magnetic resonance
OPA	oxaphosphetane
PBB	{4'-[methyl(diphenyl)phosphino]biphenyl-4-yl}triphenylborate
Ph	phenyl
ppm	parts per million
R	any hydrocarbon group
SHG	second-harmonic generators
thf	tetrahydrofuran
TMS	tetramethylsilane
UV/Vis	ultraviolet/visible

Chapter 1

1. INTRODUCTION

1.1 Preamble

There has been a long standing interest in the inorganic chemistry of ylides.[1, 2] Our interest lies in the isolation and structural characterisation of phosphonium salts (e.g. aryloxide, amide, phosphide) formed via the deprotonation of the acidic precursors with basic phosphonium ylides or iminophosphoranes. Furthermore, all of these compounds contain both acidic CHs and 'naked' anions which promote extensive hydrogen bonding.

The following chapter aims to outline two disparate topics which are both central to the work contained in this thesis. Firstly, the theoretical and physical properties of phosphonium ylides and iminophosphoranes and secondly, the nature of hydrogen bonding, in particular weak C-H...X interactions and its importance on solid-state structure.

1.2 Ylides

1.2.1 Historical Perspective

Although ylide chemistry originated over a century ago with the work of Michaelis et al,[3] they failed to proffer an ylide structure for the substance they had prepared. Instead acclaim must go to Staudinger et al who in 1919[4] prepared and isolated the first ylides and imines to be

---

[1]see for example: H. Schmidbaur, *Acc. Chem. Res.*, 1975, **8**, 62; *Angew. Chem.*, 1983, **95**, 980; *Angew. Chem. Int. Ed. Eng.*, 1983, **22**, 907.
[2]A. W. Johnson with special contributions by W. C. Kaska, K. A. O. Starzewski and D. A. Dixon, *'Ylides and Imines of Phosphorus'*, John Wiley & Sons Inc., New York, 1993, and references cited therein.
[3]A. Michaelis and H. V. Gimborn, *Chem. Ber.*, 1894, **27**, 272.
[4]H. Staudinger and J. Meyer, *Helv. Chim. Acta.*, 1919, **2**, 635.

recognised as such. However, it was with the Nobel Prize winning work of Georg Wittig in the 1950s that ylide chemistry came to fruition. This work led to the discovery of the reaction which bears his name. The Wittig reaction has found widespread prominence in organic synthesis being 'of unmatched importance for specific introduction of C - C double bonds in a known location.'[5]

Wittig coined the term ylid in the German language,[6] (ylide being the anglicised, and now generally accepted form) which is derived from 'yl' indicating an open valence (as in methyl) and 'id' denoting anionicity (as in acetylid).

An ylide is defined as 'a substance in which a carbanion is attached directly to a heteroatom carrying a substantial degree of positive charge and in which the positive charge is created by the sigma bonding of substituents to the heteroatom'.[7] This definition can be portrayed by two canonical formulae (Scheme 1.1).

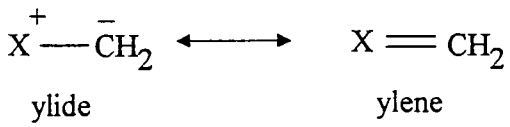

Scheme 1.1

On the left is shown the ylide formula emphasising the dipolar zwitterionic nature of the onium centre next to the carbanionic function, while on the right the ylene formula proposes a double bond between the onium centre and the ylidic carbon atom. Ylides are known for a variety of

[5]E. Vedejs, *Science*, 1980, **210**, 600.
[6]D. G. Gilheany, *Chem. Rev.*, 1994, **94**, 1339.
[7]A. W. Johnson with special contributions by W. C. Kaska, K. A. O. Starzewski and D. A. Dixon, *'Ylides and Imines of Phosphorus'*, John Wiley & Sons Inc., New York, 1993, page 2.

heteroatoms, X (e.g. X = R_2S,[8, 9] R_3As,[10, 11]), but one of the most common, and certainly the most stable and useful being phosphorus(X = R_3P).

1.2.2 Structure and Bonding

The structure of a typical phosphonium ylide is that of 'an easily pyramidalized carbanion stabilised by an adjacent tetrahedral phosphonium centre.'[12] Figure 1.1 illustrates a typical phosphonium ylide, where C_{yl} is the ylidic carbon atom, with its substituent groups represented by X and Y, while R_u is known as the unique substituent on the phosphorus atom. The P-C_{yl} bond length is shorter than a typical P-C single bond (1.8 Å). The barrier to rotation about the P-C bond is very low. For example, this has been calculated to be 0.24 kcal/mol for H_3PCH_2, compared to 21.2 kcal/mol for the sulphonium ylide H_2SCH_2.[13, 14]

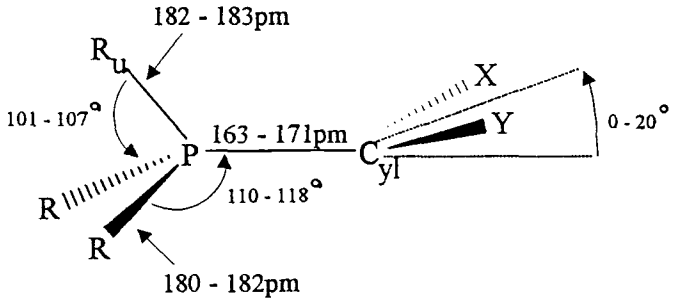

Figure 1.1

[8]T. Christensen and W. G. Witmore, *Acta. Cryst.*, 1969, **B25**, 73: A. F. Cook and J. G. Moffat, *J. Am. Chem. Soc.*, 1968, **90**, 740.
[9]B. F. Yates, W. J. Bouma and L. Radom, *J. Am. Chem. Soc.*, 1987, **109**, 2250.
[10]A. Strich, *New J. Chem.*, 1979, **3**, 105.
[11]D. Lloyd, *Chem. Soc. Rev.*, 1987, **16**, 45.
[12]H. Schmidbaur, A. Schier, W. Graf, D. L. Wilkinson and G. Muller, *New J. Chem.*, 1989, **13**, 341.
[13]D. A. Dixon, T. H. Dunning, R. A. Eades and P. G. Gassman, *J. Am. Chem. Soc.*, 1983, **105**, 7011.
[14]R. A. Eades, P. G. Gassmann and D. A. Dixon, *J. Am. Chem. Soc.*, 1981, **103**, 1066.

X-ray and theoretical studies[9, 13, 15, 16, 17, 18] have revealed that the plane defined by the atoms C_{yl}, X and Y is oriented at right angles to the plane defined by the atoms R_u, P and C_{yl}. A detailed study of triphenylphosphonium methylide (Ph_3PCH_2) was undertaken by Schmidbaur et al[12] which revealed such a deviation from carbanion planarity the angle sum at carbon being only 349°. These structural features have been instrumental in influencing the bonding models proposed for ylides.

Phosphonium ylides are especially stable carbanion-like species. This significant stabilisation is often attributed to the ability of the positively charged phosphorus atom to facilitate delocalisation of the negative charge from the carbanion. There is debate as to how this delocalisation occurs and studies have concentrated on the nature of the P-C bond. Most discussions talk in terms of a hybrid between a dipolar and double bond form (Scheme 1.2).[19]

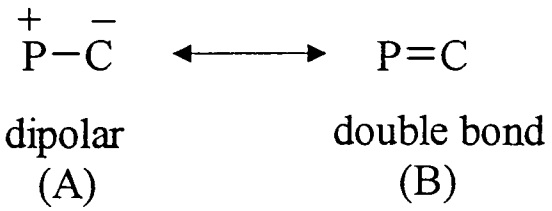

Scheme 1.2

For the purposes of chemical reactivity (A) is considered more important. Previously the double bond character in (B) was explained by dπ - pπ bonding. It was thought that there

---

[15]A. W. Johnson with special contributions by W. C. Kaska, K. A. O. Starzewski and D. A. Dixon, *'Ylides and Imines of Phosphorus'*, John Wiley & Sons Inc., New York, 1993, chapter 2.
[16]S. M. Bachrach, *J. Org. Chem.*, 1992, **57**, 4367.
[17]M. T. Nguyen and A. F. Hegarty, *J. Chem. Soc., Perkin Trans. (2)*, 1987, 47.
[18]S. G. Lias, J. F. Liebman and R. D. Levein, *J. Phys. Chem. Ref. Data*, 1984, **13**, 695.
[19]see for example: A. J. Kirby and S. G. Warren, *'The Organic Chemistry of Phosphorus'*, Elsevier, Amsterdam, 1967; J. Emsley and D. Hall, *'The Chemistry of Phosphorus.'* Harper and Row, London, 1976; H. Goldwhite, *'Introduction to Phosphorus Chemistry.'* Cambridge University Press, Cambridge, 1981; H. J. Bestmann and R. Zimmermann, *'Organic Phosphorus Compounds.'* Wiley, Chichester, 1972.

was back donation of electron density from a doubly occupied 2p orbital of the ylidic carbon into a vacant phosphorus 3d orbital (Figure 1.2).

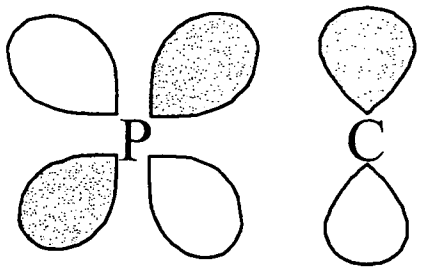

Figure 1.2 π type orbital overlap

This model was used to explain a number of properties of phosphonium ylides[6, 20, 21] especially the fact that they are more stable than their nitrogen analogues, as nitrogen does not have the requisite low energy vacant d orbitals.[22] However in light of theoretical studies it is now widely accepted that d orbitals play no part in this bond and instead alternative models have been proposed to account for the structure and reactivity of ylides. The first model suggests a lone pair of electrons from the R_3P moiety forms a σ bond to carbon completing its octet, the resulting charge density being, formally, a lone pair of electrons in a p orbital on carbon. In this model d orbitals on phosphorus are discarded and an alternative set of orbitals, namely the LUMO of the R_3P moiety, is envisaged. This LUMO is of σ^*[23] e symmetry. The extra charge density in the p orbital of the carbon atom goes into this LUMO forming a π bond. Figure 1.3 shows the overlap scheme.

---

[20]A. W. Johnson, *'Ylid Chemistry.'* Academic Press, New York, 1966.
[21]D. G. Gilheany *'The Chemistry of Organophosphorus Compounds'*, Wiley - Interscience, Chichester, 1993.
[22]I. Zugravescu and M. Petrovanu, *'Nitrogen Ylid Chemistry.'* McGrawHill, New York, 1976.
[23]B. J .Dunne, R. B. Morris and A. G. Orpen, *J. Chem. Soc., Dalton Trans.*, 1991, 653; S.-X. Xiao, W. C. Trogler, D. E. Ellis and Z. Berkovitch-Yellin, *J. Am. Chem. Soc.*, 1983, **105**, 7033; H. Oberhammer, Schmutzler and O. Stelzer, *Inorg. Chem.*, 1978, **17**, 1254.

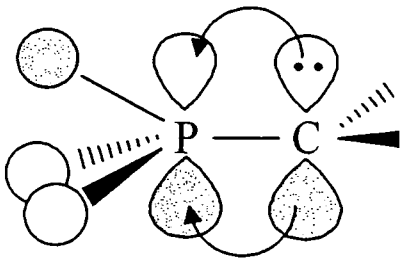

Figure 1.3 Description of the PC bond as a σ bond and a π bond

This is analogous to the bonding seen in phosphine oxides and in transition metal phosphine complexes which is known as negative hyperconjugation.[24] Strong support for this model is provided by their overall structure. This model assumes back bonding from a π orbital on the anionic carbon into an antibonding orbital on the R_3P moiety. The proposed overlap between the p orbital on the carbon atom and the LUMO of the R_3P moiety results in the orbital of the R_u substituent, that contributes to the LUMO, being eclipsed by the p orbital of carbon (this is not the case for the other two R substituents). Therefore the back bonding into the proposed LUMO would result in a greater weakening of the PR_u bond than the other two PR bonds and the PR_u bond length would be expected to be longer than the other PR bonds, as is indeed observed. Mitchell et al demonstrated that this model shows how back bonding is possible to antibonding orbitals in both the perpendicular and parallel conformations hence explaining why there is a low barrier to rotation about the P-C bond.[25]

The second model describes the bonding in terms of so called Ω or τ bonds[13, 26] (banana bonds[27]/ bent multiple bonds). This unorthodox view describes neither a σ nor a π bond but instead two curved regions of electron density located between the phosphorus and the carbon (Figure 1.4).

---

[24]A. E. Reed and P. von R. Schleyer, *J. Am. Chem. Soc.*, 1990, **112**, 1434.
[25]D. J. Mitchell, S. Wolfe and H. B. Schlegel, *Can. J. Chem.*, 1981, **59**, 3280.
[26]R. P. Messmer, P. A. Schultz, R. C. Tatar and H-J. Freund, *Chem. Phys. Lett.*, 1986, **126**, 176.
[27]I. N. Levine, *'Quantum Chemistry.'* 3rd. Edn., Allyn and Bacon, Boston, 1983.

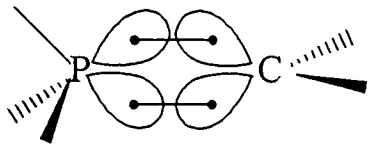

Figure 1.4 Description of the PC bond as two banana bonds

Calculations have shown both bond pairs near carbon but one slightly closer than the other. [28] It is interesting to note that although the idea of Ω bonds appears unorthodox it is not a new one, in fact Pauling introduced it in 1931.[29]

A third model worthy of note considers the P-C bond as simply a σ single bond formed by donation of the phosphorus lone pair into a vacant p orbital on the carbon atom. The phosphorus atom subsequently carries a positive charge and the carbon atom a negative one [model (A) scheme 1.2]. It is the proximity of these two opposite charges resulting in an electrostatic shortening, due to the coulombic attraction between the two components of the P-C bond, that is, in this view, accountable for the ylidic bond.[13]

1.2.3 Preparation of Ylides

There are various methods available for the preparation of phosphonium ylides and the one ultimately chosen generally depends on the nature of the substituents of the desired ylide. The most prolific method is the 'salt method'.

The 'salt method' is the formation of ylides by the conversion of a phosphonium salt (which has either been pre-prepared, or in some cases is commercially available) to a phosphonium ylide via the removal of an α-proton from the carbon atom which will become known as the ylidic carbon atom (Scheme 1.3).

---

[28]P. Molina, M. Alajarin, C. L. Leonardo, R. M. Claramunt, M. C. Foces, F. H. Cano, J. Catalan, J. L. G. de Paz and J. Elguero, *J. Am. Chem. Soc.*, 1989, **111**, 355; H. Lischka, *J. Am. Chem. Soc.*, 1977, **99**, 353.
[29]L. Pauling, *J. Am. Chem. Soc.*, 1931, **53**, 1367.

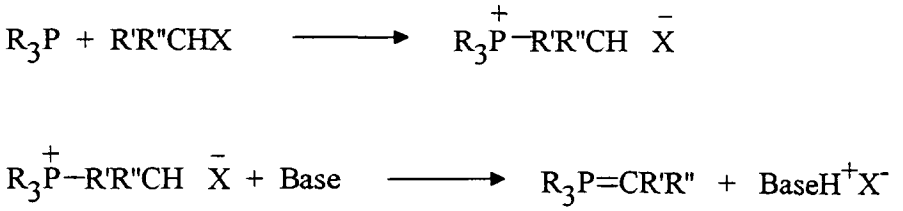

Scheme 1.3

Reaction conditions tend to be mild, although in some cases heat may be necessary. The phosphonium halide precursor for the phosphonium ylide is typically formed via a S_N2 quaternisation reaction between a trialkyl, -aryl, -acyl phosphine and an alkyl halide. Although a wide range of solvents can be employed, it must be remembered that since carbon, nitrogen or oxygen bases are used in the latter deprotonation step (e.g. NaH, $NaNH_2$, $KOBu^t$, etc.), the solvent chosen should be inert to reaction with both the base and obviously the ylide. The choice of base should be made not only by the considering the strength required (dependant on the nature of the phosphonium groups and the nature of the carbon substituents) but also by considering the ylide's tolerance to the by-products of the reaction and how these may effect any subsequent reactions (e.g. Wittig reactions), since many ylide reactions are performed in situ. In the 1950s most ylide preparations used organolithium reagents as the base, producing a lithium halide as a by-product. However, it was soon realised that these lithium salts complexed to the phosphonium ylides and complexation also occurred during the Wittig reaction. To avoid this undesirable side effect, which reduced the stereochemical control, several methods were developed to produce so called 'salt-free' ylide solutions. Koster et al employed $NaNH_2$ as the base and found THF to be one of the better solvents,[30] Schmidbaur et al also used the solvent THF but employed NaH as the base.[31] In fact most of these solvents did contain salts; they were, however, free from lithium cations.

---

[30]R. Koster, D. Simic and M. Grassberger, *Liebigs Ann. Chem.*, 1970, **739**, 281.
[31]H. Schmidbaur, H. Stuher and W. Vornberger, *Chem. Ber.*, 1972, **105**, 1084.

Due to the wide availability of triphenylphosphine (Ph_3P) it is by far the most commonly used precursor for the phosphonium salts. It also has the advantages of being safe and easy to handle, crystalline, air-stable and cheap. Also, the phosphorus-bound tertiary carbon atoms have no protons to compete in the deprotonation step.

Ylides can also be formed by the reaction of a carbene and phosphine, in effect direct coupling of the two chemical components of an ylide. This method has a limited usefulness and is only commonly employed to generate halo-substituted ylides (Scheme 1.4).

$$PhHgCXYBr + PPh_3 \longrightarrow (Ph_3P{=}CXY) + R_2CO \longrightarrow R_2C{=}CXY$$

eg X = Y = Br
or X = H, Y = Cl

Scheme 1.4

1.2.4 Reactions of Phosphonium ylides

Due to their unique electronic and molecular structure phosphonium ylides can undergo a wide range of reactions. Some reactions are dependant on their carbanionic nature with the adjacent phosphonium group having little effect, at least initially. Others involve both the carbanion and phosphonium portion of the ylide, thought not necessarily simultaneously.

A complete account of the reactions ylides undergo is beyond the scope of this introduction, however some of the more relevant reactions are shown in (Scheme 1.5).

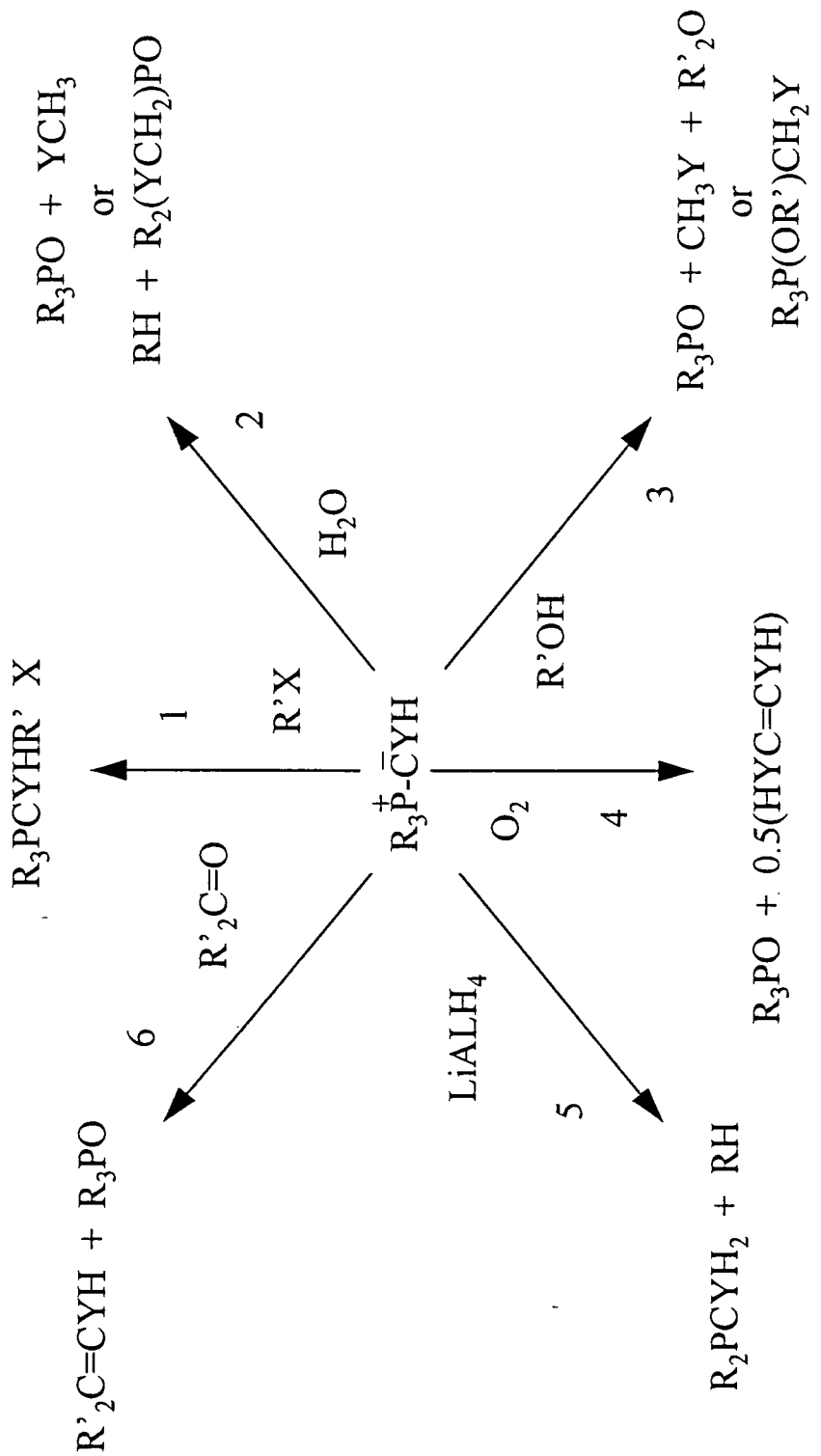

Scheme 1.5 A summary of the common reactions of phosphonium ylides

1.2.4.1 Basicity

Phosphonium ylides can generally be classed as one of three types:[32] stabilised, semi-stabilised, and non-stabilised (or reactive), reflecting the degree of delocalisation and their basicity.

Stabilised ylides contain strongly electron withdrawing groups on the ylidic carbon (for example cyclopentadienyl) which has the ability to provide significant delocalisation for the carbanion.

Semi-stabilised ylides have moderately conjugating groups (such as phenyl) on the ylidic carbon and are of intermediate reactivity.

Non-stabilised ylides include those which contain alkyl groups (e.g., $RCH{=}PPh_3$, R=alkyl) on the ylidic carbon. Due to their propensity to react readily with moisture, they are generally prepared and used in situ. These ylides tend to be highly coloured, from yellow through to red-purple, hence monitoring colour changes provides a means by which to follow the formation and/or disappearance of ylides during a reaction.

The basicity of an ylide is dependant on both the phosphorus and ylidic carbon atom substituents, stabilising groups reducing the basicity of the ylide. Early clues as to their basicity evolved from observations of the process of transylidation. Bestmann reported that reaction of triphenylphosphonium methylide with phenacyltriphenylphosphonium bromide afforded high yield of the phenacylide[33] (Scheme 1.6).

$$Ph_3P{=}CH_2 + Ph_3\overset{+}{P}CH_2COPh \rightleftharpoons Ph_3\overset{+}{P}CH_3 + Ph_3P{=}CHCOPh$$

Scheme 1.6

[32]G. Wittig and G. Geissler, *Liebigs Ann. Chem.*, 1953, **580**, 44.
[33]H. J. Bestmann, *Chem. Ber.*, 1962, **95**, 58.

Consequently he was able to construct a hierarchy of 'acidifying groups' (PhCO > COOR > Ph > Alkyl) for phosphonium salts. Conversely the group is better able to stabilise the ylide through electron delocalisation.

The basicity of ylides is measured by their pKa's and has been used to determine the influence of substituents on ylide stability. Electron withdrawing groups stabilise the ylidic carbon, decreasing its basicity. With a few exceptions the substituents on phosphorus in phosphonium ylides have been phenyl or simple alkyl groups, with studies showing that trialkylphosphonium ylides are in general more basic than the triphenylphosphonium ylides.[34] The dominant effect of the phenyl groups on the phosphonium cation is the inductive withdrawal effect,[35] stabilising the ylides.

1.2.4.2 Ylides as nucleophiles

By using phosphonium ylides as nucleophiles new C-C single bonds can be formed and the ability to later remove the phosphonium groups makes ylides useful synthetic reagents (Scheme 1.5 - 1).

However, of greater synthetic importance is the ability of ylides to react with carbonyl compounds resulting in regiospecific (and often stereospecific) C=C double bond formation, the principle step in the Wittig reaction[32] (Scheme 1.5 - 6).

1.2.4.3 Hydrolysis and Alcoholysis

In general phosphonium ylides are susceptible to hydrolytic cleavage, resulting in the formation of a hydrocarbon and a phosphine oxide. The driving force of the reaction is the formation of the energetically stable phosphorus-oxygen bond (Scheme 1.5 - 2).

---

[34]K. Issleib and R. Linder, *Liebigs Ann. Chem.*, 1967, **707**, 120.
[35]M. I. Kabachnik and T. A. Mastryukova, *J. Gen. Chem.*, 1984, **54**, 1931.

The susceptibility to hydrolysis varies with the reactivity of the ylide. Some ylides are so sensitive that they need to be prepared and handled in a moisture-free atmosphere, while others are more robust and can resist hydrolysis under severe conditions.

Triphenlyphosphonium alkylides, which are generally non-stabilised react so rapidly with water they need to be handled and stored in an inert atmosphere. For example Coffmann and Marvel observed immediate decolourisation of triphenylphosphonium ethylide in the presence of water leading to the formation of ethyldiphenylphosphine oxide (Scheme 1.7).[36]

$$Ph_3P{=}CHCH_3 \xrightarrow{H_2O} Ph_2P(O)C_2H_5 + C_6H_6$$

Scheme 1.7

In contrast Freeman et al found that the highly stabilised ylide Triphenylphosphonium 2,3,4,5-tetraphenylcyclopentadienylide (Figure 1.5) to be unaffected even after prolonged reflux in alcoholic sodium hydroxide.[37]

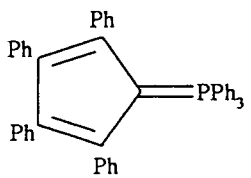

Figure 1.5 Triphenylphosphonium 2,3,4,5-tetraphenylcyclopentadienylide

However, Krohnke reported that the semi-stablised ylide triphenylphosphonium *p*-nitrobenzylide (Figure 1.6) could be prepared from its precursor salt by treatment with cold aqueous sodium hydroxide but on extended contact or on heating hydrolysis does occur.[38]

---

[36]D. D. Coffman and C. S. Marvel, *J. Am. Chem. Soc.*, 1929, **51**, 3496.
[37]B. H. Freeman, D. Lloyd and M. I. C. Singer, *Tetrahedron*, 1972, **28**, 343.
[38]F. Kronke, *Chem. Ber.*, 1950, **83**, 291.

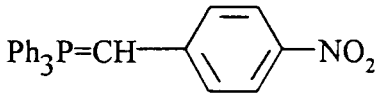

Figure 1.6 Triphenylphosphonium *p*-nitrobenzylide

In general the stability of an ylide towards hydrolysis parallels its basicity, the most basic being the most susceptible.

Although in much ylide chemistry hydrolysis is to be regarded as undesirable, it can be useful for P-C cleavage reactions under controlled conditions. Studies by Fenton and Ingold[39] revealed the group leaving the phosphorus as a hydrocarbon is that which produces the most stable carbanion with the preference for hydrocarbon formation being benzyl > phenyl > alkyl.

Alcoholysis of phosphonium ylides seems to occur by a similar mechanism (Scheme 1.5 - 3). Grayson and Keough[40] found that on heating triphenylphosphonium ρ-nitrobenzylide in ethanol that ρ-nitrotoluene, triphenylphosphine oxide and diethylether were produced. They rationalised the first step was an equilibrium between a phosphonium ylide and a phosphonium salt with the slow step of the reaction being the attack of ethoxide on tetravalent phosphorus. The resulting pentavalent phosphorane was proposed to eject the most stable carbanion in this example *p*-nitrobenzyl anion with ethoxide reacting with the tetravalent phosphonium cation to form triphenylphosphine oxide and diethylether (Scheme 1.8).

[39]G. W. Fenton and C. K. Ingold, *J. Chem. Soc.*, 1929, 2342.
[40]M. Grayson and P. T. Keough, *J. Am. Chem. Soc.*, 1960, **82**, 3919.

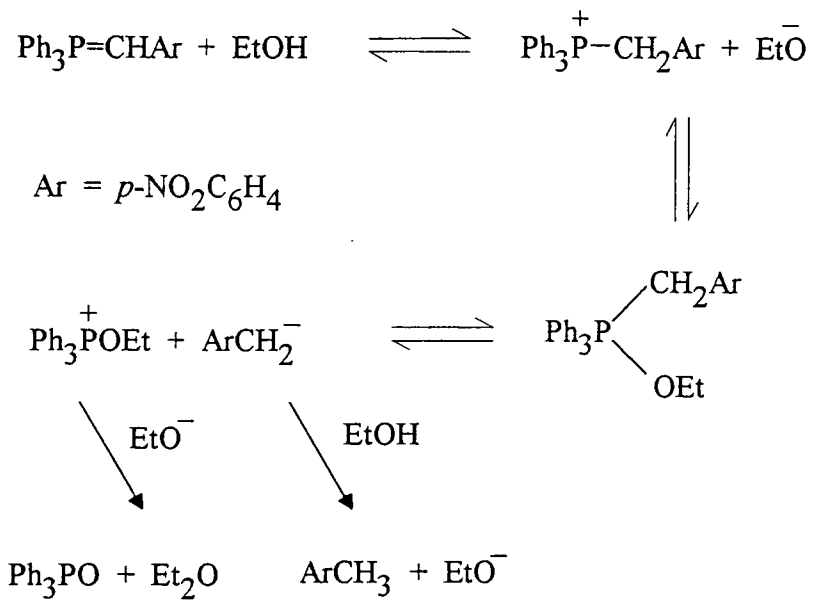

Scheme 1.8

Schmidbaur et al observed that triphenylphosphonium methylide formed tetramethyl(methoxy)phosphorane by the addition of anhydrous methanol (Scheme 1.9), a similar reaction being observed with ethanol.[41]

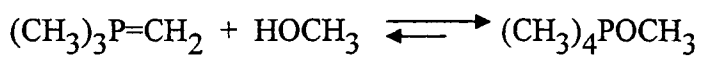

Scheme 1.9

In a few examples, alcoholysis of phosphonium ylides derived from phosphines other than triphenylphosphine has led to cleavage other than that of the ylidic carbon-phosphorus bond and Burgada et al found that during methanolysis of an ylide methoxy groups were ejected to some extent in competition with a stabilised carbanion.[42]

---

[41]H. Schmidbaur, H. Stuhler and W. Buchner, *Chem. Ber.*, 1973, **106**, 1238.
[42]R. Burgada, Y. O. El Khoshnieh and Y. Leroux, *Phosphorus Sulfur*, 1985, **22**, 225.

1.2.4.4 Oxidation

The oxidation of phosphonium ylides effects cleavage of the carbanion-phosphorus bond. The carbanion portion of the ylide in some instances reacts with unconverted ylide producing a symmetric alkene, while the phosphonium centre appears as a phosphine oxide and, again, it is the formation of the strong phosphorus-oxygen bond which is probably the driving force for the reaction (Scheme 1.5 - 4).

1.2.4.5 Reduction

Reduction also results in the cleavage of the carbanion-phosphorus bond. However, it is not as regiospecific as the aforementioned hydrolysis and oxidation reactions. Reduction of phosphonium ylides generally results in the formation of an alkane and a tertiary phosphine. Predicting which carbon-phosphorus bond will be cleaved is problematic. $LiAlH_4$ is the reducing agent of choice (Scheme 1.5 - 5).

1.2.4.6 Wittig Reaction

The Wittig reaction[32] is one of the most effective and widely used methods of synthesising alkenes. It was in the early 1950s that Wittig et al divulged a means for the preparation of alkenes where the double bond can be unambiguously positioned. The reaction involves the condensation of a carbonyl compound (aldehyde/ketone) with a phosphonium ylide.

Due to its simplicity, effectiveness and generality, the Wittig reaction became widely used, changing the course of olefin synthesis for all time.[3] The reaction, which is regiospecific, proceeds with ease under mild conditions, resulting in high yields of alkene. By-products such as triphenylphosphine oxide may be easily separated (Scheme 1.5 - 6).

In some cases the Wittig reaction can also be highly stereoselective. The selectivity for (Z)- or (E)-alkenes is dependant on: the type of carbonyl; the reaction conditions employed; and the type of ylide employed.

In general, the stabilised ylides usually favour the production of (E)-alkenes, while non-stabilised ylides, which lack conjugating substituents on the ylidic carbon, afford the (Z)-alkene. Semi-stabilised ylides show no great preference, often forming a mixture of the isomers.

A detailed account of the Wittig reaction is beyond the scope of this introduction. However, by the 1970s the mechanism of the Wittig reaction was widely accepted to be the reversible nucleophilic addition of a phosphonium ylide to the carbonyl species giving two possible intermediate betaine species which cyclise to the respective oxaphosphetane (OPA) which is followed by irreversible decomposition to give an alkene and phosphine oxide (Scheme 1.10).

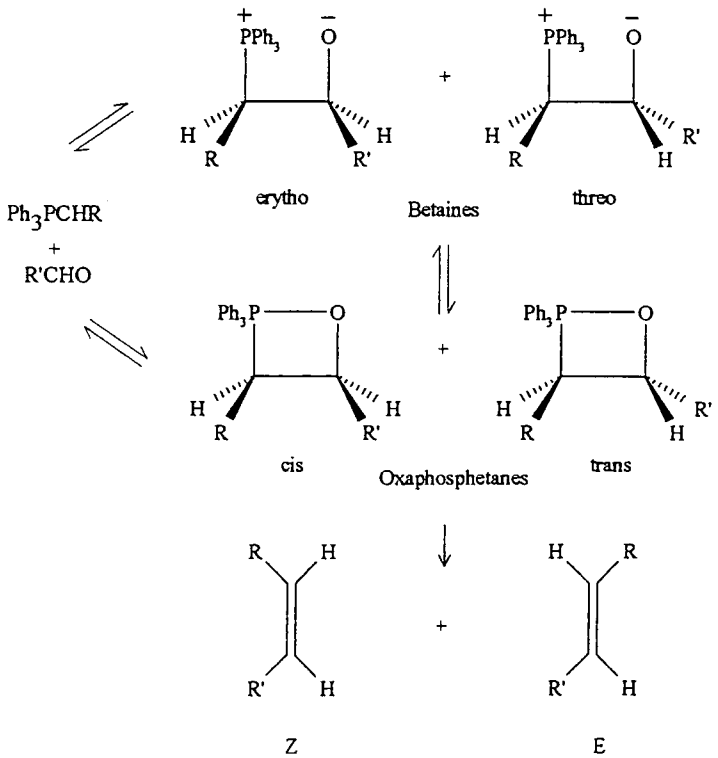

Scheme 1.10

Since then many modifications to the mechanism of this reaction have been suggested.[7] The most recent evidence suggests that the OPA is in fact the intermediate, with the betaine as a model for a transition state. The Wittig-Schlosser method[43] resulted in a complete reversal of the Wittig reaction stereochemistry, producing predominantly (E)-alkenes when using non-stabilised ylides (Scheme 1.11).

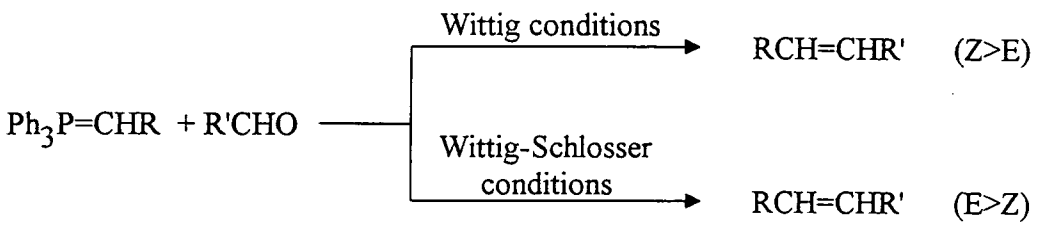

Scheme 1.11

1.3 Iminophosphoranes

Iminophosphoranes are isoelectronic with phosphonium ylides. They are compounds of the general type $R_3P{=}NR'$, with a four coordinate phosphorus atom and a formal phosphorus-nitrogen double bond, which, as in phosphonium ylides, can be considered as essentially a single P-N bond either with or without a degree of electronic delocalisation (Scheme 1.12).

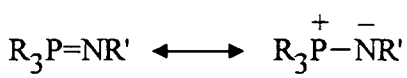

Scheme 1.12

Iminophosphoranes are considerably more stable than their phosphonium ylide analogues. This stabilisation has been attributed to the nature of the phosphorus-nitrogen bond and especially to delocalisation of electron density from nitrogen to phosphorus. They are basic,

[43]M. Schlosser and K. F. Christmann, *Angew. Chem. Int. Ed. Eng.*, 1966, 5, 126.

with proton attack occurring at the iminic nitrogen atom,[44] for example $[(Me_2N)_3P{=}N]_3P{=}N\text{-}Bu^t$ is the strongest neutral base known.[45]

1.3.1 Preparation of Iminophosphoranes

The first synthesis of an iminophosphorane was reported in 1919 by Staudinger and Meyer.[4] Now known as the Staudinger reaction it involves the reaction of an azide with a tertiary phosphine and has been widely employed for the high yield synthesis of a large range of imines (Scheme 1.13).

$$R_3P + R'N_3 \longrightarrow \left[R_3PN_3R'\right] \longrightarrow R_3P{=}NR'$$

Scheme 1.13

This reaction proceeds by nucleophilic attack of the phosphorus on the terminal nitrogen of the azide to afford a linear phosphazide (usually not detectable) which then dissociates, probably via a four-centred transition state analogous to an OPA (Scheme 1.10), to give the iminophosphorane product and N_2.

Another method employed is the direct conversion of a wide variety of aromatic amines to iminophosphoranes by their reaction with triphenylphosphine dibromide.[46] The reaction appears to proceed by nucleophilic displacement of bromine from phosphorus by nitrogen followed by deprotonation (Scheme 1.14).

$$ArNH_2 + Ph_3PBr_2 \xrightarrow{-HBr} \left[ArNH{-}PPh_3\right]^+ Br^- \xrightarrow{-HBr} ArN{=}PPh_3$$

Scheme 1.14

---

[44]R. D. Wilson and R. Bau, *J. Am. Chem. Soc.*, 1974, **96**, 7601.
[45]R. Schwesinger and H. Schlemper, *Angew. Chem. Int. Ed. Eng.*, 1987, **26**, 1167.
[46]L. Homer and H. Oediger, *Liebigs Ann. Chem.*, 1959, **627**, 142.

For alkyl-, rather than arylamines deprotonation is not spontaneous and requires further addition of a strong base (Scheme 1.15).[47]

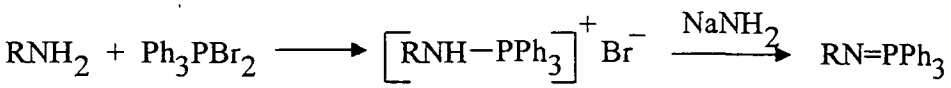

Scheme 1.15

1.3.2 Reactions of Iminophosphoranes

Iminophosphoranes undergo hydrolysis to give amines and phosphine oxides (the driving force of the reaction) under both basic and acidic conditions. The ease of the reaction is dependant on the nitrogen substituents. The alkylimines (R=alkyl) often hydrolyse in moist air (although not as readily as the phosphonium ylide analogues) but aryl imines (R=aryl) are generally stable in air and often water, but hydrolyse in dilute acid or base conditions.

Iminophosphoranes can also undergo oxidation reactions, resulting in the formation of amines and phosphine oxides though imines with more electron withdrawing substituents such as carbonyl or sulphonyl groups are more difficult to oxidise. Reduction can also take place and, as with their ylide counterparts, $LiAlH_4$ is the reducing agent often used.

The reaction of iminophosphoranes with aldehydes and ketones, discovered by Staudinger, is known as the Aza-Wittig reaction and is analogous to the Wittig reaction (Scheme 1.16).[48]

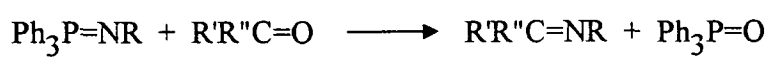

Scheme 1.16

---

[47]H-J. Cristau, L. Chiche, J. Kadoura and E. Torreilles, *Tetrahedron Lett.*, 1989, **29**, 3931.
[48]A. W. Johnson with special contributions by W. C. Kaska, K. A. O. Starzewski and D. A. Dixon, *'Ylides and Imines of Phosphorus'*, John Wiley & Sons Inc., New York, 1993, page 423.

The reaction proceeds via nucleophilic attack of the imine nitrogen atom on the carbonyl compound followed by transfer of oxygen to phosphorus. The nature of the intermediates of the Aza-Wittig reaction have not been proven, neither a betaine nor a oxazaphosphetane have been observed. The reaction is usually carried out in neutral solvents, without a catalyst and generally at mild reflux temperatures resulting in high yields.

Intramolecular Aza-Wittig reactions have also been observed leading to cyclisations (Scheme 1.17).[49]

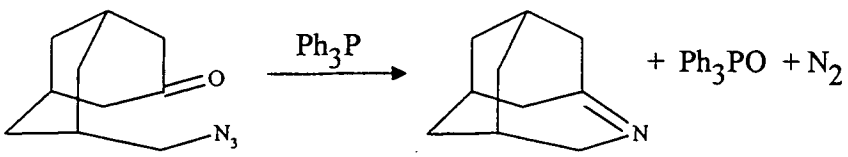

Scheme 1.17

1.4 Hydrogen Bonding

1.4.1 Historical Perspective

In 1940 Pauling[50] defined the hydrogen bond as follows;

> *"It has been recognised in recent years that under certain conditions an atom of hydrogen is attracted by rather strong forces to two atoms, instead of only one, so that it may be considered to be acting as a bond between them. This is called the hydrogen bond. It is now recognised that [...] the hydrogen bond is largely ionic in character, and is formed only between the most electronegative atoms [...]. Although the hydrogen bond is not a strong bond [...] it has great significance in determining the properties of substances."*

---

[49]T. Sasaki, S. Eguchi and T. Okano, *J. Am. Chem. Soc.*, 1983, **105**, 3912.
[50]L. Pauling, *'The Nature of the Chemical Bond and the Structure of Molecules and Crystals - An Introduction to Modern Structural Chemistry.'* 2nd Edn., Oxford University Press, London, 1940.

Today it is recognised that a hydrogen bond cannot simply be defined in terms of the elements which partake in it. However certain elements (e.g. some of the most electronegative elements F, O, N, Cl) or groups show a higher propensity than other elements for such bonding hence these were the earliest recognised and referred to in Pauling's description. Although a definitive description of what a hydrogen bond is has not yet been, and probably never will be, reached, hydrogen bonding is generally regarded as a weak association occurring between atoms, molecules or ions (positive or negative) in the gas, liquid or solid state, where an interaction between a donor D-H and an acceptor A specifically involves the H atom. This attraction is described simply as being predominantly electrostatic between the centre of high electron density on A (for example a lone pair of electrons) and the positive end of the polar covalent bond $D^{\delta-}$-$H^{\delta+}$. The notation employed is D-H...A, the term hydrogen bond referring to the H...A interaction. In this description the distance r(D-H) is shorter than r(H...A). Hydrogen bonds may be simple (i.e. involving just one acceptor and one donor), 3 centred, four centred etc. (Figure 1.7).

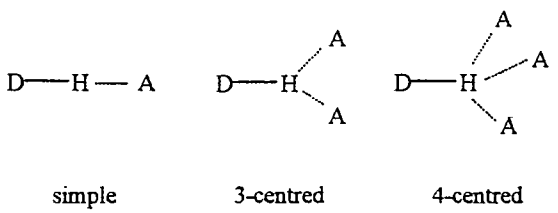

Figure 1.7

It is also well established that not all hydrogen bonds have this character. In some hydrogen bonds it is clear that the proton is not bonded covalently to either D or A, but instead is equally attracted to both. Known as 'strong' or 'very strong' hydrogen bonds the name refers to the whole system and is written as D...H...A or D-H-A.[51] In addition today there is wide agreement that the weaker C-H...O interactions such as those involved in acidic C-H groups also warrant the label hydrogen bonds. Nevertheless, despite the wide range of experimental and theoretical work supporting their existence, the concept of weak hydrogen bonds has

[51] J. Emsley, *Chem. Soc. Rev.*, 1980, **9**, 91.

repeatedly been questioned. In the 1960s, in answer to work by Sutor (who had concluded that weak hydrogen bonds existed in caffeine, theophylline and other compounds)[52, 53] an article by Donohue[54] disregarded such bonds, claiming they did not exist. His remarks resulted in a decade of structural chemists ignoring the idea that a C-H group could form a hydrogen bond with electronegative elements.

1.4.2 C-H...O Hydrogen bonds

In 1982 a landmark study conducted by Taylor and Kennard[55] revealed evidence supporting the existence of C-H...O hydrogen bonding in crystals. Their study aimed to answer two questions. (1) What crystallographic evidence was there for the existence of hydrogen bonds? (2) In what type of crystal structures do they occur? Their source of crystallographic data was the Cambridge Structural database and a total of 113 organic compounds. All of these structures had been determined by neutron diffraction (for accurate C-H positions) and contained at least one C-H group and one potential hydrogen bond acceptor atom (O, N, Cl and S were studied).[50]

They concluded that: (1) C-H atoms have a statistically significant tendency to form short intermolecular contacts to oxygen atoms, C-H...O contacts with d > 0.3 Å (d = υ(H) + υ(O) - r(H...O), where υ(H) = the van der Waals radius of H, υ(O) = van der Waals radius of O and r(H...O) = C-H...O interatomic distance), were found to occur frequently in the studied structures; (2) this tendency could not be attributed to steric effects, nor could the preference for short C-H...O contacts be explained by the van der Waals repulsion energies. The determining factor is the electrostatic energy, which in the case of oxygen, will almost always be attractive and therefore stabilise the C-H...O contacts; (3) the proton in the majority of cases was found to lie within 30 ° of the plane containing the oxygen lone pair orbitals with the optimum C-H...O arrangement being linear.

---

[52]D. J. Sutor, *Nature*, 1962, **68**, 195.
[53]D. J. Sutor, *J. Chem. Soc.*, 1963, 1105.
[54]J. Donohue, *'Structural Chemistry and Molecular Biology.'* W. H. Freeman, San Francisco, 1968, 459.
[55]R. Taylor and O. Kennard, *J. Am. Chem. Soc.*, 1982, **104**, 5063.

More recently extensive statistical database studies[56, 57, 58] have shown that the mean C...O distance in C-H...O contacts correlates convincingly with conventional C-H acidities where in general shortened C-H...O contacts are obtained for more acidic C-H groups. These studies revealed that systematic gradation in C...O distances for different weakly acidic C-H groups are apparent well beyond the 'conventional' van der Waals limit. Hence the C-H...O contact can be considered, not as a van der Waals interaction, but as primarily electrostatic in nature.

The debate still continues and as recently as 1997 a paper published by Cotton et al claimed that the typical C-H...O/N hydrogen bond represents 'nothing more than a classical van der Waals interaction'.[59] However this claim was disputed by others. In 1998 Mascal argued that C-H...N hydrogen bonds were real,[60] and Desiraju and Steiner outlined the differences in directionality characteristics between C-H...O hydrogen bonds and the van der Waals interaction.[61]

Considering C-H...O hydrogen bonds in a wider context there is a hierarchy of electrostatic interactions (Figure 1.8).[62] At the top (i.e. the strongest) are O-H...O and N-H...N hydrogen bond interactions, typically having energies of 20 - 40 $kJmol^{-1}$ (Figure 1.8a) while at the bottom are interactions between benzene rings (Figure 1.8d-e). In between these two extremes there are C-H...O hydrogen bonds (energies of 2 - 20 $kJmol^{-1}$) or C-H...X hydrogen bonds, where X is an electronegative heteroatom (Figure 1.8b), and π-facial hydrogen bonds (Figure 1.8c).

---

[56]G. R. Desiraju, *J. Chem. Soc., Chem. Commun.*, 1989, 179.
[57]G. R. Desiraju, *J. Chem. Soc., Chem. Commun.*, 1990, 454.
[58]V. R. Pedireddi and G. R. Desiraju, *J. Chem. Soc., Chem. Commun.*, 1992, 988 and references cited therein.
[59]F. A. Cotton, L. M. Daniels, G. T. Jordan IV and C. A. Murillo, *Chem. Commun.*, 1997, 1673.
[60]M. Mascal, *J. Chem. Soc., Chem. Commun.*, 1988, 303.
[61]T. Steiner and G. R. Desiraju, *Chem. Commun.*, 1998, 891.
[62]L. R. Hanton, C. A. Hunter and D. H. Purvis, *J. Chem. Soc., Chem. Commun.*, 1992, 1134.

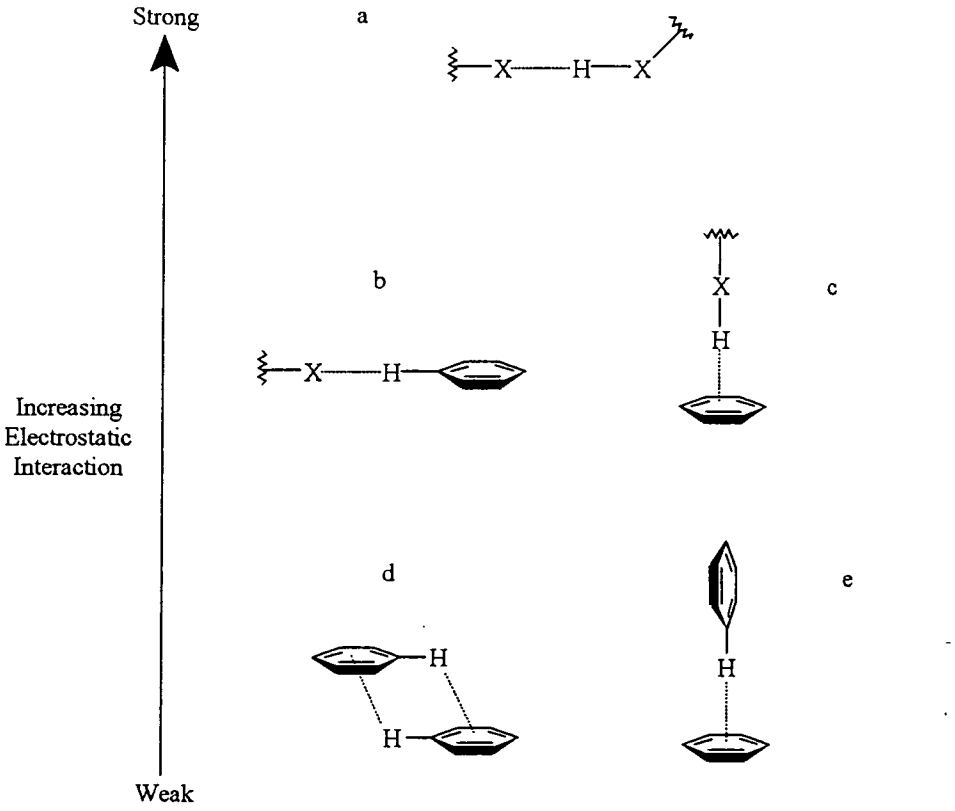

Figure 1.8 Hierarchy of electrostatic interactions

Other interactions are those involving carbon based acceptor groups (A) and C-H donor groups (D). This type of interaction can be loosely divided into two categories. Firstly, C-H···π interactions. Here the acceptor is an electron rich π-bonded system, for example arene[63, 64] or alkyne[65] acceptor. Secondly, the C-H···C interaction. In this case the acceptor possess a lone pair of electrons (for example carbanions, carbenes). It is only very recently, in the X-ray crystal structures of two closely related bis(carbene)-proton complexes[66] that the first such 3-centre 4-electron hydrogen bond has been observed.

---

[63]R. Hunter, R. H. Haueisen and A. Irving, *Angew. Chem. Int. Ed. Eng.*, 1994, **33**, 566.
[64]C. A. Hunter, *Chem. Soc. Rev.*, 1994, 101.
[65]T. Steiner, *J. Chem. Soc., Chem. Commun.*, 1995, 95.
[66]A. J. Arduengo, S. F. Gamper, M. Tamm, J. C. Calabrese, F. Davidson and H. A. Craig, *J. Am. Chem. Soc.*, 1995, **117**, 572.

1.4.3 Hydrogen bonds role in Controlled Synthesis

One major aspect of hydrogen bond studies is their use in controlled synthesis of organic solids. This is sometimes referred to as 'crystal engineering', a term introduced over 25 years ago by Gerhard Schmid.[67] Desiraju describes this area as 'the understanding of intermolecular interactions in the context of crystal packing and in the utilisation of such understanding in the design of new solids with desired physical and chemical properties'.[68] Today it is recognised as being an important form of supramolecular synthesis and it is useful in tailoring the properties of a compound which are dependent on structure. This is of particular interest in the fields of advanced and biomedical materials.

Crystal structures are mediated by intermolecular interactions (the easiest way to obtain reliable data being through crystallography). C-H...X (X = O, N, Cl, S) hydrogen bonds are relatively long with definite orientations directed by electrostatic interactions. Due to the weakness of the interaction C-H...O hydrogen bonds can be easily bent so that directionality is blurred if steric hinderance or competition with other stronger hydrogen bonding groups play a part. This is clearly observed for C-H...O contacts in carbohydrates where O-H...O hydrogen bonds are the dominant intermolecular interactions forming a framework in which the weaker C-H...O interactions have to adjust. However, when stronger hydrogen bonds are not able to dominate, they can play an important role in determining a structure. This can be illustrated by considering the anomalous crystal structures of 4-chlorophenylprop-2-ynoic acid (A) and 3,5-dintitrocinnamic acid (B) (Figure 1.9).

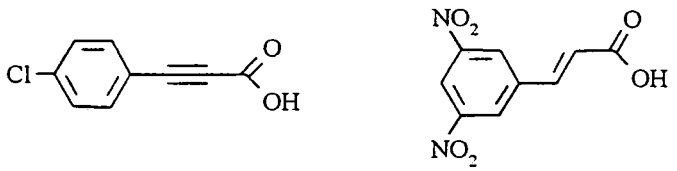

(A) (B)

Figure 1.9

[67]G. M. J. Schmidt, *Pure Appl. Chem.*, 1971, **27**, 647.
[68]G. R. Desiraju, *'Crystal Engineering. The Design of Organic Solids.'* Material Science Monographs 54, Elsevier, Amsterdam, 1989.

Usually in carboxylic acids with aromatic groups a dimeric structure is observed (Scheme 1.18).

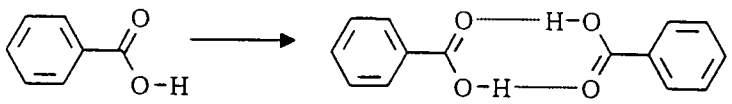

Scheme 1.18

As expected (B) does indeed form an O-H...O dimer ring, but this ring lies on a 2 fold axis rather than on an inversion centre.[69] However, (A) adopts a rare structure containing two symmetry independent molecules in which one carboxyl group has a syn conformation while in the other it is anti (Figure 1.10).[70]

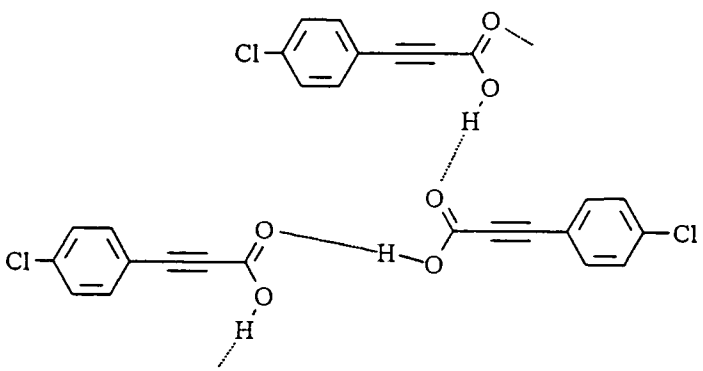

Figure 1.10

In acid (B) C-H...O hydrogen bonds are dominant and numerous, enabling them to play a significant enough role to change the site of symmetry in the dimer ring. On the other hand C-H...O hydrogen bonds are absent in (A) due to the lack of a large number of acidic C-H groups, hence the structure observed.

A further example of the significance of C-H...X interactions was reported by Desiraju et al who identified such directional preferences in several crystal structures of planar oxygenated

[69]G. R. Desiraju and C. V. K. Sharma, *J. Chem. Soc., Chem. Commun.*, 1991, 1239.
[70]G. R. Desiraju, B. N. Murty and K. V. R. Kishan, *Chem. Matr.*, 1990, 2, 447.

compounds[71] where the packing arrangement can only be understood by consideration of weak C-H...O bonds. The significance of these C-H...O interactions is dependent on their number relative to the stronger O-H...O or N-H...O interactions.

In other cases where the stronger N/O-H...O hydrogen bonds are not available, isomorphous crystal structures in which the C-H...O interactions isofunctionally replace these bonds are observed. A good example of this is seen in the the isomorphous complexes of urea-barbital and acetamide barbital (Figure 1.11).[72]

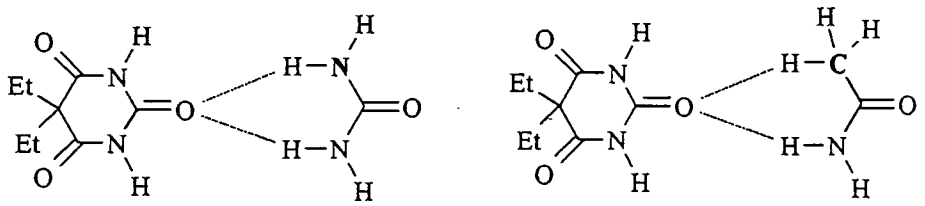

urea - barbital acetamide - barbital

Figure 1.11

Another example can be seen by studying the linear ribbon structures of piperazine-2,5-dione, 1,4-benzoquinone and 1,4-dicyanobenzene. All three have equivalent networks although the former is constituted with strong hydrogen bonds while the latter two are constituted with weak hydrogen bonds.

Structures containing only weaker C-H...O hydrogen bonding are less common. Some examples include the layered structure formed via the 1:1 cocrystallisation of 1,3,5-tricyanobenzene and hexamethylbenzene. Each layer is entirely assembled with C-H...N hydrogen bonds.[73]

---

[71] J. A. R. P. Sarma and G. R. Desiraju, *J. Chem. Soc., Perkin Trans. (2)*, 1987, 1195.
[72] Z. Berkovitch-Yellin and L. Leiserowitz, *J. Am. Chem. Soc.*, 1980, **102**, 7677.
[73] D. S. Reddy, B. S. Goud, K. Panneerselvam and G. R. Desiraju, *J. Chem. Soc., Chem. Commun.*, 1993, 663.

More recently there have been examples of crystalline adducts where short C-H...O contacts dictate the structures observed. One such structure is an adduct of trinitromethane, $CH(NO_2)_3$, with dioxane, $O(CH_2CH_2)_2O$.[74] This yields the triple aggregate $(O_2N)_3CH...O(CH_2CH_2)_2O...HC(N_2O)_3$ in which the structure is held together by a backbone of C-H...O interactions. A second illustration of this phenomenon can be seen in the crystalline complex of triphenylsilylacetylene ($Ph_3SiC{=}CH$) and triphenylphosphine oxide. This structure contains four symmetry independent molecular dimers which are connected by C=C-H...O=P hydrogen bonds. These hydrogen bonds have H...O separations of between 1.99 and 2.05 Å and are the shortest reported for an acetylene donor. This reflects the fact that this bond has been formed between the strongest known C-H donor and the strongest O acceptor.[75]

In summary there is little doubt that C-H...O hydrogen bonds are important, even if in some cases less than obvious, determinants of crystal packing especially in the absence of strong O-H...O and N-H...O hydrogen bonds. In general their strength and effectiveness is dependent on the C-H carbon acidities and on O-atom basicity. The criteria for the significance of a particular C-H...O bond have been the source of debate but it should be noted that the C-H...O hydrogen bond is not really a van der Waals contact but primarily electrostatic, its strength falling off more slowly with distance. This means that even long C....O separations (approximately 4.00 Å) have to be considered, and these weak hydrogen bonds will have an effect on the overall structure.

---

[74]H. Bock, R. Dienelt, H. Schodel and Z. Havlas, *J. Chem. Soc., Chem. Commun.*, 1993, 1792.
[75]T. Steiner, J. van der Maas and B. Lutz, *J. Chem. Soc., Perkin Trans. (2)*, 1997, 1287.

Chapter 2

2. GENERAL EXPERIMENTAL TECHNIQUES

2.1 Inert-Atmosphere Techniques

The experimental work contained in this thesis generally involves the use of air-sensitive and hygroscopic starting materials and products which rapidly decompose on exposure to air. It was therefore necessary to carry out synthesis, isolation and analyses in a dry, inert atmosphere (Ar or N_2).

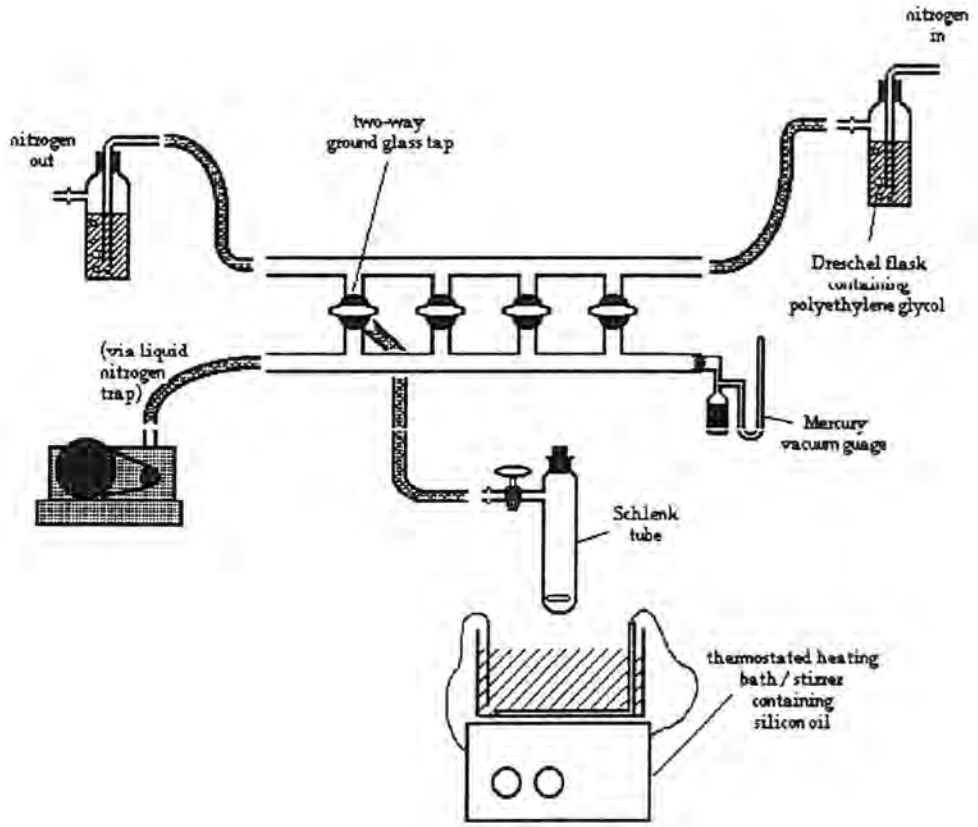

Figure 2.1 A schematic representation of a vacuum line.

Two basic types of apparatus were employed, namely a vacuum line and a glove box. All synthetic work was carried out using either a bench top, or in some cases, a fume hood vacuum and nitrogen line which is shown schematically in Figure 2.1.

Generally, standard inert-atmosphere Schlenk techniques were employed.[1] Reactions were performed in Schlenk tubes which had been dried at about 100 °C prior to evacuation to less than 0.1 torr three times, being filled with dry nitrogen between each evacuation. Air-sensitive reagents were weighed out in the glove box (Figure 2.2) and either added to the Schlenk tube directly in the glove box or placed into an air-tight vial then added to the Schlenk tube (already attached to vacuum/nitrogen line), under a back pressure of nitrogen.

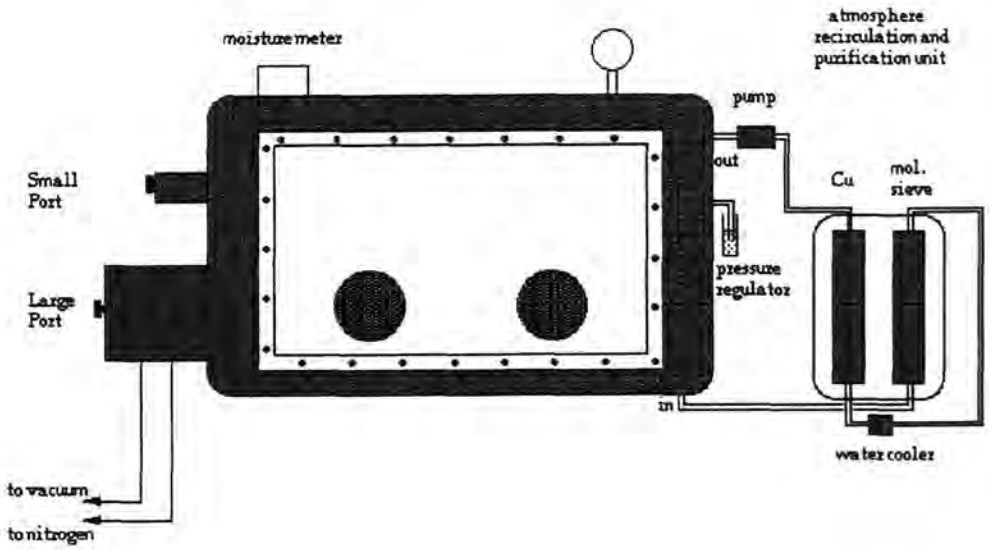

Figure 2.2 A schematic representation of a glove box.

All solvents and liquid reagents were introduced directly to the nitrogen filled Schlenk tube by a dry syringe. All products were isolated using a filter stick of the appropriate porosity. The filter stick being attached to a second Schlenk tube, evacuated and flushed with nitrogen three times as above. The other end of the filter stick being quickly placed into the neck of the Schlenk tube containing the liquid requiring filtration, and the apparatus

[1] D. F. Schriver and M. A. Drezdzon. *'The Manipulation of Air Sensitive Compounds.'*, 2nd Edn., Wiley, New York, 1986.

inverted to complete the filtration, with the whole process taking place under dry nitrogen gas. The isolated products were then dried under vacuum and taken into the glove box, prior to analysis. Handling and storage of all products was carried out under the nitrogen atmosphere of a glove box (Figure 2.2). Samples and equipment were introduced into the glove box through one of the two ports. The ports were evacuated and filled with nitrogen three times before opening the inner doors. Monitoring of the glove box atmosphere was performed by a moisture meter, the moisture level being maintained to between 2-4 parts per million.

2.2 Starting Materials and Solvents

All the starting materials obtained were of the highest purity available. The phosphonium salts and organic acids were obtained from Aldrich or Lancaster. In general they did not have to be stored in a glove box, but in order to remove any residual moisture they were pumped under a vacuum in the Schlenk tube prior to performing a reaction. Where appropriate, liquid reagents were dried for at least 24 hours prior to use over molecular sieves (13X or 4A).

The solvents used (thf, toluene, hexane, acetonitrile) were freshly distilled over the appropriate drying agents and used directly. Deuterated solvents, for use in NMR were stored over molecular sieves in the glove box or supplied in 0.5 mL glass ampoules which were opened in the glove box for immediate use.

2.3 Nuclear Magnetic Resonance (NMR) Spectroscopy

Due to the presence of phosphorus nuclei in all products both ^{31}P as well as ^{1}H NMR studies were routinely carried out.

All the samples were prepared in the glove box by dissolving the compound in a known volume of a suitable, pre-dried, deuterated solvent, in a NMR tube (1-5 mg in 0.5 mL of solvent for ^{1}H NMR, 10-15 mg in 0.5 mL of solvent for ^{31}P NMR). Before removing from the glove box the NMR tubes were sealed with an air-tight plastic cap and plastic film. The data were acquired as soon as possible to minimise any decomposition.

All spectra were acquired at room temperature. ^{1}H NMR spectra were recorded at 200 MHz using a Varian VXR200 or a Mercury-200 NMR spectrometer or at 250 MHz using a Bruker AC 250FT NMR spectrometer or at 400 MHz using a Gemini-400 NMR spectrometer. All chemical shifts (δ) reported are relative to TMS and all coupling constants are quoted in Hz.

^{31}P NMR spectra were recorded at 101.2 MHz using a Bruker AC 250 FT NMR spectrometer or at 80.9 MHz using a Mercury-200 NMR spectrometer. All chemical shifts reported are relative to 85% H_3PO_4 and all coupling constants are quoted in Hz.

^{19}F NMR spectra were recorded at 75.3 MHz on a Bruker AC 250 FT NMR spectrometer. All chemical shifts reported are relative to $CFCl_3$ and all coupling constants are quoted in Hz.

2.4 Infra-Red (IR) Spectroscopy

The IR spectra of isolated products were obtained as nujol mulls on NaCl plates using a Perkin Elmer 1720 × FTIR spectrometer. Due to the air-sensitive nature of the products the mulls were prepared in a glove box using nujol dried over molecular sieves. To minimise the effects of air exposure all spectra were obtained within approximately 5 minutes of their removal from the glove box. In some cases the mull was then exposed to the atmosphere for a few minutes and another spectrum recorded, in order to observe the effects of air and moisture exposure and indeed this is a useful method for determining the resistance of air-sensitive compounds to decomposition.

2.5 Melting Point Determinations

Melting points were determined by differential scanning calorimetry (DSC) using a Mettler FP80 control unit coupled to a Mettler FP85 thermal analysis cell. 5-10 mg of the sample was loaded into an aluminium capsule in the glove box, sealed and then removed from the glove box. The capsule was then immediately placed in the furnace, in which a nitrogen atmosphere was maintained. The melting points quoted in Chapter 3 are calculated as the minimum value of the exotherm recorded by the DSC. It should be noted that the onset of melting would be at a lower temperature.

2.6 Elemental Analysis

Carbon, hydrogen, nitrogen and phosphorus content (percentages by mass) were determined for characterised products. Samples were prepared in the glove box to avoid any degradation or hydrolysis of the compound. For C, H and N analysis between 1-2 mg of the sample was sealed into a pre-weighed aluminium capsule. This capsule was then removed from the glove box and accurately weighed before analysis. Analysis was performed using an Exeter Analytical CE-440 apparatus.

For phosphorus analysis between 6-10 mg of the sample was placed into a gelatine capsule (the exact amount being dependent on the expected amount of phosphorus in the compound). The sample was then acid-digested in a 1:1 solution of sulphuric:perchloric acid. A portion of this solution was reacted with ammonium molybdate to form a coloured phosphomolybdate complex which was defined spectroscopically using a Pye Unicam UV spectrometer.

2.7 X-Ray Diffraction Studies

The principal tool for solid-state structure determination is X-ray Crystallography. The technique requires single crystals ideally no smaller in dimension than $0.1 \times 0.1 \times 0.1$ mm^3 and no greater than $0.5 \times 0.5 \times 0.5$ mm^3. Crystals were grown in the Schlenk tubes under nitrogen at temperatures ranging from -80 °C in a freezer, 5 °C in a refrigerator, to room temperature of 25 °C. Products were all characterised by IR and NMR spectroscopy before X-ray analysis was performed.

Due to the air-sensitive nature of these compounds they must be treated before study in order to prevent decomposition. One method employed is the use of inert, perfluorinated polyether oil as a coating for the crystal. These oil-coated crystals are then examined under a microscope and a suitable single crystal is selected. This is then attached to the diffractometer head by means of a glass fibre. Once placed onto the diffractometer, a cold dry nitrogen gas stream is applied which freezes the oil around the crystal, fixing the orientation and preventing air from hydrolysing, oxidising or drying the sample. Data collection then takes place, at low temperature, in order to minimise atom vibrations. The time taken depends on the type of diffractometer, lattice type, unit cell dimensions and the intensity of reflections and can take anything from 6 hours to 5 days.

Appendix A contains a summary of data and atomic coordinates for all compounds characterised by this technique. For the purpose of quoting hydrogen bond distances, apart from compounds (19), (24) and (25), all C-H groups, which were initially located and freely refined, were normalised by extending the C-H distance along the C-H bond vector to a distance of 1.08 Å (a typical C-H neutron distance). All OH and NH groups were freely refined.

2.8 Neutron Diffraction

Data were collected at 20 K on the D19 instrument at the Institut Laue Langevin, Grenoble. The air-sensitive crystals (15-20 mm^3) were mounted on aluminium pins in an argon-filled glovebox and sealed under quartz domes prior to removal and transportation to Grenoble. Structures were refined using the X-ray coordinates of the heavy atoms as a starting point. Appendix A contains a summary of data and atomic coordinates for all compounds characterised by this technique.

2.9 Cryoscopic Relative Molecular Mass (Mr) Measurements

Specially designed apparatus was used for measuring cryoscopic data.[2] Cryoscopic grade benzene (melting point 5.2 °C) was obtained from Fisons Analytical, degassed using dry nitrogen and stored over molecular sieves. The cryoscopic constant, Kc, of benzene was then determined for each new batch by dissolving a known mass of freshly sublimed biphenyl (Mr = 154.2) in a known volume of the benzene and measuring the depression in the freezing point of the benzene, ΔT, due to the solute. From Equation 2.1, Kc could then be obtained.

$$Kc = \frac{\Delta T \times \text{mass of benzene} \times 154.2}{1000 \times \text{mass of biphenyl}}$$

Equation 2.1

With a known value of Kc, the Mr of a compound could be determined by dissolving a known mass (typically 50 - 500 mg) of the sample in a known volume (and therefore mass) of benzene (typically 20 - 25 mL) whose freezing point has already been determined. The freezing point of the solution was found several times to ensure that an accurate value has been obtained. With the aid of a hand held magnifying lens the Beckmann thermometer

---

[2]M. G. Davidson, R. Snaith, D. Stalke and D. S. Wright, *J. Org. Chem.*, 1993, **58**, 2810.

could be read to an accuracy of ± 0.001 °C. The depression in freezing point of benzene, ΔT, caused by the solute was thus determined and, from Equation 2.2, the Mr of the sample could be calculated.

$$M_r = \frac{\text{mass of solute x Kc x 1000}}{\Delta T \text{ x mass of benzene}}$$

Equation 2.2

Usual precautions were taken to prevent any hydrolysis of the compound before measurements were made.

The apparatus used was composed of an inner sleeve into which a known volume of benzene was added whilst maintaining a flow of nitrogen through the apparatus via a vacuum line. The sample was then added directly into this inner sleeve. Cooling of the solution was achieved by means of recirculating ethanol. The apparatus is shown in Figure 2.3. Errors were calculated with regard to the accuracy of the thermometer reading and the variation in values found for ΔT.

2.10 UV/Visible Absorption Spectroscopy

UV/Visible absorption spectra were carried out with an ATI Unicam UV2-100 spectrometer. Spectra were performed using quartz cells over an appropriate wavelength (usually 200 nm to 600 nm). A base line was obtained using a suitable solvent prior to use.

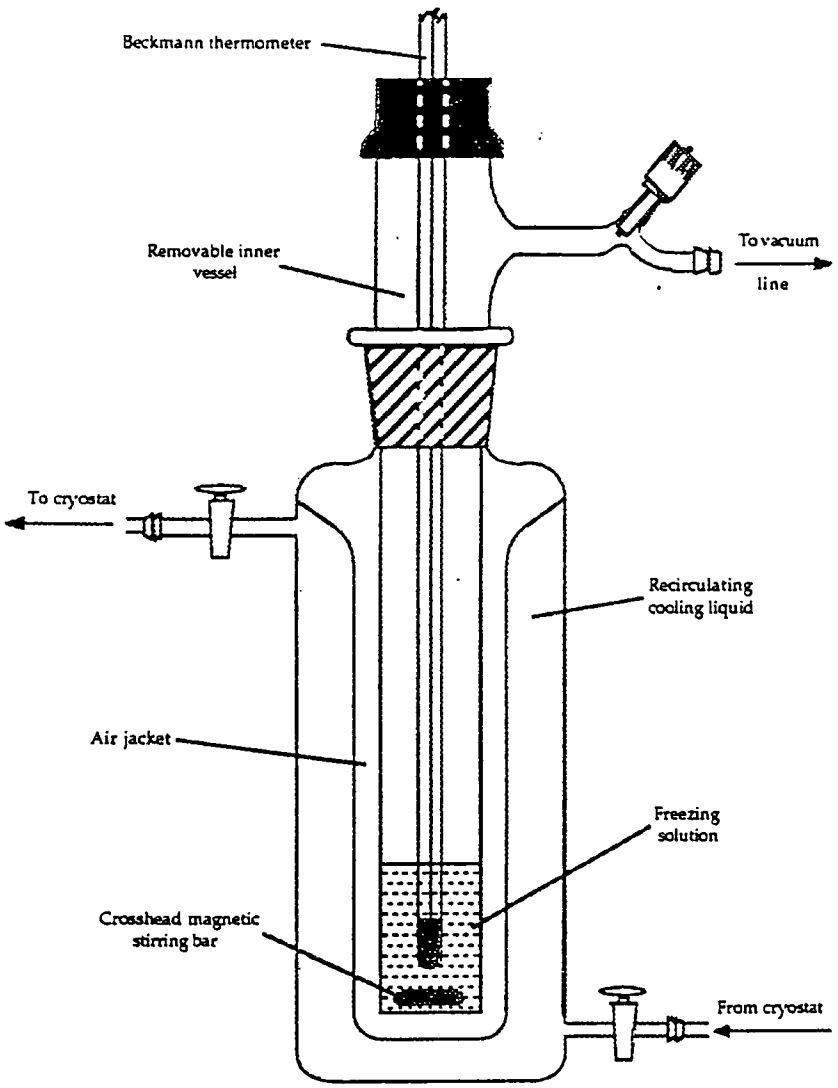

Figure 2.3 Apparatus for cryoscopic measurements.

Chapter 3

3. RESULTS

This chapter reports the synthesis and characterisation of both starting materials, namely the phosphonium ylides and the iminophosphorane [(1) to (4)], and all complexes [(5) to (27)] which will be discussed in subsequent chapters (the numbering scheme employed here will remain the same throughout). Single crystal X-ray diffraction data were obtained for all complexes except (18) and (27). Single crystal neutron diffraction data were also obtained for complexes (7) and (10). All crystal data and structure refinement information is provided in Appendix A, while selected parameters are detailed in the relevant discussion chapters. Where neutron data were obtained it is these data, not X-ray data, that are quoted.

These experimental results will be divided into five areas. The first area outlines details of the starting materials synthesised. The further four areas divide the complexes according to the discussion chapters in which they appear. Table 3.1 lists the formulae and numbers of complexes along with the chapter in which they are discussed.

Table 3.1 The complexes described in the subsequent chapters of the thesis.

Numbers used in text	Formula	Discussion Chapter
(5)	$[(Ph_3PMe)^+(OC_6H_5)^-]_n$	4
(6)	$[(Ph_3PEt)^+(OC_6H_5)^-]_n$	4
(7)	$[(Ph_3PMe)^+(OC_6H_3Ph_2\text{-}2,6)^-]_2$	4
(8)	$[(Ph_3PEt)^+(OC_6H_3Ph_2\text{-}2,6)^-]_2$	4
(9)	$(Ph_3PMe)^+(OC_6H_2{}^tBu_2\text{-}2,6\text{-}Me\text{-}4)^-.thf$	4
(10)	$[(Ph_3PEt)^+(OC_6H_2{}^tBu_2\text{-}2,6\text{-}Me\text{-}4)^-]_n$	4
(11)	$[(Ph_3PC(Ph)H_2)Br.2CH_3CN]_n$	4
(12)	$[(Ph_3AsC(Ph)H_2)Br.2CH_3CN]_n$	4
(13)	$(Ph_3PEt)^+(NPh_2)^-$	5
(14)	$[(Ph_3PEt)^+(C_{12}H_8N)^-]_2$	5
(15)	$[(Ph_3PMe)^+(Ar_2P)^-]_2$ [i]	5
(16)	$[(Ph_3PEt)^+]_2[CH_2(2,6\text{-}{}^tBu_2\text{-}C_6H_2O)_2]^{2-}$	6
(17)	$(Ph_3PNH)_2[CH_2(2,6\text{-}{}^tBu_2\text{-}C_6H_2OH)_2]$	6
(18)	$[(Ph_3PMe)^+]_2[CH_2(2,6\text{-}{}^tBu_2\text{-}C_6H_2O)_2]^{2-}$	6
(19)	$[(Ph_3PEt)^+(C_6H_5O_2)^-]_2$	6
(20)	$[(Ph_3PEt)^+(Hsalen)^-.xCH_3CN]_n$	6
(21)	$[(Ph_3PMe)^+(LH_3)^-.2CH_3CN]_n$	6
(22)	$(Ph_3PEt)^+(LH_3)^-.2CH_3CN$	6
(23)	$[(Ph_3PNH_2)^+(LH_3)^-.2CH_3CN]_n$	6
(24)	$(Ph_3P^+C(H)=C(H)C_6H_4O^-).C_7H_8$	7
(25)	$Ph_3P^+C(Ph)=C(H)C_6H_4O^-$	7
(26)	$[Ph_3PC(H)=C(H)C_6H_4OH]^+Cl^-$	7
(27)	$[Ph_3PC(H)=C(H)C_6H_4OMe]^+I^-$	7

i $Ar_2PH = [C_6H_2(CF_3)_3\text{-}2,4,6]_2PH$
ii H_2salen = N,N'-ethylenebis(salicylideneimine)
iii LH_4 = *p*-tert-butylcalix[4]arene

3.1 Preparation of Starting Materials (1) to (4)

Preparations of the ylides were performed using the standard 'salt-free' method of preparation.[1] The preparation of iminotriphenylphosphorane was modified from syntheses found in the literature.[2,3]

3.1.1 Formation of (1), Triphenylphosphonium methylide

$$Ph_3PCH_3^+ Br^- + NaNH_2 \longrightarrow Ph_3PCH_2 + NaBr + NH_3$$

(1)

Dry thf (150 mL) was added, under nitrogen, to a round-bottom flask containing methyltriphenylphosphonium bromide (35.6 g, 100 mmol) and sodium amide (4.6 g, 110 mmol). This was heated to 40 °C and allowed to stir overnight resulting in a yellow solution with a precipitate of sodium bromide. After filtration to remove the NaBr and any unreacted $NaNH_2$, almost all the thf was evaporated under vacuum and the remaining suspension was redissolved in hexane (80 mL) and toluene (8 mL) to give a slightly cloudy yellow solution. On leaving this solution at room temperature a crop of yellow crystals was obtained.

Yield: 19.8 g (72 %)

Melting point: 101.3 °C (Literature value 96.0 °C)[1]

IR Spectrum: ν 2920 cm^{-1}, 2850 cm^{-1} and 1460 cm^{-1} C-H stretches of nujol mull,
ν 880 cm^{-1} P-C stretch of ylide.

---

[1] R. Koster, D. Simic and M. Grassberger, *Liebigs Ann. Chem.*, 1970, **739**, 281.
[2] H. Staudinger and J. Meyer, *Helv. Chim. Acta.*, 1919, **2**, 635; L. Bickofer and S. M. Kim, *Chem. Ber.*, 1963, **96**, 3099; H-J. Cristau, J. Kadoura, L. Chiche and E. Toreilles, *Bull. Soc. Chim. Fr.*, 1989, **4**, 515.
[3] R. Appel and A. Hauss, *Chem. Ber.*, 1960, **93**, 405.

^{1} H NMR spectrum: 200 MHz, solvent C_6D_6

δ (ppm)	Integral	Multiplicity	Assignment
0.9	2H	doublet	$Ph_3PC\mathbf{H}_2$
7.2-7.8	15H	multiplet	ArH

^{31} P NMR spectrum: 101.2 MHz, solvent C_6D_6

δ (ppm)	Multiplicity	Assignment
20.7	singlet	$Ph_3\mathbf{P}CH_2$

3.1.2 Formation of (2), Triphenylphosphonium ethylide

$$Ph_3PC(Me)H_2^+ Br^- + NaNH_2 \longrightarrow Ph_3PC(Me)H + NaBr + NH_3$$

(2)

Dry thf (180 mL) was added, under nitrogen, to a round-bottom flask containing ethyltriphenylphosphonium bromide (37.0 g, 100 mmol) and sodium amide (4.6 g 110 mmol). This was heated to 40 °C and allowed to stir overnight resulting in a red solution with a precipitate of sodium bromide. After filtration to remove the NaBr and any unreacted $NaNH_2$, almost all the thf was evaporated under vacuum and the remaining suspension was redissolved in hexane (20 mL) to give a slightly cloudy red solution. On leaving this solution at room temperature a crop of red crystals was obtained.

Yield: 16.0 g (55 %)

Melting point: 112.5 °C

IR Spectrum: ν 2920 cm^{-1}, 2850 cm^{-1} and 1460 cm^{-1} C-H stretches of nujol mull,
ν 820 cm^{-1} P-C stretch of ylide.

^{1}H NMR spectrum: 200 MHz, solvent C_6D_6

δ (ppm)	Integral	Multiplicity	Assignment
1.0	1H	doublet of quartets	$Ph_3PC(Me)\mathbf{H}$
2.1	3H	doublet of doublets	$Ph_3PC(\mathbf{Me})H$
7.0 - 7.1	9H	multiplet	m,p-ArH
7.1-7.7	6H	multiplet	o-ArH

^{31}P NMR spectrum: 101.2 MHz, solvent C_6D_6

δ (ppm)	Multiplicity	Assignment
14.6	singlet	$Ph_3\mathbf{P}C(Me)H$

3.1.3 Formation of (3), Triphenylphosphonium benzylide

$$Ph_3PC(Ph)H_2^+ Br^- + NaH \longrightarrow Ph_3PC(Ph)H + NaBr + H_2$$

(3)

Dry thf (150 mL) was added, under nitrogen, to a round bottom flask containing benzyltriphenylphosphonium bromide (23.0 g, 53.1 mmol) and sodium hydride (1.3 g, 55 mmol). This was allowed to stir at room temperature for 48 hours resulting in an orange solution with a precipitate of sodium bromide. After filtration to remove the NaBr and any unreacted NaH, almost all the thf was evaporated under vacuum and the remaining suspension was redissolved in toluene (50 mL) to give a clear orange/red solution. Refrigeration of this solution to 5 °C for 48 hours yielded orange crystals suitable for X-ray analysis.

Yield: 14.7 g (79 %)

Melting point: 167.5 °C

IR Spectrum: ν 2920 cm^{-1}, 2850 cm^{-1} and 1460 cm^{-1} C-H stretches of nujol mull,
ν 880 cm^{-1} P-C stretch of ylide.

^{1}H NMR spectrum: 250 MHz, solvent C_6D_6

δ (ppm)	Integral	Multiplicity	Assignment
2.9	1H	broad singlet	$Ph_3PC(Ph)\mathbf{H}$
6.6-7.9	20H	multiplet	ArH

^{31}P NMR spectrum: 101.2 MHz, solvent C_6D_6

δ (ppm)	Multiplicity	Assignment
9.7	singlet	$Ph_3PC(Ph)H$

3.1.4 Formation of (4), Iminotriphenylphosphorane

$$Ph_3PNH_2^+ Br^- + NaH \longrightarrow Ph_3PNH + NaBr + H_2$$

(4)

Dry toluene (15 mL) was added, under nitrogen, to a mixture of amino(triphenyl) phosphonium bromide (1.79 g, 5 mmol) and sodium hydride (0.20 g, 5 mmol) in a Schlenk tube. The solution was stirred at 100 °C for 48 hours. The solution was filtered hot, and cooled to room temperature. Storage of the solution at -40 °C for 24 hours yielded a crop of colourless crystals suitable for X-ray analysis.

Yield: 1.0 g (75 %)
Melting point: 128 °C (Literature value 128 °C)[3]

IR Spectrum: ν 2920 cm^{-1}, 2850 cm^{-1} and 1460 cm^{-1} C-H stretches of nujol mull,
ν 1189 cm^{-1} P-N stretch of imine (Literature value 1193 cm^{-1})[4]
ν 3349 cm^{-1} N-H stretch

^{1}H NMR spectrum: 200 MHz, solvent C_6D_6

δ (ppm)	Integral	Multiplicity	Assignment
1.1	1H	broad singlet	Ph_3PNH
7.1-7.3	9H	multiplet	m,p-ArH
7.34	6H	multiplet	o-ArH

^{31}P NMR spectrum: 101.2 MHz, solvent C_6D_6

δ (ppm)	Multiplicity	Assignment
17.5	singlet	Ph_3PNH

[4]M. Schlosser, *Topics Stereochem.*, 1970, **5**, 1.

3.2 Synthesis and characterisation of complexes (5) to (12)

3.2.1 Formation of (5)

(1) (5)

Dry acetonitrile (7 mL) was added under nitrogen to solid Ph_3PCH_2, (1), (0.69 g, 2.5 mmol) and solid phenol (0.24 g, 2.5 mmol) in a Schlenk tube. Stirring at room temperature for 5 minutes resulted in the formation of a yellow precipitate in a yellow solution, which on warming for a further 5 minutes dissolved to give a clear yellow solution. Standing at -30°C yielded a crop of yellow crystals suitable for X-ray analysis.

Yield: 0.4 g (38 %)

Melting point: 110.2 °C

^{1}H NMR spectrum: 200 MHz, solvent CD_3CN

δ (ppm)	Integral	Multiplicity	Assignment[i]
2.0	-	singlet	CH_3CN
5.9 - 6.8	5H	multiplet	ArH of phenol
7.7-7.9	15H	multiplet	ArH of Ph_3PCH_3

i Ph_3PCH_3 not observed

^{31}P NMR spectrum: 101.2 MHz, solvent CD_3CN

δ (ppm)	Multiplicity	Assignment
28.6	singlet	Ph_3PCH_3

Elemental Analysis: $C_{25}H_{23}PO$

	C	H	P	O
Calculated % by mass	81.1	6.3	8.4	4.3
Observed % by mass	78.1	6.2	-	-

3.2.2 Formation of (6)

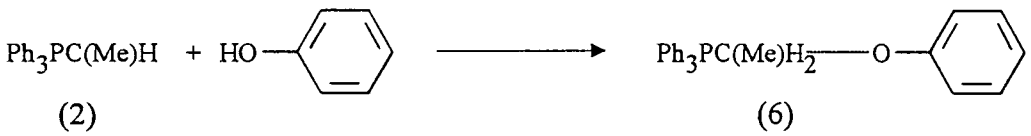

(2) (6)

Dry acetonitrile (10 mL) was added under nitrogen to solid $Ph_3PC(Me)H$ (2.90 g, 10 mmol) and solid phenol (0.94 g, 10 mmol) in a Schlenk tube. Stirring at room temperature for 5 minutes resulted in the formation of a pale yellow precipitate in a yellow solution. On stirring at room temperature for a further 5 minutes the precipitate dissolved to give a clear yellow solution. Standing at -30°C yielded a crop of yellow crystals suitable for X-ray analysis.

Yield: 2.6 g (66 %)

Melting point: 129 °C

^{1}H NMR spectrum: 200 MHz, solvent CD_3CN

δ (ppm)	Integral	Multiplicity	Assignment[i]
1.3	3H	triplet	$Ph_3PC(\mathbf{Me})H_2$
7.6 - 7.8	20H	multiplet	ArH

i $Ph_3PC(Me)\mathbf{H_2}$ not observed

^{31}P NMR spectrum: 101.2 MHz, solvent C_6D_6

δ (ppm)	Multiplicity	Assignment
27.5	singlet	$Ph_3PC(Me)H_2$

Elemental Analysis: $C_{26}H_{25}PO$

	C	H	P	O
Calculated % by mass	81.2	6.5	8.1	4.2
Observed % by mass	78.3	6.4	-	-

3.2.3 Formation of (7)

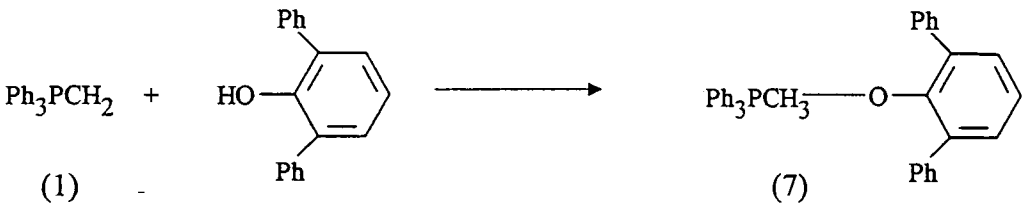

(1) (7)

Dry toluene (10 mL) was added under nitrogen to solid Ph_3PCH_2 (0.69 g, 2.5 mmol) and solid diphenylphenol (0.62 g, 2.5 mmol) in a Schlenk tube. On stirring and heating a pale yellow precipitate in a yellow solution was immediately obtained. Addition of more toluene (10 mL) and further heating afforded no change. On addition of acetonitrile (5 mL) the precipitate dissolved to give a clear orange solution. Standing at room temperature yielded a crop of yellow block like crystals suitable for X-ray diffraction.

Yield: 0.9 g (70 %)

Melting point: 206.5 °C

^{1}H NMR spectrum: 250 MHz, solvent C_6D_6

δ (ppm)	Integral	Multiplicity	Assignment
3.0	3H	doublet	Ph_3PCH_3
6.7-8.2	36H	multiplet	ArH

^{31}P NMR spectrum: 101.2 MHz, solvent C_6D_6

δ (ppm)	Multiplicity	Assignment
25.7	singlet	Ph_3PCH_3

Elemental Analysis: $C_{37}H_{31}OP$

	C	H	P	O
Calculated % by mass	85.1	5.9	5.9	3.1
Observed % by mass	84.1	5.6	6.0	-

3.2.4 Formation of (8)

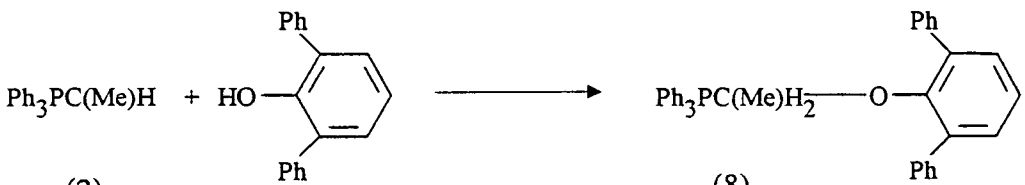

(2) (8)

Dry thf (10 mL) was added under nitrogen to solid Ph3PC(Me)H (0.73 g, 2.5 mmol) and solid diphenylphenol (0.62 g, 2.5 mmol) in a Schlenk tube. On stirring and heating a pale yellow precipitate in a yellow solution was immediately obtained. On addition of dry acetonitrile (5 mL) the precipitate dissolved resulting in a clear yellow solution. Standing at room temperature yielded a crop of yellow crystals suitable for X-ray diffraction.

Yield: 0.9 g (65 %)

Melting point: 203 °C

^{1}H NMR spectrum: 250 MHz, solvent C_6D_6

δ (ppm)	Integral	Multiplicity	Assignment
0.5	3H	doublet of triplets	$Ph_3PC(\mathbf{Me})H_2$
3.8	2H	doublet of quartets	$Ph_3PC(Me)\mathbf{H_2}$
6.8-8.3	32H	multiplet	ArH

^{31}P NMR spectrum: 101.2 MHz, solvent C_6D_6

δ (ppm)	Multiplicity	Assignment
27.4	singlet	$Ph_3\mathbf{P}C(Me)H$

Elemental Analysis: $C_{38}H_{33}PO$

	C	H	P	O
Calculated % by mass	85.0	6.2	5.8	3.0
Observed % by mass	83.5	6.2	5.7	-

3.2.5 Formation of (9)

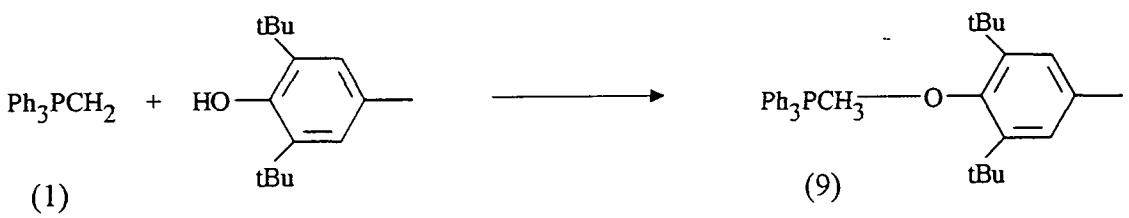

(1) (9)

Dry thf (20 mL) was added under nitrogen to solid Ph_3PCH_2 (0.69 g, 2.5 mmol) and solid 2,6-di-tert-butyl-4-methylphenol (0.55 g, 2.5 mmol) in a Schlenk tube. Stirring at room temperature for 5 minutes resulted in the formation of a yellow precipitate in an orange

solution, which on warming for a further 5 minutes dissolved to give a clear dark red solution. Standing at room temperature yielded a crop of yellow crystals suitable for X-ray analysis. Prolonged exposure to light results in the yellow crystals and solution turning deep green.

Yield: 0.7 g (59 %)

Melting point: 126.7 °C

^{1}H NMR spectrum: 200 MHz, solvent C_6D_6

δ (ppm)	Integral	Multiplicity	Assignment
1.4	-	multiplet	thf
1.5	18H	singlet	**di^{t}Bu**Mephenol
2.3	3H	singlet	di^{t}Bu**Me**phenol
3.6	-	multiplet	thf
3.6	3H	broad singlet	Ph_3PCH_3
7.0-7.7	-	multiplet	ArH

However when exposed to light the crystals turn green in colour and the ^{1}H NMR spectrum no longer contains thf peaks.

^{31}P NMR spectrum: 101.2 MHz, solvent C_6D_6

δ (ppm)	Multiplicity	Assignment
24.1	singlet	Ph_3PCH_3

Elemental Analysis: $C_{34}H_{41}PO.C_4H_8O$

	C	H	P	O
Calculated % by mass	80.3	8.6	5.5	5.6
Observed % by mass	79.8	8.7	5.4	-

3.2.6 Formation of (10)

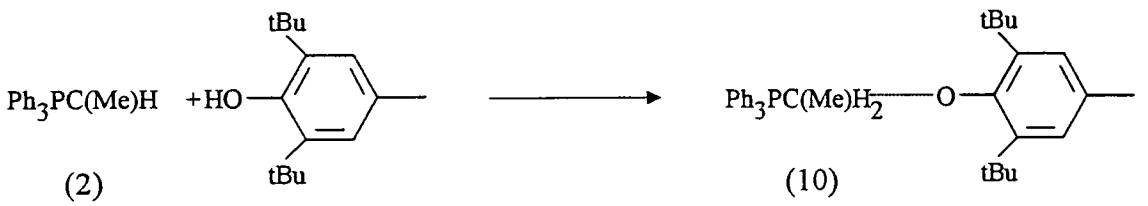

Dry thf (12 mL) was added under nitrogen to solid $Ph_3PC(Me)H$ (0.73 g, 2.5 mmol) and solid 2,6-di-tert-butyl-4-methylphenol (0.55 g, 2.5 mmol) in a Schlenk tube. Stirring at room temperature for 5 minutes resulted in the formation of an orange precipitate in a red solution, which on warming for a further 5 minutes dissolved to give a clear deep red solution. Standing at room temperature yielded a crop of orange block like crystals suitable for X-ray analysis.

Yield: 0.4 g (32 %)

Melting point: 190.3 °C

^{1}H NMR spectrum: 200 MHz, solvent C_6D_6

δ (ppm)	Integral	Multiplicity	Assignment
1.1	3H	doublet	$Ph_3PC(\mathbf{Me})CH_2$
1.8	18H	singlet	**di^{t}Bu**Mephenol
2.6	3H	singlet	di^{t}Bu**Me**phenol
4.5	2H	broad singlet	$Ph_3PC(Me)C\mathbf{H_2}$
7.0-7.5	11H	multiplet	m,p-ArH of $Ph_3PC(Me)CH_2$ and ArH of phenol
7.6	6H	multiplet	o-ArH of $Ph_3PC(Me)CH_2$

^{31}P NMR spectrum: 101.2 MHz, solvent C_6D_6

δ (ppm)	Multiplicity	Assignment
26.3	singlet	$Ph_3\mathbf{P}(Me)CH_2$

Elemental Analysis: $C_{35}H_{43}PO$

	C	H	P	O
Calculated % by mass	82.4	8.4	6.1	3.1
Observed % by mass	81.3	8.4	6.0	-

3.2.7 Formation of (11)

$$Ph_3P + PhCH_2Br \longrightarrow Ph_3PC(Ph)H_2^{+}\,Br^{-}$$

(11)

Dry CH_3CN (50 mL) and benzyl bromide (11.6 mL, 95.3 mmol) was added, under nitrogen, to a round bottom flask containing triphenylphosphine (25.0 g, 95.3 mmol). On

stirring at room temperature a white crystalline solid immediately precipitated out of solution. This was allowed to stir overnight before isolation.

Yield: 45.0 g (99 %)

Melting point: 291 °C

^{1}H NMR spectrum: 200 MHz, solvent $CDCl_3$

δ (ppm)	Integral	Multiplicity	Assignment
2.0	-	singlet	CH_3CN
5.4	2H	doublet	$Ph_3PC(Ph)H_2$
7. 1-7.8	20H	multiplet	ArH

^{31}P NMR spectrum: 101.2 MHz, solvent $CDCl_3$

δ (ppm)	Multiplicity	Assignment
23.5	singlet	$Ph_3PC(Ph)H_2$

3.2.8 Formation of (12)

$$Ph_3As + PhCH_2Br \longrightarrow Ph_3AsC(Ph)H_2^{+}\ Br^{-}$$

(12)

Dry CH_3CN (60 mL) and benzyl bromide (4.16 mL, 35.0 mmol) was added, under nitrogen, to a round bottom flask containing triphenylarsine (10.7 g, 35.0 mmol). On stirring at room temperature for 48 hours a white crystalline solid was formed. This redissolved on heating. On standing at 5 °C for 72 hours crystals suitable for X-ray diffraction were obtained.

Yield: 10.4 g (67 %)

Melting point: 324.8 °C

^{1}H NMR spectrum: 200 MHz, solvent $CDCl_3$

δ (ppm)	Integral	Multiplicity	Assignment
5.4	2H	singlet	$Ph_3AsC(Ph)\mathbf{H}_2$
7.0-7.6	20H	multiplet	ArH

IR Spectra:

In the spectra of compounds (5) to (10) a peak due to P-C (≈ 880 cm^{-1}) was present. Absorptions due to the acidic protons of the phenol derivatives were found to be absent in all products. After air exposure for 5 minutes broad OH stretches (≈ 3300 cm^{-1}) were observed indicating the products are all hygroscopic. In the spectra of (11) a peak due to P-C (≈ 880 cm^{-1}) was present while that for of (12) revealed a peak due to As-C (≈ 692 cm^{-1}).

3.3 Synthesis and characterisation of complexes (13) to (15)

3.3.1 Formation of (13)

$$Ph_3PC(Me)H + Ph_2NH \longrightarrow Ph_3PC(Me)H_2{-}{-}NPh_2$$

Dry toluene (20 mL) was added under nitrogen to solid Ph_2NH (0.42 g, 2.5 mmol) and solid $Ph_3PC(Me)H$ (0.73 g, 2.5 mmol) in a Schlenk tube. After stirring for 15 minutes at room temperature a red precipitate was formed which dissolved by gentle heating to give a clear red solution. Refrigeration of this solution to 5 °C overnight yielded a crop of red crystals suitable for X-ray analysis.

Yield: 0.4 g (37 %)

Melting point: 111.6 °C

^{1}H NMR spectrum: 200 MHz, solvent C_6D_6

δ (ppm)	Integral	Multiplicity	Assignment
2.1	3H	doublet	$Ph_3PC(\mathbf{Me})H_2$
3.9	2H	broad singlet	$Ph_3PC(Me)\mathbf{H_2}$
6.8-7.7	25H	multiplet	ArH

^{31}P NMR spectrum: 101.2 MHz, solvent $CDCl_3$

δ (ppm)	Multiplicity	Assignment
26.1	singlet	$Ph_3\mathbf{P}C(Me)H_2$

Elemental Analysis: $C_{32}H_{30}NP$

	C	H	N	P
Calculated % by mass	83.7	6.5	3.1	6.7
Observed % by mass	82.2	6.3	3.4	6.4

3.3.2 Formation of (14)

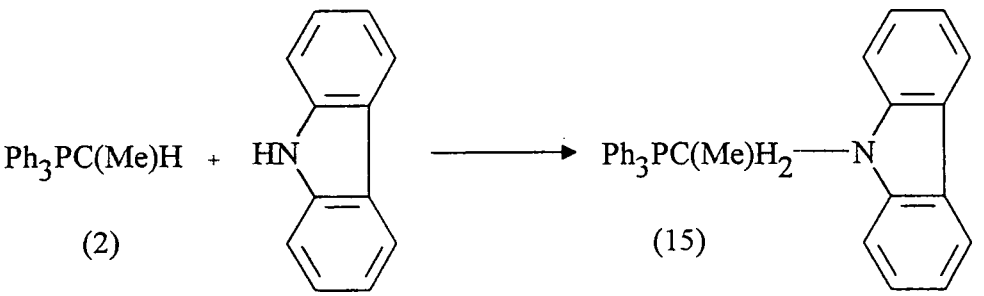

(2) (15)

Dry thf (15 mL) was added under nitrogen to solid $Ph_3PC(Me)H$ (0.73 g, 2.5 mmol) and solid carbazole (0.42 g, 2.5 mmol) in a Schlenk tube. Heating this solution immediately resulted in the formation of a yellow precipitate in an orange solution. On addition of dry acetonitrile (5 mL) the precipitate dissolved to give a clear orange solution. Standing at room temperature yielded a crop of yellow needles suitable for X-ray analysis.

Yield: 0.4 g (38 %)

Melting point: 156.8 °C

^{1}H NMR spectrum: 200 MHz, solvent C_6D_6

δ (ppm)	Integral	Multiplicity	Assignment
1.0	3H	doublet of triplets	$Ph_3PC(\mathbf{Me})H_2$
1.8	2H	doublet of quartets	$Ph_3PC(Me)\mathbf{H_2}$
6.5 - 6.9	12H	multiplet	m,p-ArH of $Ph_3PC(Me)H_2$
7. - 7.4	6H	multiplet	m,p-ArH of carbazolyl
7.7 - 7.8	3H	multiplet	o-ArH of $Ph_3PC(Me)H_2$
8.3 - 8.3	15H	multiplet	o-ArH of carbazolyl

^{31}P NMR spectrum: 101.2 MHz, solvent C_6D_6

δ (ppm)	Multiplicity	Assignment
27.4	singlet	$Ph_3\mathbf{P}C(Me)H_2$

Elemental Analysis: $C_{32}H_{28}NP$

	C	H	N	P
Calculated % by mass	84.0	6.2	3.1	6.8
Observed % by mass	81.4	6.0	3.6	-

3.3.3 Formation of (15)

$$Ph_3PCH_2 + Ar_2PH \longrightarrow Ph_3PCH_3{-}PAr_2$$

Dry Toluene (5 mL) was added under nitrogen to solid Ph_3PCH_2 (0.14 g, 0.5 mmol) and solid Ar_2PH (0.30 g, 0.5 mmol) in a Schlenk tube. The resulting deep blue solution was stirred at room temperature for 15 minutes, during which time a red precipitate formed. On further addition of toluene (15 mL) and gentle warming the precipitate dissolved to give a blue solution. Standing at room temperature for 2 hours yielded a crop of dark red, plate like crystals suitable for X-ray analysis.

Yield: 0.2 g (55 %)

Melting point: 129.5 °C

^{1}H NMR spectrum: 200 MHz, solvent C_6D_6

δ (ppm)	Integral	Multiplicity	Assignment
2.3	3H	doublet	$Ph_3PC\mathbf{H}_3$
7.0 - 6.6	15H	multiplet	ArH of Ph_3PCH_3
7.6	4H	singlet	$\mathbf{Ar}_2P$

^{31}P NMR spectrum: 101.2 MHz, solvent C_6D_6

δ (ppm)	Integral	Multiplicity	Assignment
21.0	1P	multiplet	$Ar_2\mathbf{P}$
21.6	1P	singlet	$Ph_3\mathbf{P}CH_3$

^{19}F NMR spectrum: 235.3 MHz, solvent C_6D_6

δ (ppm)	Integral	Multiplicity	Assignment
- 61.2	12F	doublet	o-CF_3
- 62.3	6F	singlet	p-CF_3

Elemental Analysis: $C_{37}H_{23}P_2F_{18}$

	C	H	P	F
Calculated % by mass	51.1	2.7	7.1	39.3
Observed % by mass	50.8	2.5	-	-

IR Spectra:

In the spectra of compounds (13) to (15) a peak due to P-C ($\approx$ 880 cm^{-1}) was present. Absorptions due to the acidic protons of the phenol derivatives were found to be absent in all products. After air exposure for 5 minutes broad OH stretches ($\approx$ 3300 cm^{-1}) were observed indicating the products are all hygroscopic.

3.4 Synthesis and characterisation of complexes (16) to (23)

3.4.1 Formation of (16)

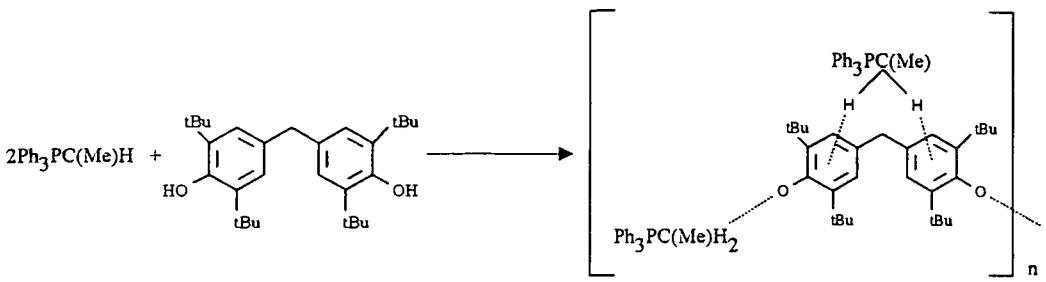

(2) (16)

Solid $Ph_3PC(Me)H$ (0.58 g, 2 mmol) was added under nitrogen to solid 4,4-methylenebis(2,6-di*tert*butylphenol) (0.42 g, 1 mmol) in a Schlenk tube and vigorously stirred under vacuum, resulting in a pale purple solid. On addition of dry acetonitrile (3 mL) a pale red precipitate in a dark red solution was immediately obtained. On heating the precipitate dissolved resulting in a clear dark red solution. Standing at room temperature yielded a crop of red crystals suitable for X-ray diffraction.

Yield: 0.8 g (75 %)

Melting point: 139.3° C

^{1}H NMR spectrum: 200 MHz, solvent C_6D_6

δ (ppm)	Integral	Multiplicity	Assignment[i]
1.6	3H	doublet of triplets	$Ph_3PC(\mathbf{Me})H_2$
1.3	36H	singlet	^{t}Bu of phenol
3.8	2H	singlet	CH_2 of phenol
6.9	4H	singlet	ArH of phenol
7.7 - 7.9	30H	multiplet	ArH of $Ph_3PC(Me)H_2$

i $Ph_3PC(Me)\mathbf{H_2}$ not observed

^{31}P NMR spectrum: 101.2 MHz, solvent C_6D_6

δ (ppm)	Multiplicity	Assignment
26.6	singlet	$Ph_3\mathbf{P}C(Me)H_2$

Elemental Analysis: $C_{69}H_{82}P_2O_2$

	C	H	P	O
Calculated % by mass	82.5	8.2	6.2	3.2
Observed % by mass	81.2	8.8	-	-

3.4.2 Formation of (17)

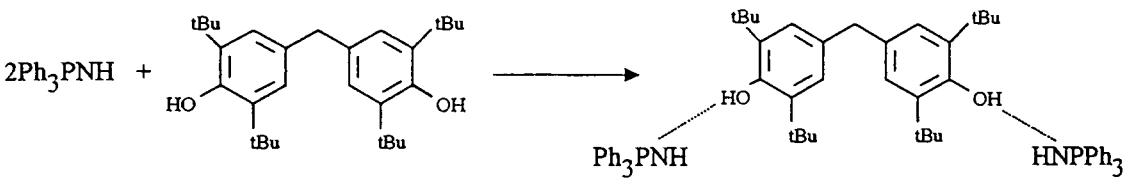

(4) (17)

Dry acetonitrile (5 mL) was added under nitrogen to solid Ph_3PNH (0.55 g, 2 mmol) and solid 4,4-methylenebis(2,6-di*tert*-butylphenol) (0.42 g, 1 mmol) in a Schlenk tube. On stirring a white precipitate in a deep purple solution was immediately obtained. On heating the precipitate dissolved resulting in a clear deep purple solution. Standing at room temperature yielded a crop of red crystals suitable for X-ray diffraction.

Yield: 0.8 g (80 %)

Melting point: 145.7 °C

^{1}H NMR spectrum: 200 MHz, solvent $CDCl_3$

δ (ppm)	Integral	Multiplicity	Assignment
0.8	2H	broad singlet	Ph_3PNH
1.4	36H	singlet	^{t}Bu of bisphenol
3.8	2H	singlet	CH_2 of bisphenol
5.1	2H	broad singlet	OH of bisphenol
7.0	4H	singlet	ArH of bisphenol
7.4 - 7.5	12H	multiplet	m,p-ArH of Ph_3NH
7.6 - 7.7	18H	multiplet	o-ArH of Ph_3NH

^{31}P NMR spectrum: 101.2 MHz, solvent $CDCl_3$

δ (ppm)	Multiplicity	Assignment
23.4	singlet	Ph_3PNH

Elemental Analysis: $C_{65}H_{74}N_2P_2O_2$

	C	H	N	P	O
Calculated % by mass	79.7	7.8	2.9	6.3	3.3
Observed % by mass	80.4	8.0	3.8	-	-

3.4.3 Formation of (18)

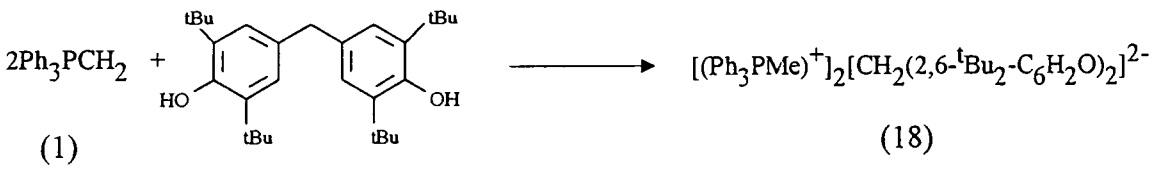

(1) (18)

Solid Ph_3PCH_2 (0.55 g, 2 mmol) was added under nitrogen to solid 4,4-methylenebis(2,6-di*tert*butylphenol) (0.42 g, 1 mmol) in a Schlenk tube and thoroughly

mixed together, resulting in a pale purple solid. On addition of dry acetonitrile (3 mL) a pale red precipitate in a dark red solution was immediately obtained. On heating the precipitate dissolved resulting in a clear dark red solution. Standing at room temperature yielded a crop of red crystals.

Yield: 0.6 g (62 %)

Melting point: 161.7 °C

^{1}H NMR spectrum: 200 MHz, solvent $CDCl_3$

δ (ppm)	Integral	Multiplicity	Assignment[i]
1.4	36H	singlet	^{t}Bu of bisphenol
3.8	2H	singlet	CH_2 of bisphenol
7.0	4H	singlet	ArH of bisphenol
7.7 - 7.8	30H	multiplet	ArH of Ph_3PCH_3

i Ph_3PCH_3 not observed

^{31}P NMR spectrum: 80.9 MHz, solvent $CDCl_3$

δ (ppm)	Multiplicity	Assignment
22.9	singlet	Ph_3PCH_3

Elemental Analysis: $C_{65}H_{78}P_2O_2$

	C	H	P	O
Calculated % by mass	81.9	8.3	6.5	3.4
Observed % by mass	79.9	8.1	7.4	-

3.4.4 Formation of (19)

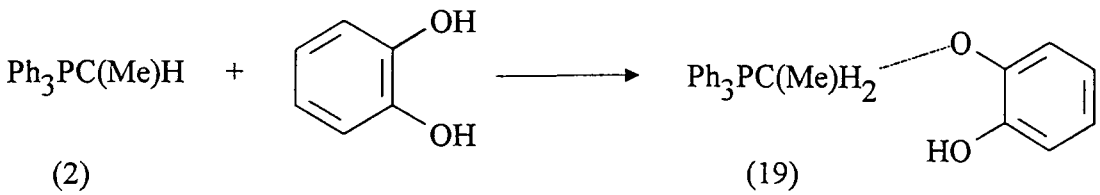

(2) (19)

Dry acetonitrile (15 mL) was added under nitrogen to solid $Ph_3PC(Me)H$ (0.73 g, 5 mmol) and solid catechol (0.28 g, 2.5 mmol) in a Schlenk tube. Stirring at room temperature resulted in the immediate formation of a yellow precipitate. On heating the precipitate dissolved to give a clear yellow solution. Standing at room temperature yielded a crop of yellow needles suitable for X-ray analysis.

Yield: 0.7 g (66 %)

Melting point: 159.9 °C

^{1}H NMR spectrum: 200 MHz, solvent $CDCl_3$

δ (ppm)	Integral	Multiplicity	Assignment
1.3	3H	doublet of triplets	$Ph_3PC(\mathbf{Me})H_2$
6.5	4H	double of multiplets	ArH of catechol
6.8	1H	broad singlet	OH of catechol
7.7 - 7.6	15H	multiplet	ArH of $Ph_3PC(Me)H_2$

^{31}P NMR spectrum: 101.2 MHz, solvent $CDCl_3$

δ (ppm)	Multiplicity	Assignment
29.3	singlet	$Ph_3\mathbf{P}C(Me)H_2$

Elemental Analysis: $C_{26}H_{25}PO_2$

	C	H	P	O
Calculated % by mass	78.0	6.3	7.7	8.0
Observed % by mass	76.8	6.3	-	-

3.4.5 Formation of (20)

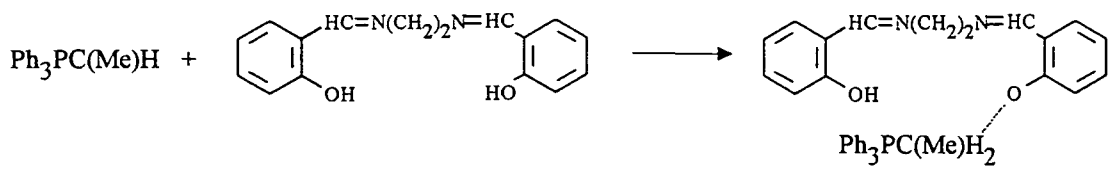

(2) (20)

A dry acetonitrile solution (20 mL) was added under nitrogen to solid H_2salen, (0.67 g, 2.5 mmol) and solid $Ph_3PC(Me)H$ (0.73 g, 2.5 mmol) in a Schlenk tube. Heating the solution resulted in the formation of a yellow precipitate which on further warming gave a clear orange solution. This solution on standing at room temperature for 1 hour yielded a crop of orange crystals suitable for X-ray analysis.

Yield: 1.1 g (75 %)

Melting point: 141.5 °C

^{1}H NMR spectrum: 200 MHz, solvent CD_3CN

δ (ppm)	Integral	Multiplicity	Assignment
1.3	3H	doublet of triplets	$Ph_3PC(\mathbf{Me})H_2$
1.9	4H	multiplet	$\mathbf{CH_3}CN$ and OH
3.3	2H	doublet of quartets	$Ph_3PC(Me)\mathbf{H_2}$
3.8	4H	singlet	N- $\mathbf{CH_2}$-$\mathbf{CH_2}$-N
6.4 - 7.8	29H	multiplet	ArH
8.6	2H	singlet	(-N=C**H**-)$_2$

^{31}P NMR spectrum: 101.2 MHz, solvent $CDCl_3$

δ (ppm)	Multiplicity	Assignment
28.9	singlet	$Ph_3\mathbf{P}C(Me)H_2$

Elemental Analysis: $C_{36}H_{35}N_2PO_2$

	C	H	N	P	O
Calculated % by mass	77.4	6.3	5.0	5.5	5.7
Observed % by mass	77.5	6.3	5.1	5.1	-

3.4.6 Formation of (21)

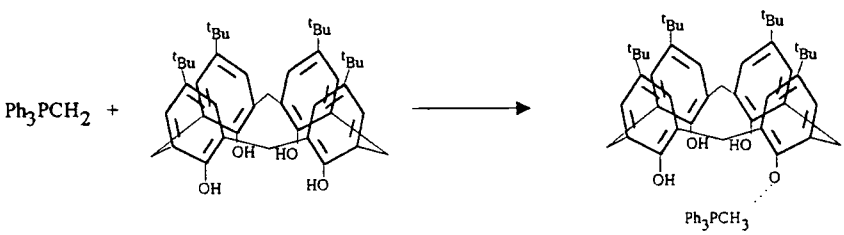

(1) (21)

Dry acetonitrile (5 mL) was added under nitrogen to solid tert-butyl-calix[4]arene, (LH_4), (0.33 g, 0.5 mmol) and solid Ph_3PCH_2 (0.55 g, 2 mmol) in a Schlenk tube. On stirring a yellow precipitate in a yellow solution was immediately obtained. On heating the precipitate dissolved resulting in a clear yellow solution. Standing at room temperature yielded a crop of pale yellow plate like crystals suitable for X-ray diffraction.

Yield: 0.5 g (67 %)

Melting point: 118.5 °C

^{1}H NMR spectrum: 200 MHz, solvent $CDCl_3$

δ (ppm)	Integral	Multiplicity	Assignment
1.3	36H	singlet	^{t}Bu of LH_3^-
2.0	-	singlet	CH_3CN
3.2	4H	doublet	CH_2 of LH_3^-
3.3	3H	doublet	$Ph_3PC\mathbf{H}_3$
4.3	4H	doublet	CH_2 of LH_3^-
6.9	8H	singlet	ArH of LH_3^-
7.6 - 7.8	15H	multiplet	ArH of Ph_3PCH_3
13.3	3H	broad singlet	OH of LH_3^-

^{31}P NMR spectrum: 101.2 MHz, solvent $CDCl_3$

δ (ppm)	Multiplicity	Assignment
21.7	singlet	$Ph_3\mathbf{P}CH_3$

Elemental Analysis: $C_{63}H_{73}PO_4.C_4H_6N_2$

	C	H	N	P	O
Calculated % by mass	79.9	7.9	2.9	3.4	6.9
Observed % by mass	80.3	8.0	2.3	-	-

3.4.7 Formation of (22)

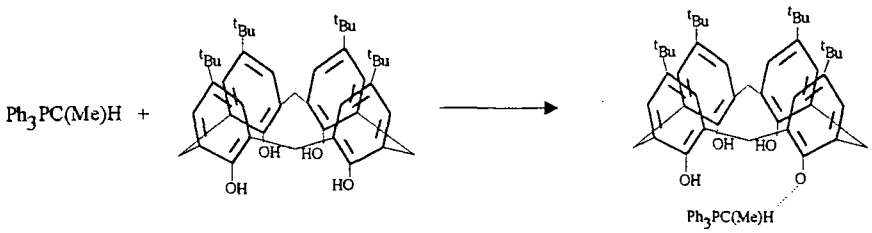

(2) (22)

Dry acetonitrile (15 mL) was added under nitrogen to solid tert-butyl-calix[4]arene, (LH_4), (0.33 g, 0.5 mmol) and solid $Ph_3PC(Me)H$ (0.58 g, 2 mmol) in a Schlenk tube. On stirring a yellow precipitate in an orange solution was immediately obtained. On heating the precipitate dissolved resulting in a clear orange solution. Standing at room temperature yielded a crop of yellow crystals suitable for X-ray diffraction.

Yield: 0.2 g (36 %)

Melting point: 177.5 °C

^{1}H NMR spectrum: 200 MHz, solvent $CDCl_3$

δ (ppm)	Integral	Multiplicity	Assignment
1.2	36H	singlet	^{t}Bu of LH_3^-
1.5	3H	doublet of triplets	$Ph_3PC(\mathbf{Me})H_2$
3.2	4H	doublet	CH_2 of LH_3^-
3.8	2H	doublet of quartets	$Ph_3PC(Me)\mathbf{H_2}$
4.4	4H	doublet	CH_2 of LH_3^-
4.7	8H	singlet	ArH of LH_3^-
7.7 - 7.9	15H	multiplet	ArH
10.2	3H	singlet	OH of LH_3^-

^{31}P NMR spectrum: 101.2 MHz, solvent $CDCl_3$

δ (ppm)	Multiplicity	Assignment
26.4	singlet	$Ph_3PC(Me)H_2$

Elemental Analysis: $C_{64}H_{75}PO_4$

	C	H	P	O
Calculated % by mass	87.8	8.6	3.5	7.3
Observed % by mass	81.1	7.9	-	-

3.4.8 Formation of (23)

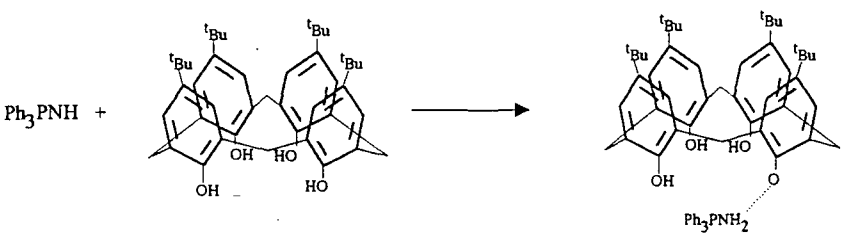

(4) (23)

Dry acetonitrile (15 mL) was added under nitrogen to solid tert-butyl-calix[4]arene, (LH_4), (0.33 g, 0.5 mmol) and solid Ph_3PNH (0.56 g, 2 mmol) in a Schlenk tube. On stirring a white precipitate in a pale yellow solution was immediately obtained. On heating and the addition of dry toluene (3 mL) the precipitate dissolved resulting in a clear pale yellow solution. Standing at room temperature yielded a crop of pale yellow needle like crystals suitable for X-ray diffraction.

Yield: 0.3 g (69 %)

Melting point: 167.2 °C

^{1}H NMR spectrum: 200 MHz, solvent C_6D_6

δ (ppm)	Integral	Multiplicity	Assignment[i]
1.3	36H	singlet	^{t}Bu of LH_3^-
3.3	4H	doublet	CH_2 of LH_3^-
4.6	4H	doublet	CH_2 of LH_3^-
6.8 - 7.0	9H	multiplet	m,p-ArH of Ph_3PNH_2
7.1	8H	singlet	ArH of LH_3^-
7.4 - 7.5	6H	multiplet	o-ArH of Ph_3PNH_2
10.2	3H	broad singlet	OH of LH_3^-

i Ph_3PNH_2 not observed

^{31}P NMR spectrum: 101.2 MHz, solvent C_6D_6

δ (ppm)	Multiplicity	Assignment
31.5	singlet	$Ph_3\mathbf{P}NH_2$

Elemental Analysis: $C_{62}H_{72}NPO_4.2CH_3CN$

	C	H	N	P	O
Calculated % by mass	78.7	7.8	4.1	3.1	6.4
Observed % by mass	76.9	7.4	4.2	-	-

IR Spectra:

In the spectra of compounds (16) to (23) a peak due to P-C (≈ 880 cm^{-1}) was present except for the spectra of compounds (17) and (23) in which a peak due to P-N (≈ 1190 cm^{-1}) was observed. Absorptions due to the acidic protons of the phenol derivatives were found to be absent in (16) and (18). After air exposure for 5 minutes broad OH stretches (≈ 3300 cm^{-1}) were observed for all products indicating they are all hygroscopic.

3.5 Synthesis and characterisation of complexes (24) to (27)

3.5.1 Formation of (24)

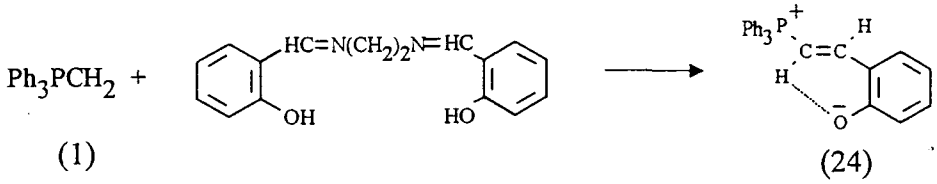

(1) (24)

Dry toluene (25 mL) was added under nitrogen to solid H_2salen (2.0 g, 7.5 mmol) and solid Ph_3PCH_2 (2.1 g, 7.5 mmol) in a Schlenk tube. Heating this solution (to about 60 °C) resulted in the formation of a yellow precipitate which on further warming gave a red solution with an immiscible orange oil. After stirring for half an hour at room temperature, addition of dry acetonitrile (14 mL), followed by gentle warming, caused complete dissolution of the oil into a red solution. This solution on standing at room temperature for 24 hours yielded a crop of orange X-ray quality crystals.

Yield: 2.4 g (66 %)

Melting point: 230.5 °C

^{1}H NMR spectrum: 400 MHz, solvent $CDCl_3$

δ (ppm)	Integral	Multiplicity	Assignment
2.3	3H	singlet	toluene
6.1	1H	triplet	ArH
6.7	1H	doublet	ArH
6.8	1H	doublet	ArH
7.0-7.7	22H	multiplet	ArH and P-CH=C**H**-C
8.7	1H	doublet of doublets	P-C**H**=CH-C

^{31}P NMR spectrum: 101.2 MHz, solvent $CDCl_3$

δ (ppm)	Multiplicity	Assignment
20.9	singlet	**P**-CH=CH-C

^{1}H{^{31}P} NMR spectrum: 400 MHz, solvent $CDCl_3$

δ (ppm)	Integral	Multiplicity	Assignment
2.3	3H	singlet	toluene
6.1	1H	triplet	ArH
6.7	1H	doublet	ArH
6.8	1H	doublet	ArH
7.0-7.7	22H	multiplet	ArH and
		(signals lost in multiplet)	P-CH=C**H**-C
8.7	1H	doublet	P-C**H**=CH-C

COSY; See Figure 3.1

Elemental Analysis: $C_{26}H_{21}OP.C_7H_8$

	C	H	P	O
Calculated % by mass	83.9	6.2	6.6	3.4
Observed % by mass	83.2	6.2	6.6	-

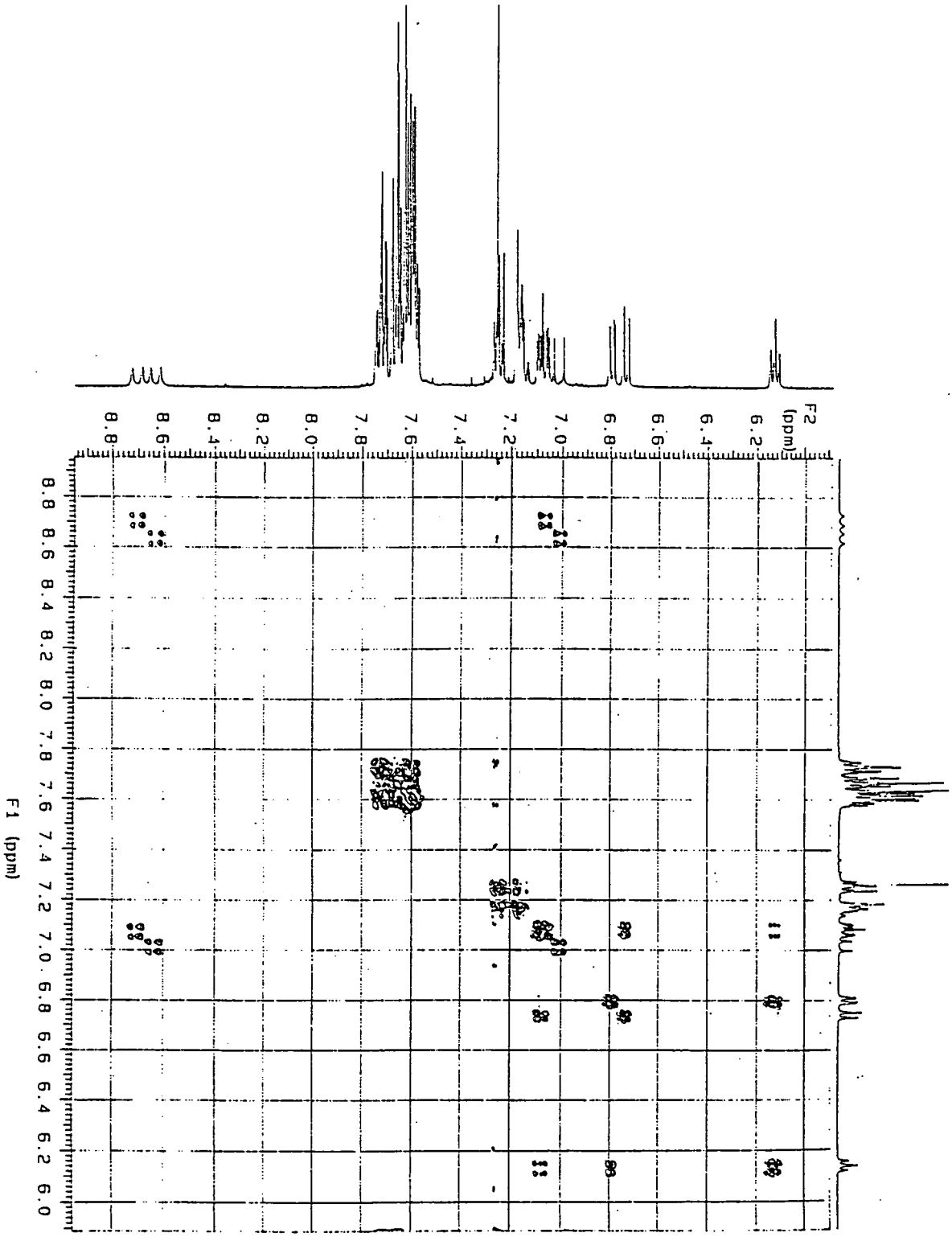

Figure 3.1 COSY spectrum of (24)

3.5.2 Formation of (25)

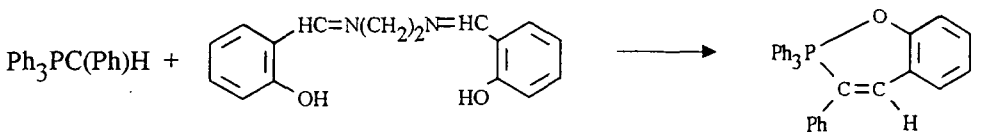

Dry toluene (10 mL) was added under nitrogen to solid (H_2salen) (0.67 g, 2.5 mmol) and solid $Ph_3PC(Ph)H$ (0.88 g, 2.5 mmol) in a Schlenk tube. Heating this solution resulted in the formation of an orange precipitate which on further warming gave a clear red solution. On cooling to room temperature an immiscible red oil formed. After stirring for half an hour at room temperature, addition of dry acetonitrile (2 mL), followed by gentle warming, caused complete dissolution of the oil into a red solution. This solution on standing at room temperature for 72 hours yielded a crop of orange X-ray quality crystals.

Yield: 0.4 g (34 %)

Melting point: 228-232 °C

^{1}H NMR spectrum: 200 MHz, solvent $CDCl_3$

δ (ppm)	Integral	Multiplicity	Assignment
2.1	-	singlet	toluene
6.7-7.6	23H	multiplet	ArH
8.2	1H	doublet	P-C(Ph)=C**H**-C

^{31}P NMR spectrum: 101.2 MHz, solvent $CDCl_3$

δ (ppm)	Multiplicity	Assignment
-51.9	singlet	**P**-C(Ph)=CH-C

Elemental Analysis: $C_{32}H_{25}PO$

	C	H	P	O
Calculated % by mass	84.2	5.5	6.8	3.5
Observed % by mass	83.5	5.6	6.6	-

3.5.3 Formation of (26)

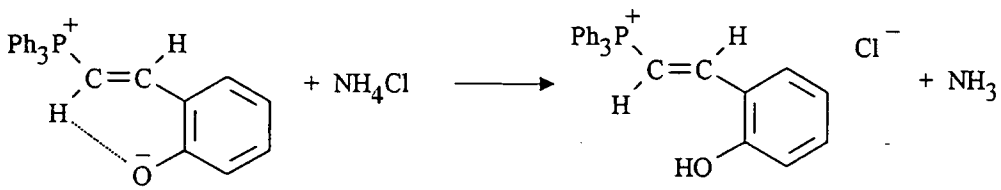

Dry acetonitrile (100 mL) was added under nitrogen to solid $Ph_3PC(H)=CH(C_6H_4O^-)$ (2.36 g, 5 mmol) and solid NH_4Cl (0.27 g, 5 mmol) in a two-necked round-bottom flask. On stirring for half an hour a yellow precipitate in an orange solution was obtained. On heating (to about 90 °C) for 12 hours the precipitate dissolved resulting in a clear orange solution. Standing at room temperature yielded a crop of yellow crystals suitable for X-ray diffraction.

Yield: 1.5 g (69 %)

Melting point: 258.9 °C

^{1}H NMR spectrum: 200 MHz, solvent C_6D_6

δ (ppm)	Integral	Multiplicity	Assignment
6.6 - 6.7	1H	triplet	P-C**H**=CH-C
7.1 - 7.8	20H	multiplet	ArH and P-CH=C**H**-C
11.5	1H	singlet	OH

^{31}P NMR spectrum: 101.2 MHz, solvent C_6D_6

δ (ppm)	Multiplicity	Assignment
20.6	singlet	Ph_3**P**C(H)=

Elemental Analysis: $C_{26}H_{22}POCl$

	C	H	P	O	Cl
Calculated % by mass	74.9	5.3	7.4	3.8	8.5
Observed % by mass	74.5	5.3	-	-	-

3.5.4 Formation of (27)

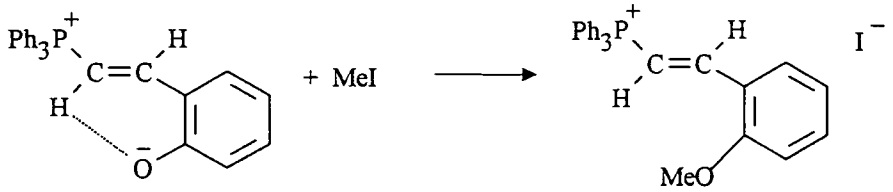

Dry acetonitrile (15 mL) was added under nitrogen to solid $Ph_3PC(H)=CH(C_6H_4O^-)$ (1.18 g, 2.5 mmol) in a Schlenk tube to give a clear orange solution. Methyl iodide (0.16 mL, 2.5 mmol) was added dropwise to give a clear yellow solution. On standing at -30 °C a pale yellow solid was obtained.

Yield: 0.5 g (35 %)

Melting point: 136.8 °C

^{1}H NMR spectrum: 200 MHz, solvent C_6D_6

δ (ppm)	Integral	Multiplicity	Assignment
1.9	-	singlet	C**H**$_3$CN
3.8	3H	singlet	MeO
7.0 - 8.1	21H	multiplet	ArH and P-C**H**=C**H**-C

^{31}P NMR spectrum: 101.2 MHz, solvent C_6D_6

δ (ppm)	Multiplicity	Assignment
21.5	singlet	Ph$_3$**P**C(H)=

Elemental Analysis: $C_{27}H_{25}POI$

	C	H	P	O	I
Calculated % by mass	62.0	4.8	5.9	3.1	24.3
Observed % by mass	61.5	4.9	-	-	-

Chapter 4

4. DISCUSSION - SIMPLE PHOSPHONIUM ARYLOXIDES

As discussed in the introduction of this thesis (Section 1.4), the role of 'strong' X-H...Y hydrogen bonding (e.g. where X and Y = N or O) in the structure, physical properties and reactivity of organic compounds has been well established.[1] However, it is increasingly apparent that weaker C-H...X interactions can also have a significant influence over the structure of solids.[2, 3, 4] Consequently, considerable interest is now focused on their study. Such C-H...X interactions, where X = O or N are the most commonplace, though it has been shown that carbon based π - bonded systems, such as alkynes[3, 4, 5] and arenes,[6] can also function as acceptors to acidic C-H groups. Amongst compounds able to participate in strong C-H...X hydrogen bonding, and those that have been most extensively studied are X_3CH (where X = Cl, NO_2, etc.)[7] and R-C≡C-H.[8] However, other systems containing acidic C-H groups have also been shown to participate in structurally significant C-H...X interactions.[9] As Steiner recently highlighted,[8] one such class of compounds where investigation has, up to now, been limited, is Group 15 'onium' cations.

---

[1]C. B. Aakeroy and K. R. Seddon, *Chem. Soc. Rev.*, 1993, 397; G. R. Desiraju, *Angew. Chem. Int. Ed. Eng.*, 1995, **34**, 2328, and references cited therein.
[2]G. R. Desiraju, *Acc. Chem. Res.*, 1991, **24**, 290, and references cited therein.
[3]F. H. Allen, J. A. K. Howard, V. J. Hoy, G. R. Desiraju, D. S. Reddy and C. C. Wilson, *J. Am. Chem. Soc.*, 1996, **118**, 4081.
[4]G. R. Desiraju, *Chem. Commun.*, 1997, 1475, and references cited therein.
[5]T. Steiner, *J. Chem. Soc., Chem. commun.*, 1995, 95.
[6]R. Hunter, R. H. Haneisen and A. Irving, *Angew. Chem. Int. Ed. Engl.*, 1994, **33**, 566; C. A. Hunter, *Chem. Soc. Rev.*, 1994, 101.
[7]V. R. Pedireddi and G. R. Desiraju, *J. Chem. Soc., Chemm Commun.*, 1992, 988; G. R. Desiraju, *ibid.*, 1990, 454; G. R. Desiraju, *ibid.*, 1989, 179.
[8]T. Steiner, *Chem. Commun.*, 1997, 727.
[9]M. G. Davidson, T. G. Hibbert, J. A. K. Howard, A. Mackinnon and K. Wade, *Chem. Commun.*, 1996, 2285.

This chapter will discuss our recent results in this field concerning the protonation of triphenylphosphonium alkylides with OH - monoacidic organic compounds and will reveal a facile and versatile route to hydrocarbon soluble, crystalline phosphonium aryloxides. In these salts, the absence of strong hydrogen bond donors, coupled with a profusion of potential C-H donor groups and the availability of electron rich acceptor anions, provides an ideal platform for the study of C-H...X interactions. This includes discussion relating to the synthesis and characterisation of complexes (5) to (10) in the preceding chapter. X-ray crystal structures were obtained for all these complexes and further characterisation by single crystal neutron diffraction was carried out for complexes (7) and (10).

It was the synthesis and structural characterisation of the first ever reported phosphonium aryloxide $[(Ph_3PMe)^+(OC_6H_2Me_3\text{-}2,4,6)^-]_2$,[10] (A), which initiated our interest in such systems. It was formed via the deprotonation of mesitol (2,4,6-trimethylphenol) with triphenylphosphonium methylide (1) and was shown by X-ray crystallography to be a discrete dimeric structure aggregated solely through C-H...O hydrogen bonds involving both the alkyl and aryl donors within the phosphonium cations (Figure 4.1). The resulting central motif was an eight membered $(O...H\text{-}C\text{-}H...)_2$ ring in which the methyl group of each cation bridges the two anions through two of its three hydrogen atoms and each oxygen is clamped between two *ortho*-hydrogen atoms of phenyl groups thereby providing each oxygen atom with four hydrogen bonds. All four C-H...O hydrogen bonds (average C...O distance, C-H...O angle, 3.275 Å and 167 °) were shown to be well within the accepted criteria of distance and angle used to define the existence of an electrostatic C-H...O interaction.[2, 11] Further evidence that these were indeed hydrogen bonds came from the orientation of the hydrogen bond donor groups which, although free to rotate, were all ideally aligned to participate in hydrogen bonding.

Having observed the unusual mode of aggregation in (A) further investigation was undertaken and the effect of a methyl group on the ylidic carbon was studied by reacting triphenylphosphonium ethylide (2) with mesitol. The resulting phosphonium aryloxide,

---

[10] M. G. Davidson, *J. Chem. Soc., Chem. Commun.*, 1995, 919.
[11] R. Taylor and O. Kennard, *J. Am. Chem. Soc.*, 1982, **104**, 5063.

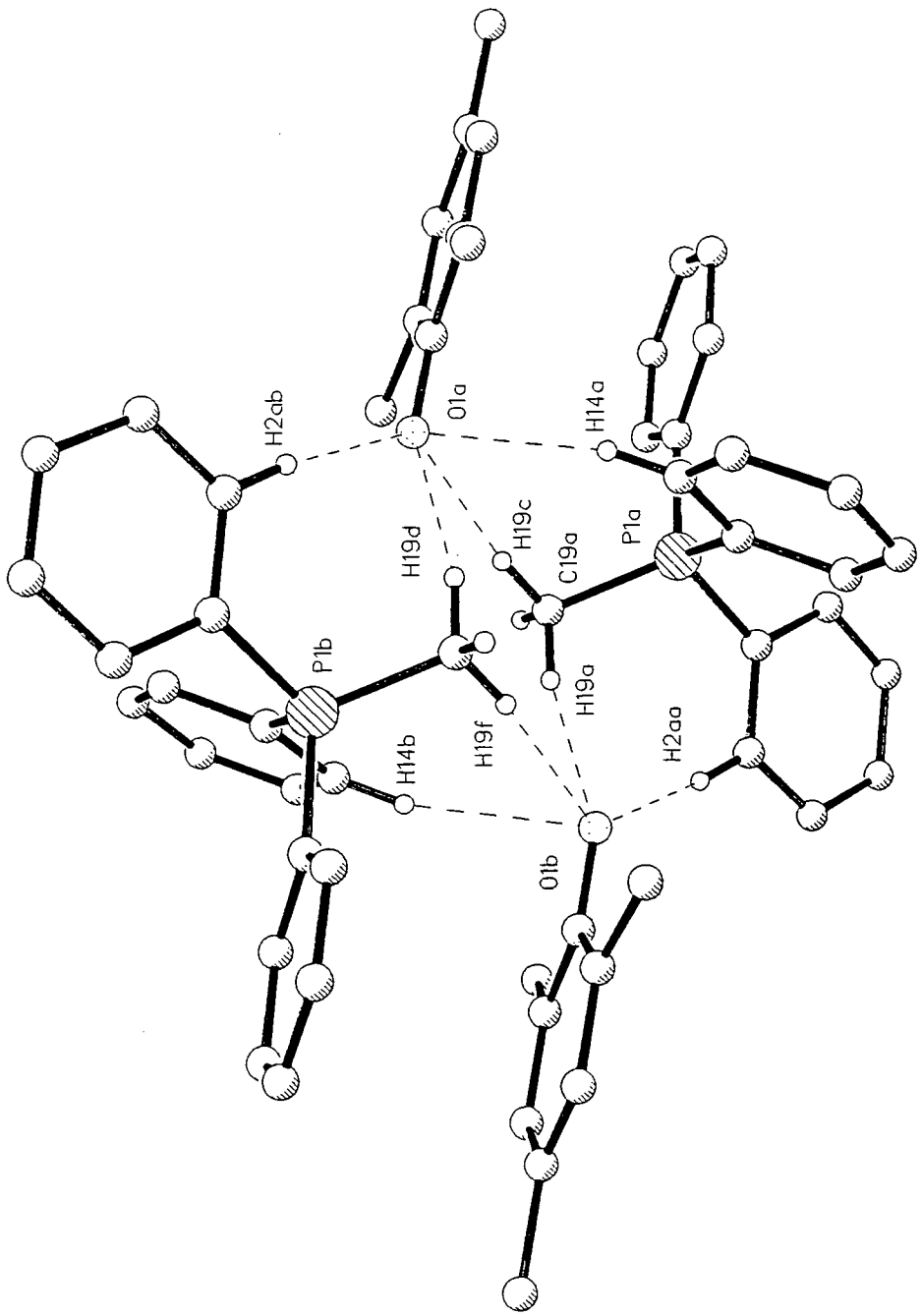

Figure 4.1. The molecular structure of $[(Ph_3PMe)^+(OC_6H_2Me_3\text{-}2,4,6)^-]_2$, (A). All aryl hydrogen atoms except those involved in C-H...O hydrogen bonding have been omitted for clarity.

$[(Ph_3PEt)^+(OC_6H_2Me_3\text{-}2,4,6)^-]_2$, (B), (Figure 4.2), was also found to have a dimeric structure which was again aggregated via C-H...O hydrogen bonds with the motif of chelating C(alkyl)-H and C(aryl)-H donors apparent. As in (A) there was a central motif of an eight membered $(O...H\text{-}C\text{-}H...)_2$ ring. Although the structures of (A) and (B) were similar, subtle differences were apparent. For example, unlike (A) each oxygen was found to be only trifurcated as only one C(aryl)-H donor interacts with the anion. Another noticable difference was that unlike (A) where the phosphonium cations were trans to one another here they were cis to one another (Scheme 4.1). It was these subtle changes in supramolecular structure that led us to investigate further.

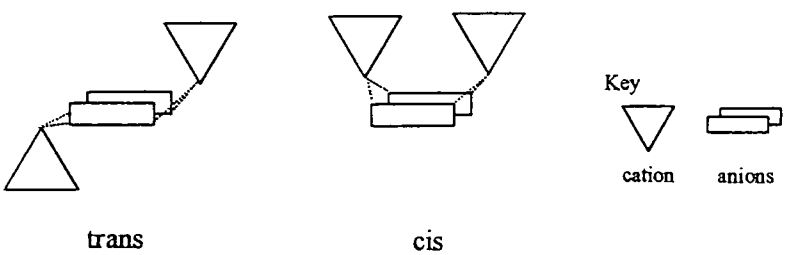

Scheme 4.1 Schematic to illustrate the position of the cations in the trans and cis configurations

In so doing, a series of phosphonium aryloxide salts were synthesised from a wide range of commercially available phenol derivatives of the general formula $2,4,6\text{-}R\text{-}C_6H_2OH$, where the R groups were any combination of H, Me, Ph or ^{t}Bu. The resulting compounds (5) - (10) will be discussed (Table 4.1).

Deprotonation of phenol with triphenylphosphonium methylide (1), yielded a yellow crystalline solid. As expected preliminary characterisation indicated the formation of the phosphonium aryloxide salt $[(Ph_3PMe)^+(OC_6H_5)^-]_n$ (5), effected by the transferral of the acidic proton from the phenol to the basic carbon atom of the ylide. This was confirmed by X-ray crystallography which revealed all bond lengths and angles within the cations and anions were normal.

As observed for (A) and (B), (5) is aggregated via C-H...O hydrogen bonds and the structural motif of C(alkyl)-H...O and C(aryl)-H...O hydrogen bonds chelating the oxygen centre of the anion is present. These being favoured by the profusion of acidic (C-)H

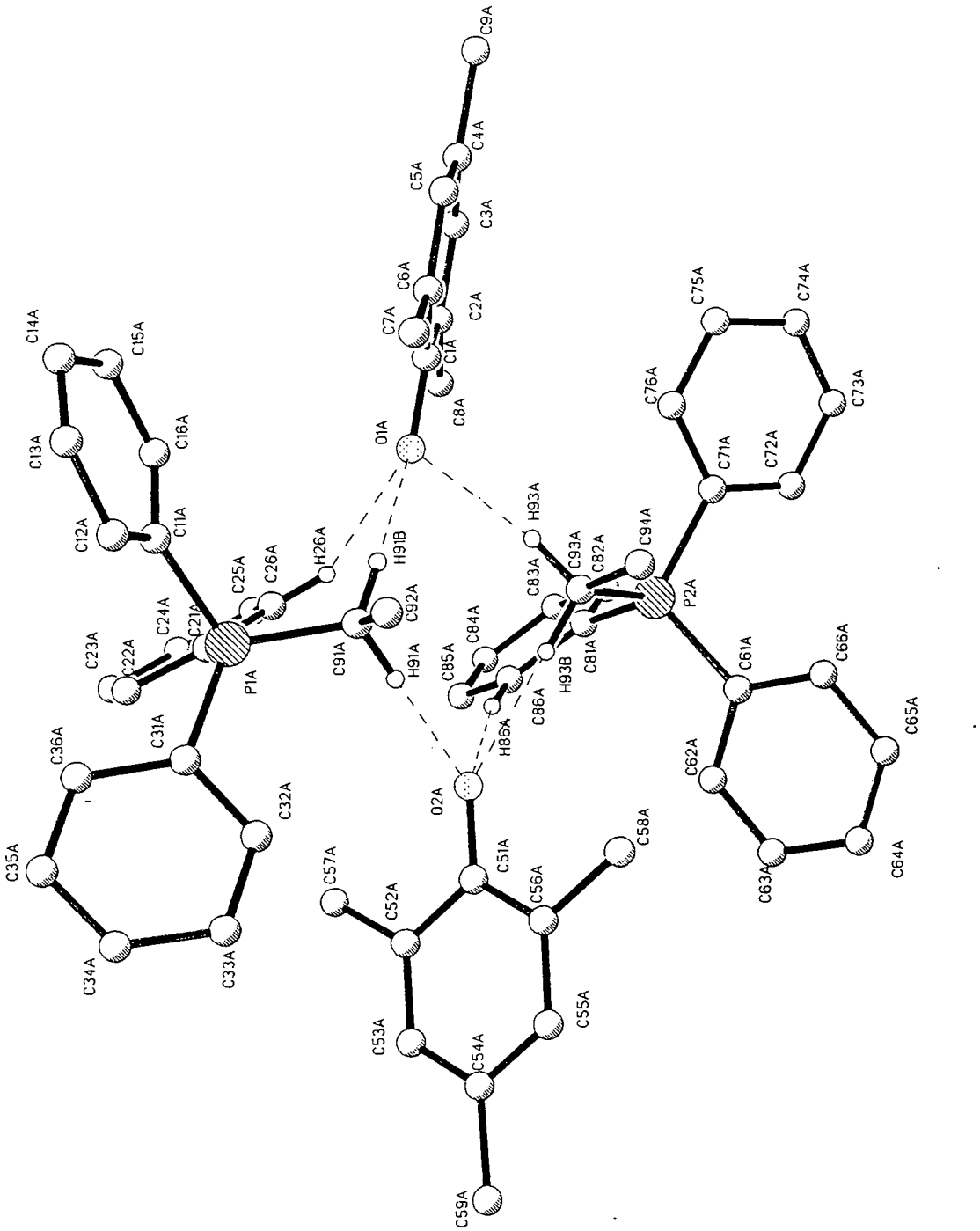

Figure 4.2. The molecular structure of $[(Ph_3PEt)^+(OC_6H_2Me_3\text{-}2,4,6)^-]_2$, (B). All hydrogen atoms except those involved in C-H...O hydrogen bonding have been omitted for clarity.

Table 4.1 Summary of compounds (5) - (10) together with (A) and (B) for comparison.

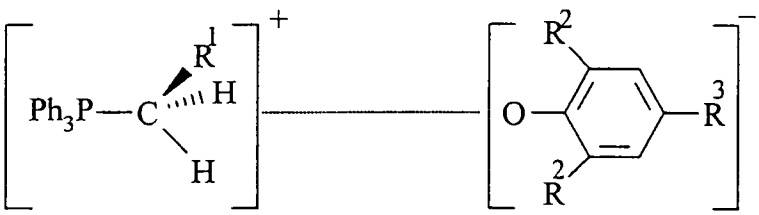

	R^1	R^2	R^3	Structure
(A)	H	Me	Me	tetrafurcated dimer
(B)	Me	Me	Me	trifurcated dimer
(5)	H	H	H	pentafurcated polymer
(6)	Me	H	H	tetrafurcated polymer
(7)	H	Ph	H	trifurcated dimer
(8)	Me	Ph	H	trifurcated dimer
(9)	H	^{t}Bu	Me	bifurcated monomer
(10)	Me	^{t}Bu	Me	bifurcated monomer + thf

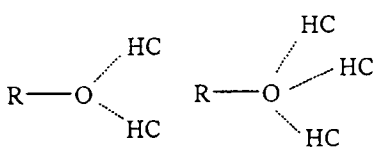

bifurcated trifurcated etc

atoms which are good hydrogen bond donors in the presence of highly anionic oxygen atoms which are excellent hydrogen bond acceptors. All hydrogen bond parameters for (5) are shown in Table 4.2.

Table 4.2 Hydrogen bond parameters for (5).

Interaction	C...O distance (Å)	H...O distance (Å)	C-H...O angle (°)
C7AB-H7BD...O1AB	3.222	2.165	165.7
C7AB-H7CD...O1B	3.446	2.469	149.8
C22J-H22J...O1B	3.392	2.324	169.8
C16J-H16J...O1AB	3.305	2.227	175.2
C24I-H24I...O1AB	3.368	2.374	152.3

The asymmetric unit consists of two crystallographically independent monomeric (Ph_3PCH_3...OR) units which contain different bond lengths and angles but are chemically identical. As seen before dimeric $(Ph_3PCH_3...OR)_2$ units are observed, however, due to the two crystallographically independent monomers two distinct dimeric units are observed, both with the cations in a trans configuration (Figure 4.3a).

In both dimeric units the central motif is again an $(O...H\text{-}C\text{-}H...)_2$ eight membered ring with the methyl group of each cation bridging the two anions through two of its three hydrogen atoms. In addition, two *ortho*-hydrogen atoms of phenyl groups belonging to different cations interact with each oxygen atom (Table 4.2). Unlike (A) and (B) these dimeric units are further aggregated with each oxygen atom being further chelated by an *ortho*- phenyl hydrogen atom of a cation from a neighbouring dimeric unit (Table 4.2). This results in a polymeric structure in which each oxygen atom is pentafurcated (Figure 4.3b). All of the five C-H...O hydrogen bonds lie within the accepted criteria for distance and angle.

The increase in both the number of hydrogen bonds to each oxygen atom and the more extensive aggregation compared to (A) and (B) can be attributed to the reduction in steric bulk of the anion. It no longer has the bulkier Me groups in the *ortho* and *para* positions to block further aggregation.

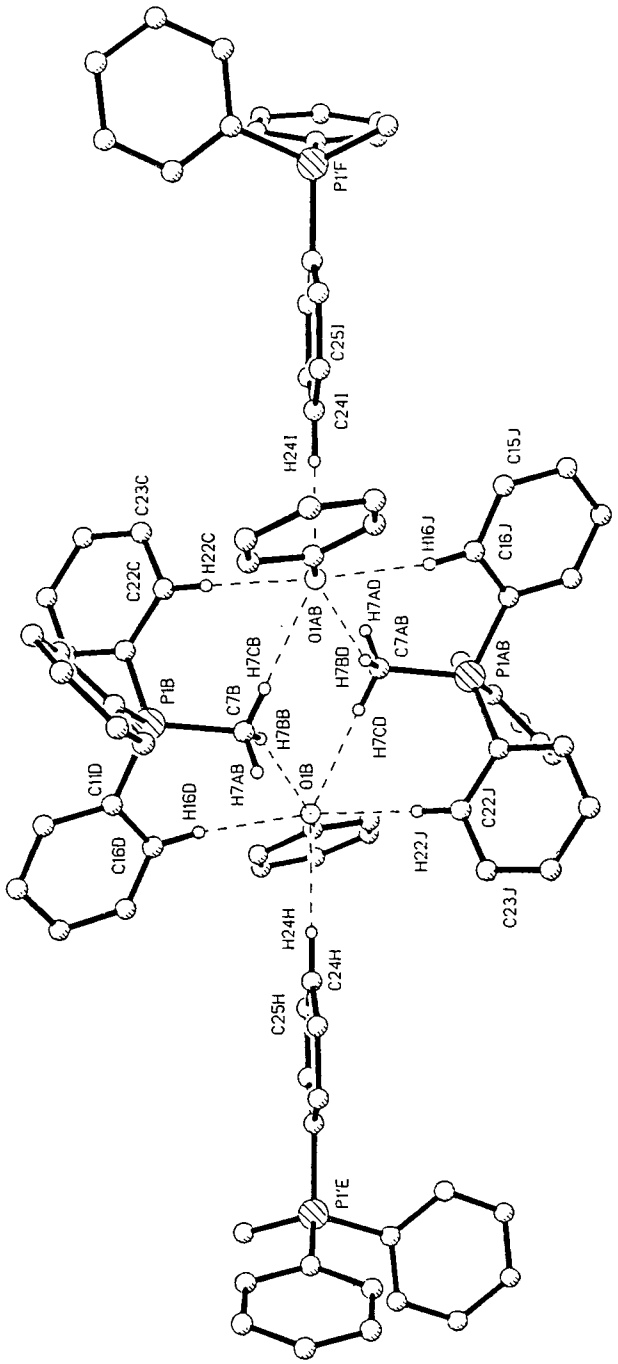

Figure 4.3a. The dimeric unit of $[(Ph_3PMe)^+(OC_6H_5)^-]_n$, (5), (only one of two geometrically similar dimers is shown) also showing further aggregation to other dimeric units. All aryl hydrogen atoms except those involved in C-H...O hydrogen bonding have been omitted for clarity.

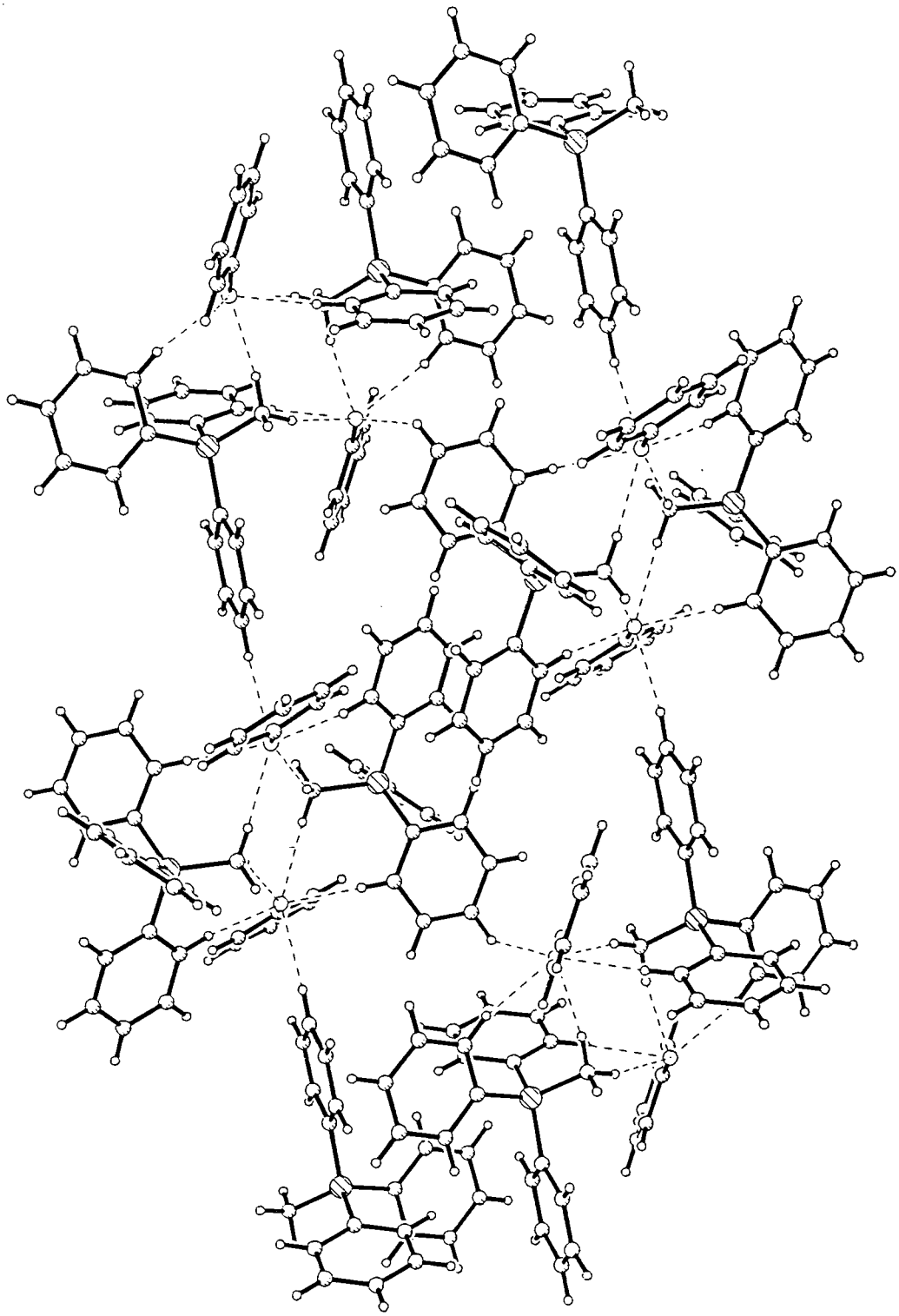

Figure 4.3b. The polymeric structure of $[(Ph_3PMe)^+(OC_6H_5)^-]_n$, (5).

Synthesis of the yellow crystalline solid $[(Ph_3PEt)^+(OC_6H_5)^-]_n$, (6), was achieved by reaction of triphenylphosphonium ethylide (2) with phenol in a dry acetonitrile solution. Initial analysis provided evidence for the formation of the expected phosphonium salt (6) via the transfer of the acidic phenolic proton to the basic ylidic carbon atom and this was confirmed by X-ray crystallography.

The geometry of the cations and anions is normal, but again it is the mode of aggregation which is of interest. As observed previously, on the supramolecular level this structure is aggregated via C-H...O hydrogen bonds. It too exhibits the structural motif of C(alkyl)-H...O and C(aryl)-H...O hydrogen bonds. All hydrogen bond parameters are shown in Table 4.3. Dimeric units are observed in which the cations are trans to one another (Figure 4.4).

Table 4.3 Hydrogen bond parameters for (6).

Interaction	C...O distance (Å)	H...O distance (Å)	C-H...O angle (°)
C7C-H71C...OOB	3.163	2.094	169.9
C7C-H72C...OOC	3.254	2.194	166.7
C34A-H34A...OOC	3.383	2.329	164.8
C36C-H36C...OOB	3.322	2.253	170.1

The central motif is an $(O...H\text{-}C\text{-}H...)_2$ eight membered ring in which the CH_2 groups of the cations bridge the anions through both of their hydrogen atoms. However, in this case, unlike (5), only one *ortho*-hydrogen atom of a phenyl group of each cation is interacting with the oxygen atoms. This may be attributed to the increased steric requirement of the ethyl group on the ylidic carbon atom resulting in the other two phenyl rings of the cation not already involved in C(aryl)-H...O hydrogen bonding being in unfavourable orientations for interaction with the anion. As for (5) these dimeric units are further associated via *ortho*-hydrogen atoms of phenyl groups belonging to cations of neighbouring dimeric units (Table 4.3). This again results in a polymeric structure but here the oxygen atoms are only tetrafurcated. It is interesting to note that in the case of (5) and (6) no switch from a trans to a cis configuration, as was seen on going from (A) and (B), is observed.

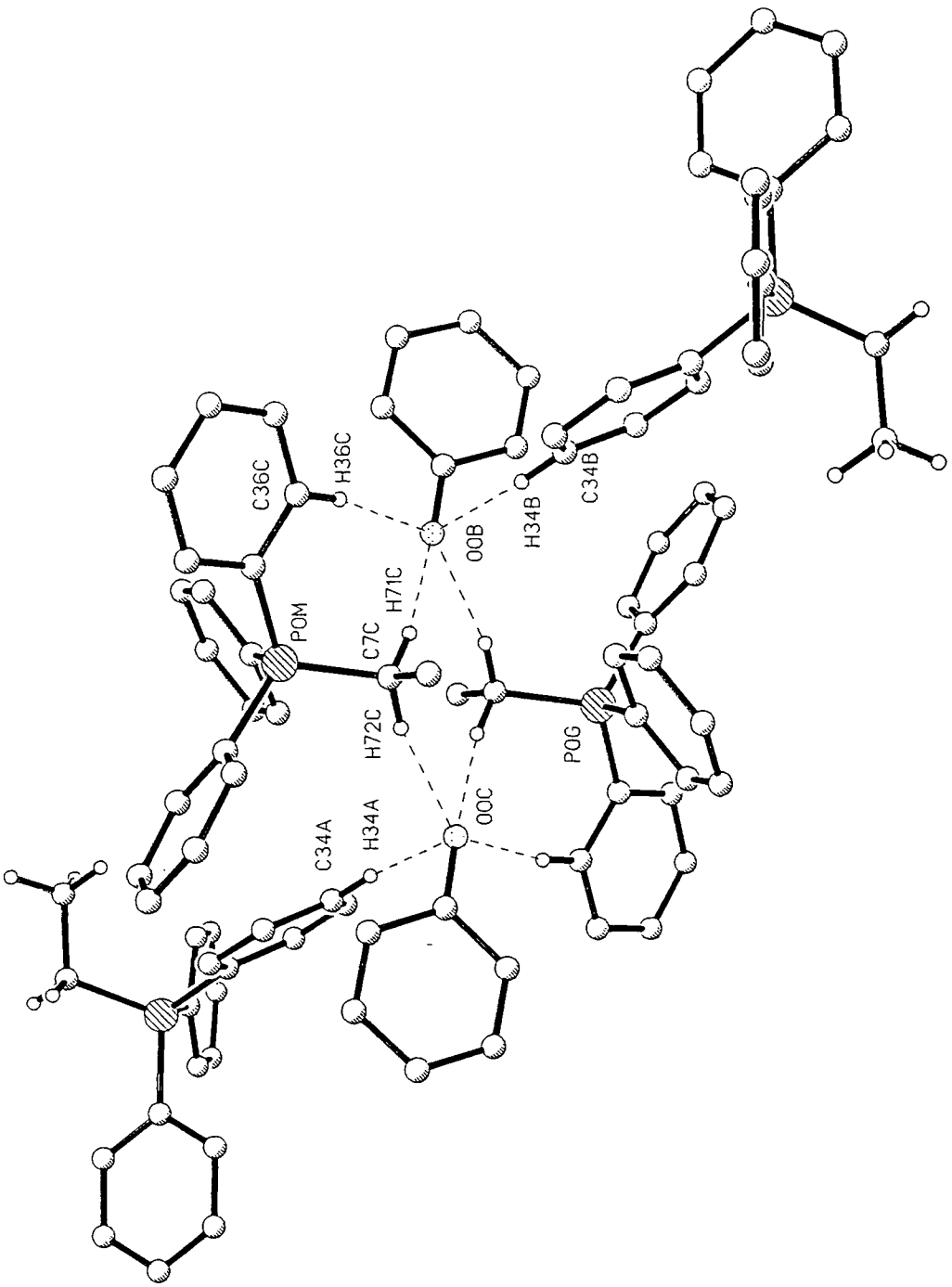

Figure 4.4 The dimeric units of $[(Ph_3PEt)^+(OC_6H_5)^-]_n$, (6), showing further aggregation from neighbouring dimers. All hydrogen atoms of the dimeric unit except those involved in C-H...O hydrogen bonding have been omitted.

Having observed the enhanced aggregation resulting from a decrease in the steric bulk of the phenol derivative, it was felt prudent to investigate how an increase in steric bulk would affect the bonding observed. An obvious starting point was to study the effect of phenyl substituents on the phenol. 2,6-diphenylphenol was used for this purpose and phosphonium salts were obtained via its deprotonation by (1) and (2).

Deprotonation of 2,6-diphenylphenol with (1) in a dry toluene:acetonitrile solution yielded a yellow crystalline solid. Preliminary characterisation indicated the expected formation of the phosphonium aryloxide salt $[(Ph_3PMe)^+(OC_6H_3Ph_2\text{-}2,6)^-]_2$ (7), (Figure 4.5). The solid-state structure of (7) was initially determined by an X-ray study, however, these crystals were of a suitable size for single crystal neutron diffraction (Section 2.8). Single crystal neutron diffraction has the advantage over single crystal X-ray diffraction in that it can precisely locate the positions of the hydrogen atoms and hence has obvious significance in the study of C-H...O hydrogen bonding. Therefore, the solid-state structure of (7) was subsequently characterised by low temperature (20 K) neutron diffraction (it is the bond lengths and angles from these neutron diffraction data that will be quoted here). The molecular geometries of both cation and anion are as expected. On the supramolecular level (7) adopts the by now familiar C-H...O hydrogen bonded dimeric structural motif. All hydrogen bond parameters are shown in Table 4.4.

Table 4.4 Hydrogen bond parameters for (7).

Interaction	C-H distance (Å)	H...O distance (Å)	C-H...O angle (°)
C21-H21a...O21a	1.102(4)	2.119(4)	157.8(4)
C21-H21b...O21	1.105(5)	1.935(5)	166.9(4)
C246-H24e...O21	1.095(5)	2.118(5)	174.0(4)
C11-H11b...O11^{i}	1.098(5)	2.033(5)	161.4(4)
C11-H11a...O11a^{i}	1.100(5)	1.968(5)	167.7(4)
C142-H14a...O11a^{i}	1.090(4)	2.166(4)	168.2(4)

i - not shown in Figure 4.5

As observed for (5) two chemically similar but crystallographically independent centrosymmetric dimers are found in the crystallographic unit cell and only one of these will be discussed further. Within each dimer, the structural motif of C(alkyl)-H...O and

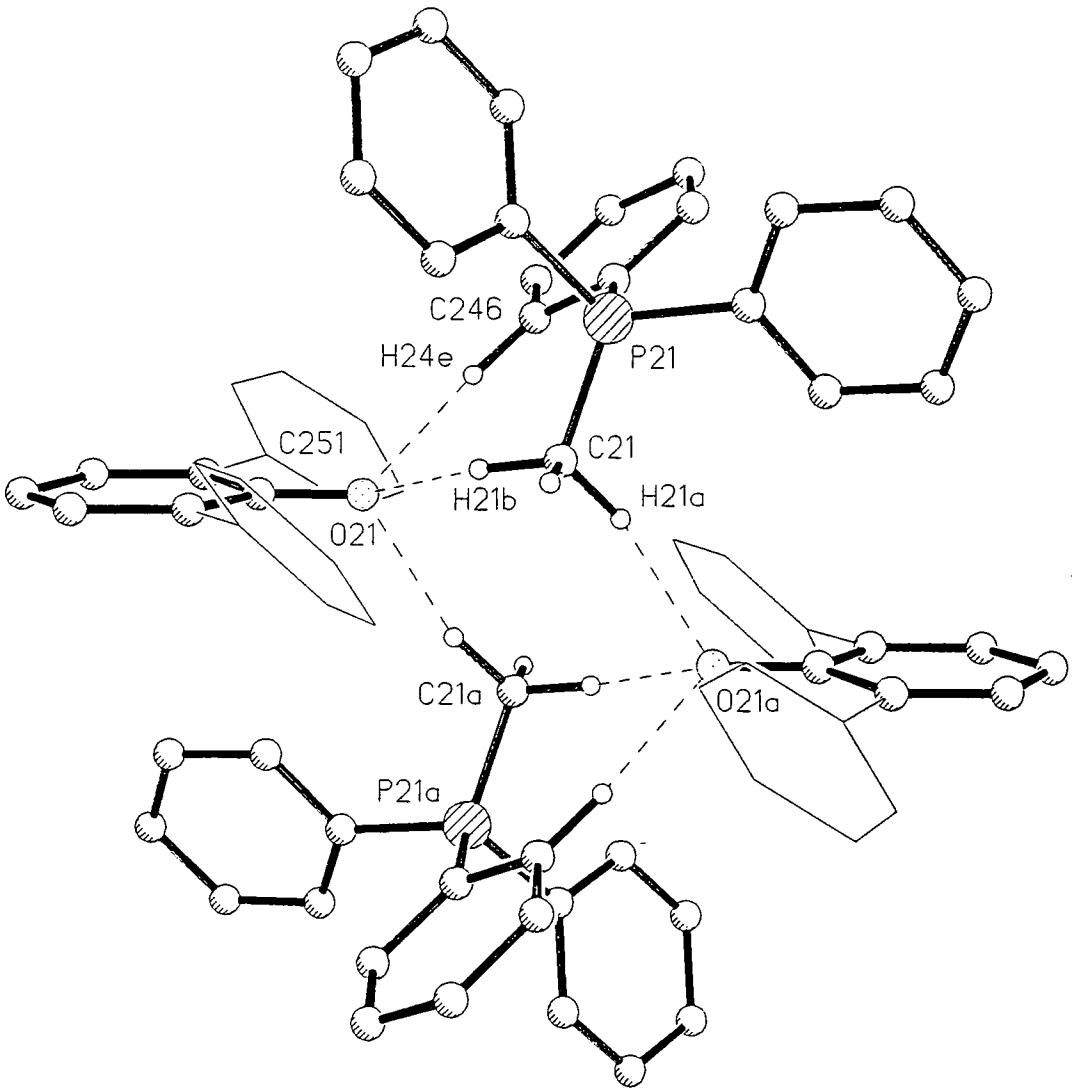

Figure 4.5. The molecular structure of $[(Ph_3PMe)^+(OC_6H_3Ph_2\text{-}2,6)^-]_2$, (7), (only one of the two geometrically similar dimers is shown). All aryl hydrogen atoms except those involved in C-H...O hydrogen bonding have been omitted, and the anion substituent groups shown in outline for clarity.

C(aryl)-H...O hydrogen bonds is observed. The methyl group of each cation interacts with the two anionic oxygen centres. This (...H-C-H...) bridge is slightly asymmetric. The tri-coordination of the oxygen atom is completed by interaction with one *ortho*-hydrogen from a phenyl group of the cation. The change from a tetrafurcated oxygen observed in (A) to a trifurcated oxygen in (7) presumably results from the differing steric requirements of the *ortho*-Me groups of (A) and the *ortho*-Ph groups of (7). Remarkable in (7) are the short H...O distances clustered around 2 Å (Table 4.4) which is at the lower limit for previously observed 'strong' C-H...O hydrogen bonds[8] and H21b...O21 [1.933(5) Å] is by some way the shortest C-H...O interaction yet characterised by neutron diffraction, being over 5% shorter than the shortest C-H...O hydrogen bond found in the Cambridge Structural Database (CSD) [in 1-methylthymine H...O = 2.045 Å].[12, 13] This emphasises the propensity of both 'onium' cations and aryloxide anions to participate in strong hydrogen bonding of this type.

Reaction of (2) and 2,6-diphenylphenol in a dry thf:acetonitrile solution resulted in the formation of a yellow crystalline solid. Characterisation, ultimately by X-ray diffraction, revealed the expected formation of the phosphonium salt $[(Ph_3PEt)^+(OC_6H_3Ph_2\text{-}2,6)^-]_2$ (8), again with the transfer of the phenolic proton to the ylidic carbon atom having occurred. Once again the same structural motifs are observed, (Figure 4.6). All hydrogen bond parameters are shown in Table 4.5.

Table 4.5 Hydrogen bond parameters for (8).

Interaction	C...O distance (Å)	H...O distance (Å)	C-H...O angle (°)
C1A-H1AA...O1B	3.191	2.211	149.58
C26A-H26A...O1B	3.170	2.095	173.3
C36A-H36A...O1A	3.111	2.327	128.0

However, the pattern of C-H...O hydrogen bonding observed in this structure is subtly different from that in the dimers previously studied. Here there is no central motif of an $(O...H\text{-}C\text{-}H...)_2$ eight membered ring as, although the oxygen atom is trifurcated, these

[12]F. H. Allen and O. Kennard, *Chem. Des. Autom. News*, 1993, **8**, 1.
[13]A. Kvick, T. F. Koetzle and R. Thomas, *J. Chem. Phys.*, 1974, **61**, 2711.

three hydrogen bonds do not consist of two alkyl and one aryl donors. Instead two aryl donors, that is, two *ortho*-hydrogens of phenyl groups, one from each cation, interact with the anion and only one of the cation's CH_2 protons is involved in a C(alkyl)-H...O hydrogen bond (Table 4.5). The second CH_2 proton is in a position unfavourable for interaction presumably as a result of the steric requirements of both the methyl group on the ylidic carbon and the *ortho*-phenyl substituents on the phenol. No further aggregation is observed. Yet again this illustrates how variation in the steric requirements of the cations and anions alters the structures observed. It should also be noted that an acetonitrile molecule is present in the lattice (one per monomer unit); however, it plays no obvious part in the stabilisation of the phosphonium salt and there appears to be no interaction between it and either the cation or anion.

In order to increase the steric demand of the anion still further the final two phosphonium aryloxides formed involved a phenol with bulky ^{t}Bu substituents in the *ortho*-positions, namely 2,6-di^{t}butyl-4-methylphenol.

Deprotonation of 2,6-di^{t}butyl-4-methylphenol by reaction with (1) in a dry thf solution resulted in the formation of a yellow, crystalline solid. X-ray crystallography revealed it to be the phosphonium salt $(Ph_3PMe)^+(OC_6H_2{}^tBu_2\text{-}2,6\text{-}Me\text{-}4)^-$.thf, (9). The cations and anions are of expected geometry and, as in all these salts, on the supramolecular level the anion and cation are held together by C-H...O hydrogen bonds with the same structural motif of C(alkyl)-H...O and C(aryl)-H...O hydrogen bonds being observed. All hydrogen bond parameters are shown in Table 4.6. However, in this case the resulting structure is that of a monomer (Figure 4.7). The oxygen atom of the anion is bifurcated with one alkyl donor from the methyl group of the cation and with one aryl donor, namely an *ortho*-hydrogen atom of one of the cation's phenyl groups (Table 4.6).

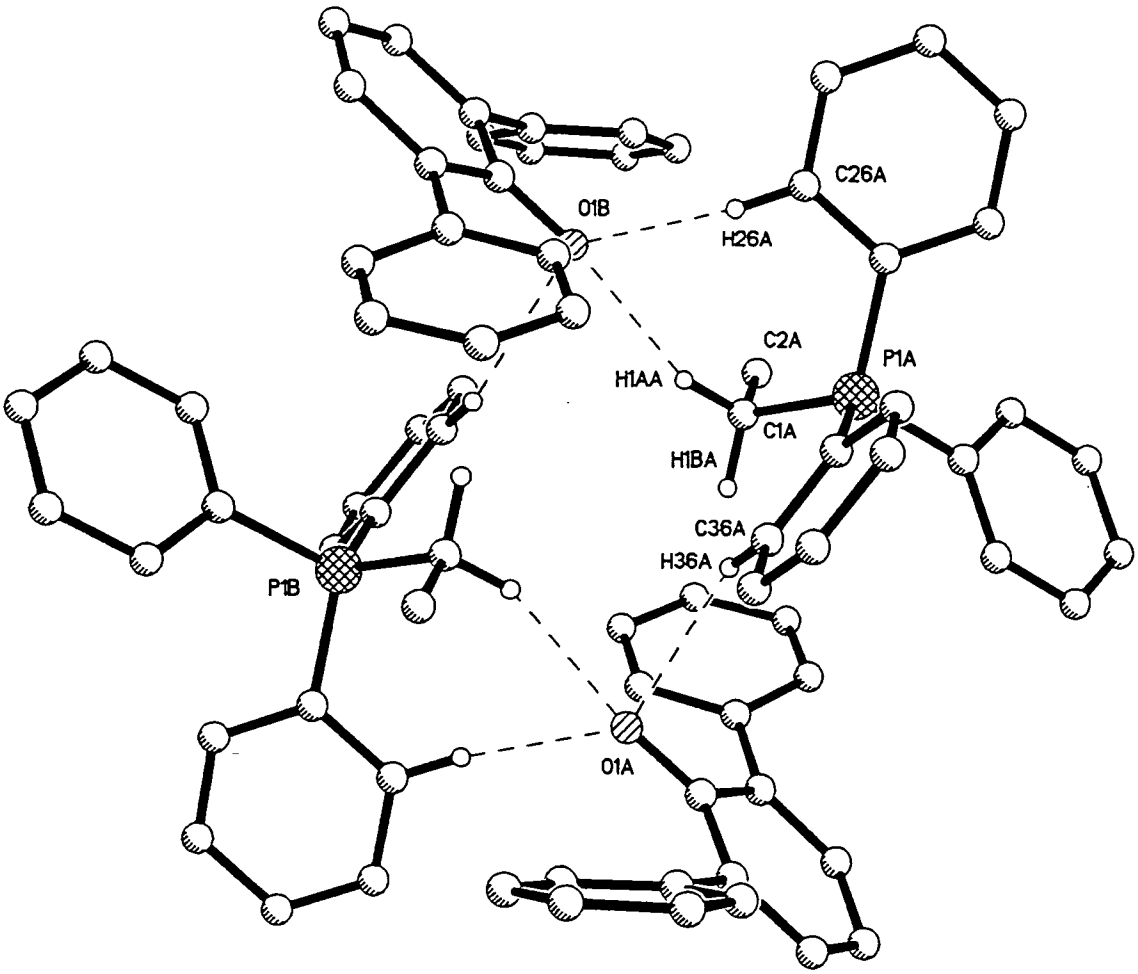

Figure 4.6. The molecular structure of $[(Ph_3PEt)^+(OC_6H_3Ph_2\text{-}2,6)^-]_2$, (8). All aryl hydrogen atoms except those involved in C-H...O hydrogen bonding have been omitted for clarity.

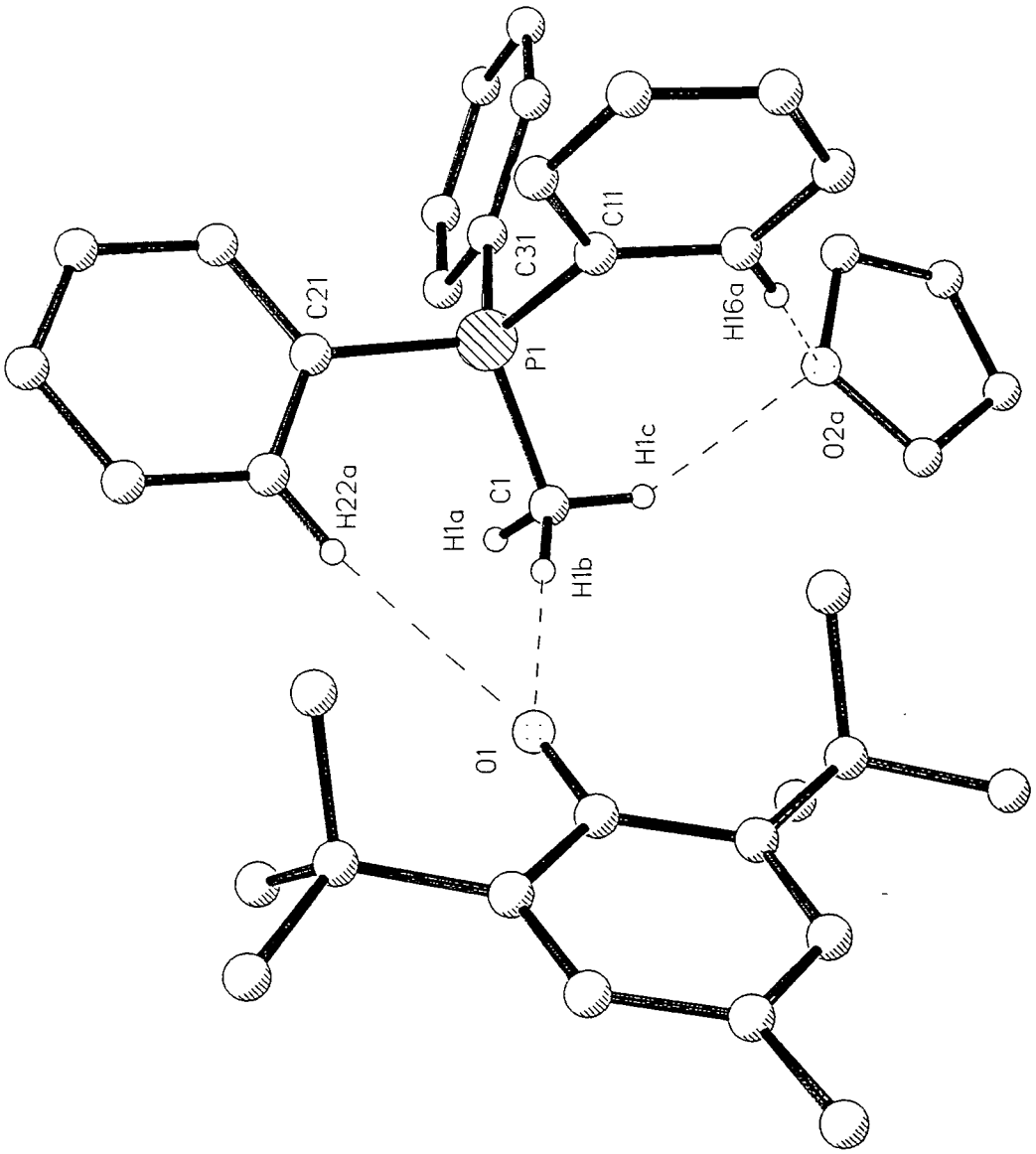

Figure 4.7. The molecular structure of $(Ph_3PMe)^+(OC_6H_2{}^tBu_2\text{-}2,6\text{-}Me\text{-}4)^-.thf$, (9), showing the incorporation of a thf molecule in the monomer. All thf, aryl and ^tBu hydrogen atoms except those involved in C-H...O hydrogen bonding have been omitted for clarity.

Table 4.6 Hydrogen parameters for (9).

Interaction	C...O distance (Å)	H...O distance (Å)	C-H...O angle (°)
C1-H1b...O1	3.252	2.173	178.7
C22-H22a...O1	3.495	2.427	169.8
C1-H1c...O2a	3.390	2.415	149.4
C16-H16a...O2a	3.215	2.1584	165.3

This decrease in the degree of aggregation is presumably attributable to the steric protection of the oxygen atom afforded by the ^{t}Bu groups. These seemingly prevent further C-H...O hydrogen bonding occurring between the phosphonium cation of one monomer and the aryloxide anion of another as occurs in the salts (5) - (8).

Although no dimers are observed each cation has a thf molecule associated with it and once more the structural motif of C(alkyl)-H and C(aryl)-H donors to the oxygen atom of the thf is observed, one being a hydrogen atom of the cation's methyl group, the other being an *ortho*-hydrogen atom of a phenyl group (Table 4.6).

A further feature of note is that if the solution is left for several days before isolation or indeed on isolation in a glove box, the yellow crystals rapidly change colour to green. ^{1}H NMR of the green crystals is similar to that obtained for the yellow crystals, however, one noticeable difference is the loss of the thf peaks suggesting desolvation occurs. Whether the desolvation and colour change are related is not known.

Reaction of (2) with 2,6-di^{t}butyl-4-methylphenol in a dry thf solution resulted in the formation of an orange crystalline solid. These crystals were of a suitable size for single crystal neutron diffraction (Section 2.8). Therefore, preliminary spectroscopic characterisations and collection of single crystal X-ray diffraction data was followed by a low temperature (20 K) neutron diffraction study. The product was found to be $[(Ph_3PEt)^{+}(OC_6H_2{}^{t}Bu_2\text{-}2,6\text{-}Me\text{-}4)^{-}]_n$ (10), as expected. As observed previously on the supramolecular level the principal mode of cation-anion association is C-H...O hydrogen bonding. All hydrogen bond parameters obtained by neutron diffraction are shown in Table 4.7.

Table 4.7 Hydrogen bond parameters for (10).

Interaction	C-H distance (Å)	H...X distance (Å)	C-H...X angle (°)
C1-H1a...O1	1.103(3)	2.271(3)	168.3(2)
C22-H22a...O1	1.092(3)	1.998(3)	179.3(3)
C13a-H13b...π	1.089(3)	2.419(3)[i]	145.0(3)[ii]
C32b-H32c...π	1.088(3)	2.341(3)[i]	144.2(3)[ii]
C33b-H33c...O1	1.088(3)	2.353(3)	160.0(3)

i perpendicular distance from the H atom to the plane of the ring (C41-C46)
ii angle between the C-H bond and the centroid of C41-C46

Once again the motif of short C(alkyl)-H...O and C(aryl)-H...O hydrogen bonds from the phosphonium cation to the oxygen atom of the anion is observed. However, in (10), unlike in (7), but similarly to (9), dimerisation of the monomeric units does not occur. Again, as in (9), this is presumably due to the protection afforded by the bulky ^{t}Bu groups of the anion (Figure 4.8a).

In spite of this steric hindrance, the electronic factors (i.e., acidic C-H groups and an electron rich anionic centre) which favour aggregation prevail and for (10) an alternative mode of aggregation operates. Longer range, out-of-plane C-H...π interactions take place between aryl C-H groups and an electron-rich π-system of both faces of the anion (Figure 4.8b). Adjacent *ortho-* and *meta-* C-H groups of one phosphonium cation interact with one face of the anion's π-system, including the coplanar p-orbital of the oxygen. The distances involved (Table 4.7) are at the lower end of the range seen for similar interactions.[6] Further evidence that these are genuine interactions is provided by the orientation of the groups involved. Firstly the H33c...O1 bond vector lies along the only open approach to the anionic oxygen atom (all other approaches being blocked by the organic framework of the monomeric unit). Secondly, the two aryl groups are almost orthogonal to each other [angle between the planes defined by C31b-C36b and C41-C46 = 79.7(1)°]. Thirdly, H32c and H33c are essentially equidistant from the plane defined by the ring C41-C46 [2.341(3) Å and 2.353(3) Å for H32c and H33c, respectively]. Finally, H32c lies almost directly above the centroid of C41-C46.

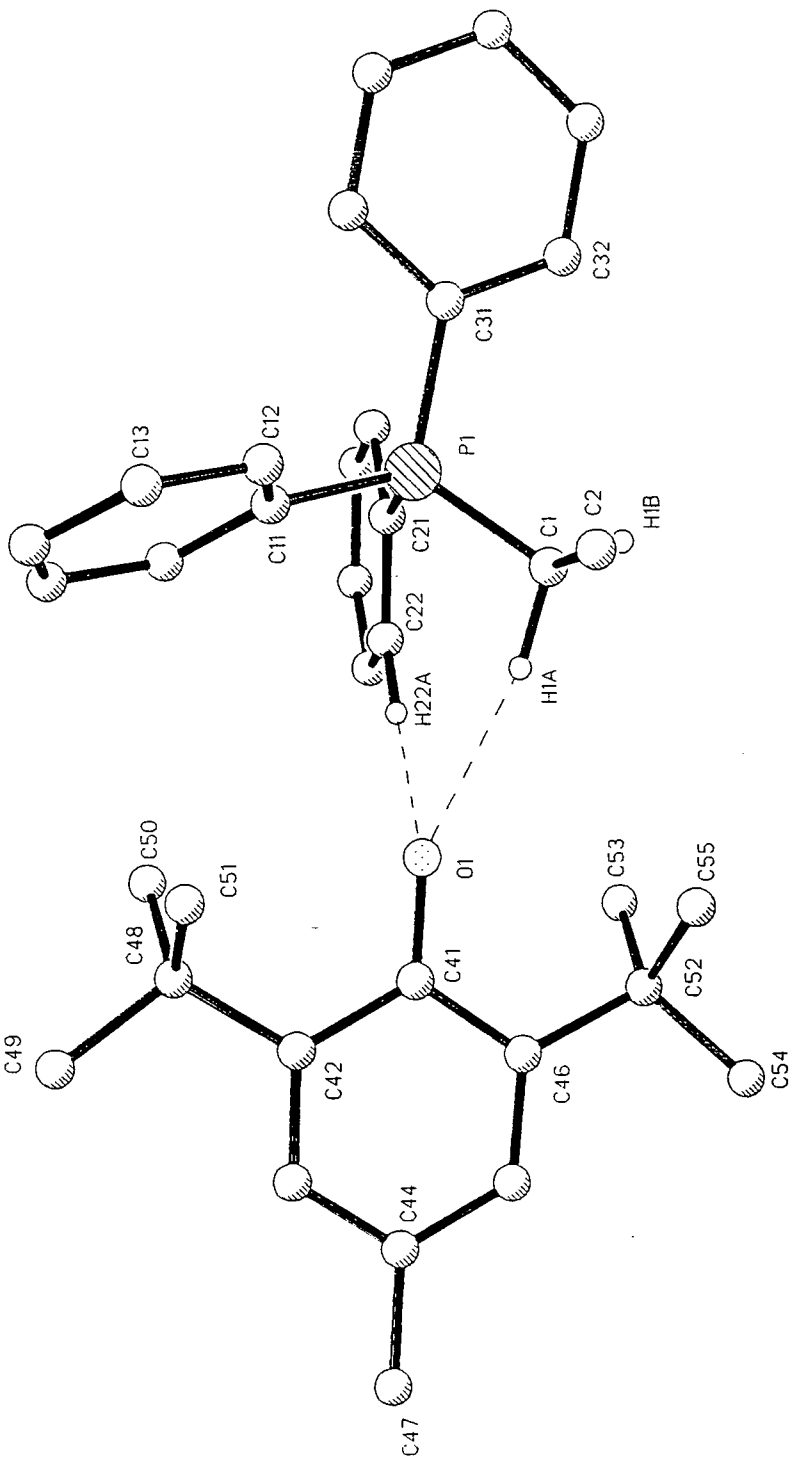

Figure 4.8a The structure of $[(Ph_3PEt)^+(OC_6H_2{}^tBu_2\text{-}2,6\text{-}Me\text{-}4)^-]$, (10) dervied from neutron diffraction data. All hydrogens except those involved in C-H...O hydrogen bonding have been omitted for clarity.

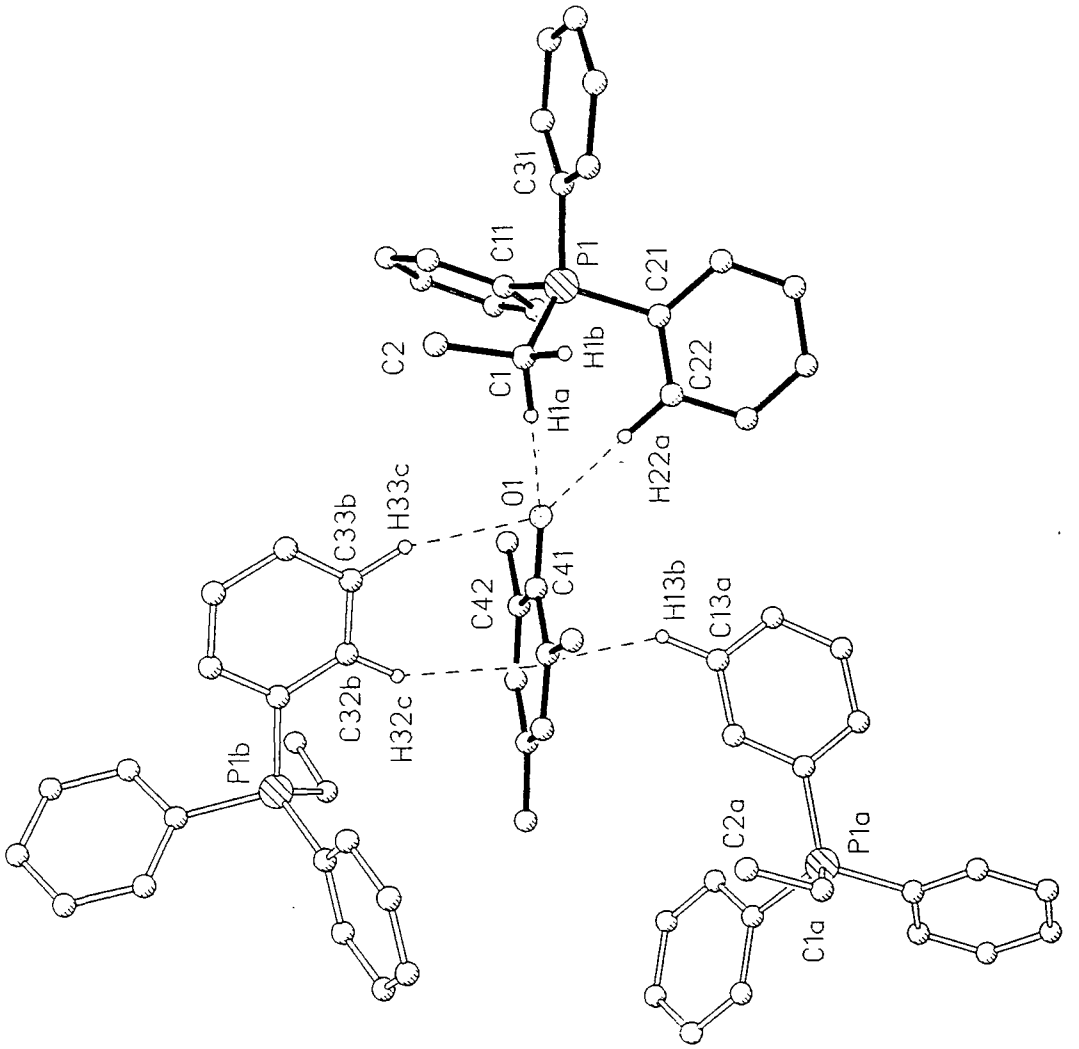

Figure 4.8b The molecular structure of $[(Ph_3PEt)^+(OC_6H_2{}^tBu_2\text{-}2,6\text{-}Me\text{-}4)^-]_n$, (10), showing the out-of-plane C-H...π interactions. All hydrogens except those involved in C-H...O/π hydrogen bonding, and the anion's ^{t}Bu substituents have been omitted for clarity.

The other face of the anion is also involved in a C-H...π interaction with H13b, a *meta*-C-H group of a symmetry related cation, which completes the unusual though not unprecedented,[6] C-H...π...H-C interaction. Again the relative orientation of the groups involved, suggests an attractive interaction. The two aryl groups are orthogonal to each other [angle between the planes defined by C11a-C16a and C41-C46 = 86.4(1)], C11a-C16a is also orientated such that only one hydrogen atom (H31b) comes into close contact with C41-C46. At this face no additional interaction with the oxygen atom is possible since the close approach to O1 is blocked by the cation (specifically by C21-C26).

A number of points are worthy of mention concerning all structures discussed so far. All the hydrogen bonds described here are well within the accepted criteria of distance and angle used to define such an interaction. However, it could be said that distance alone is rather an unconvincing criterion upon which to judge the validity of C-H...O hydrogen bonds. The hydrogen bonding observed in all these structures is favoured by a number of factors. The phenol derivatives are all sufficiently acidic to act as proton donors and hence proton transfer to an ylide (which is in effect acting as a proton sponge), to give O...H-C adducts is effected. This hydrogen bonding is favoured by a combination of highly anionic oxygen atoms which are excellent hydrogen bond acceptors and the alkyl phosphonium hydrogen atoms, which are inherently acidic, being potentially good hydrogen bond donors. It should also be noted that the relative orientations of the donor groups involved provide further evidence that these interactions are genuine. All these groups are free to rotate, however, they are all found to be ideally aligned to participate in hydrogen bonding.

Searches of the CSD revealed this series of phosphonium aryloxide salts to be unique in several respects. No other phosphonium aryloxides or alkoxides were found in the CSD although examples of phosphonium thiolates and selenates are known.[14] Also Hunter et al reported the cation Ph_3PMe^+, as a hydrogen bond donor to a boron containing anion. As observed in our structures the phosphonium cation utilises both C(alkyl)-H and C(aryl)-H donors. In this case three hydrogen bonds were formed. One involved a C(alkyl)-H donor

[14]J. M. Ball, P. M. Boorman, J. F. Fait, A. S. Hinman and P. J. Lundmark, *Can. J. Chem.*, 1989, **18**, 751.

to the boron anion. Two further interactions of the C-H...π type were also formed. These involved one C(alkyl)-H and one C(aryl)-H interacting with a furan molecule.[15]

Although no phosphonium aryloxides or alkoxides were found the CSD does contain a number of examples where such C-H...O hydrogen bonding, involving the types of cations we have observed, is evident. Fifteen structures which exhibit short intermolecular C...O distances between an alkyl phosphonium cation and an oxygen were found. Of these, four involve C-H interactions with neutral solvent molecules, two with methanol[16, 17] and two with water.[18, 19] A further ten involve C-H...O interactions with anions including perchlorate,[20, 21, 22] hydrogen sulphate,[23] nitrite,[24] trinitromethanide,[25] formate,[24] 2,3-dicyano-1,4-napthoquinone[26] and triflate[27, 28] anions and one involves close contact to both an acetate anion and a neutral acetic acid in the same structure.[29] Of these, five involve the phosphonium cation, $(Ph_3PCH_3)^+$.[23, 24, 25, 26]

As has been shown, on the supramolecular level (5) to (10) are all extensively hydrogen bonded, with a common motif of alkyl and aryl donors. These structural features can be illustrated by simple schematic diagrams which show at a glance the degree of aggregation (i.e. monomer, dimer, etc) and the number of hydrogen bond donors to each anionic oxygen (i.e. bifurcation, trifurcation etc.).

---

[15]R. Hunter, R. H. Haueisen and A. Irving, *Angew. Chem. Int. Ed. Eng.*, 1994, **33**, 566.
[16]D. Matt, R. Ziessel, A. De Cian and J. Fischer, *New J. Chem.*, 1996, **20**, 1257.
[17]H. Schmidbaur, C. Paschalidis, O. Steigelmann, D. L. Wilkinson and G. Muller, *Chem. Ber.*, 1989, **122**, 1857.
[18]Mazar-Ul-Haque, W. Horne, S. E. Cremer and J. T. Most, *J. Crystallogr. Spectrosc. Res.*, 1989, **19**, 317.
[19]Mazar-Ul-Haque, W. Horne and S. E. Cremer, *J. Crystallogr. Spectrosc. Res.*, 1988, **18**, 533.
[20]M. R. Churchill, L. A. Buttrey, W. G. Feighery, J. B. Keister and J. W. Ziller, *J. Crystallogr. Spectrosc. Res.*, 1990, **20**, 89.
[21]M. Cygler and J. Skolimowski, *Can. J. Chem.*, 1983, **61**, 427.
[22]N. Gurusamy, K. D. Berlin, D. van der Helm and M. B. Hossain, *J. Am. Chem. Soc.*, 1982, **104**, 3107.
[23]F. Schmock, A. El-Kholi, U. Muller and K. Dehnicke, *Z. Naturforsch., Teil B*, 1988, **43**, 1069.
[24]M. E. Essawi, H. Gosmann, D. Fenske, F. Schmock and K. Dehnicke, *Z. Naturforsch., Teil B*, 1988, **43**, 1279.
[25]K. D. Scherfise, F. Weller and K. Dehnicke, *Z. Naturforsch., Teil B*, 1985, **40**, 906.
[26]M. R. Bryce, S. R. Davies, M. Hasan, G. J. Ashwell, M. Szablewski, M. G. B. Drew, R. Short and M. B. Hursthouse, *J Chem. Soc., Perkin Trans. 2*, 1989, 1285.
[27]D. C. R. Hockless, M. A. McDonald, M. Pabel and S. B. Wild, *J. Chem. Soc., Chem. Commun.*, 1995, 257.
[28]H. J. Bestmann, D. Hadawi, H. Behl, M. Bremer and F. Hampel, *Angew. Chem. Int. Ed. Eng.*, 1993, **32**, 1205.
[29]E. Vedjes and S. T. Diver, *J. Am. Chem. Soc.*, 1993, **115**, 3358.

Figure 4.9 reveals how at first a monomer, and then, by extending these simple principles, a dimer, can be illustrated using simple geometric shapes to represent cation and anions, with arrows representing the hydrogen bonds.

In order to investigate whether or not such structural motifs are restricted to phosphonium aryloxides, we have structurally characterised some inorganic salts. Benzyltriphenylphosphonium bromide, (11) and Benzyltriphenylarsonium bromide, (12) were synthesised following the same procedure and their resulting structures are analogous.

Salt (11) was formed by reacting triphenylphosphine with benzyl bromide in a dry acetonitrile solution. Characterisation ultimately by X-ray diffraction revealed the formation of the inorganic salt $[(Ph_3PC(Ph)H_2)Br.2CH_3CN]_n$, (11). In common with the phosphonium aryloxide salts on the supramolecular level the cations and anions are held together with a series of C-H...X interactions (where X = Br). Dimeric units are observed in which the bromide anion is chelated by C(alkyl)-H and C(aryl)-H donors again reminiscent of the phosphonium aryloxides. All C-H...Br parameters are given in Table 4.8.

Table 4.8 Hydrogen bond parameters for (11).

Interaction	C...Br distance (Å)	H...Br distance (Å)	C-H...Br angle (°)
C1A-H1BA...BrA	3.824	2.779	162.7
C1A-H1AA...BrB	3.831	2.793	161.1
C32A-H32A...BrB	3.893	2.827	169.4
C46A-H46A...BrA	3.714	2.674	161.4
C3D-H3BD...BrA	3.896	2.836	167.1
C3A-H3CA...BrA	3.836	2.846	152.4

Here it can be seen that both of the cation's CH_2 hydrogen atoms are involved in C-H...X interactions and form a bridge between the two Br anions. Furthermore, two aryl donors,

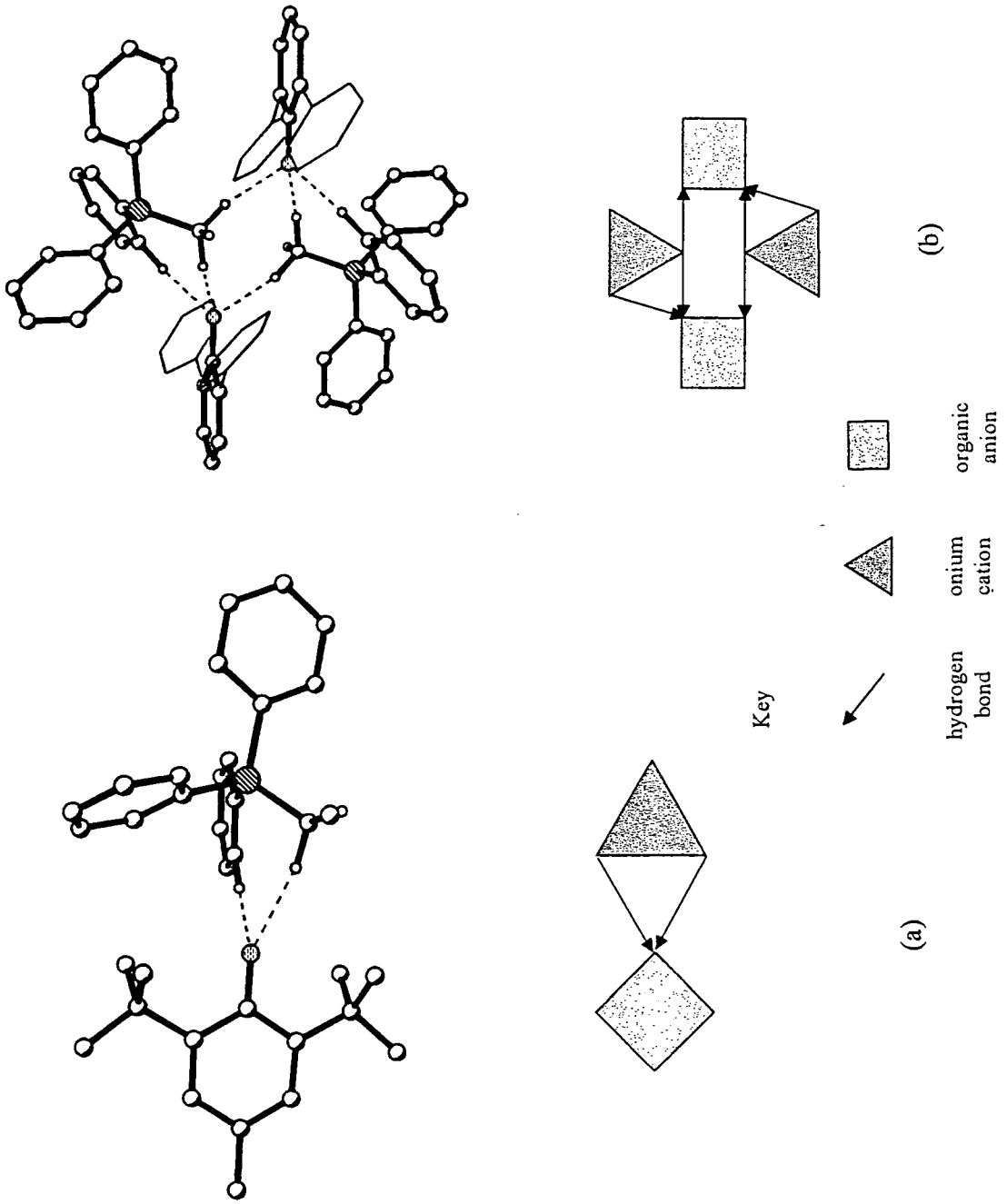

Figure 4.9 Simple geometric representation a monomer and a dimer;

(a) shows the bifurcated monomer (10)

(b) shows the trifurcated dimer (7)

that is two *ortho*-phenyl hydrogens (one from each cation) interact with the bromide anions (Figure 4.10a).

However, further aggregation is observed in this salt, and this can be rationalised by considering the fundamental differences between the anions in these inorganic salts compared with those in the phosphonium aryloxides. Unlike the aryloxide anion the bromide anion has a spherically symmetrical charge distribution which means that it can be coordinated from all directions. Conversely, in the aryloxide anion, the anionic oxygen is effectively protected or blocked from coordination on one side by its organic group. Subsequently, in this inorganic salt, the bromide anion undergoes further C-H...X interactions with the methyl groups of two acetonitrile molecules. These acetonitrile molecules bridge the dimers, resulting in the formation of a polymeric structure in which the bromide anion is hexafurcated. As for the phosphonium aryloxides, this structure can also be represented by a simple schematic diagram, (Figure 4.10b).

All these features are observed in the analogous arsonium salt, $[(Ph_3AsC(Ph)H_2)Br.2CH_3CN]_n$, (12), (Figure 4.11). This also has a polymeric structure resulting from bridging acetonitrile molecules between dimeric cation-anion units All C-H...Br parameters are shown in Table 4.9.

Table 4.9 Hydrogen bond parameters for (12).

Interaction	C...Br distance (Å)	H...Br distance (Å)	C-H...Br angle (°)
C7AA-H72A...BrAB	3.790	2.723	169.7
C7AA-H71A...BrAA	3.817	2.760	166.0
C22A-H22A...BrAA	3.725	2.659	168.8
C32A-H32A...BrAB	3.933	2.858	173.6
C9AB-H92C...BrAB	3.852	2.801	164.4
C9BB-H91D...BrAB	3.901	2.842	166.8

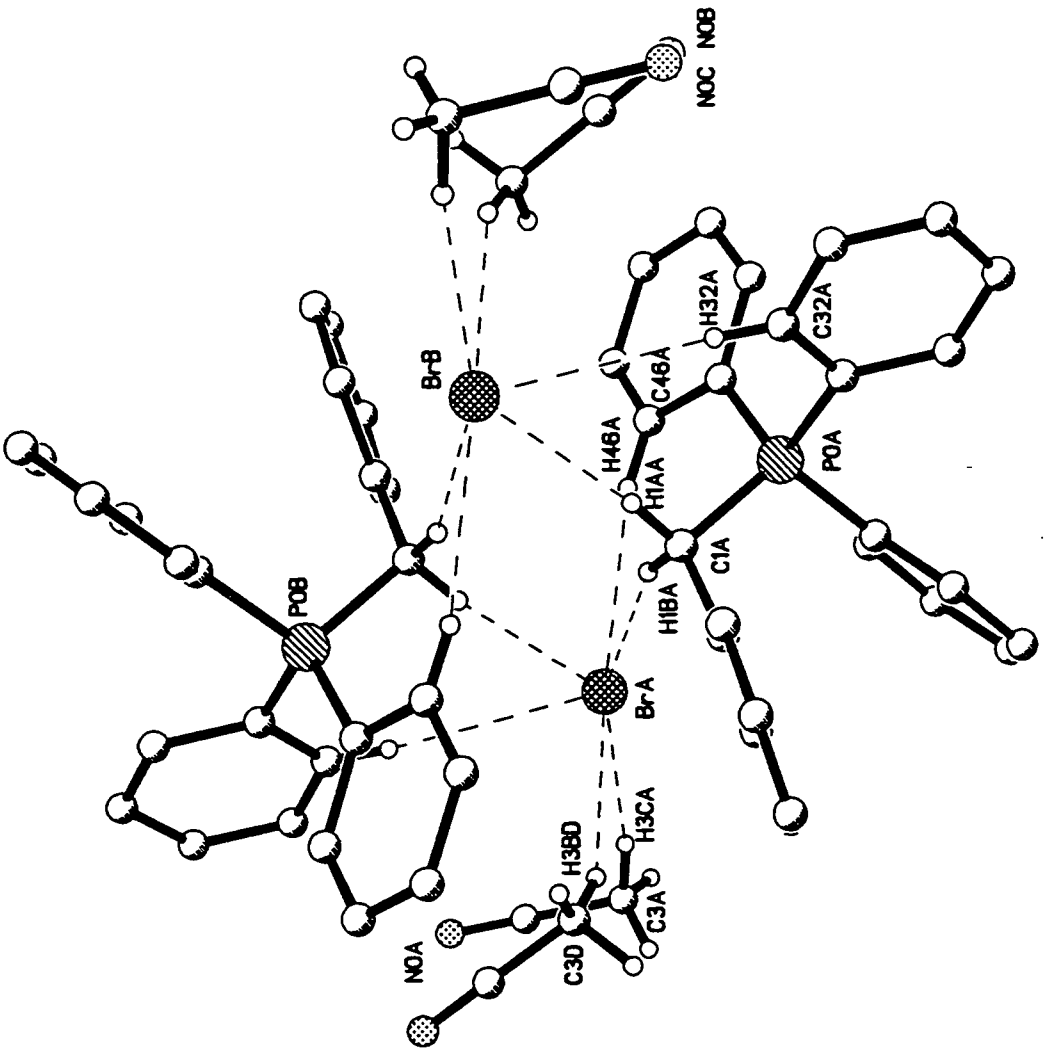

Figure 4.10a. The dimeric unit of $[(Ph_3PC(Ph)H_2)Br.2CH_3CN]_n$, (11). All aryl hydrogen atoms except those involved in C-H...X hydrogen bonding have been omitted for clarity.

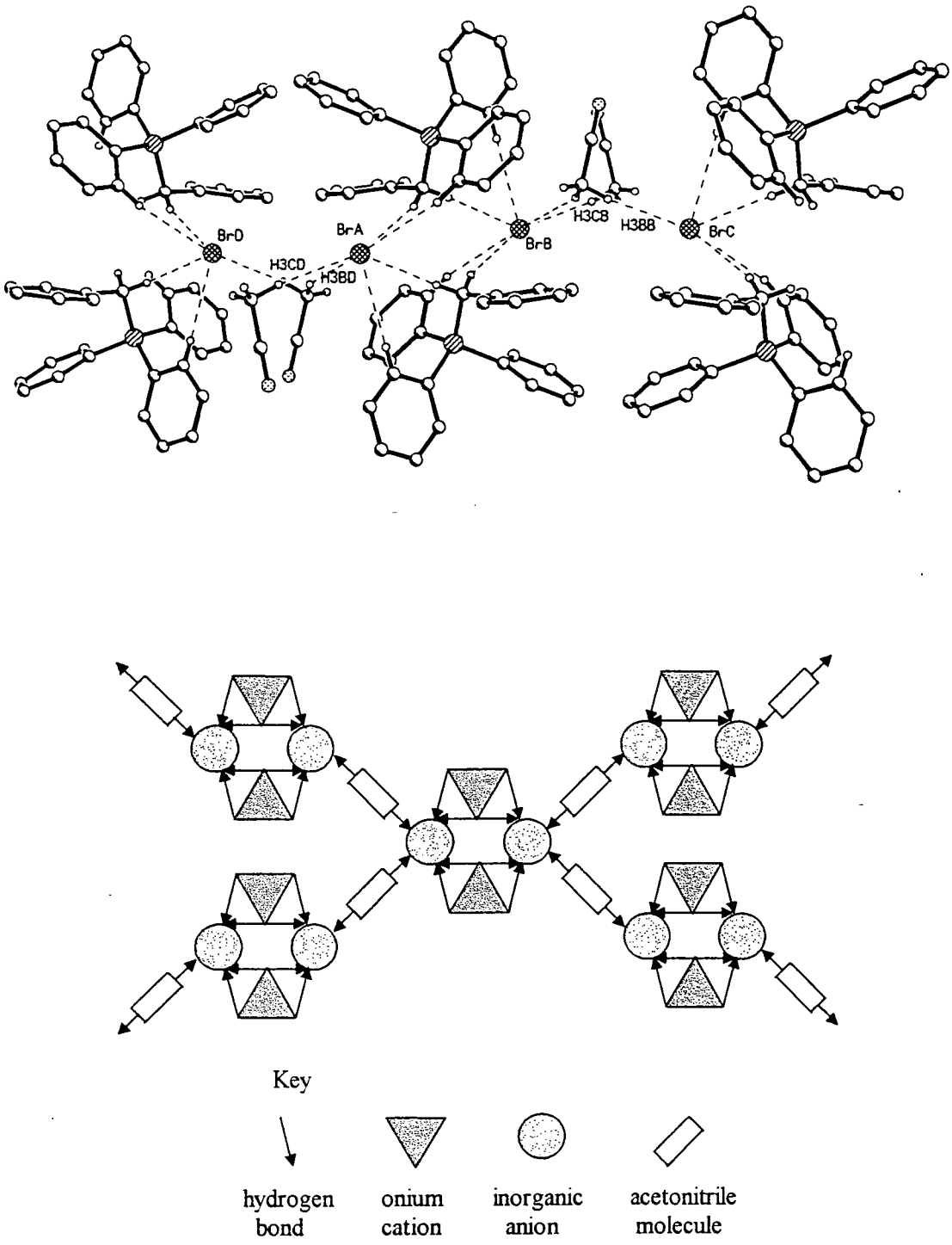

Figure 4.10b. The polymeric structure of $[(Ph_3PC(Ph)H_2)\ Br.2CH_3CN]_n$, (11), showing the bridging CH_3CN molecules, with a more extended schematic representation below.

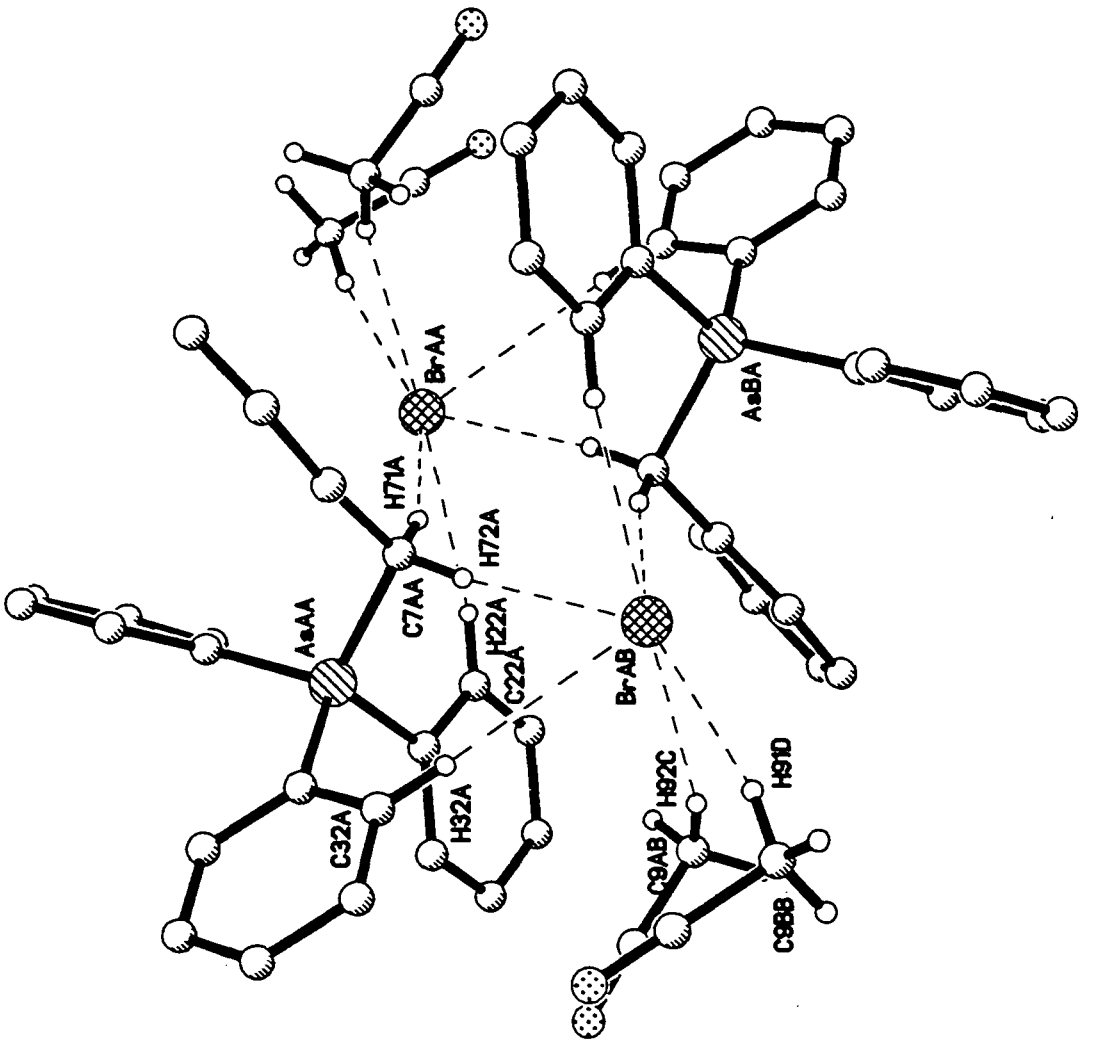

Figure 4.11. The dimeric unit of $[(Ph_3AsC(Ph)H_2)Br.2CH_3CN]_n$, (12). All aryl hydrogen atoms except those involved in C-H...X hydrogen bonding have been omitted for clarity.

From the results in this chapter a number of conclusions can be drawn about the synthesis of phosphonium aryloxide salts.

(i) Deprotonation of a range of phenol derivatives with the non-stabilised ylides (1) and (2) in a combination of hydrocarbons (e.g. toluene) and more polar solvents (e.g. acetonitrile, thf) under mild conditions yields crystalline phosphonium aryloxide salts.

(ii) In all, eight salts, (A), (B), (5) - (10) have now been isolated and their solid-state structures characterised by single crystal X-ray diffraction (See Table 4.1) In order to characterise these structures more fully the neutron diffraction structures of two of these salts, (7) and (10), were obtained.

iii) A wide range of phenol derivatives of the general formula 2,4,6-R-C_6H_2OH were employed in which the R groups were any one of H, Me, Ph or ^{t}Bu groups. This allowed a variation in the steric requirements of the aryloxide anions and in so doing, gave control over a number of factors including the degree of aggregation, the number of hydrogen bond donors to each oxygen atom and the degree of solvent incorporation: in effect what could be described as a form of crystal engineering.

(iv) On the supramolecular level, all eight structures are extensively C-H...O hydrogen bonded and a common structural motif of C(alkyl)-H and C(aryl)-H hydrogen bond donors to the anionic oxygen atom of the aryloxide is observed. This emphasises that alkyltriphenyl-phosphonium cations are strong and versatile hydrogen bond donors and aryloxide anions are strong and versatile hydrogen bond acceptors.

(v) A neutron diffraction study of (7) revealed it to contain a C-H...O interaction that is over 5% shorter than any other such interaction characterised by this technique.

(vi) These structural motifs are not unprecedented and can also be observed in inorganic salts such as (11) and (12).

Chapter 5

5. DISCUSSION - PHOSPHONIUM AMIDES AND PHOSPHIDES

The preparation and structural characterisation of compounds containing 'naked' organic and organometallic anions has attracted much attention. Their use in organic[1] and polymer[2] synthesis, their geometry[3, 4, 5, 6] and their participation in weak intermolecular interactions[4] are of particular interest. Several strategies have been employed in the synthesis of such ion-separated systems, for example, lithiation of organic acids in the presence of crown ether ligands,[3, 4] deprotonation of organic acids using strong, nitrogen containing organic bases[7, 8] or cleavage of Si-element bonds using fluorosilicate anions.[1, 6] Having established a strategy for generating phosphonium aryloxides via the deprotonation of phenol derivatives with non stabilised phosphonium ylides as described in the previous chapter, it led us to the more general use of phosphonium ylides as an alternative means of generating organic anions to those strategies outlined above. This chapter will report our results relating to the extension of this work describing the formation of two phosphonium amides (13) and (14) and a phosphonium phosphide (15). Numbering of these complexes is consistent with those used previously. X-ray structures were obtained for all three compounds.

---

[1]R. Noyori, I. Nishida and J. Sakata, *J. Am. Chem. Soc.*, 1983, **105**, 1598.
[2]M. T. Reetz, S. Hutte, S. Goddard and R. Minet, *J. Chem. Soc., Chem. Commun.*, 1995, 275.
[3]H. Hope, M. M. Olmstead, P. P. Power and X. Xu, *J. Am. Chem. Soc.*, 1984, **106**, 819.
[4]M. M .Olmstead and P. P. Power, *J. Am. Chem. Soc.*, 1985, **107**, 2174; R. A. Bartlett, H. V. Rasika Dias, H. Hope, B. D. Murray, M. M. Olmstead and P. P. Power, *ibid.*, 1986, **108**, 6921.
[5]R. Hunter, R. H. Haueisen and A. Irving, *Angew. Chem. Int. Ed. Eng.*, 1994, **33**, 566.
[6]J. Wessel, U. Behrens, E. Lork and R. Mews, *ibid.*, 1995, **34**, 443.
[7]M. J. Peräkylä, *J. Organomet. Chem.*, 1996, **61**,7420; J. A. Platts and S. T. Howard, *ibid.*, 1996, **61**, 4480; R. W. Alder, *Chem. Rev.*, 1989, **89**, 1215; H. A. Staab and T. Saupe, *Angew. Chem. Int. Ed. Eng.*, 1988, **27**, 865.
[8]R. Schwesinger, C. Hasenfratz, H. Schlemper, L. Walz, E.-M. Peters, K. Peters and H. G. von Schnering, *Angew. Chem. Int. Ed. Eng.*, 1993, **32**, 1361.

Reaction of (2) with Ph_2NH in a dry toluene solution resulted in the formation of a bright red precipitate which dissolved on heating. Cooling to room temperature yielded a crop of red crystals. Characterisation ultimately by single crystal X-ray diffraction confirmed the expected formation of the phosphonium amide $(Ph_3PEt)^+(NPh_2)^-$, (13), (Figure 5.1). This, to our knowledge, is the first example of a phosphonium amide to be isolated and structurally characterised. Furthermore, the crystal structure contains the first example of an essentially 'naked' Ph_2N^- anion.

The cation and anion are held together by hydrogen bonds. Both C(alkyl)-H and C(aryl)-H donors from the cation chelate the anionic nitrogen, forming two C-H...N hydrogen bonds. All hydrogen bond parameters are given in Table 5.1. This motif of chelating alkyl and aryl hydrogen bond donor groups is reminiscent of that found in the phosphonium aryloxides.

Table 5.1 Hydrogen bond parameters for (13)

Interaction	C...N distance (Å)	H...N distance (Å)	C-H...N angle (°)
C1-H1B...N1	3.543	2.487	165.6
C32-H32A...N1	3.387	2.317	170.7

The geometry of the cation is not unusual but that of the $(Ph_2N)^-$ anion is of considerable interest. Others have tried and failed to isolate this anion in a crystal. Power et al were able to achieve ion separation with isoelectronic $(Ph_2X)^-$ anions (where X = CH, P, As or Sb) by lithiation of Ph_2XH and crystallisation in the presence of crown ethers to give solvent-separated ion pairs.[3, 4] However, this strategy was unsuccessful in the case of Ph_2NH (due to strong Li-N bond) the result being an ion-contacted monomer $Ph_2NLi(12\text{-}c\text{-}4)$.[1] The structural characterisation of this 'naked' anion has until now, remained elusive. The geometry of the anion in (13) does not differ significantly from that found in the ion-contacted lithium amide, which reflects the predominantly ionic nature of the Li-N bond in lithium amides.[9] In the anion of (13) the bond lengths of N1-C11 and N1-C21 were 1.380(5) Å and 1.365(3) Å respectively with the C11-N1-C21 angle being 121.5(3)°, the average corresponding parameters in $Ph_2NLi(12\text{-}c\text{-}4)$ being 1.388 Å and 119.1°.

[9]K. Gregory, P. von R. Schleyer and R. Snaith, *Adv. Inorg. Chem.*, 1991, **37**, 47, and references therein.

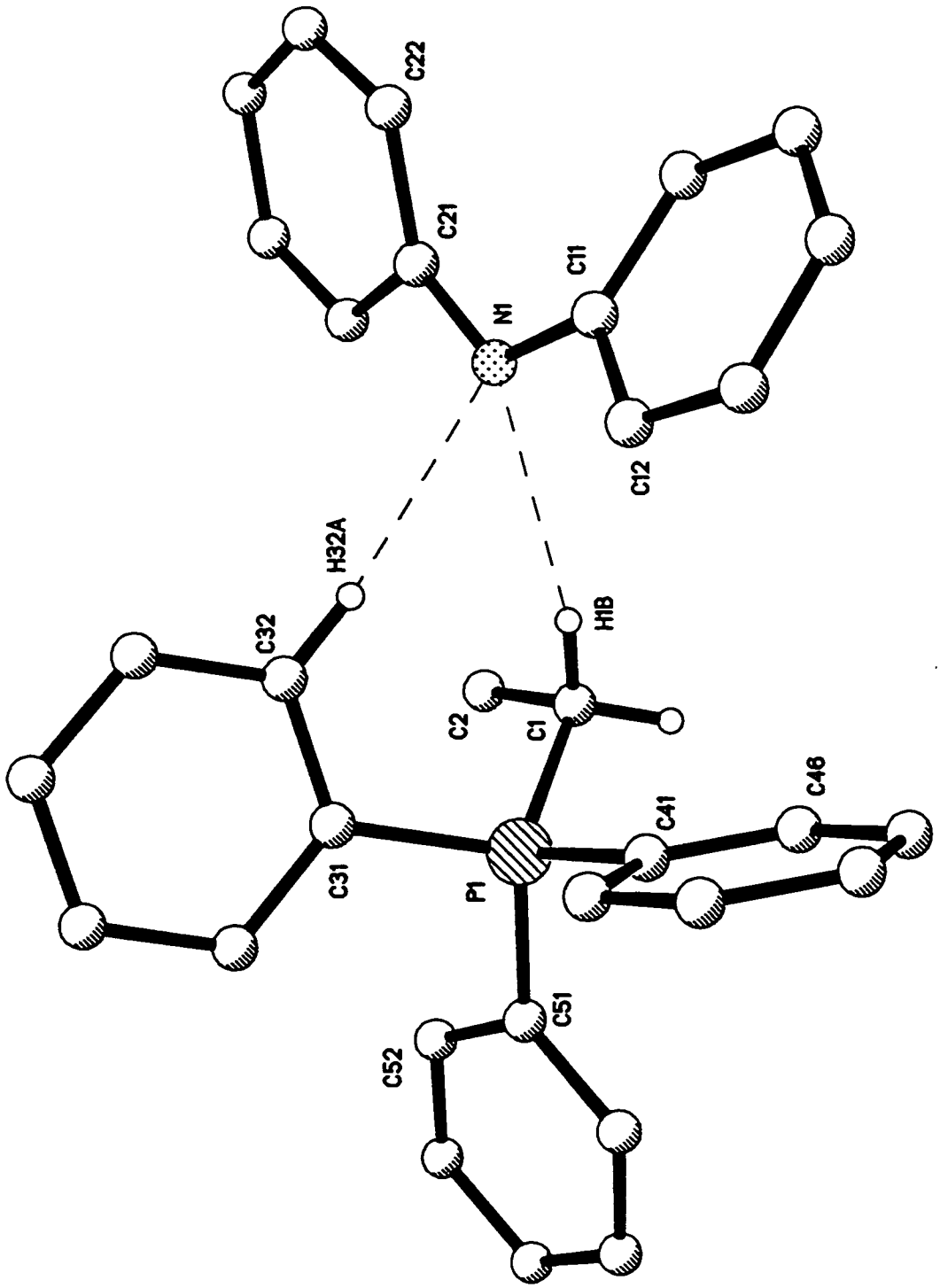

Figure 5.1 The molecular structure of $(Ph_3PEt)^+(NPh_2)^-$, (13). All aryl hydrogen atoms except those involved in C-H...N hydrogen bonding have been omitted for clarity.

In the lithium amide the anionic nitrogen is three-coordinate and planar (indicative of sp^2 hybridisation) and although ion-separation in the case of (13) precludes a similar definitive analysis, in view of its similar geometry to the lithium amide, we postulate that N1 in (13) is similarly sp^2 hybridised. Significantly, if one examines the bisector of the two C-H...N hydrogen bond vectors it can be seen to almost perfectly complete the trigonal planar geometry about N1. This implies that the C-H...N interactions are both with a lone pair of electrons in an sp^2 orbital of nitrogen. It is well established that weak hydrogen bonds can exhibit such electrostatic directionality.[10] Consequently, this leaves the lone pair in the nitrogen p orbital to interact with the π-system of the phenyl rings. In spite of this proposed interaction, the nitrogen-bound phenyl rings are not coplanar as would be necessary for ideal overlap of the nitrogen p orbital with both phenyl π-systems, but are tilted at an angle of 39.9° to each other. This is presumably to relieve steric strain between the hydrogen atoms bound to C22 and C16 rather than for compelling electrostatic reasons.

Cryoscopic RMM measurements[11] were carried out for (13) to ascertain the stability of this ion-pair in solution. These results revealed a relative molecular mass of 280 ± 10 for 8.0×10^{-3} M benzene solution, corresponding to a degree of association, n [relative to monomeric $(Ph_3PEt)^+(NPh_2)^-$] of 0.62 ± 0.03. These measurements suggest that the ion pairs observed in the solid state are not maintained in benzene solution. ^1H NMR and ^{31}P NMR spectroscopies are consistent with the existence of phosphonium and amide ions in solution, however, in view of the expected similarity in the pKa of Ph_3PEt^+ and Ph_2NH,[12] the operation of an equilibrium (fast on the NMR time scale) between the ionic and molecular species in solution cannot be discounted.

Following on from the successful reaction of (2) with Ph_2NH it was postulated that another NH-containing species, carbazole (Figure 5.2), whose structure is similar to that of Ph_2NH may also be seen to undergo deprotonation to form a 'naked' organic anion. Carbazole is closely related to indole and both are benzologs of pyrrole (Figure 5.2).

---

[10]G. R. Desiraju, *Angew. Chem. Int. Ed. Eng.*, 1995, **34**, 2328; G. R. Desiraju, *Acc. Chem. Res.*, 1991, **24**, 290.

[11]see chapter 2, section 2.9 for details on cryoscopic techniques.

[12]F. G. Bordwell, *Acc. Chem. Res.*, 1988, **21**, 456.

However, of the three, carbazole is the most acidic,[13] and therefore of more potential use in our systems.

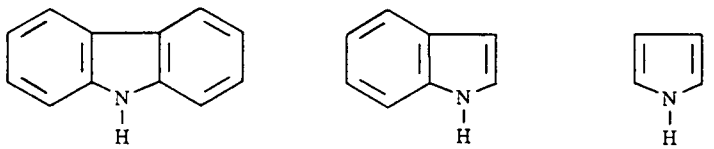

carbazole indole pyrrole

Figure 5.2 The structures of carbazole and its related compounds.

Reaction of (2) with carbazole in a dry thf solution resulted in the formation of a yellow precipitate which dissolved on addition of acetonitrile. On cooling to room temperature a crop of yellow needle-like crystals was obtained. Solid-state characterisation, as predicted, reveals that the carbazole has undergone deprotonation to give the salt, $[(Ph_3PEt)^+(C_{12}H_8N)^-]_2$, (14), (Figure 5.3). The dimeric structure is aggregated via C-H...N hydrogen bonds, though in this case the nitrogen atoms are not chelated by C(alkyl)- and C(aryl)- hydrogens, but instead one cation bridges the anions by utilising two C(alkyl)-H donors from its CH_2 group, meanwhile the other uses only one such proton, the second C(alkyl)-H donor being from its CH_3 group (Figure 5.4). All hydrogen bond parameters are given in Table 5.2. These dimers then stack in columns of alternating cations and anions. There are no interactions between neighbouring dimeric units.

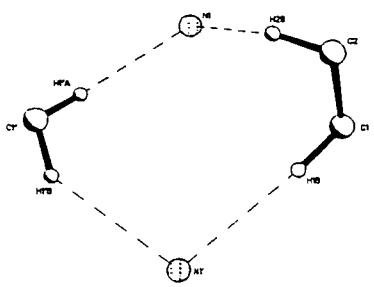

Figure 5.4 The central motif of the dimeric units of (14), highlighting the C-H...N hydrogen bonding motif

[13]M. Balon, M. C. Carmona, M. A. Munoz and J. Hidalgo, *Tetrahedron*, 1989, **45**, 7501.

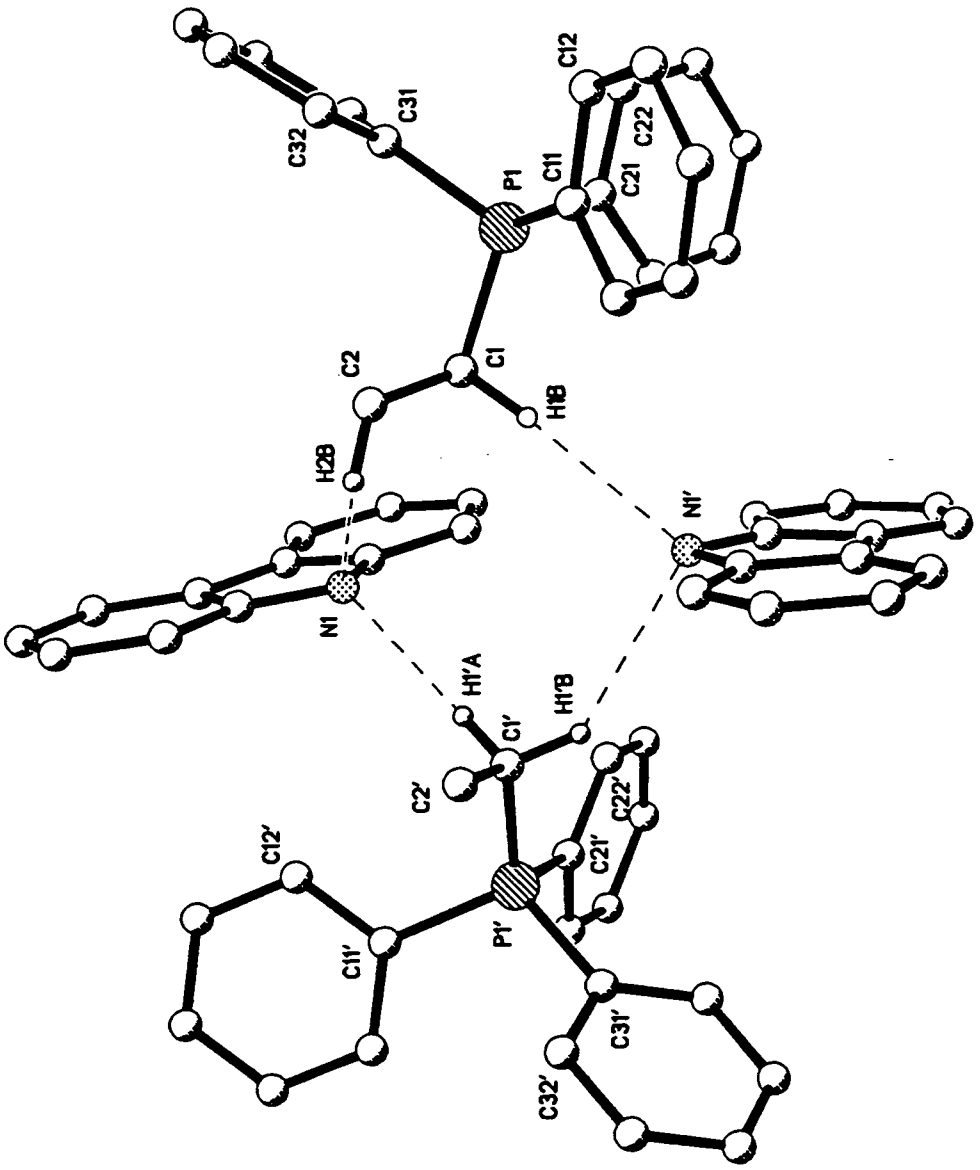

Figure 5.3 The dimeric unit of $(Ph_3PEt)^+(C_{12}H_8N)^-$, (14). All hydrogen atoms except those involved in hydrogen bonding have been omitted for clarity.

Table 5.2 Hydrogen bond parameters of (14)

Interaction	C...N distance (Å)	H...N distance (Å)	C-H...N angle (°)
C1'-H1'A...N1	3.223	2.189	159.7
C1'-H1'B...N1'	3.511	2.600	141.6
C1-H1B...N1'	3.646	2.602	162.2
C2-H2B...N1	3.218	2.407	130.8

A search of the Cambridge Structural Database (CSD), revealed other species in which carbazole anions have been observed, for example in the structures of, $(C_{12}H_8N)^-([^tBuOH]_2Li)^+.2thf$,[14] $(C_{12}H_8N)^-Li^+.2thf$[15] and $[(C_{12}H_8N)^-(NBu^n_4)^+]_n$.[2] The latter is the only one to contain a nonmetallic cation. Its anions are also stabilised by two C-H...N hydrogen bonds from neighbouring cations, one cation being more closely associated with the anion than the other. However chains, not dimers are formed, resulting in a polymeric structure of alternating cations and anions, (C...N distances 3.339(7) Å and 3.674(7) Å). These C...N distances are comparable with those observed in our structure (C...N of 3.218 - 3.646 Å). The bond lengths and angles observed within the anions of all the above examples are very similar to the ones observed in (14), however all the anions have more acute C-N-C angles than in the neutral carbazole, (103 - 106°, 109° for the anions and carbazole respectively), while the C-C bond bridging the two six-membered rings is longer in carbazole than in the anions (1.451 Å, 1.431 - 1.438 Å for carbazole and the anions respectively).

Having demonstrated that our strategy can be transferred to reaction with amides we turned our attention to the possibility of forming a stable phosphide anion. Previous work in which bulky electron-withdrawing groups such as $C_6H_2(CF_3)_3$-2,4,6, (Ar), were utilised to stabilise a variety of low-coordinate phosphonium compounds, such as diphosphenes[16, 17, 18] phosphaalkenes[19] and their transition metal derivatives,[16, 18, 19] suggested that Ar_2PH could be a species which would potentially form a stable phosphide

[14]C. Lambert, P. von R. Schleyer and F. Hampel, *Angew. Chem. Int. Ed. Eng.*, 1992, **31**, 1209.
[15]R. Hacker, E. Kaufmann, P. von R. Schleyer, W. Mahdi and H. Dietrich, *Chem. Ber.*, 1987, **120**, 1533.
[16]K. B. Dillon and H. P. Goodwin, *J. Organomet. Chem.*, 1992, **429**, 169.
[17]K. B. Dillon, V. C. Gibson and L. J. Sequeira, *J. Chem. Soc., Chem. Commun.*, 1995, 2429.
[18]K. B. Dillon, V. C. Gibson, J. A. K. Howard, L. J. Sequeira and J. W. Yao, *Polyhedron*, 1996, **15**, 4173.
[19]K. B. Dillon and H. P. Goodwin, *J. Organomet. Chem.*, 1994, **469**, 125.

anion, Ar_2P^-, in our system. Reaction of (1) with Ar_2PH in a dry toluene solution at room temperature resulted in the immediate formation of a red precipitate in a deep blue solution. The precipitate dissolved on addition of more toluene and heating. On cooling to room temperature a crop of deep red plate-like crystals was obtained. Single crystal X-ray diffraction confirmed the expected formation of the phosphonium salt $[(Ph_3PMe)^+(Ar_2P)^-]_2$, (15), (Figure 5.5). As might be expected, on the basis of the previously characterised phosphonium salts, the cations and anions are held together and aggregation occurs via C-H...P interactions, between acidic C-H groups of the cation and the basic phosphonium centre of the anion. In the monomeric unit there is one C(alkyl)-H...P interaction (Figure 5.6). However, a C(aryl)-H...P interaction, from a cation of one monomeric unit to the anion of another, leads to the formation of dimers. Also a further, slightly longer, C(alkyl)-H...P interaction, (H19C...P2A), may also reinforce aggregation although it should be noted that the geometry of the dimer imposed by the other interactions necessitates this close contact. All hydrogen bond parameters are given in Table 5.3.

Table 5.3 Hydrogen bond parameters of (15)

Interaction	C...P distance (Å)	H...P distance (Å)	C-H...P angle (°)
C19-H19A...P2A	3.820	2.790	159.3
C12-H12...P2	3.926	2.902	158.3
C19-H19C...P2A	4.156	3.089	169.6

The geometry of the cation is as expected, however it is the geometry of the anion that is again of interest. Such ion-separated R_2P^- anions have been observed before in the solid state, for example in the structures of $Li(12\text{-c-}4)_2^+Ph_2P^-$,[3] $Na(18\text{-c-}6)^+P(CN)^-_2.thf$,[20] $[K(18\text{-c-}6)^+P(CN)_2^-]_\infty$[21] and $Ph_3PNPPh_3^+P(CN)Ph^-$,[22] although only the latter contains a nonmetallic cation. The geometry of the anion in (15) is influenced greatly by the sterically bulky Ar groups. The C29-P2-C20 angle of 109.1(1)° is greater than that found for any of the above examples whose angles range from 95.2 to 105.2,° and the angle between the

[20]W. S. Sheldrick, J. Kroner, F. Zwaschka and A. Schmidpeter, *Angew. Chem. Int. Ed. Eng.*, 1979, **18**, 934.
[21]A. Schmidpeter, G. Burget, F. Zwaschka and W. S. Sheldrick, *Z. Anorg. Allg. Chem.*, 1985, **527**, 17.
[22]A. Schmidpeter, K.-H. Zirzow, G. Burget, G. Huttner and I. Jibril, *Chem. Ber.*, 1984, **117**, 1695.

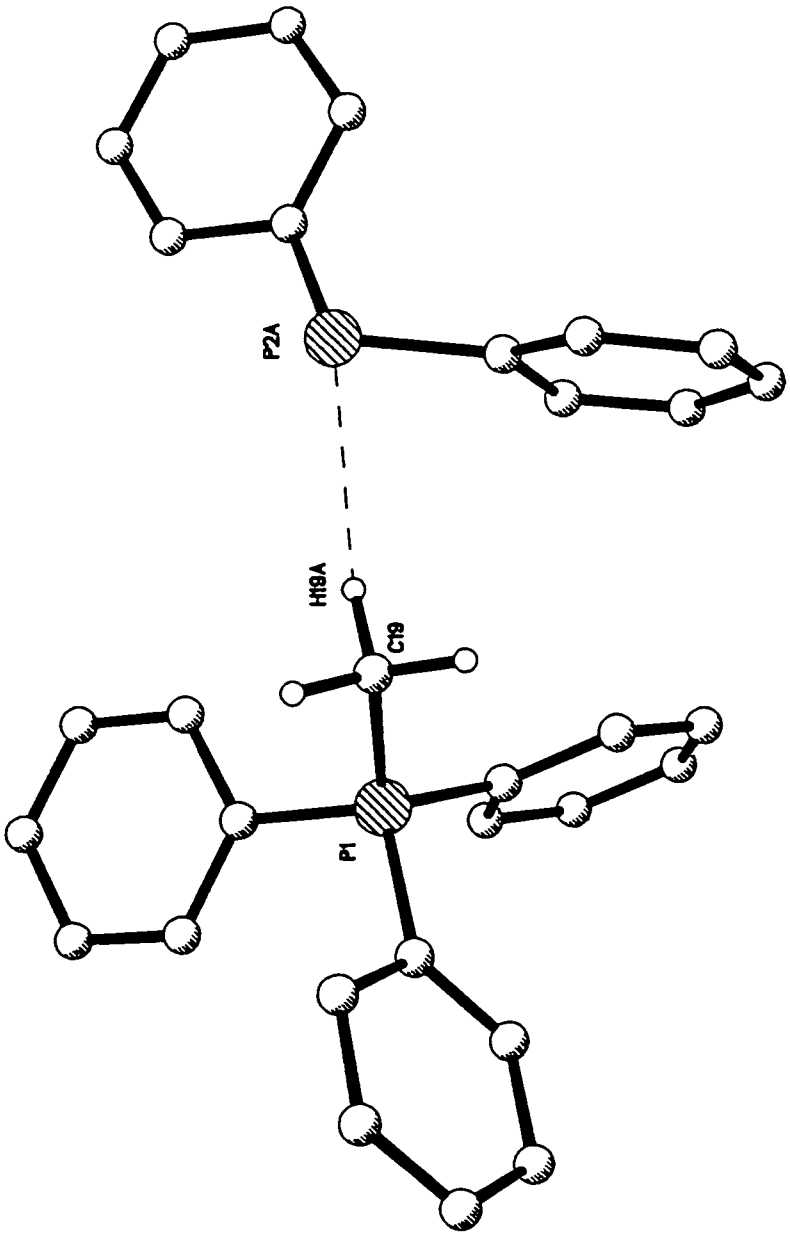

Figure 5.5 The monomeric unit of $[(Ph_3PMe)^+(Ar_2P)^-]_2$, (15). All CF_3 groups and aryl hydrogen atoms except those involved in hydrogen bonding have been omitted for clarity.

planes defined by the two aryl groups in (15) of 84.3° is far greater than the angle of 43.4° found for the equivalent parameter in the Ph_2P^- anion of $[Li(12\text{-}c\text{-}4)_2]^+Ph_2P^-$. Although the twisting may occur primarily to relieve the steric interactions between bulky ortho-CF_3 groups of the two aryl substituents, it also appears to have electronic consequences. The two P-C(ipso) bond lengths of the anion differ significantly, and while the longer of these two bond vectors essentially lies in the plane defined by the aryl group C20 to C25, (P2-C20-X angle is 177°, where X = centroid of C20 to C25), the other deviates in such a way that P2 lies significantly above the aryl plane defined by C29 to C34, (P2-C29-X angle is 166°, where X = centroid of C29 to C34), (Figure 5.7). Both the inequivalent P2-C(ipso) bond lengths and the unusual conformation of the anion suggest greater delocalisation of the negative charge into one aryl group. Delocalisation of negative charge into the Ar groups is further evidenced by the irregularity of bond lengths within the two aromatic rings of the anion (Table 5.7).

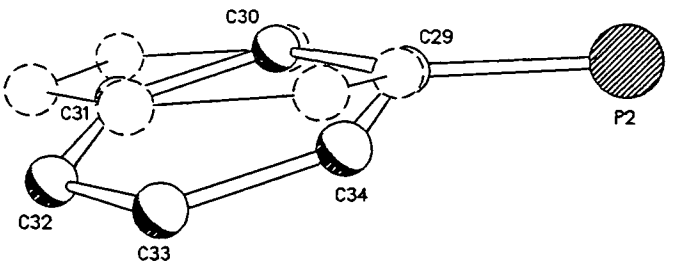

Figure 5.7 Superimposition of the two Ar-P groups highlighting the distortion from planarity of one of them (C29 to C34, solid lines and atoms). All hydrogen atoms and CF_3 groups omitted for clarity.

Table 5.4 Bond lengths in the two Ar rings

Bond	Bond length (Å)	Bond	Bond length (Å)
C29 - C30	1.447(3)	C20 - C21	1.420(3)
C30 - C31	1.390(3)	C21 - C22	1.394(3)
C31 - C32	1.383(3)	C22 - C23	1.382(3)
C32 - C33	1.383(3)	C23 - C24	1.389(3)
C33 - C34	1.391(3)	C24 - C25	1.391(3)
C34 - C29	1.450(3)	C25 - C20	1.433(3)

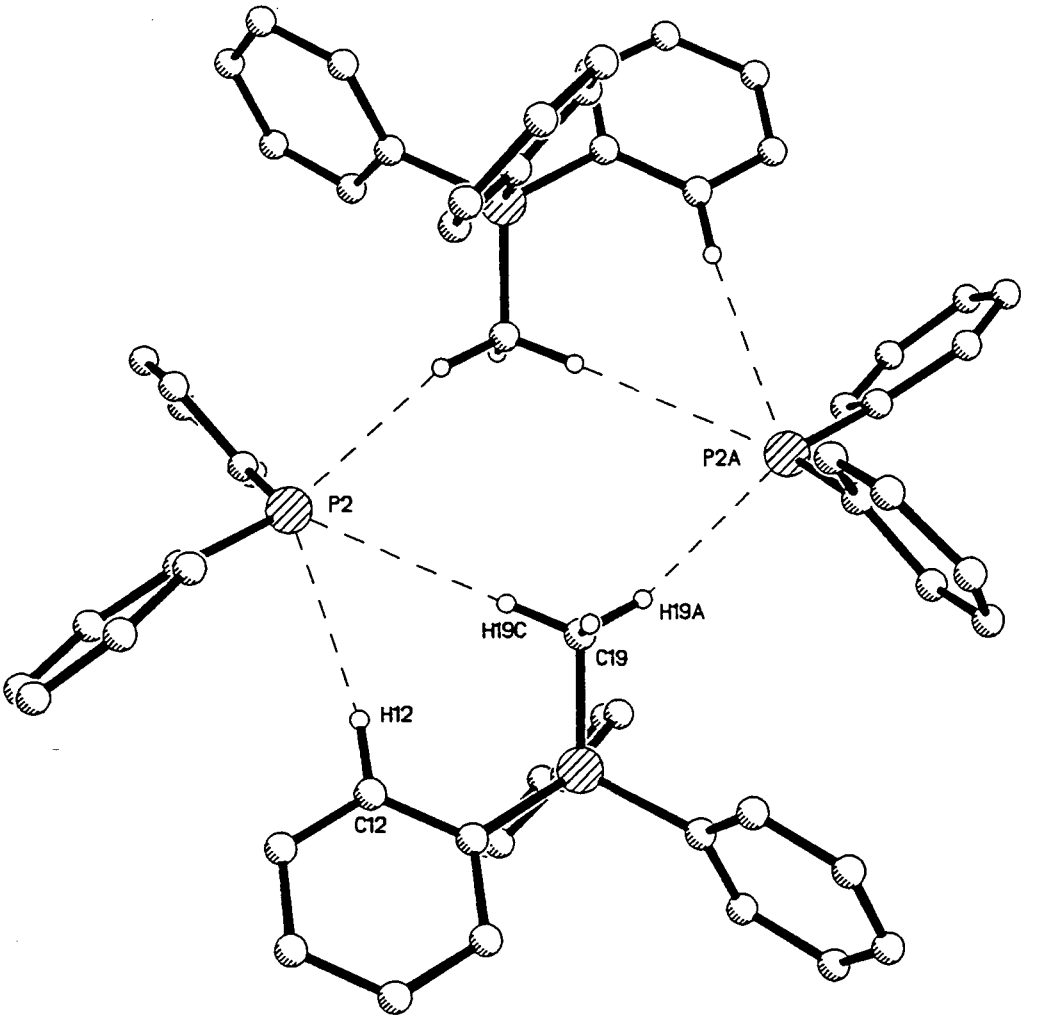

Figure 5.6 Dimers of (15), all CF_3 groups and aryl hydrogen atoms, except those involved in hydrogen bonding, have been omitted for clarity.

In conclusion, the following points highlight the salient results of the experimental investigations reported in this chapter.

(i) This work demonstrates that the strategy of deprotonating phenolic organic acids with basic phosphonium ylides to form aryloxide salts can be extended, resulting in the formation of phosphonium amides and phosphides.

(ii) Two amides, (13) and (14), and one phosphide, (15), were isolated and characterised by single crystal X-ray diffraction. As previously, for the phosphonium aryloxides, these were also found to be extensively hydrogen bonded.

(ii) Reaction of (2) with diphenylamine resulted in the formation of the first example of a 'naked' Ph_2N^- anion, something that had been unobtainable by previous strategies. Another secondary amine, carbazole, was also shown to form a phosphonium amide with (2).

(iii) Further investigation into the generality of this method resulted in the formation of a phosphonium phosphide (15), the first example of its kind.

These results suggest that the mode of aggregation via hydrogen bonding is one that can be observed generally in alkytriphenylphosphonium salts and these compounds offer a general base for studying weak hydrogen bonds in the absence of other more dominating intermolecular interactions.

Chapter 6

6. DISCUSSION - MULTIFUNCTIONAL PHENOLS

We have previously shown how the reactions of phosphonium ylides with simple organic acids led to the isolation of hydrogen bonded organic phosphonium salts (Chapters 4 and 5). In extending this work we were interested in the reactions of phosphonium ylides and imines with multifunctional compounds, that is those containing more than one acidic proton. The following chapter will discuss our investigation of interactions with organic acids possessing two phenolic groups, resulting in compounds (16) to (20) and those possessing four phenolic groups resulting in compounds (21) to (23), the numbering of compounds is consistent with that seen previously. All compounds were characterised by single crystal X-ray diffraction except for (18).

One type of multifunctional organic acid we chose to study was the bisphenol, 4,4'-methylenebis(2,6-di^{t}butylphenol), (Figure 6.1). Obvious comparisons can be drawn with the monofunctional phenol derivative , 2,6-di^{t}butyl-4-methylphenol, and the bisphenol was therefore expected to form complexes with phosphonium ylides and the related iminotriphenylphosphorane, Ph_3PNH, (4).

Reaction of (2) with bisphenol in a 2:1 ratio in a dry acetonitrile solution resulted in the formation of a red precipitate which dissolved on further heating. On cooling bright red crystals were formed. Characterisation ultimately by X-ray diffraction revealed the expected formation of a phosphonium salt, $[(Ph_3PEt)^+]_2[CH_2(2,6,-{}^tBu_2\text{-}C_6H_2O)_2]^{2-}$, (16), (Figure 6.2). The bisphenol is doubly deprotonated with the transfer of its acidic phenolic protons to the basic ylidic carbons. This results in units consisting of two cations associated with one anion. This structure is not symmetrical, instead each cation is interacting with the anion in two very different ways. One cation (cation A) is interacting with an anionic oxygen in a way that has come to be expected. The resulting motif of the

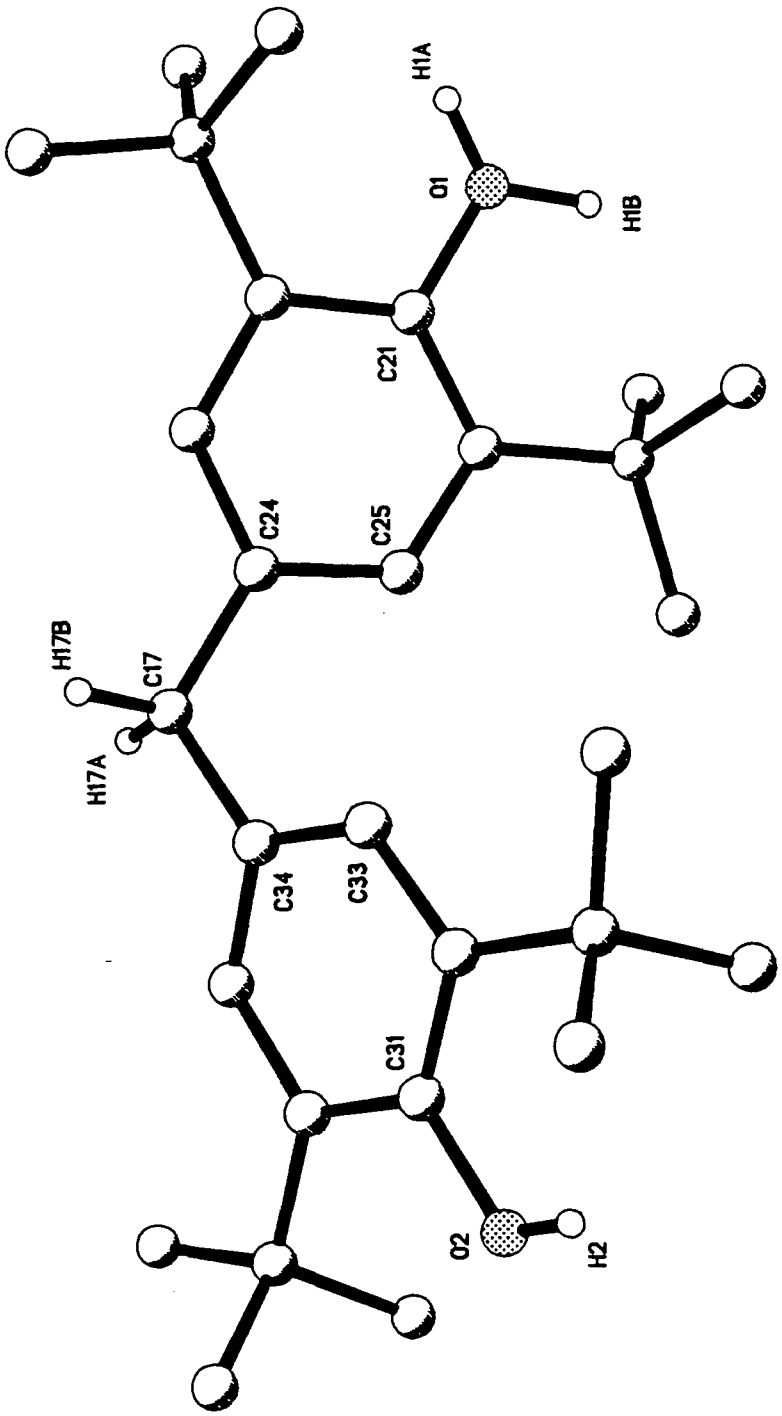

Figure 6.1 The molecular structure of 4,4'-methylenebis(2,6-di^{t}butylphenol), (bisphenol). All aryl and ^{t}butyl hydrogen atoms have been omitted for clarity. H1A and H1B on O1 are each at 50% occupancy.

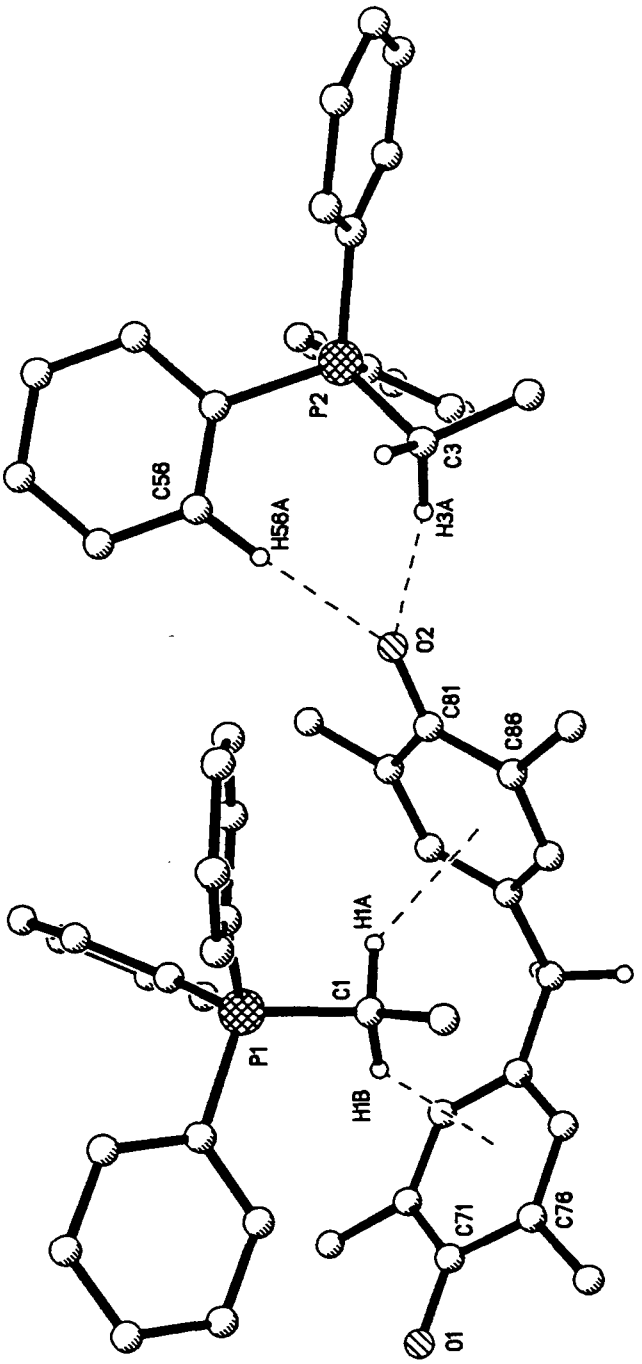

Figure 6.2 The molecular structure of $[(Ph_3PEt)^+]_2[CH_2(2,6,\text{-}^tBu_2\text{-}C_6H_2O)_2]^{2-}$, (16). All aryl hydrogen atoms, except those involved in hydrogen bonding, and the methyl groups of each ^{t}Bu have been omitted for clarity.

oxygen (O2) being chelated by an alkyl and aryl (C)-H donor in a manner previously observed for the phosphonium salts discussed in the previous chapters.

In contrast the second cation (cation B) sits above the bisphenol in the cup-like region the bisphenol defines with the two hydrogen atoms of its CH_2 group directed towards the arene rings of the bisphenol. Consequently two C-H...π hydrogen bonds are observed. All hydrogen bonds parameters are given in Table 6.1.

Table 6.1 Hydrogen bond parameters of (16)

Interaction	C...X distance (Å)	H...X distance (Å)	C-H...X angle (°)
C56-H56A...O2	3.357	2.281	174.0
C3-H3B...O2	3.225	2.164	167.1
C1-H1A...π	3.476	2.520[i]	147.0
C1-H1B...π	3.455	2.513[ii]	145.2
C35-H35B...O1	2.942	2.023	140.9

i perpendicular distance from the H atom to the plane of the ring (C81-C86)
ii perpendicular distance from the H atom to the plane of the ring (C71-C76)

This mode of interaction leaves the second anionic oxygen (O1) unprotected and a potential hydrogen bond acceptor. On the supramolecular level these anion-cation units can be seen to polymerise via the interaction of this second anionic oxygen with a para C(aryl)-H of a phenyl group belonging to a cation of type B in a neighbouring unit (Figure 6.3).

Reaction of the iminophosphorane (4) with bisphenol, again in a 2:1 ratio in a dry acetonitrile solution resulted in the formation of a red precipitate which dissolved on heating. Cooling to room temperature yielded red crystals suitable for X-ray diffraction. Characterisation by ^{1}H NMR spectroscopy suggested that in this case (4) had not deprotonated the bisphenol as two broad peaks assignable to two OH groups and two NH groups were observed. Single crystal X-ray diffraction confirmed this with the solid-state

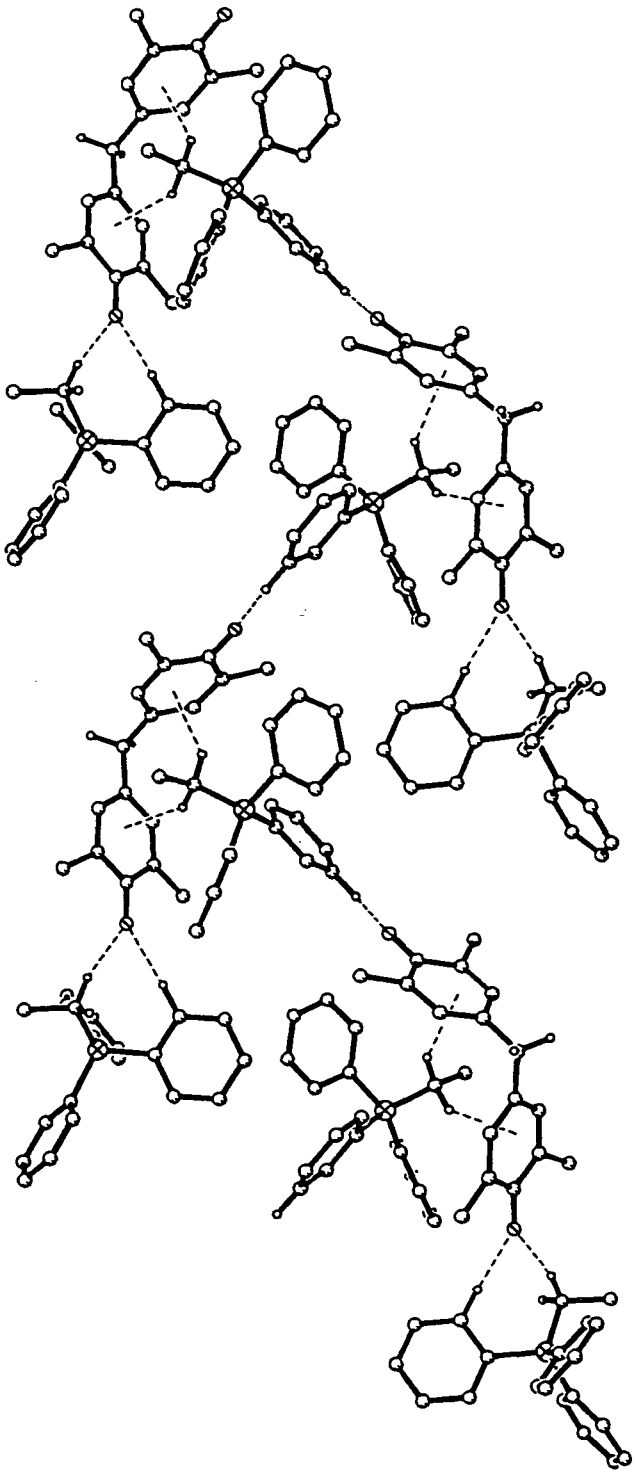

Figure 6.3 The polymeric structure of (16). All aryl hydrogen atoms, except those involved in hydrogen bonding, and the methyl groups of each ^{t}Bu have been omitted for clarity.

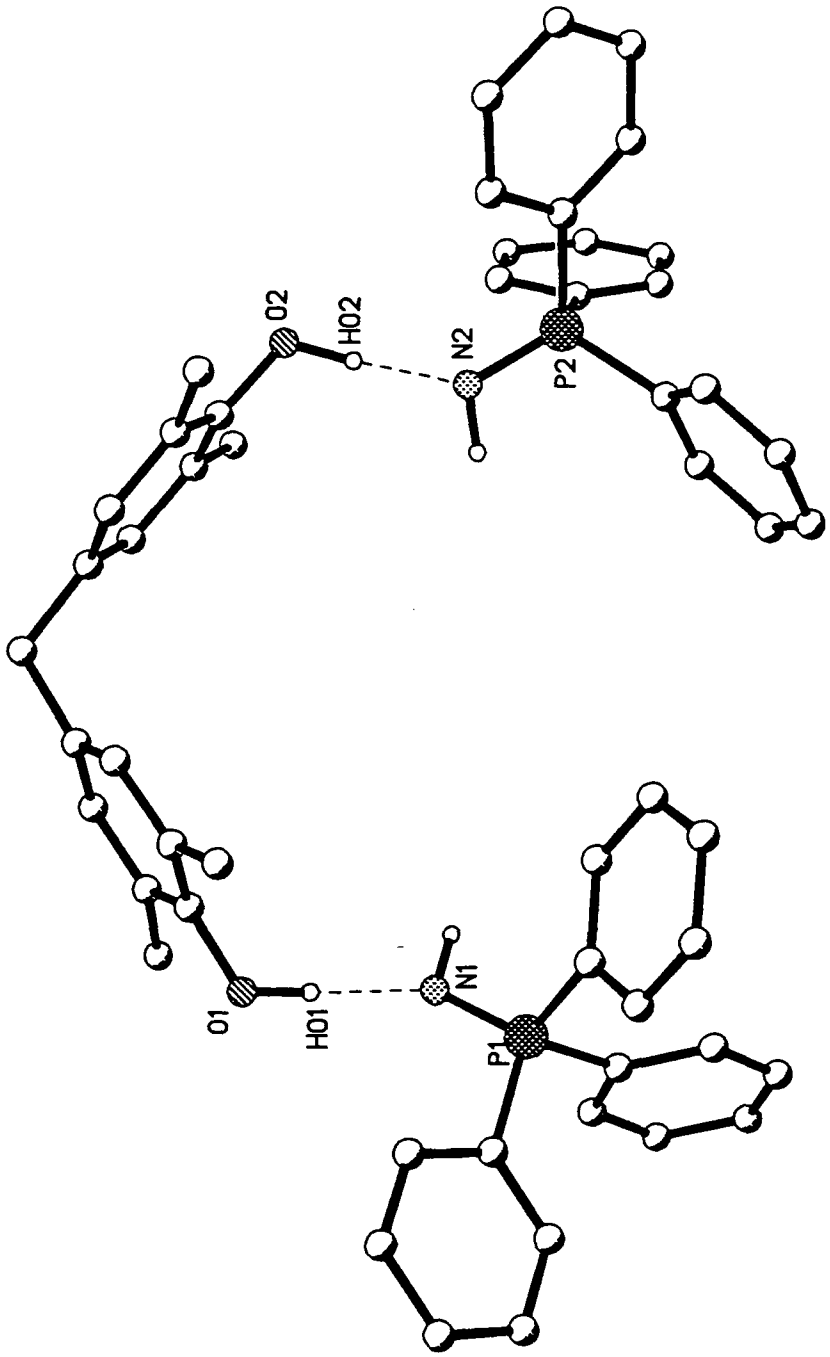

Figure 6.4 The molecular structure of $[Ph_3PNH]_2[CH_2(2,6,\text{-}^tBu_2\text{-}C_6H_2OH)_2]$, (17). All aryl hydrogen atoms and the methyl groups of each ^{t}Bu have been omitted for clarity.

structure being that of the adduct $[Ph_3PNH]_2.[CH_2(2,6,-^tBu_2-C_6H_2OH)_2]$, (17), (Figure 6.4). The two components of this adduct are linked by two O-H...N hydrogen bonds, an iminophosphorane being associated with each phenolic group of the bisphenol. All hydrogen bond parameters are given in Table 6.2. The lack of deprotonation in (17) is possibly attributable to the fact that iminophosphoranes such as (4) are less basic than phosphonium ylides. Consequently, in this case, (4) is presumably insufficiently basic to deprotonate the bisphenol.

On the supramolecular level, the adducts can be seen to stack in parallel columns. However neighbouring columns pack so the bisphenols are orientated with their linking CH_2 groups pointing in opposite directions and the phenyl groups of imines in neighbouring columns interlock (Figure 6.5). This results in the imines of neighbouring columns sitting above the cup like cavity defined by the bisphenol with a phenyl group sitting inside this cup. On closer examination there seems a possibility the two of these C(aryl)-H are involved in C-H...π interactions, with the arene rings of the bisphenol, (Figure 6.6 and Table 6.2a).

Table 6.2 Hydrogen bond parameters of (17)

Interaction	O...N distance (Å)	H...N distance (Å)	O-H...N angle (°)
O1-HO1...N1	2.736(3)	1.742(7)	159.9(7)
O2-HO2...N2	2.684(3)	1.664(7)	174.3(4)

This mode of interaction is not unprecedented. Results reported by Glidewell et al[1] on the interactions of the related 4,4'-bisphenols of the type $X(C_6H_4OH)_2$ with hexamethylenetetramine, $(CH_2)_6N_4$, (HMTA), have led to similar adducts. One difference that should be noted is that HMTA is capable of accepting two hydrogen bonds therefore unlike (17) forms 1:1 adducts leading to chains where the adducts are linked not isolated adducts in stacks as in (17). Reaction of HMTA with the bisphenols where X = S or SO_2 leads to the formation of adducts in which the HMTA and bisphenols interact via O-H...N hydrogen bonds. The HMTA can be seen to bridge between two bisphenols via two O-H...N hydrogen bonds to form chains or alternating amines and phenols. These O-

[1]P. I. Coupar, C. Glidewell and G. Ferguson, *Acta Cryst., Sect. B*, 1997, **53**, 521.

H...N hydrogen bonds are of comparable lengths to those observed in (17), (Table 6.2), the O...N distance being 2.728(3) and 2.715(4) Å for X = S and X = SO_2 respectively. These chains pack in a similar manner to the stacks in (17) with the X groups of the bisphenols forming parallel chains pointing in opposite directions and the amines of one chain sitting above the cup defined by the bisphenol in the neighbouring chain. Here two C-H...π interactions are reported with two hydrogen atoms from a CH_2 group of HMTA being directed towards the arene rings of the bisphenols. H...C contacts from the HMTA hydrogen atoms to the carbon atoms of the rings range from 2.76 - 3.05 Å where X = S and 2.87 - 3.06 Å where X = SO_2. These are comparable with the analogous distances for the proposed C-H...π interactions in (17), (Table 6.2a). Considering the C-H...π interactions observed in the HMPTA adducts and those in (16) it would seem that these bisphenols are good C-H...π hydrogen bond acceptors and hence those proposed in (17) are feasible.

By comparing the structure of bisphenol itself with those of (16) and (17) it allows us to observe how the bisphenol component is affected by deprotonation and co-crystallisation respectively. Examination of the C-O bonds reveal that, as expected, the bond lengths of the bisphenol and (17) are very similar, while in (16) the anionic oxygen atoms form C-O bonds which are significantly shorter, and probably have partial double bond character (Table 6.3). However, the angles at the methylene bridge are almost identical for bisphenol and (16). Meanwhile it is more acute in (17), this is probably a requirement of the packing observed in (17) (Table 6.3).

Table 6.3 Parameters for the parent bisphenol, (16) and (17)

Compound	Average C-O bond length (Å)	Angle at methylene bridge (°)
Bisphenol	1.385	115
(16)	1.299	116
(17)	1.383	111

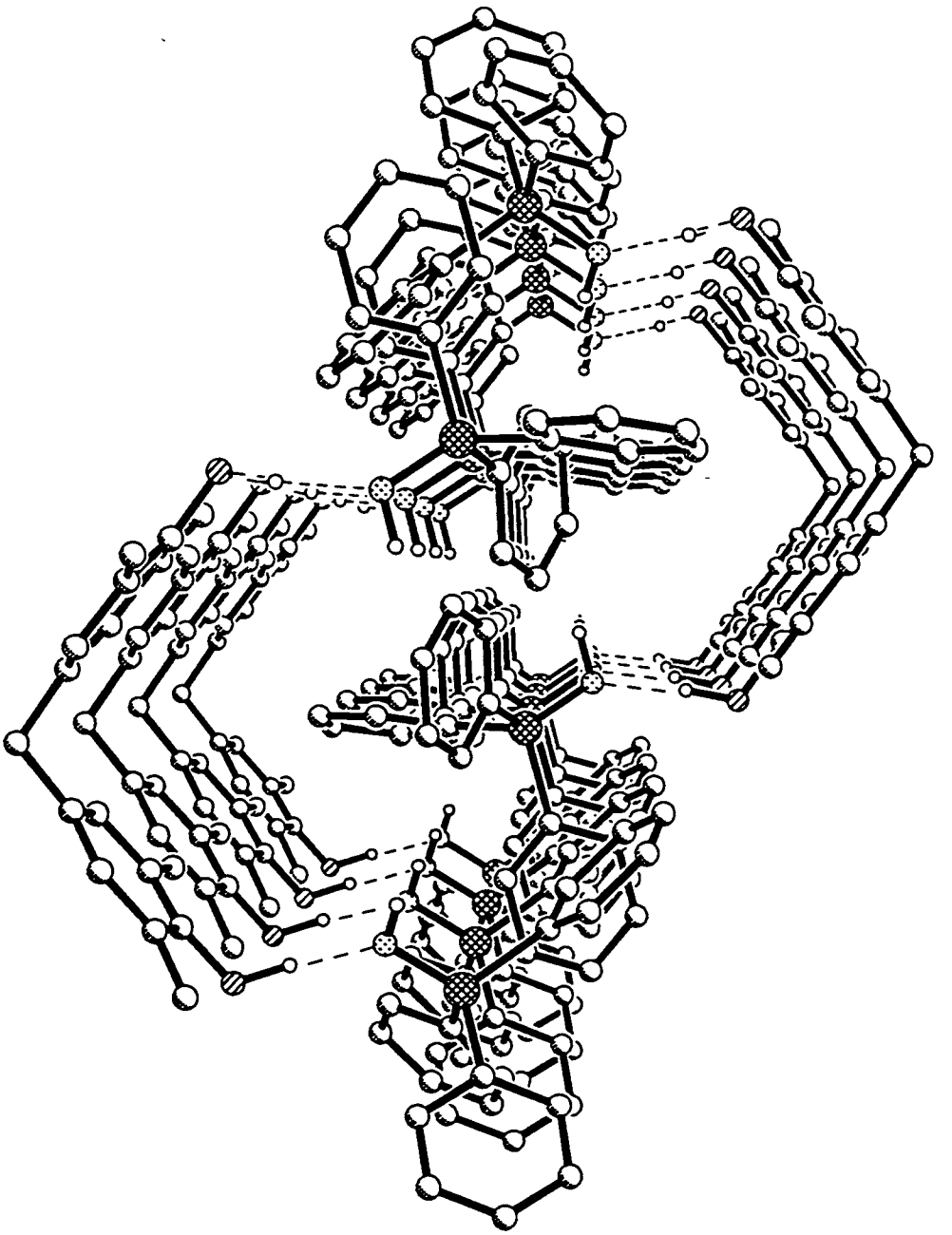

Figure 6.5 The packing arrangement of (17) viewed down the a axis. All aryl hydrogen atoms and the methyl groups of each ^{t}Bu have been omitted for clarity.

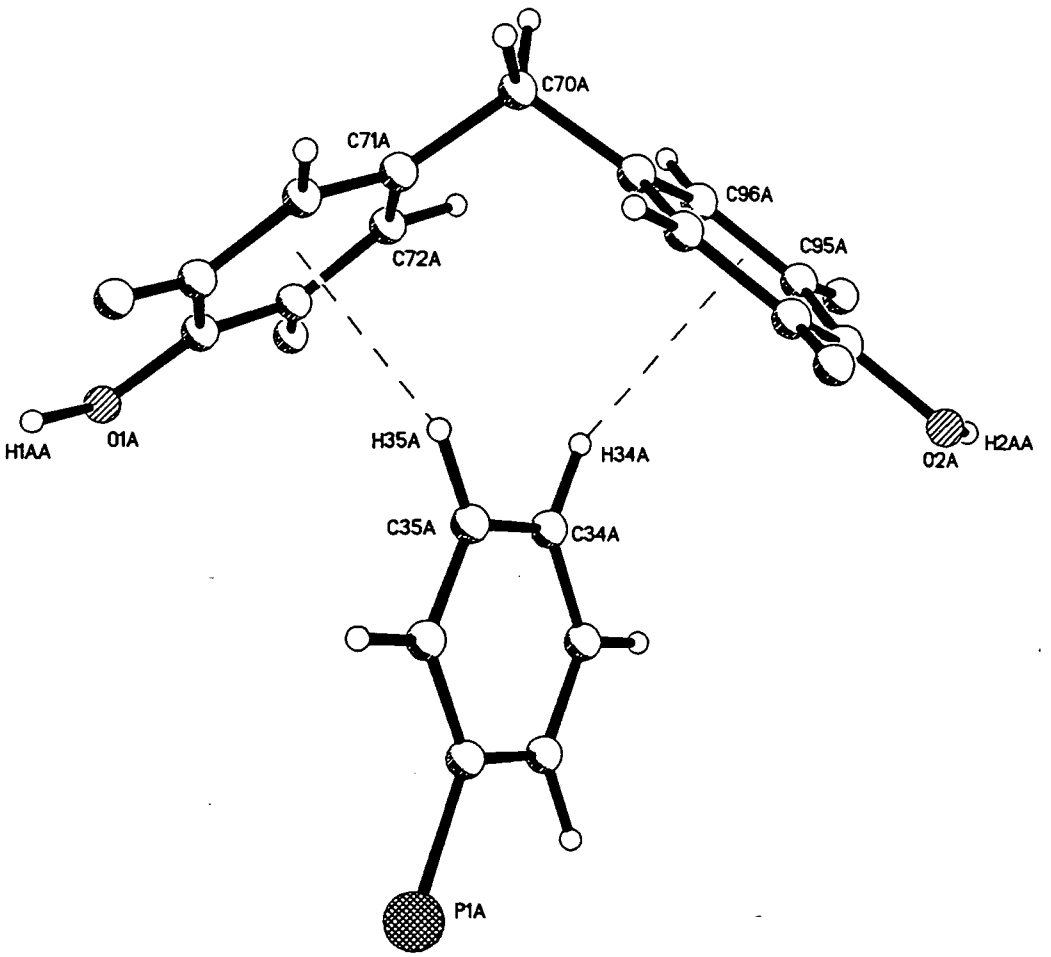

Figure 6.6 The proposed C-H...π bonding between neighbouring adducts. The methyl groups of each ^{t}Bu, and the full iminophosphorane molecule have been omitted for clarity.

Table 6.2a C-H...π interactions of (17)

Interaction	C...π distance (Å)	H...π distance (Å)	C-H...π angle (°)
C34A-H34A...π	3.609	2.93[i]	121[ii]
C35A-H35A...π	3.507(3)	2.71[iii]	130[iv]

i perpendicular distance from the H atom to the plane of the ring (C91A-C96A)
ii angle between the C-H bond and the centroid of C91A-C96A
iii perpendicular distance from the H atom to the plane of the ring (C71A-C76A)
iv angle between the C-H bond and the centroid of C71A-C76A

Another feature of interest is how the relative positions of the two arene rings alter on going from bisphenol to (16). Figure 6.7 shows all three bisphenol units. One arene ring has been drawn in the same orientation for all three to show at a glance how the relative positions of the two rings change dramatically in the three different compounds.

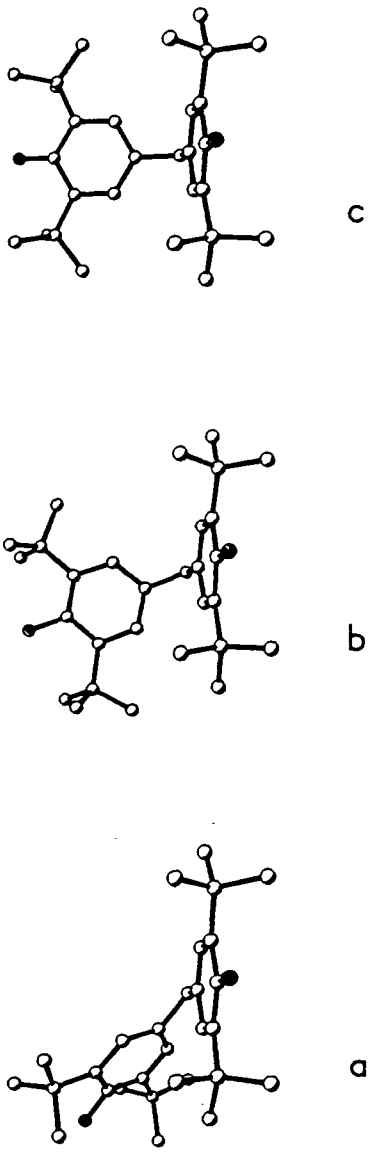

Figure 6.7 The bisphenol components of a) bisphenol, b) (17), c) (16), illustrating the variation in the relative postions of the arene rings. All hydrogen atoms have been omitted for clarity.

In the simpler case of biphenyl (Figure 6.8a), in order to calculate the relative positions of the two rings it would simply require a calculation of the torsion angle between C1-C2-C3-C4, that is the difference in angle between the bonds C1-C2 and C3-C4 when viewed down the bond C2-C3 (Figure 6.8b).

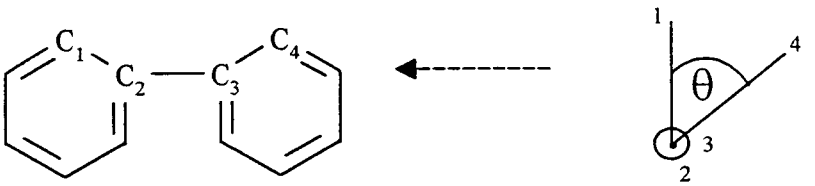

a. Biphenyl b. Torsion angle

Figure 6.8

However, in our case we have a methylene bridge between the two rings and a single parameter will not suffice. If we consider Figure 6.9 (where C3 is the methylene bridge) there is a unique position when the bonds C1'-C2 and C1-C2 eclipse C5'-C4 and C5-C4 respectively. In this eclipsed position the torsion angle of C1-C2-C3-C4 would be the same as that between C5-C4-C3-C2. Therefore any deviation from this eclipsed position would result in a difference between the two torsion angles, $\Delta\theta$. This difference in effect, quantifies the difference in the orientations between the two arene rings.

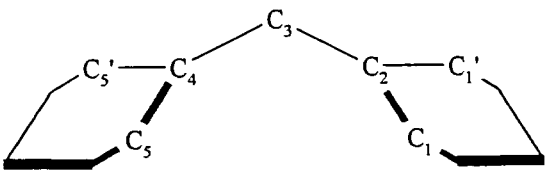

Figure 6.9

The relevant torsion angles were calculated to obtain $\Delta\theta$ for the three compounds (Table 6.4). They reveal that (16) is almost completely eclipsed, however in the parent bisphenol the arene rings are almost at right angles. (17) is between these two extreme positions

Table 6.4 $\Delta\theta$ for the parent bisphenol, (16) and (17)

Compound	$\Delta\theta$ (°)
Bisphenol	78.0
(16)	0.4
(17)	17.2

Reaction of (1) and bisphenol in dry acetonitrile resulted in a red precipitate which dissolved on heating. Cooling resulted in the formation of red crystals. Preliminary characterisations were carried out and the ^{1}H NMR pointed to the formation of a phosphonium salt $[(Ph_3PMe)^+]_2[CH_2(2,6,\text{-}^tBu_2\text{-}C_6H_2O)_2]^{2-}$, (18). Unfortunately no X-ray structure was obtained. In postulating the structure of (18), the structures of (16) and (17) were considered. Although (1) and (4) are isostructural the ^{1}H NMR of (18) does not reveal the presence of OH protons and the ^{31}P NMR spectrum points to the formation of a phosphonium salt, strongly suggesting that proton transfer has occurred. Also if one considers the interactions of (1) and (2) with the monofunctional organic acids described in the preceding chapters it would be plausible to postulate that (18) would be similar to (17).

In an extension of our investigations into the reactions of phosphonium ylides with organic acids possessing two phenolic groups, a further two such organic acids were chosen for study, namely, catechol and N,N'-ethylenebis(salicylideneimine), (H_2salen). The following section reveals how reaction of both with (2) led to partial deprotonation of the organic acid to form the phosphonium salts (19) and (20).

Reaction of (2) with catechol in a 1:1 ratio in dry acetonitrile resulted in the formation of a bright yellow precipitate which dissolved on heating. Cooling to room temperature yielded a crop of crystals. Analysis, ultimately by single crystal X-ray diffraction revealed the expected formation of the phosphonium salt $[(Ph_3PEt)^+(C_6H_5O_2)^-]_2$, (19). In the asymmetric unit there are two different anion-cation units; however, in both cases, the transfer of an acidic proton from one of the catechol's phenolic groups to the basic ylidic carbon has occurred. These two different units lead to two types of dimers. In both cases the dimers' aggregation is not through an extension of the C-H...O hydrogen bond

network, as observed for the phosphonium aryloxides in chapter 4, but instead through stronger O-H...O hydrogen bonds. This is possible due to the presence of both anionic oxygens and phenolic groups in the anions. Neighbouring units interact via two O-H...O hydrogen bonds between anions, the anions simultaneously acting as both hydrogen bond acceptors and donors (Figure 6.9).

In both dimers the anions and cations are held together by C-H...O hydrogen bonds. This difference in the two anion-cation units is manifested in one way by the mode of hydrogen bonding observed. Dimer A displays the by now familiar motif of C(alkyl)-H and C(aryl)-H donor chelating the anionic oxygen. In contrast in dimer B the orientation of the cation with respect to the anion is different and, although the C(alkyl)-H hydrogen bond is still observed, the C(aryl)-H interaction is no longer feasible. A possible second interaction involves a C(alkyl)-H from the cation's CH_3 group interacting with an oxygen (C02B...O2B 3.229 Å). This is reminiscent of the bonding pattern observed in the carbazole complex, (14), in Chapter 5. In dimer A the anions are planar, (Figure 6.9a), but dimer B, (Figure 6.9b), is stepped. The presence of two types of dimer is presumably a consequence of the packing arrangement. All hydrogen bond parameters are given in Table 6.5.

Table 6.5a Hydrogen bond parameters in dimer A of (19)

Interaction	X...O distance (Å)	H...O distance (Å)	X-H...O angle (°)
C01-H1A...O1'A	3.160	2.21	145
C32-H32...O1'A	3.346	2.29	167
O2'B-H2'B...O1'A	2.663(2)	1.84(3)	151(3)
O2'A-H2'A...O1'B	2.663(2)	1.84(3)	151(3)

Table 6.5b Hydrogen bond parameters in dimer B of (19)

Interaction	X...O distance (Å)	H...O distance (Å)	X-H...O angle (°)
C01-H1BB...O1B	3.204	2.22	150
O2B-H2B...O1A	2.592(2)	1.72(3)	156(2)
O2A-H2A...O1B	2.592(2)	1.72(3)	156(2)

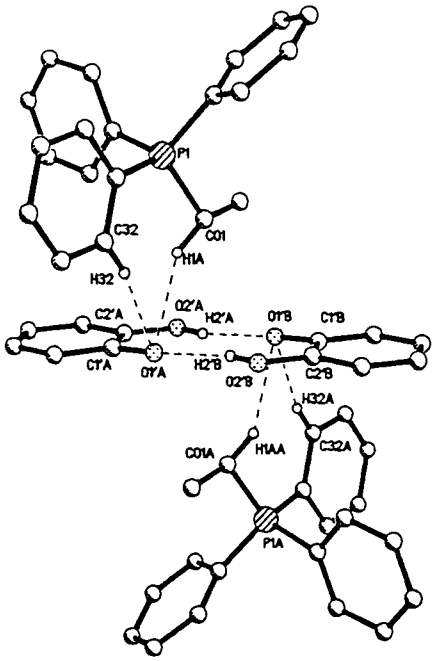

Figure 6.9a Dimer A of (19). All hydrogen atoms except those involved in hydrogen bonding have been omitted for clarity.

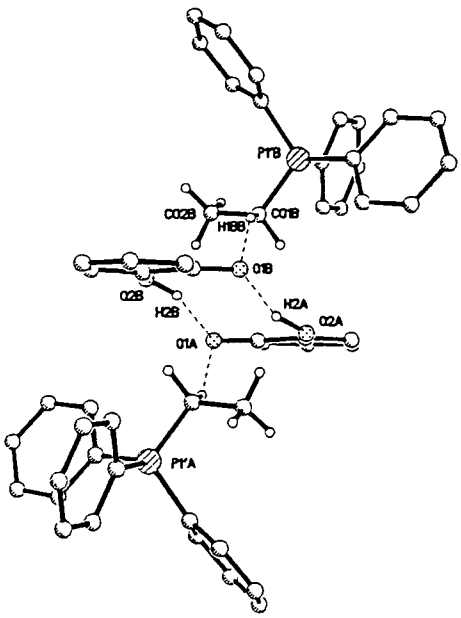

Figure 6.9b Dimer B of (19). All aryl hydrogen atoms except those involved in hydrogen bonding have been omitted for clarity.

Several structures were found that contain a monodeprotonated catechol, most commonly coordinating to metal centres.[2] However, only one example of a monodeprotonated catechol anion with a non coordinating organic cation was found, namely $(NH_4)^+(C_6H_5O_2)^-.C_6H_6O_2.H_2O$.[3] Here, however, it is the fully protonated catechol that is associated with the ammonium cation through hydrogen bonds, the monodeprotonated catechol anions interact only with the protonated catechol and not with the cation. The intramolecular average O...O distance in (19) is 2.622 Å. This, as expected, is shorter than those found in the structure of the parent catechol (average 2.770 Å).[4] However, this is not unsurprising as in this latter case the O-H...O hydrogen bonding does not involve an anionic oxygen.

In continuation of this strategy reactions with N,N'-ethylenebis(salicylideneimine) (H_2salen) were undertaken. Reaction of (1) and (3) with H_2salen led to unexpected results and these will be discussed in Chapter 7. Reaction of H_2salen with either one or two equivalents of (2) in a 1:1 acetonitrile:toluene solution yielded a yellow, crystalline solid. Preliminary analysis and an X-ray crystal structure confirmed the product to be the phosphonium salt of the monodeprotonated organic acid $[(Ph_3PEt)^+(Hsalen)^-]_n$, (20), (Figure 6.10). The crystallographic asymmetric unit also contains one molecule of acetonitrile. Considering only the ion-pair, the structure is as predicted and in accord with our previous findings. One phenolic group has been deprotonated by (2) and the cation chelates the anionic oxygen centre via both C(alkyl)-H and C(aryl)-H donors. All hydrogen bond parameters are given in Table 6.6.

Table 6.6 Hydrogen bond parameters for (20)

Interaction	X...X' distance (Å)	X...X' distance (Å)	X-H...X' angle (°)
C36-H36...O2	3.599(6)	2.666(6)	143.5(1)
C51-H51B...O2	3.412(6)	2.565(6)	143.5(1)
O1-H1-O2	2.463(4)	1.62(7)	167.53(5)
C5-H5...N1	3.624(6)	2.683(6)	171.1(1)

[2]see for example C. Nather, A. John, K. Ruppert and H. Bock, *Acta Cryst., Sect. C,* 1996, **52**, 1166; R. H. Heistand, A. L. Roe and L. Que Jr., *Inorg. Chem.*, 1982, **21**, 676.
[3]O. Kumberger, J. Riede and H. Schmidbaur, Z. Naturforsch., Teil B, 1993, **48**, 958.
[4]H. Wunderlich and D. Mootz, *Acta Cryst., Sect. B,* 1971, **27**, 1684.

To our knowledge the anion derived from H_2salen that is uncoordinated to a metal centre is unprecedented. In H_2salen itself, whose solid-state structure is known[5] the phenolic group participates only in intramolecular hydrogen bonding with the iminic N atoms to give discrete molecules in the crystal, but in (20), as in (19), the presence of both anionic oxygen atoms and phenolic OH groups gives rise to strong intermolecular O-H...O bonds. In this case dimers are not formed, instead the Hsalen$^-$ anions self assemble into infinite chains via very short O-H...O hydrogen bonds (Table 6.6). The packing of these chains is such that an array of cations interact alternatively with chains of anions lying above and below them (Figure 6.11). Taken in isolation these bilayers of cations and anions resemble an inorganic clay-like structure. However, instead of infinite two-dimensional sheets of anions, which would be required in order to take this analogy further, secondary interactions between the chains of anions are finite. Two coplanar chains are further associated by means of mutual C-H...N interactions (Table 6.6), to give molecular tapes, (Figure 6.12), which are ordered in the crystal such that they are alternatively orthogonal and staggered. In this way tunnels are defined, (Figure 6.13), in which one dimensional arrays of cations are located (Figure 6.14). Calculation of the area within the four anions defining a channel allowed the size of these infinite channels along the b axis to be obtained. The distance between one set of parallel planes was estimated to be 10.1 Å while that between the set of parallel planes perpendicular to these was estimated to be 11.0 Å. Hence, the cross-sectional area of the cavity can be said to be approximately 110 Å^2. Small voids at the intersections between orthogonal tapes are filled by non-interacting guest acetonitrile molecules. Perhaps significantly, there are no obvious intermolecular contacts between orthogonal tapes which may reduce the rigidity of the framework with respect to potential cation exchange. Overall, the monodeprotonation of H_2salen gives rise to the self assembly of a three-dimensional host lattice of anions in which large tunnel-like voids are filled by guest cations. Alternatively, the overall structure may be interpreted as two interpenetrating and nearly orthogonal bilayers of cations and anions. The question arises as to why the structure self-assembles as it does, instead of as a more obvious bilayer topology, comprising of infinite sheets of anions, especially as such an arrangement would maximise hydrogen bond interactions.

---

[5]N. B. Pahor, M. Calligaris, G. Nardin and L. Randaccio, *Acta Cryst., Sect. B*, 1978, **34**, 1360.

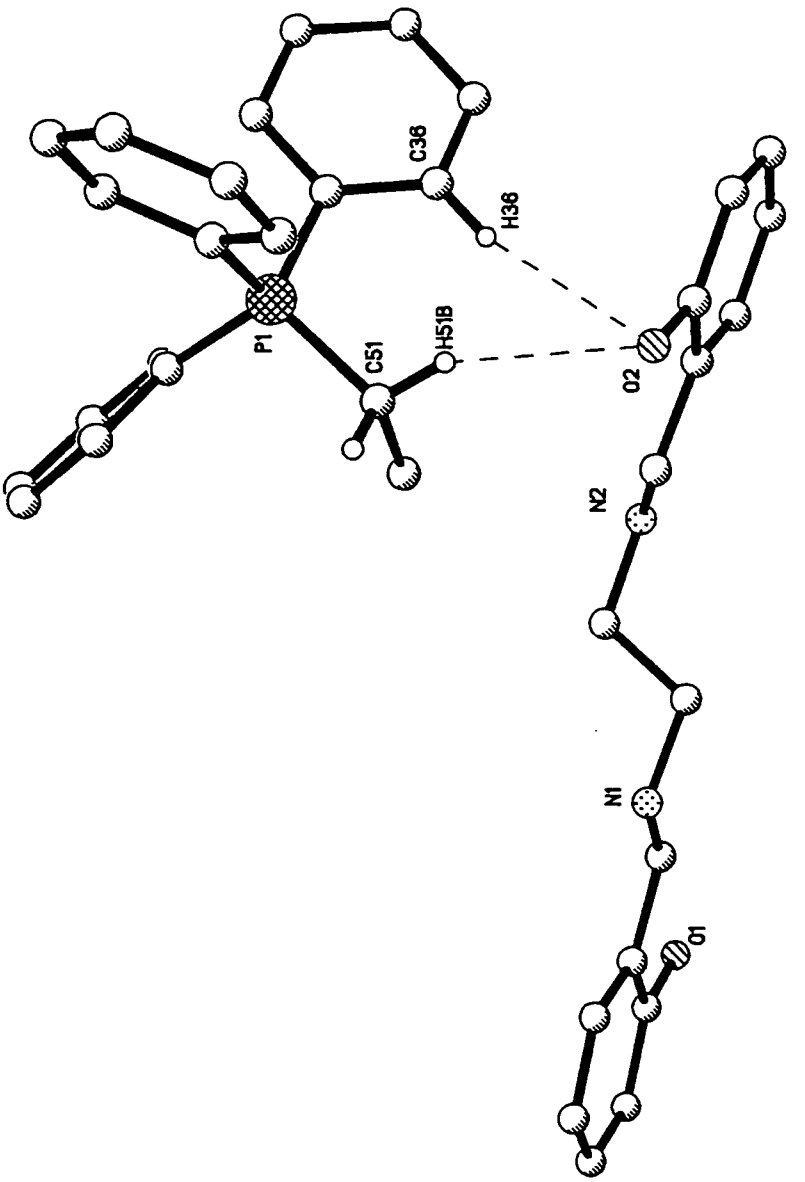

Figure 6.10 The molecular structure of $(Ph_3PEt)^+(Hsalen)^-$, (20). All hydrogen atoms except those involved in hydrogen bonding and lattice CH_3CN have been omitted for clarity.

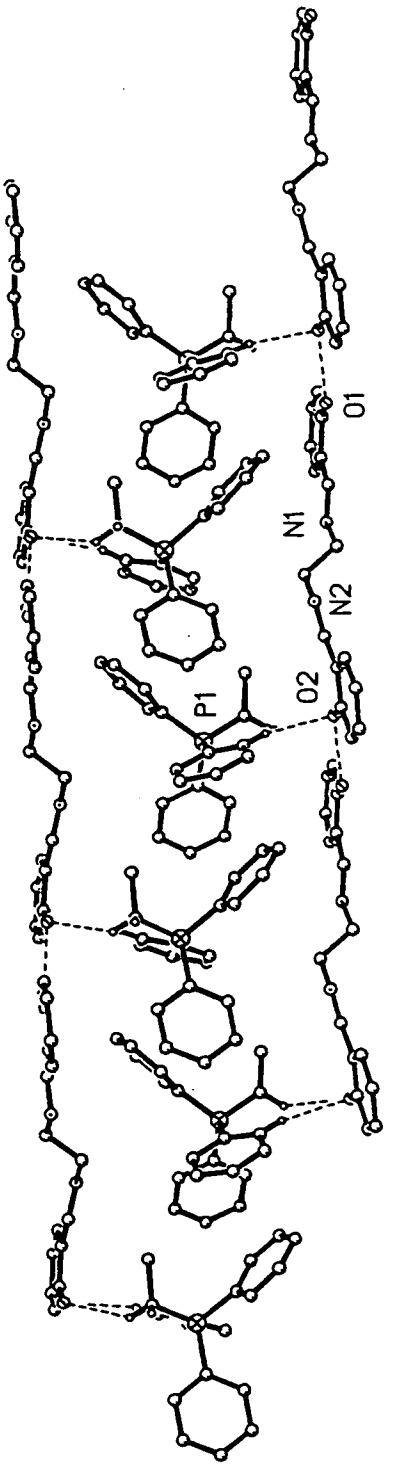

Figure 6.11 The packing of the anion chains in (20), showing how the cations interact alternately with the chain layer above and below.

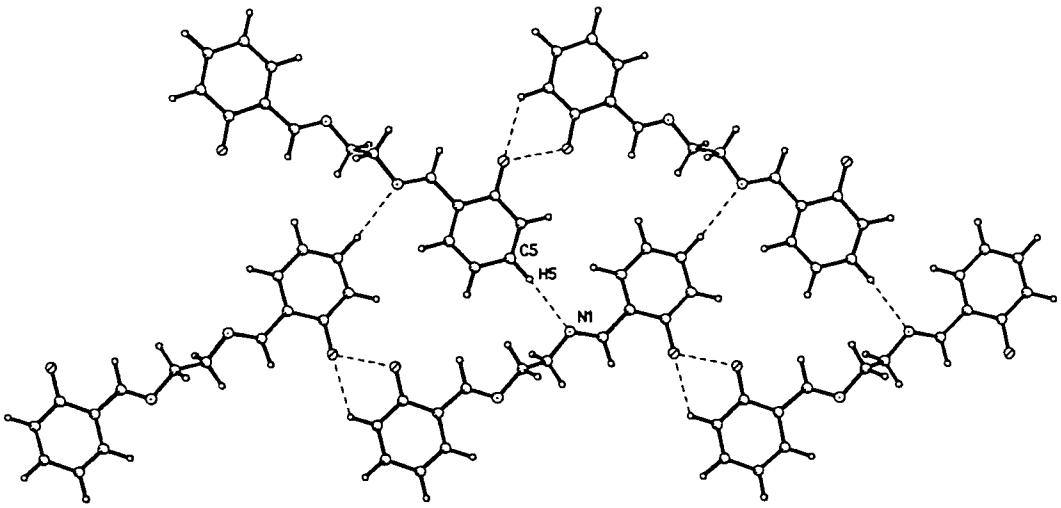

Figure 6.12 Co-planar chains associated by means of mutual C-H...N hydrogen bonds.

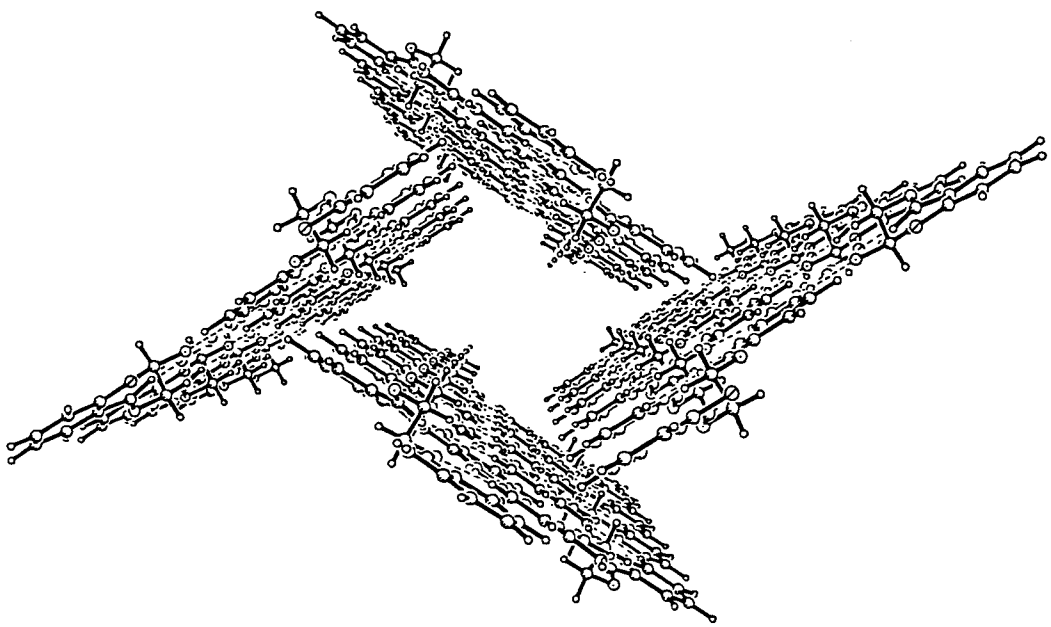

Figure 6.13 Tunnels defined by the anions of (20).

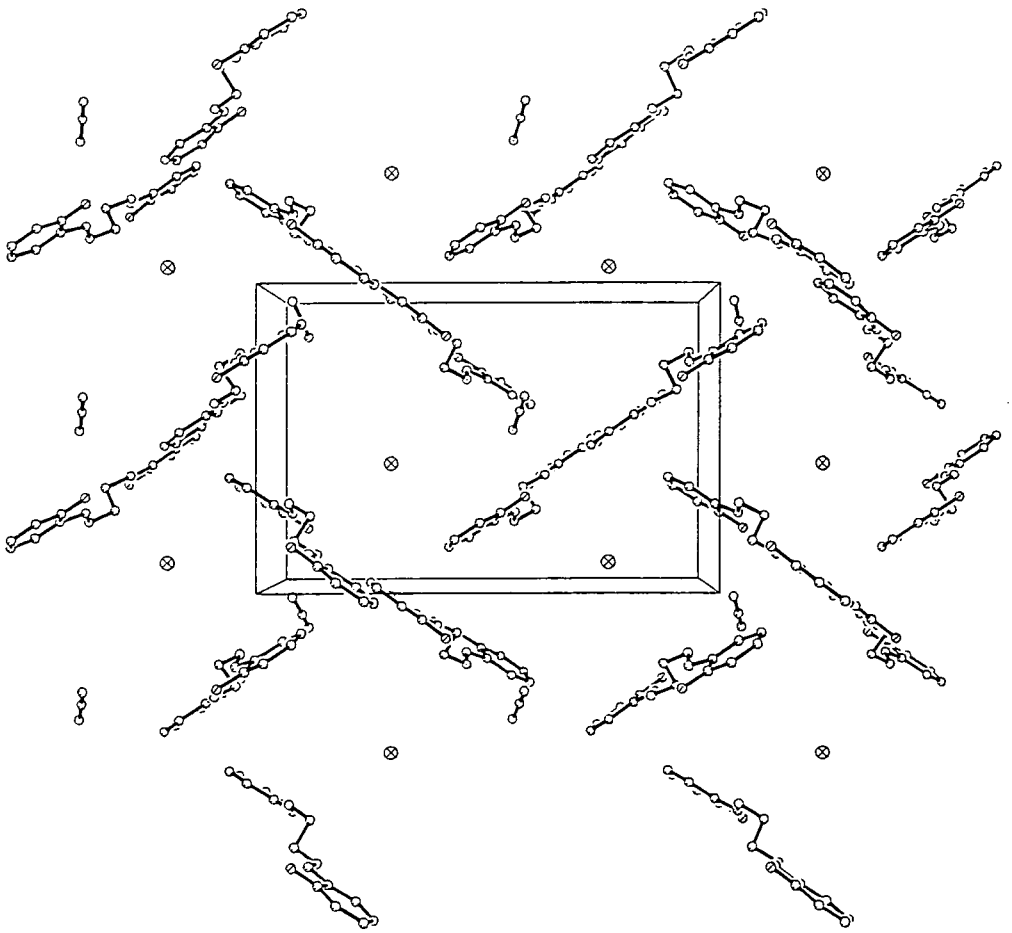

Figure 6.14 Packing of anions and cations to illustrate the location of the cations in the anion-defined tunnels. Here only the phosphorus atoms of the cations are shown.

We believe two factors favour the observed structure. Firstly, the location of cations in anionic tunnels maximises the anion-cation proximity, while minimising cation-cation interactions, which is favourable from simple electrostatic considerations. Secondly, the self-assembly of anions into tapes rather than two-dimensional sheets is entropically favoured. Such considerations as these are known to be important in predicting supramolecular structures.[6]

Both (19) and (20) demonstrate that partial deprotonation of a biphenolic precursor using an organic base gives rise to the self-assembly of anions via strong O-H...O hydrogen bonds between anionic and phenolic oxygens.

Having investigated the interaction of bifunctional phenols our attention turned to a type of compound possessing four phenolic groups namely *p-tert*-butylcalix[4]arene (LH_4) Figure 6.15. The calixarenes[7] are a type of organic compound capable of existing in a 'cone' conformation often referred to as basket-like in shape (Figure 6.15b). They possess the potential for forming host-guest complexes, the guest molecule residing within the host's cavity. Interest arose in these type of systems due to their potential as clathrating agents for organic molecules and in today's supramolecular chemistry calixarenes are a well-established class of compounds. *p-tert*-Butylcalix[n]arenes, where n = 4, 6, 8 are commercially available and many derivatives of calixarenes are based upon these parent compounds.

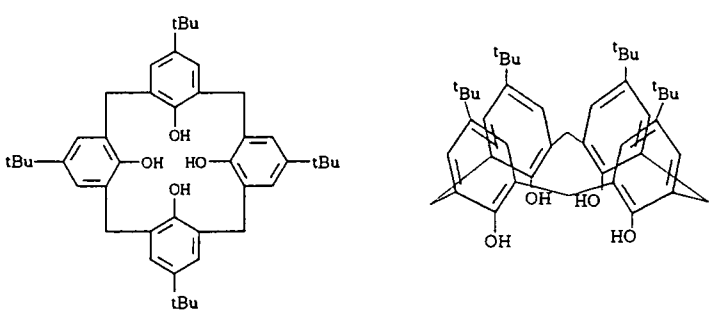

(a) LH_4 (b) cone configuration of LH_4

Figure 6.15

[6]P. R. Ashton, A. N. Collins, M. C. T. Fyfe, P. T. Glink, S. Menzer, J. F. Stoddart and D. J. Williams, *Angew. Chem. Int. Ed. Eng.*, 1997, **36**, 59.
[7]C. D. Gutsche and R. Muthukrishnan, *J. Org. Chem.*, 1978, **43**, 4905.

The cone conformation is favoured for calix[4]arenes because of the strong intramolecular hydrogen bonding between the four OH groups. These are referred to as being at the bottom or at the lower rim of the cavity. The basket-like cavity of LH_4 has already been shown to accommodate a variety of neutral guest molecules. Andreetti et al reported the formation of a LH_4:toluene clathrate in 1979.[8] The calixarene was found to be in the familiar cone configuration with four-fold symmetry, its shape mainly determined by the four intramolecular O-H...O hydrogen bonds (O...O = 2.670(9) Å). The guest toluene molecule was orientated with its C-CH_3 bond on the calixarene's four-fold axis. Interactions between the guest molecule and the cavity were mainly due to the tert-butyl groups. LH_4 has also been found to form complexes in the solid state with chloroform,[7, 9] benzene,[10] xylene,[10] anisole,[10] and acetonitrile[11] In aprotic solvents such as acetonitrile the principal attractive forces between host and guests are said to arise from coulombic charges (charge-charge or dipole-dipole interactions), hydrogen bond interactions, π interactions and/or van der Waals interactions.

It is LH_4 that we chose to study, reactions were carried out with (1), (2) and (4). The same methods were utilised in all reactions namely the reaction of (1), (2) or (4) with LH_4 in a 4:1 ratio in an acetonitrile solution to form (21), (22) and (23) respectively. All three reactions resulted in the formation of crystalline products and structures were obtained by single crystal X-ray diffraction in all three cases.[12] Despite the 4:1 ratio used in these reactions, LH_4 was only monodeprotonated. However, complexes of calix[4]arene anions and organic cations formed from the reaction of amines and calix[4]arenes studied by Gutsche et al[9, 13] were also found to form monodeprotonated products despite amine:LH_4 ratios of up to 10:1. An insight into why only monodeprotonated species are obtained can be gained from consideration of calixarene's pKa values. Unfortunately, attempts to measure pKa values of LH_4 were thwarted by their low solubility. However, the related

---

[8]G. D. Andreetti, R. Unargo and A. Pochini, *J. Chem. Soc., Chem. Commun.*, 1979, 1005.
[9]L. Bauer and C. D. Gutsche, *J. Am. Chem. Soc.*, 1985, **107**, 6063.
[10]M. Coruzzi, G. D. Andreetti, V. Bocchi, A. Pochini and R. J. Unargo, *J. Chem. Soc., Perkin Trans. (2)*, 1982, 1133.
[11]Wei Xu, R. J. Puddephatt, L. Manojlovic-Muir, K. W. Muir and C. S. Frampton, *J. Inclusion Phenom.* 1994, **19**, 277.
[12]In all three cases it became apparent, as the refinement proceeded, that the tert-butyl groups of the calixarenes were disordered and hence were modelled as such.
[13]C. D. Gutsche, M. Iqbal and I. Alam, *J. Am. Chem. Soc.*, 1987, **109**, 4314.

p-nitrocalixarenes were studied by Shinkai et al.[14] The first and second pKa values measured in a mixture of water:thf (7:3), were found to be < 0 and 10.3 ± 0.3 respectively. This large decrease in acidity on undergoing monodeprotonation would explain the lack of subsequent deprotonation by even relatively strong bases such as (1), (2) and (4). It must be emphasised that these results only provide a possible explanation for our observations as the species involved and the solvents used are different from our own. Compounds (21) and (23) were isostructural, however the structure of (22) was distinctly different. Due to these facts the subsequent discussion will begin with a description of (21) and (23), followed by an examination of (22).

Characterisation ultimately by single crystal X-ray diffraction revealed that the reaction of (1) and LH_4 had resulted in the formation of the phosphonium salt $[(Ph_3PMe)^+(LH_3)^-.2CH_3CN]_n$, (21). Transfer of an acidic proton from one of the phenolic groups of LH_4 to the basic ylidic carbon atom had been effected. The asymmetric unit contains one anion, one cation and two acetonitrile molecules. As observed in the previous series of phosphonium aryloxide salts, the cations and anions are held together by C-H...O hydrogen bonds (Figure 6.16). A C(alkyl)-H hydrogen atom is seen to bond to the deprotonated anionic oxygen. All hydrogen bond parameters are given in Table 6.7. The geometry of the cation is as expected, however, the structure of the anion is of interest.

Table 6.7 Hydrogen bond parameters of (21)

Interaction	X...X' distance (Å)	X...X' distance (Å)	X-H...X' angle (°)
C8-H8C...O1	3.153	2.11	161
C22B-H2XA...O2	3.211	2.21	153
C8-H8B...N2XB	3.214	2.41	129
O4-H4A...O1A	2.521(3)	1.47(6)	173(5)
O3-H3A...O4	2.721(3)	1.89(5)	162(5)
O2-H2A...O1	2.551(3)	1.63(5)	176(4)

[14]S. Shinkai, K. Araki, H. Koreishi, T. Tsubaki and O. Manabe, *Chem. Lett.*, 1986, 1351.

The calixarene anion adopts a familiar 'cone' configuration (Figure 6.17), although monodeprotonation reduces the symmetry. As mentioned previously there are two acetonitrile molecules in the asymmetric unit. One acetonitrile molecule is found to be a guest in the lower cavity of the calixarene anion the other is located in the lattice (vide infra). This is analogous to the host-guest behaviour exhibited when acetonitrile is a guest in neutral LH_4[11] and other calixarene anions.[15] In all these structures the acetonitrile is disposed at the level of the tert-butyl groups, orientated with the nitrogen atom projecting out of the cone.

Another feature of interest is the configuration of the actual cone itself. In the structure of LH_4 with a guest acetonitrile molecule the four oxygens form a regular square of side 2.692 Å. The hydrogens in effect 'follow' each other around the square, each pointing towards the next oxygen. However in (21) deprotonation of one of the phenolic groups leads to a disruption in the O-H...O hydrogen bonding that was observed in the neutral LH_4. The deprotonated oxygen (O1) is involved in short O-H...O hydrogen bonds with its neighbouring OH groups (O4-H4A) and (O2-H2A). The other phenolic group (O3-H3A) is involved in a longer O-H...O hydrogen bond with O4 and subsequently there is no O-H...O hydrogen bond observed between O2 and O3, as is observed in LH_4. This results in the two shortest O...O distances being observed between O2-O1 and O4-O1. Of intermediate distance is that between O3-O4 and the longest distance is between O2-O3 (Table 6.8).

Table 6.8 The O...O distances in the anion of (21)

Interaction	O...O distance (Å)
O1...O2	2.551(3)
O1...O4	2.521(3)
O3...O4	2.721(3)
O2...O3	2.945(3)

[15] J. M. Harrowfield, M. I. Ogden, W. R. Richmond, B. W. Skelton and A. H. White, *J. Chem. Soc., Perkin Trans. (2)*, 1993, 2183.

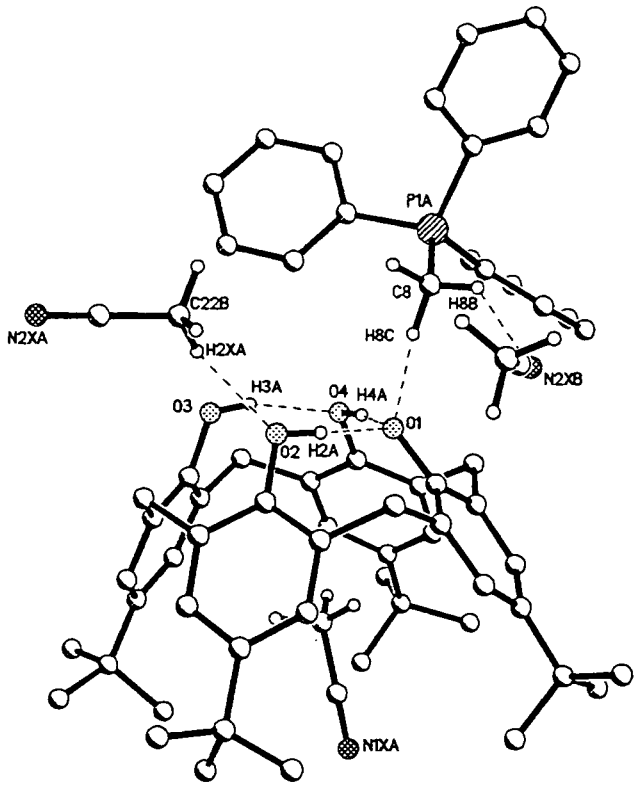

Figure 6.16 The molecular structure of $(Ph_3PMe)^+(LH_3)^-.2CH_3CN$, (21). All aryl and ^{t}butyl hydrogen atoms have been omitted for clarity.

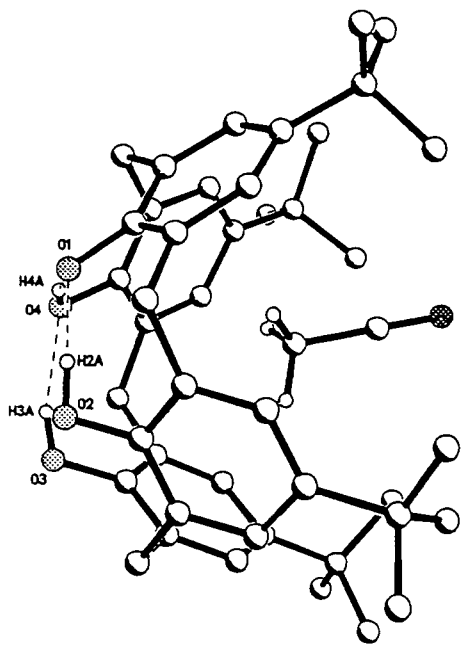

Figure 6.17 The cone configuration of the anion with guest acetonitrile molecule.

On the supramolecular level, these anions are packed in sheets. Within a sheet the anions are all orientated with their cone's lower rims at the same level, that is, either at the bottom or top of the layer (Figure 6.18). These rows of anions tilt in alternate directions and are staggered presumably to minimise the steric interactions of the tert-butyl groups (Figure 6.19).

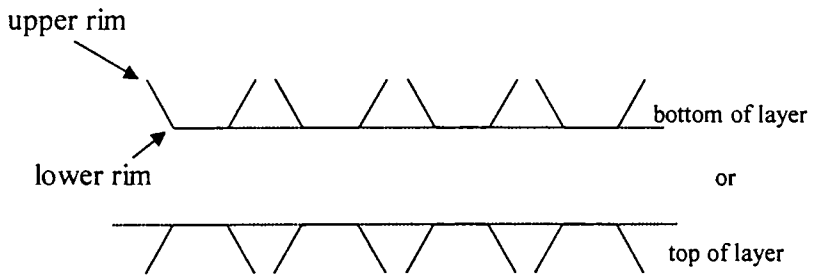

Figure 6.18 A schematic of the orientation of the anions within a sheet

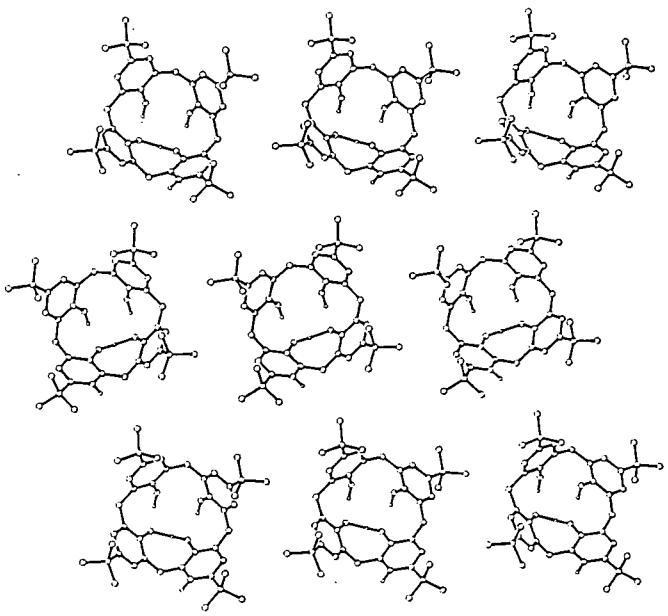

Figure 6.19 A sheet of anions from the structure of (21).

These sheets then pack in pairs with the anions in one sheet being orientated so that the top of their cone's upper rims are closest to the upper rims of the anions in the sheet below (Figure 6.20).

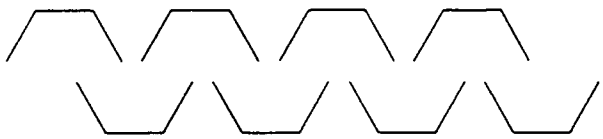

Figure 6.20 A schematic of the orientaion of anions in neigbouring sheets

It is also noteworthy that each sheet is displaced by half an anion unit compared to previous and following sheets so each cone lies beneath the space where four cones in the neighbouring layers meet.

The cation's geometry is as expected. It is however, not only involved in hydrogen bonding to the calixarene anions but is also interacting with the nitrogen atom of the second, 'free', acetonitrile forming a C-H...N hydrogen bond. This second acetonitrile is also acting as a bridge between neighbouring cation-anion units, utilising one of its methyl protons to form a C-H...O hydrogen bond with O2 (Figure 6.16 and Table 6.7). The cations and acetonitrile molecules pack in sheets. Within these sheets every second cation-acetonitrile unit sits slightly higher than its neighbouring units (Figure 6.21). There are double the number of cation-acetonitrile units in these sheets compared to the number of anion units in the anion sheets. This is because the cation-acetonitrile layer lies in the space between two layers of anions that pack lower rim to lower rim. The cations being alternately associated with an anion from the layer above then an anion from the layer below, the free acetonitrile molecules acting as bridges between these resulting in the formation of chains within the sheets. It should be noted that the neighbouring chains within these sheets do not interact to give a three-dimensional hydrogen bonded network. Similarly, although the three-layer motif (i.e. two anion layers and one cation layer) is infinitely repeated, there are no interactions between neighbouring three-layer units (Figure 6.22).

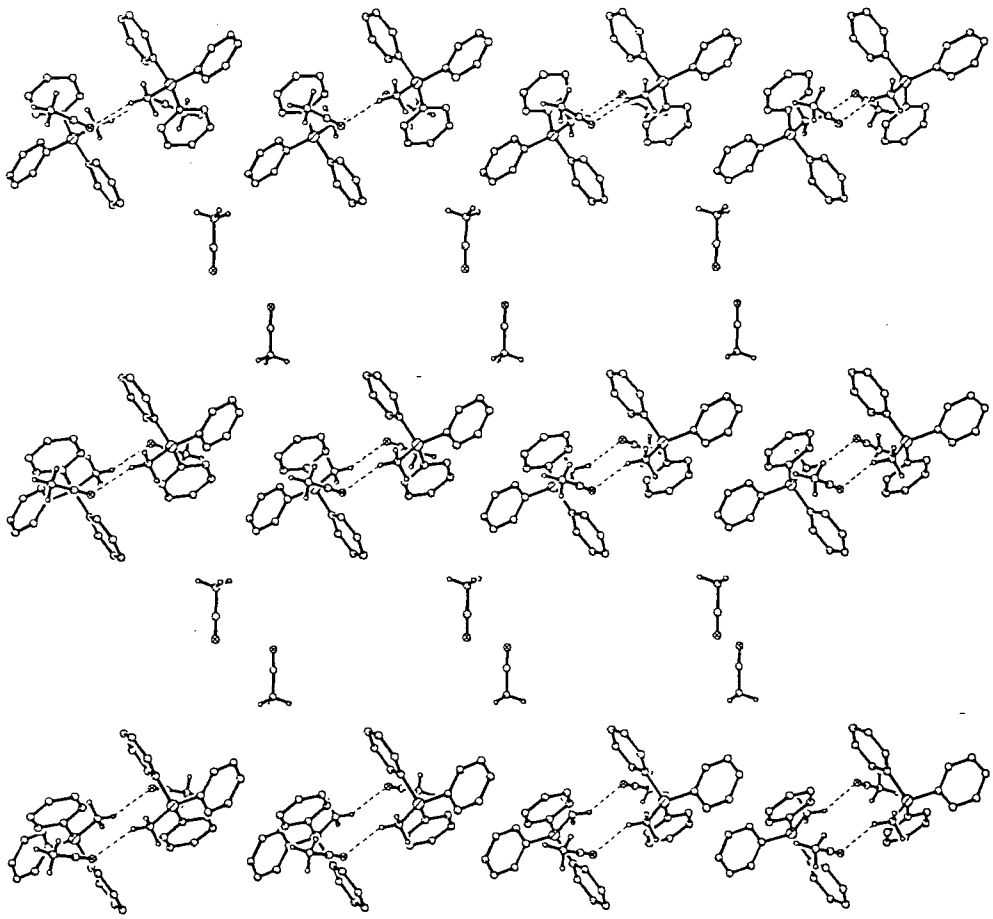

Figure 6.21 The packing of that cation layers in (21). The central acetonitrile molecules show the postions of the anions.

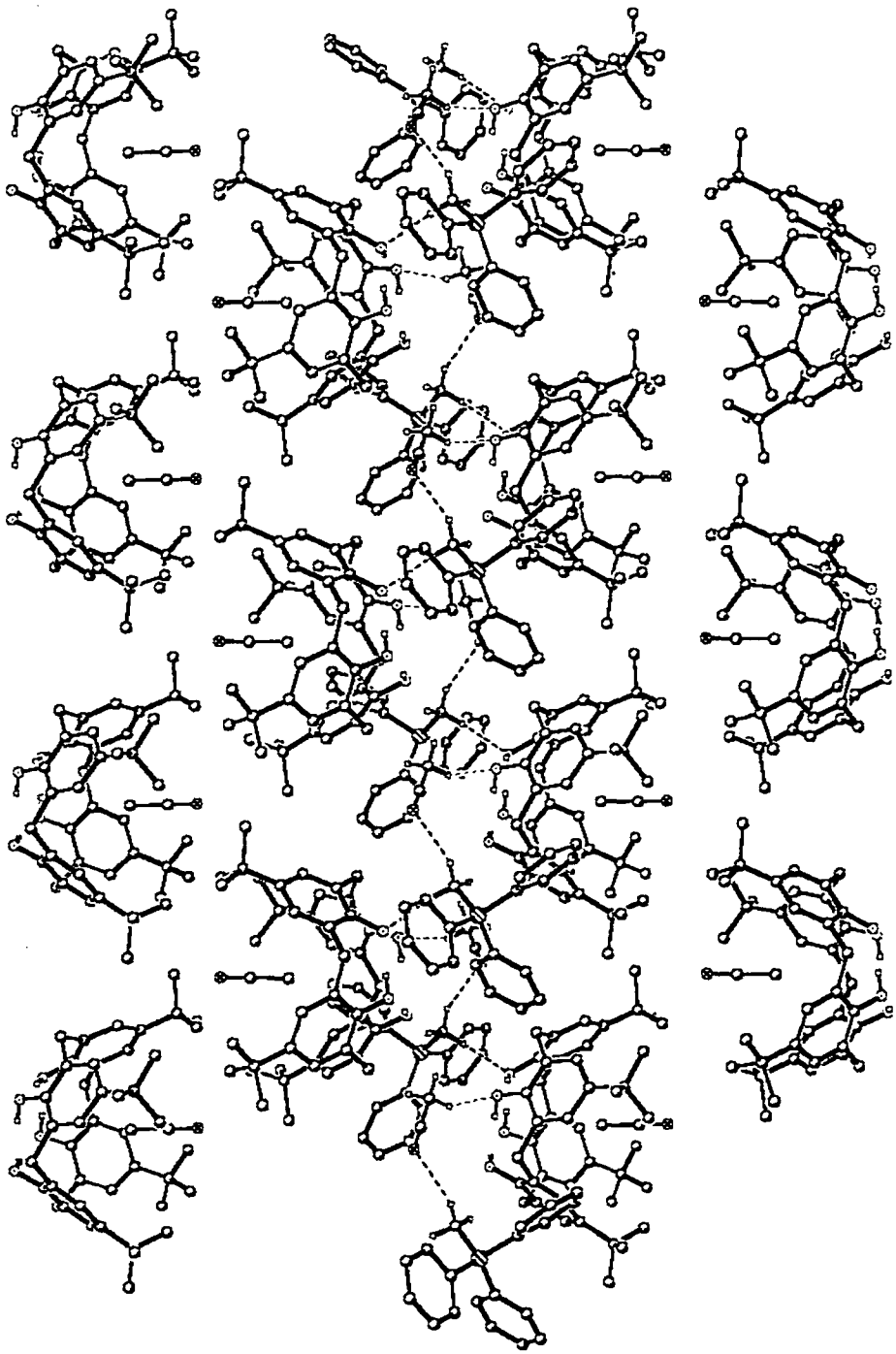

Figure 6.22 The overall packing arrangement of (21)

As mentioned previously (21) and (23) are isostructural. Single crystal X-ray diffraction revealed the solid-state structure to be $[(Ph_3PNH_2)^+(LH_3)^-.2CH_3CN]_n$, (23), (Figure 6.23). The geometry of the cation is as expected and interacts with the anion through C-H...N hydrogen bonds in an analogous manner to (21). The structure of the anion is also directly comparable with a guest acetonitrile and an irregular arrangement of the oxygens consistent with the monodeprotonation observed. These anions and cations are also seen to pack in an identical manner to that described for (21), with units being linked through the second 'free' acetonitriles. All hydrogen bond parameters are given in Table 6.9. It is interesting to note that in this case (4) has deprotonated the calixarene to form an ion-pair, in contrast to the adduct formed on its reaction with bisphenol. This is possibly attributable to the calixarene having a lower pKa value than the bisphenol (unfortunately no pKa values for bisphenol are available) and therefore being sufficiently acidic for (4) to deprotonate it.

Table 6.9 Hydrogen bond parameters of (23)

Interaction	X...X' distance (Å)	X...X' distance (Å)	X-H...X' angle (°)
N1A-H1A...O1	2.745(5)	1.86(5)	173(5)
C91B-H91E...O3	3.201	2.25	162
N1A-H1B...N2A	2.992(6)	2.26(5)	147(5)
O4-H4A...O1	2.556(4)	1.65(6)	169(6)
O3-H3A...O1	2.572(4)	1.66(5)	178(5)
O2-H2A...O4	2.728(4)	1.85(5)	171(5)

The structure of (22) is, on the whole, rather different from (21) and (23) although it does have some features in common which will be discussed first. It too contains a monodeprotonated calixarene namely, $(Ph_3PEt)^+(LH_3)^-.2CH_3CN$, (22), (Figure 6.24). The anion is in its familiar 'cone' configuration in which a guest acetonitrile resides. The cation and anion are held together by C-H...O hydrogen bonds, and there is a second 'free' acetonitrile in the lattice. These latter two features are of interest, as on examination they are found to be different from that observed previously. Firstly, consider the aggregation of the ion-separated pairs. Instead of only one, there are three close contacts between the anion and the cation. The cation hydrogen bonds to two of the oxygen atoms, both of

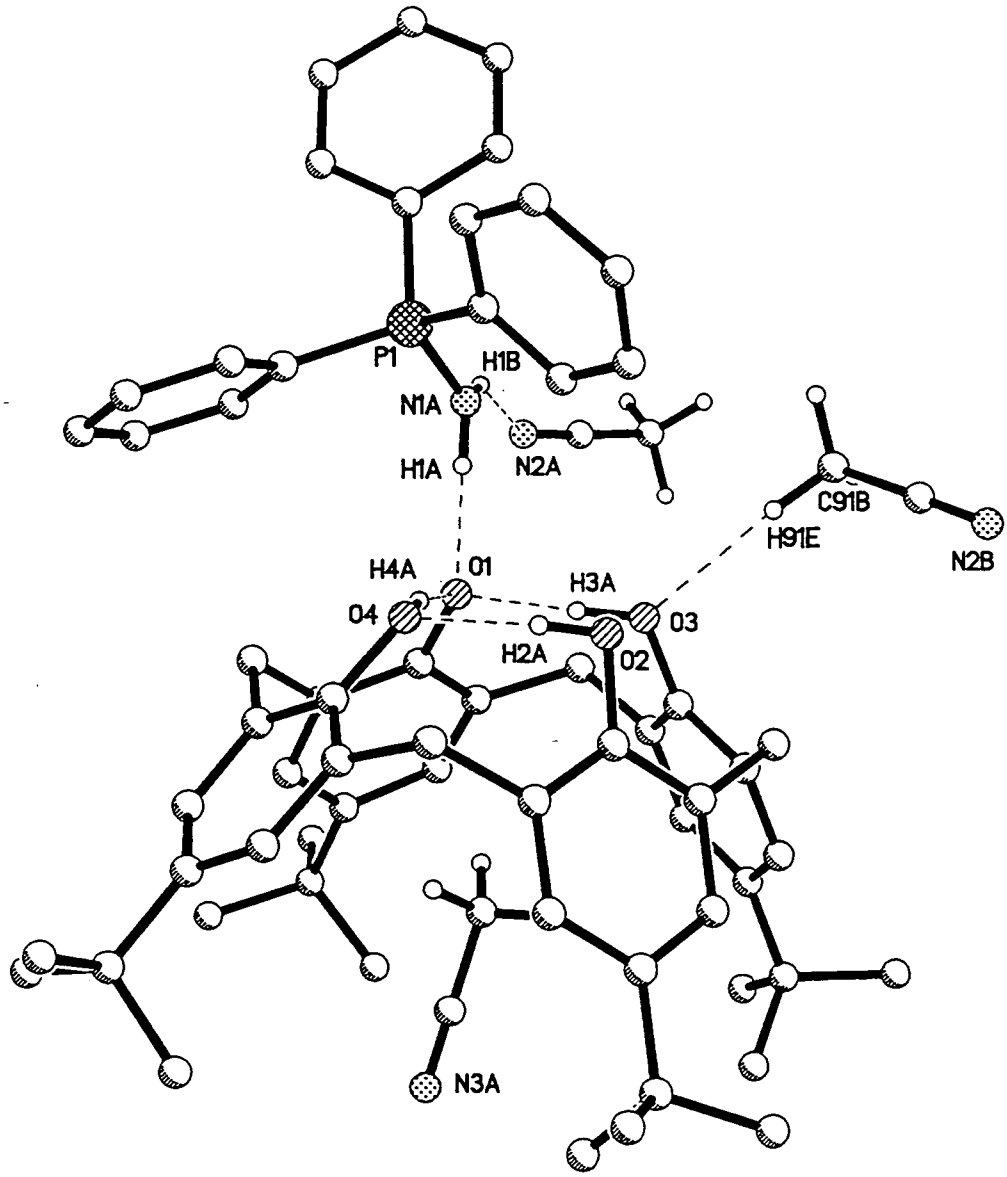

Figure 6.23 The molecular structure of $(Ph_3PNH_2)^+(LH_3)^-.2CH_3CN$, (23). All aryl and ^{t}butyl hydrogen atoms are omitted for clarity.

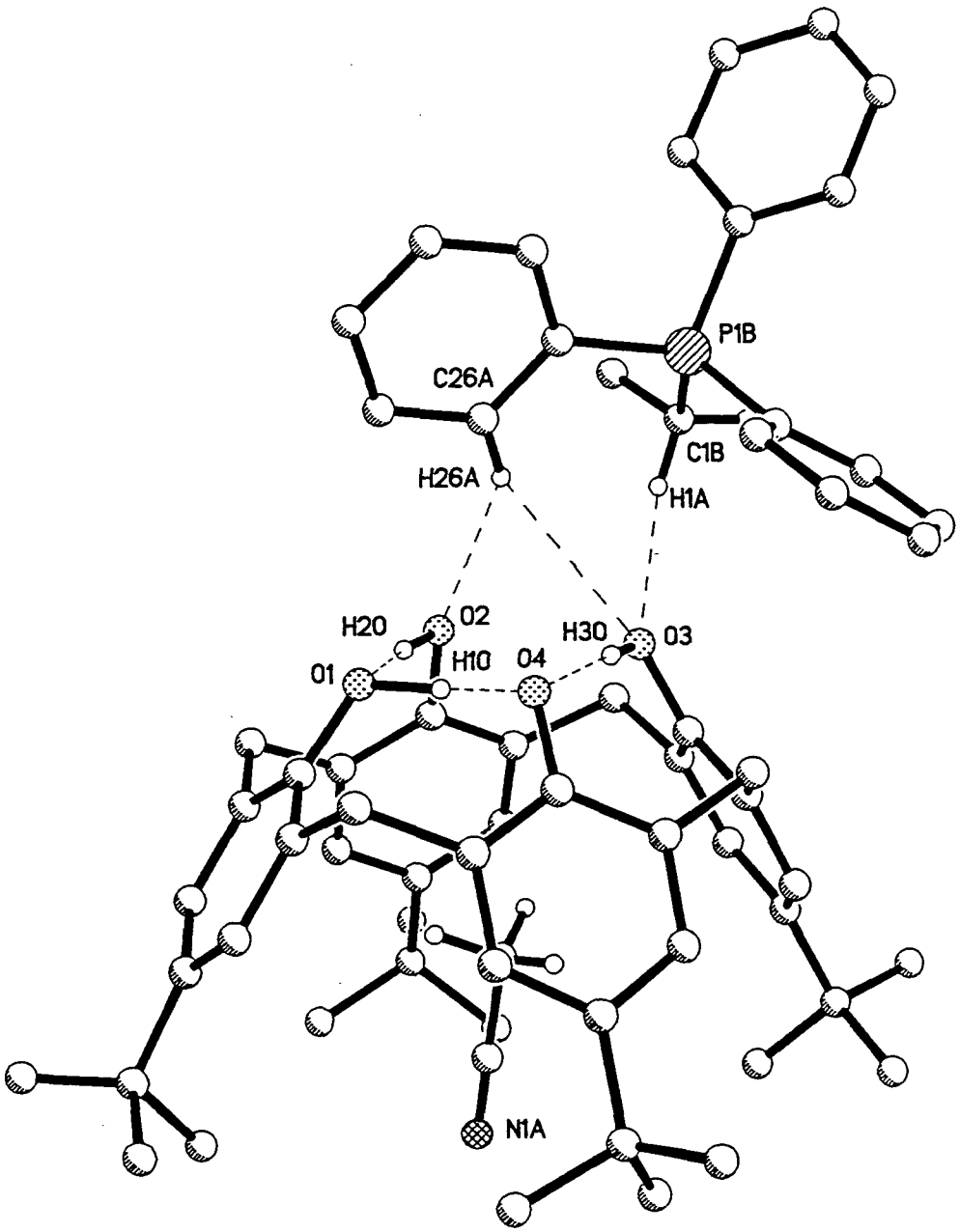

Figure 6.24 The molecular structure of (22). All ^{t}butyl and aryl hydrogen atoms, except those involved in hydrogen bonding, have been omitted for clarity.

which remain protonated, namely O2 and O3 (Figure 6.24). O3 is chelated in the usual fashion by a C(alkyl)-H and C(aryl)-H, while O2 is in close contact with the same C(aryl)-H. The cations are then involved in a C-H...N interaction with an acetonitrile group, however, the molecule involved is not the second 'free' acetonitrile. Instead the cation interacts with the guest acetonitrile of a neighbouring anion (Figure 6.25). Interestingly the free acetonitrile molecules are not involved in any interactions with either the cations or anions. All hydrogen bond parameters are given in Table 6.10.

Table 6.10 Hydrogen bond parameters of (22)

Interaction	X...X' distance (Å)	X...X' distance (Å)	X-H...X' angle (°)
C1B-H1A...O3	3.222	2.181	161
C26A-H26A...O2	3.427	2.483	145
C26A-H26A...O3	3.526	2.662	136
C12A-H12A...N1A	3.332	2.490	134
O1-H1O...O4	2.490(4)	1.26(6)	168(5)
O2-H2O...O1	2.656(4)	1.64(6)	173(5)
O3-H3O...O4	2.599(4)	1.79(6)	173(6)
O2...O3	2.963(4)	-	-

The anions stack directly over one another forming columns which pack together as illustrated by Figure 6.26. Columns of cations fit between. Figure 6.27 reveals how the cations sit above one another. The guest acetonitrile molecules are also shown, and describe the position of the anions. Altogether, the overall packing is quite different from that seen before (Figure 6.28). This quite dramatic difference is presumably due to the subtle difference between the cations in (22), (i.e. the methyl group on the ylidic carbon), compared to the isostructural cations of (21) and (23). This illustrates once again, how subtle changes in building blocks can lead to more prominent changes in the supramolecular structure.

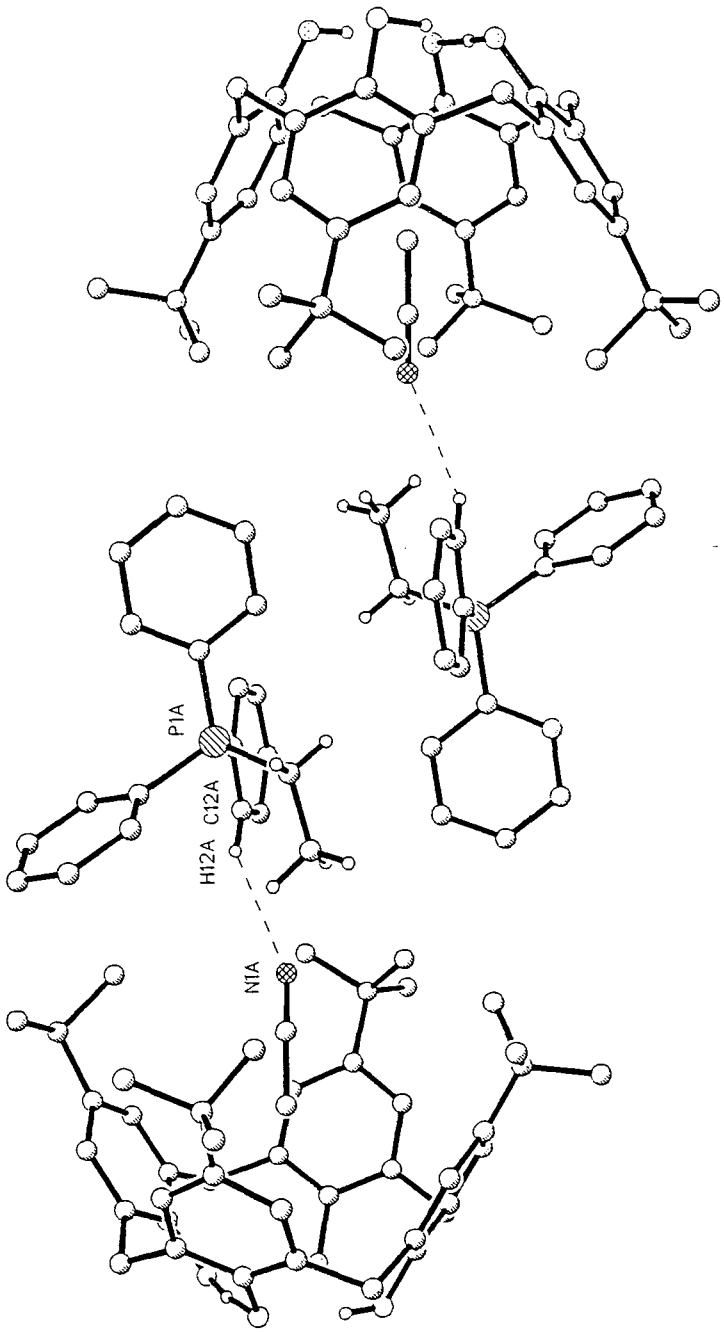

Figure 6.25 Cations of (22) interacting with guest acetonitrile molecules.

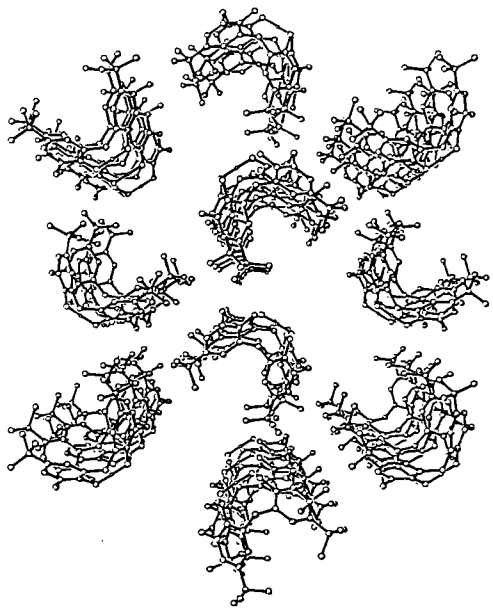

Figure 6.26 The packing arrangement of the anion columns of (22).

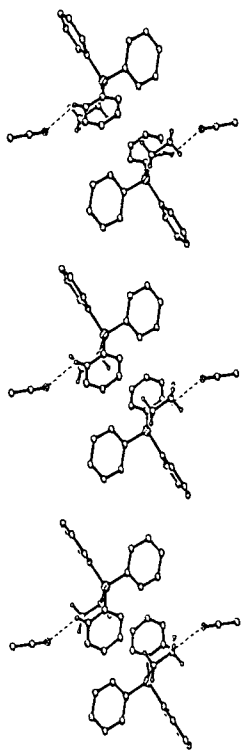

Figure 6.27 The side view of a cation column in (22).

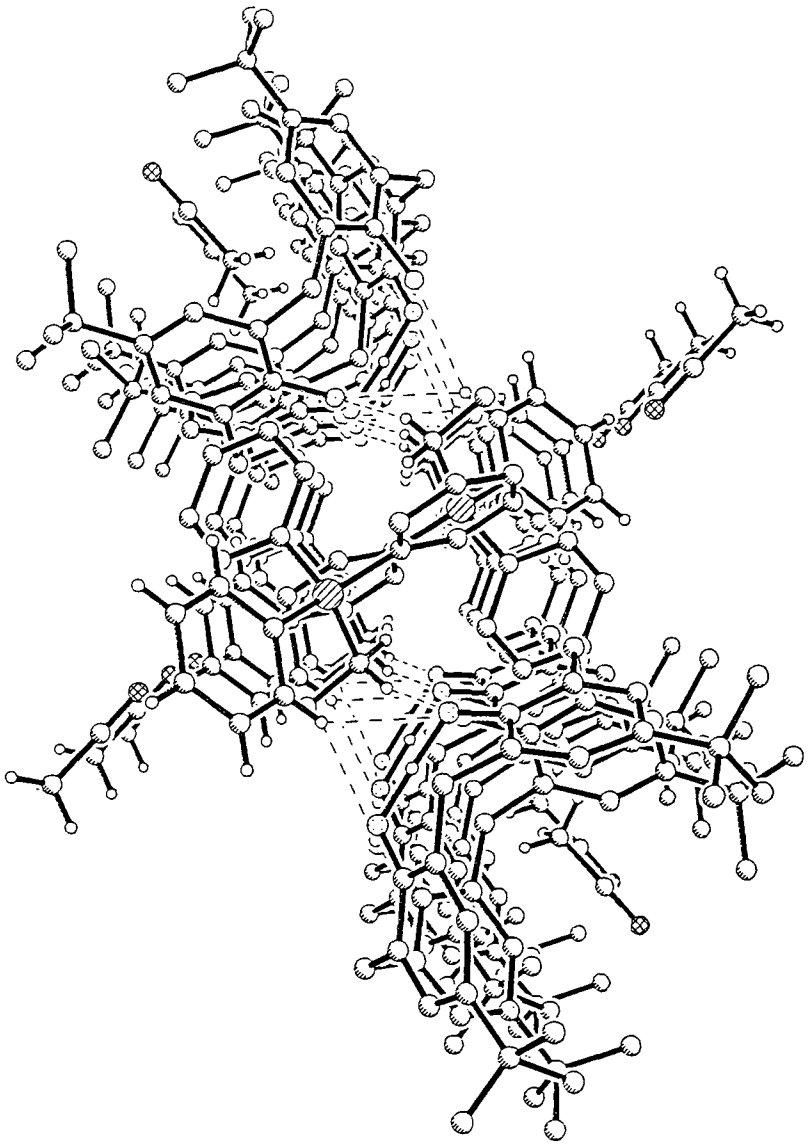

Figure 6.28 The overall packing arrangement of anions and cations of (22).

Considering all three LH_4-derived structures together, a search of the crystal data base revealed some structures that were similar to our own. A series of tetralkylammonium cations with calix[4]arenes were studied by Harrowfield et al. One of these contains a tetralkylammonium cation and a *p-tert*-butylcalix[4]arene anion (hence of particular interest), namely $NEt_4^+[LH_3]^-.24CH_3CN.0.38H_2O$.[15] This had been formed from the reaction of aqueous Et_4NOH with LH_4 in acetonitrile. As we had observed, the calixarene was monodeprotonated by the quaternary base to form the salt. The asymmetric unit contained an anion with a guest acetonitrile molecule and a NEt_4^+ cation, then one half of that. The guest acetonitrile molecule was found to be disposed at the level of the tert-butyl groups with its nitrogen atom projecting out of the cone, as observed in our structure. The anions were in two different orientations leading to alternating stacks of anions and associated cations. However, in spite of their disposition in stacks the cations were said to have no intimate association with the anions. There was also found to be a 'free' acetonitrile in the lattice, but this was found to have no anion or cation affiliation but instead occupied a void in the lattice as seen in (22). The cations were orientated directly above and below its neighbouring anions. Here, unlike our compounds, the cation is symmetrical and its position suggested that the negative charge on the anions was delocalised on all the oxygen atoms to maximise electrostatic interaction. It should also be noted that no phenolic hydrogens were assigned due to high thermal and rotational disorder, the data set having been collected at 295 K.

Another structure of interest resulted from the reaction of tert-butylamine with LH_4 in acetonitrile.[13, 16] As observed previously proton transfer occurs from the calixarene to the amine resulting in a monodeprotonated calixarene anion and the cation $[(CH_3)_3CNH_3]^+$. However, unlike the previous structures, it is not the acetonitrile molecule which is the guest of the calixarene anion but the cation instead. An 'endo-calix' complex is not observed in our structures presumably because the cations are too bulky to fit in the host. Also this type of arrangement would preclude the extensive hydrogen bond networks observed.

---

[16]L. Bauer and C.D. Gutsche, *J. Am. Chem. Soc.*, 1985, **107**, 6063.

In conclusion, a number of more complicated phosphonium salts have been isolated and characterised by X-ray diffraction, proving yet again an extension of the strategy of reaction of phosphonium ylides with organic acids, in this case the extension to multifunctional systems, has been successful. The following points summarise the work undertaken in this chapter.

(i) Reaction of 4,4'-methylenebis(2,6-di^{t}butlyphenol), bisphenol, with (2) resulted in a doubly deprotonated species (16) in which the two cations were seen to interact with the anion in two different ways. One as seen before, chelating the anionic oxygen, while the second interacted with the π-system of the anion's arene rings. Conversely reaction with (4) led to the co-crystallisation of an adduct (17). Comparison of the bisphenol components of (16) and (17) with the structure of bisphenol itself, revealed a change in relative positions of the two arene rings in all three cases.

(ii) Further investigations of the reaction of (2) with the bifunctional phenols, catechol and H_2salen revealed two mono-deprotonated species, (19) and (20) respectively. In both cases the presence of an anionic and phenolic oxygen led to the anions associating via strong O-H...O hydrogen bonds. In the latter case this aggregation was more extensive resulting in anionic tunnels in which the cations were placed.

(iii) Increasing the number of phenolic groups to four was affected by utilising p-tert-butyl-calix[4]arene. Reaction with (1), (2) and (4) all resulted in mono-deprotonated products, (21)-(23) respectively. In all three cases acetonitrile was found to be the guest molecule in the calixarene. (21) and (23) were isostructural, revealing an extensive hydrogen bond network in which 'free' acetonitriles bridged between ion-pairs. However, (22) was quite different and less extensively hydrogen bonded. This illustrates how a small change in the molecular structure of the reactants can lead to a more profound change in the supramolecular structure of the resulting product.

Chapter 7

7. DISCUSSION - REACTION OF PHOSPHONIUM YLIDES WITH THE SCHIFF BASE H_2SALEN.

During the course of our investigation into the reaction of phosphonium ylides with multifunctional organic acids, as described in the previous chapter, some unexpected results were obtained. As reported in Chapter 6, we carried out the reaction of the Schiff base N,N'-ethylenebis(salicylideneimine), (H_2salen), with triphenylphosphonium ethylide, (2), obtaining the expected phosphonium salt. However on reaction of H_2salen with triphenylphosphonium methylide, (1), and triphenylphosphonium benzylide, (3), the reactions followed different pathways. We herein report the results of these reactions, describing the complexes (24) and (25). Subsequent reactions involving (24) resulted in complexes (26) and (27). X-ray crystal structures were obtained for complexes (24) to (26). (24) and (25) were also found to exhibit some interesting physical properties investigated by UV/Vis spectroscopy and these will also be discussed. All numbering of complexes is consistent with that used previously.

The readily available Schiff base H_2salen, contains two protic sites (i.e. two phenolic groups), as well as two potentially reactive iminic functionalities. We envisaged that the reaction of H_2salen with phosphonium ylides would proceed in one of two ways. Either the imine C=N double bond of H_2salen could participate in a Wittig-like reaction to yield an iminophosphorane and an alkene (such reactions between ylides and imines are well documented[1]), or its phenolic protons could react to give a phosphonium salt of $(Hsalen)^-$ as observed in its reaction with (2), or $(salen)^{2-}$ (Scheme 7.1). It was the possibility of the latter reaction that was initially of interest to us. However, the observed mode of reaction is not so simple and leads to unexpected products.

---

[1]A. W. Johnson, *'Ylides and Imines of Phosphorus'*, Wiley, New York, 1993, page 201 and references therein.

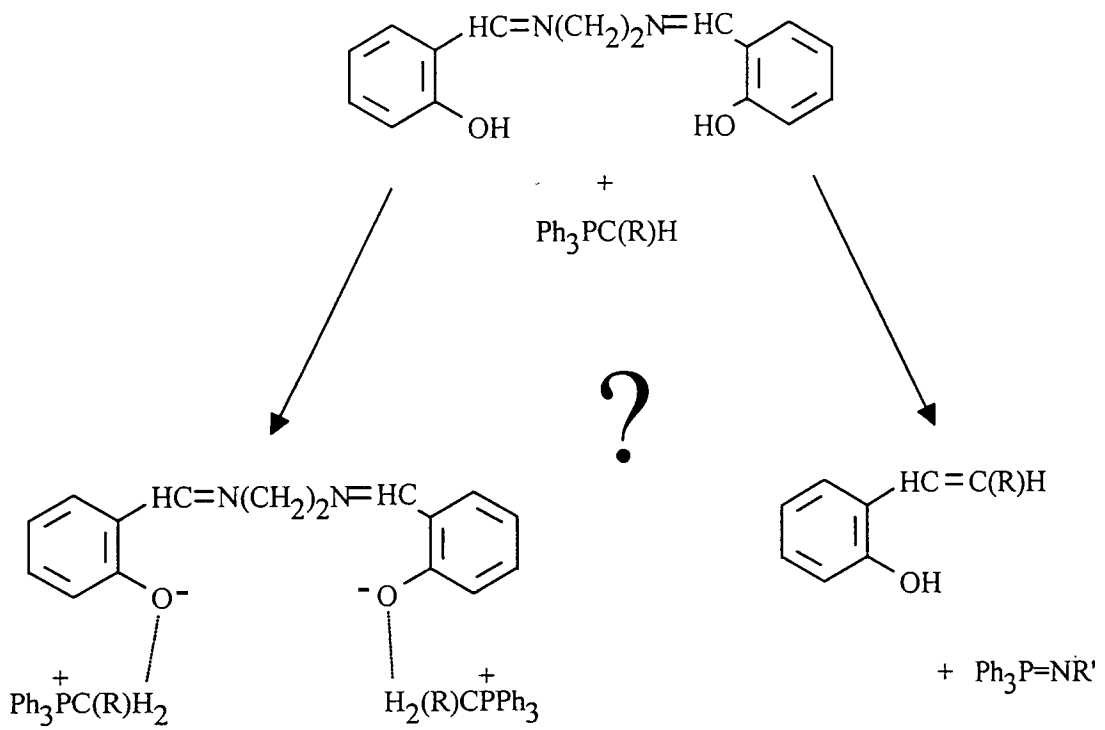

Scheme 7.1

Reaction of (1) with H_2salen in a toluene solution resulted in the formation of an insoluble, oily precipitate, which on addition of acetonitrile and warming dissolves. Cooling yields a crop of large orange crystals whose characterisation, ultimately by single crystal X-ray diffraction, led to what is best described as a zwitterionic vinylphosphonium salt, $[(Ph_3P^+C(H)=C(H)C_6H_4O^-).C_7H_8]_n$, (24), with the phosphonium and the aryloxide groups adopting a sterically favoured *E* configuration about the alkene double bond (Figure 7.1). This is a configuration also required by the intramolecular C-H...O hydrogen bond between H8 and O1. All hydrogen bond parameters are given in Table 7.1.

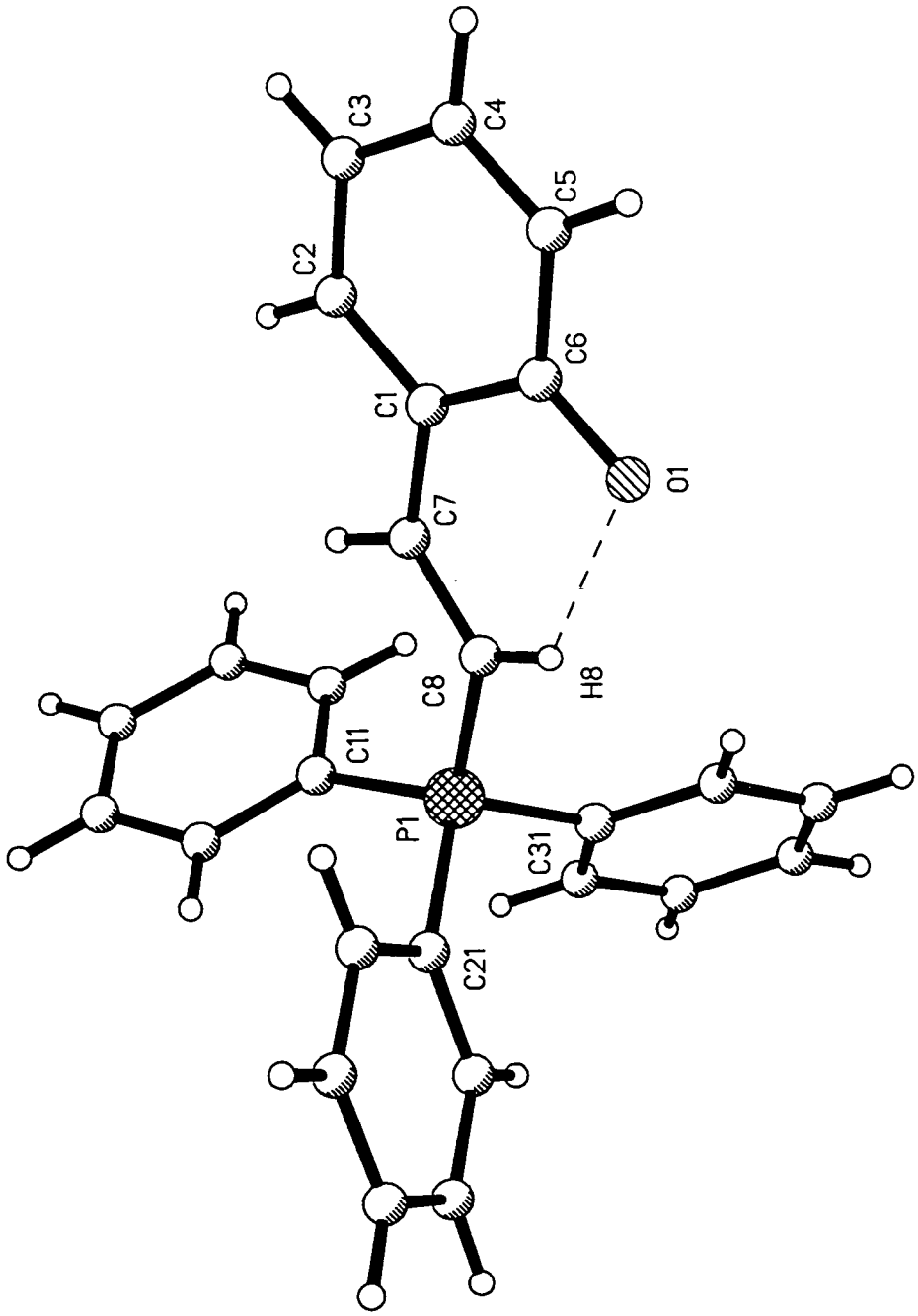

Figure 7.1 The molecular structure of $(Ph_3P^+C(H)=C(H)C_6H_4O^-)$, (24), showing the intramolecular C-H...O hydrogen bond.

Table 7.1 Hydrogen bond parameters of (24).

Interaction	C...O distance (Å)	H...O distance (Å)	C-H...O angle (°)
C8-H8...O1	2.826(3)	2.20(1)	127(1)
C15b-H15b...O1a	3.233(3)	2.52(3)	131(1)
C46a-H46c...O1a	3.407(7)	2.43(3)	172(1)

With the exception of the phenyl rings bound to P1, the molecule is planar (rms deviation from a mean plane defined by all non hydrogen atoms, excluding phenyl rings bound to P1, 0.022 Å). This suggests the possibility of delocalisation of the negative charge (formally on O1 in the description above) to the other extreme resonance form – that of a substituted ylide (Scheme 7.2). A minor but significant contribution from this latter resonance form is apparent from analysis of the bond lengths found within the crystal structure (Table 7.2). For example, C6-O1 [1.270(3) Å] is shorter than the C(aryl)-O distance found in the anion of $[(Ph_3PMe)^+(OC_6H_2Me_3\text{-}2,4,6)^-]_2$ (1.310 Å)[2] suggesting partial double bond character, and the bond lengths within the ring C1 to C6 vary significantly and consistently with the proposed delocalisation, the longest bonds being C1-C6 and C1-C2, and the shortest being C2-C3 and C4-C5 (Table 7.2). Furthermore, P1-C8 (1.753(2) Å) is shorter than a P-C single bond of a typical phosphonium salt and is more comparable to that found in structures of stabilised phosphonium ylides, e.g. $Ph_3P{=}C(CN)_2$, (1.753 Å).[3]

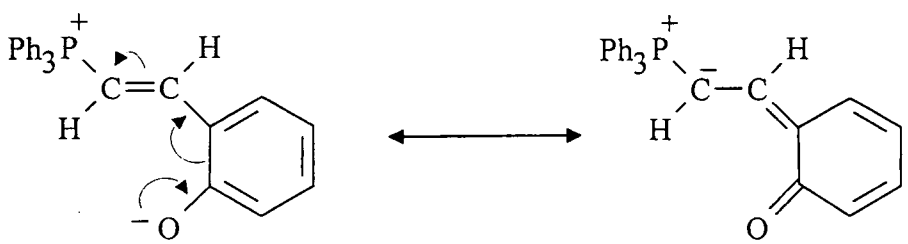

Scheme 7.2

Table 7.2 Selected bond lengths of (24).

[2]M. G. Davidson, *J. Chem. Soc., Chem. Commun.*, 1995, 919.

Bond	Bond length Å
C6-O1	1.207(3)
C1-C6	1.451(3)
C1-C2	1.407(3)
C2-C3	1.375(3)
C4-C5	1.359(3)
P1-C8	1.753(2)

At the supramolecular level, further interactions are revealed. In addition to the intramolecular C-H...O hydrogen bond, each oxygen atom participates in two further intermolecular C-H...O interactions (Figure 7.2). An aryl C-H group interacts with oxygen from a neighbouring molecule resulting in the formation of polymeric chains. Along these infinite chains there are further weak interactions from methyl groups of lattice toluene (Table 7.1).

A search of the CSD revealed no other crystal structures of zwitterionic phosphonium salts of the type R_3P^+-C(H)=C(H)RX$^-$ (where X = N, O or S) although three related structures are of interest (A.1),[4] (A.2),[5] (B.1)[6] and (B.2)[6] (Figure 7.3). In all these structures the P and O are cis with respect to the double bond resulting in close contact between these two atoms [P...O distance in (A.1), (A.2), and (B.1), 2.365, 2.144, and 1.789 Å, respectively] and there is a distortion from tetrahedral towards trigonal bipyramidal geometry about phosphorus. An open chain isomer of (B.2) was detected by ^{31}P NMR, but was found to exist only in polar solvents and was not isolated.[6] Other compounds which are pertinent to (24) have been reported. For example, monoalkoxyphosphoranes (C) were isolated but no evidence was found for the existence of zwitterionic structures rather than pentacoordinate phosphorus compounds (by ^{31}P NMR).[7] Instead a zwitterion was postulated to be a transient intermediate in the formation of the monoalkylphosphorane (D), (Figure 7.3)

[3]R. Richter, H. Hartung, S. Deresch and J. Kaiser, *Z. Anorg. Allg. Chem.*, 1980, **469**, 179.
[4]I. Kawamoto, T. Hata, Y. Kishida, and C. Tamura, *Tetrahedron Lett.*, 1971, 2417.
[5]I. Kawamoto, T. Hata, Y. Kishida, and C. Tamura, *Tetrahedron Lett.*, 1972, 1611.
[6]H. J. Bestmann, C. Riemer, R. Dotzer, *Chem. Ber.*, 1992, **125**, 225.
[7]I. Granoth, J. C. Martin, *J. Am. Chem. Soc.*, 1981, **103**, 2711.

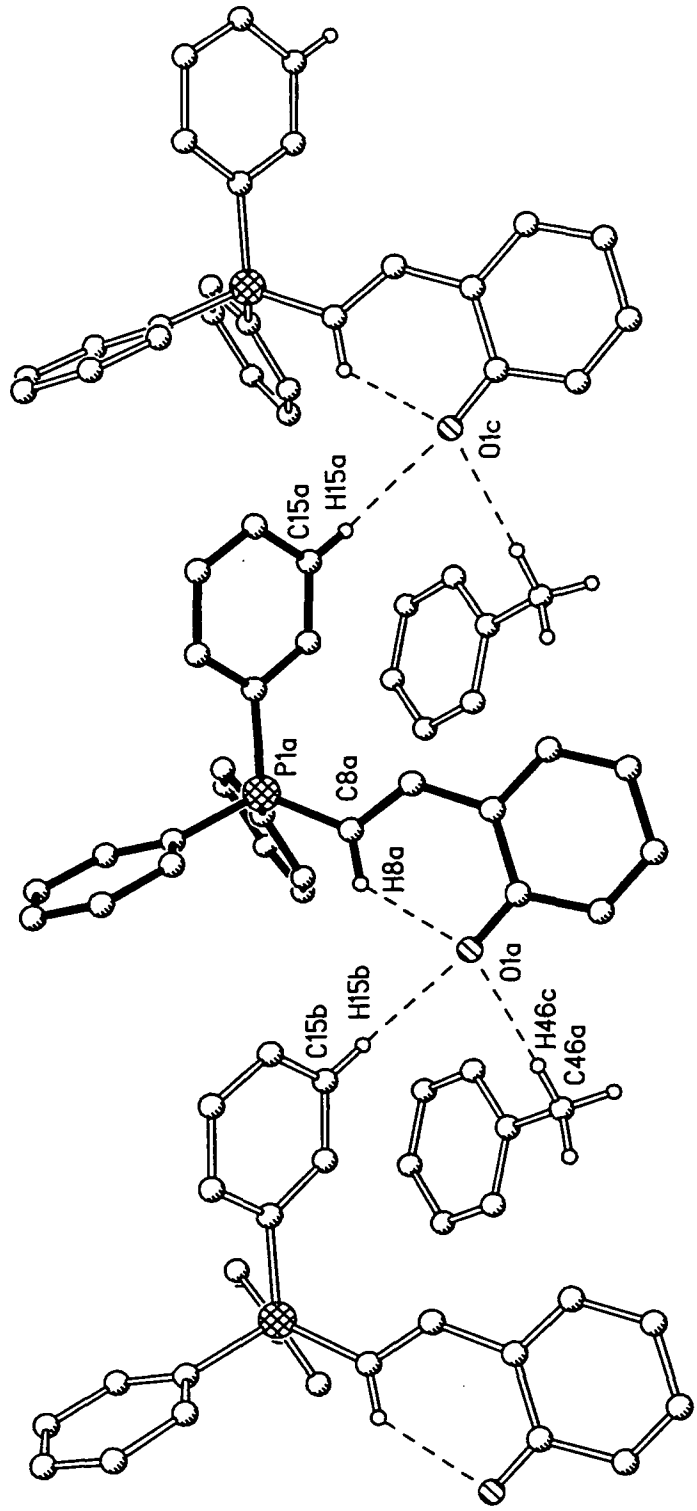

Figure 7.2 The infinite chains of (24) showing the weak interactions with lattice toluene. All aryl hydrogen atoms except those involved in hydrogen bonding have been omitted for clarity.

although the isomerisation was held to be the fast step of the reaction and irreversible.[8]

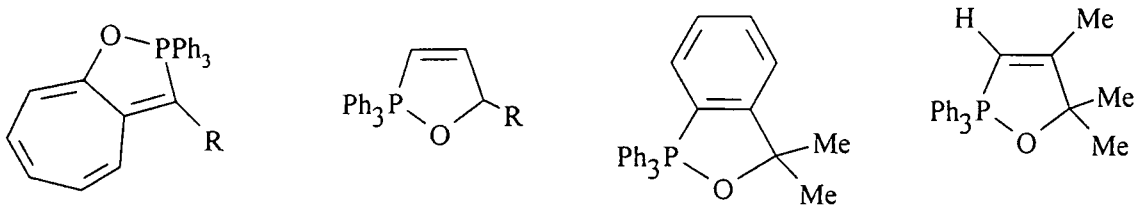

A
1: R = CN
2: R = CO_2Et

B
1: R = $C(OEt)_2$
2: R = Me

C

D

Figure 7.3

In all these examples, only compounds in which phosphorus and oxygen were cis with respect to the double bond were isolated. Therefore (24) appears to be unique and anomalous in being a stable zwitterion in the solid state and in solution. Three features which distinguish (24) from the compounds discussed above can be highlighted as possible factors in this apparently anomalous behaviour. Firstly, in (24) the *E* isomer is stabilised by an intramolecular hydrogen bond which is not available in (A) -(D). Secondly, a P-O bond in the Z isomer of (24) would be part of a six membered ring in contrast to the five membered rings formed by compounds (A)-(D) which is best able to accommodate the preferred O-P-C angle of 90 °. Thirdly, in (24) the negative charge is able to be delocalised over a greater extent than is possible in (A)-(D). This delocalisation (Scheme 7.2) may confer enhanced stability of the zwitterionic form. We have, however, observed that toluene solutions of (24) are not indefinitely stable. In fact over a number of days a resonance at -50 ppm in addition to that at 21 ppm appears in the ^{31}P NMR spectra. This observation is consistent with slow, partial conversion form the zwitterionic *E* to the *Z* isomer with a concomitant P...O interaction. These observations led to UV/Vis studies that will be discussed later on in this chapter. It is noteworthy in this context that, in a preliminary note, Bestmann and Kloeters reported the synthesis of the *Z* isomer of (24), identified by ^{1}H and ^{31}P NMR, by a different route, however, we

[8]C. F. Garbers, J. S. Malherbe and D. F. Schneider, *Tetrahedron Lett.*, 1972, 1421.

were unable to repeat their work and to our knowledge, no further experimental details have since appeared in the literature.[9]

The mechanism by which (24) is formed is of interest and an insight into the possible course of reaction of (1) with H_2salen comes from the work of Bestmann and Seng.[10] They reported that although ylides not having β-protons reacted with imines to give products typical of Wittig-type reactions (i.e. an alkene and an iminophosphorane), ylides with β-protons followed a different course (Scheme 7.3). They found that after initial nucleophilic attack of the ylidic carbon atom on the imine, to give isolable betaines (E), further heating (150-200 °C) then caused elimination of RNH_2 and PPh_3 to give allenes (F). We suggest (Scheme 7.4) that the reaction of (1) and H_2salen is similarly initiated by nucleophilic attack at the imine to give a betaine adduct (G) (although the alternative formation of a cyclic azaphosphetane, analogous to the oxaphosphetane intermediates in the Wittig reactions,[11] cannot be excluded). The presence of the hydroxyl group in (G) then permits the reaction to proceed differently to that shown in Scheme 7.3. Proton transfer from OH to give intermediates (H) can then be followed by a Hoffmann-like elimination of RNH_2. In contrast to Bestmann and Seng's reactions (Scheme 7.3) such a step does not now require the concomitant elimination of Ph_3P, but instead results in the formation of vinylphosphonium salts rather than allenes (Scheme 7.4).

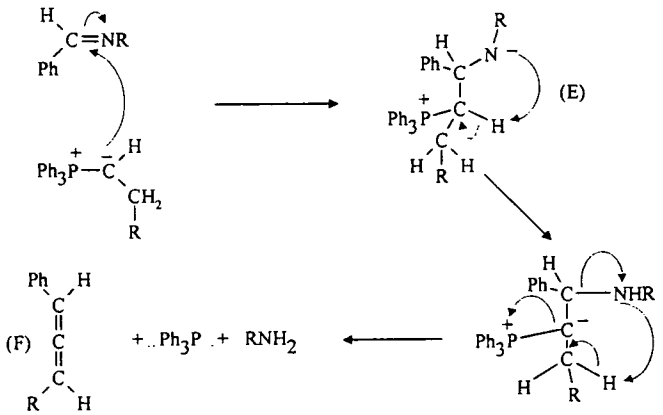

Scheme 7.3

[9]H. J. Bestmann and W. Kloeters, *Tetrahedron Letts.*, 1977, 79.
[10]H.J. Bestman and F. Seng, *Tetrahedron.*, 1965, **21**, 1373.
[11]A. W. Johnson, *'Ylides and Imines of Phosphorus'*, Wiley, New York, 1993, Chapter 9.

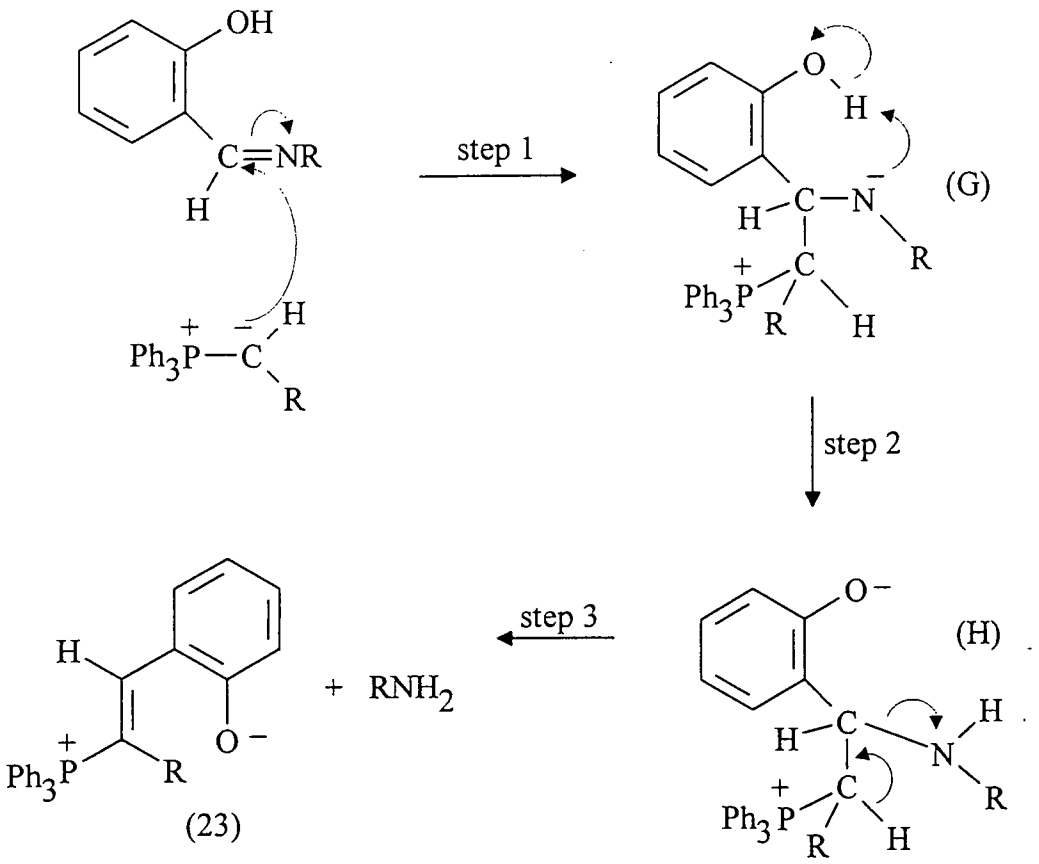

Scheme 7.4

Although initial reactions were carried out in a 1:1, (1):H_2salen ratio, on using two equivalents of (1) the isolated yield of zwitterion increases to greater than 100 % yield for the 1:1 reaction shown in Scheme 7.4. This suggests one of two things, either two ylides attack the two iminic functionalities simultaneously to form double the amount of zwitterion with the loss of ethylenediamine, or, Scheme 7.4 is continued, i.e. after the initial attack of the ylide to form the zwitterion a second ylide attacks the remaining RNH_2 species at its iminic function resulting in the formation of a second zwitterion and ethylenediamine (Scheme 7.5). The first route would require, at one stage, a high degree of negative charge on the bridging N-R-N group and hence it is the second route which would be more likely.

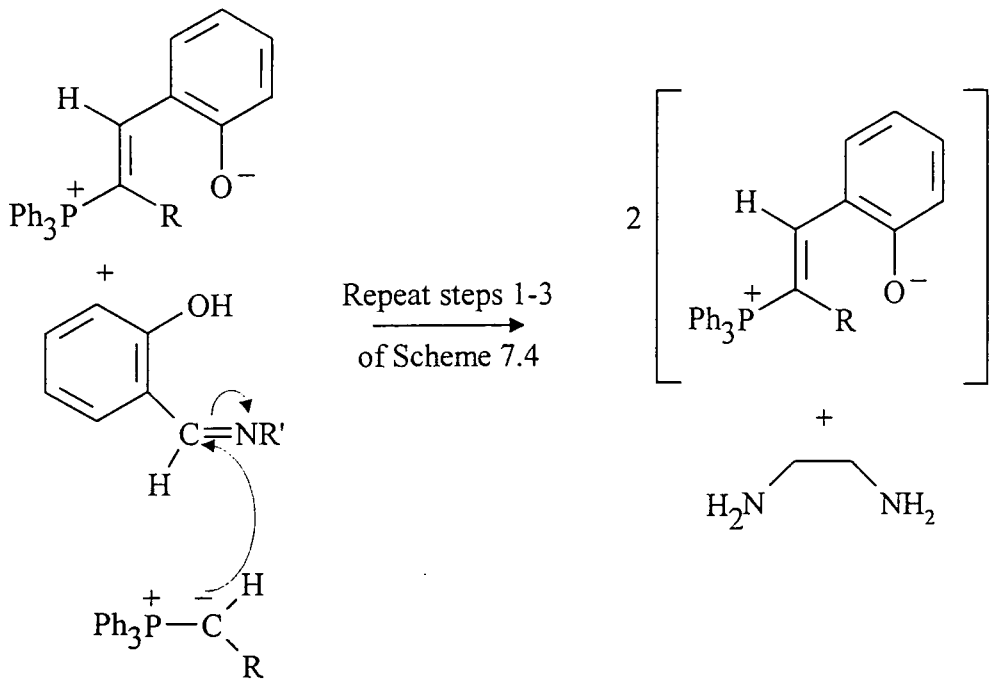

Scheme 7.5

In order to explore if this novel mode of reaction could be observed in the reaction of any other phosphonium ylides with H_2salen, to test our proposed mechanism, and to establish the degree to which the weak intramolecular C-H...O interaction found in (24) influences the unusual *E* configuration about the C=C double bond, we investigated the reaction of triphenylphosphonium benzylide, (3), with H_2salen. The reaction appeared to proceed in a similar manner with initial formation of an oil in toluene which dissolved on addition of acetonitrile. The solution then yielded a crop of orange crystals on cooling. Characterisation, ultimately by single-crystal X-ray diffraction, determined the isolated compound to be $Ph_3P^+C(Ph)=C(H)C_6H_4O^-$, (25), an aryloxyphosphorane in which the phosphorus and oxygen atoms are in cis orientation about the double bond (Figure 7.4). This is in contrast to the stable trans orientation found in the zwitterionic, (24). The coordination sphere around the phosphorus is trigonal bipyramidal with oxygen occupying one apical position and a phenyl group the other. The three equatorial positions are occupied by the two other phenyl groups and the alkenyl group. All relevant bond lengths are given in Table 7.3. The P-O bond length [1.982(2) Å] is within the range observed for similar P-O interactions found in other pentacoordinate monoalkyl- or monoaryloxyphosphoranes [(A.1), (A.2), (B), for example] and, as expected, the apical P-

Ph bond, (P-C41), is lengthened relative to those in the equatorial positions (Table 7.3). To our knowledge, the six membered P-C=C-C=C-O ring of (25) is unique in the solid state. In contrast to the planar acyclic system found in (24) the phosphorus atom lies above the plane defined by the other five atoms. This puckering is necessary in order for a six membered ring to accommodate the 90 ° C1-P-O angle required by the trigonal bipyramidal geometry at phosphorus. A further consequence of the *Z* configuration (and hence the P-O interaction) is that the extensive delocalisation of the negative charge through the conjugated system from oxygen, as seen in (24), is no longer apparent. This is manifested most obviously in the lengthening of both P-C1 and C26-O bonds and a shortening of C21-C26 and C25-C26 bonds relative to the equivalent parameters in (24) (Table 7.3). A more complete comparison is given later in Table 7.5.

Table 7.3 Selected bond lengths of (25).

Bond	Bond length (Å)
P-C1	1.821(3)
P-C41	1.905(3)
P-C31	1.828(2)
P-C51	1.823(3)
C26-O	1.330(3)
C21-C26	1.410(4)
C25-C26	1.412(4)

This configuration is also interesting as it can be compared with those commonly observed in S_N2 reactions. The phosphorus atom being surrounded by the three phenyl groups with the alkenyl group, as described above, and the oxygen, lined up in such a way as to be analogous to an attacking nucleophile. It is also noteworthy that the P-C41 bond is particularly long (1.905(3) Å) and hence could be considered to be analogous to the lengthened bond of a leaving group in an S_N2 reaction (Figure 7.5).

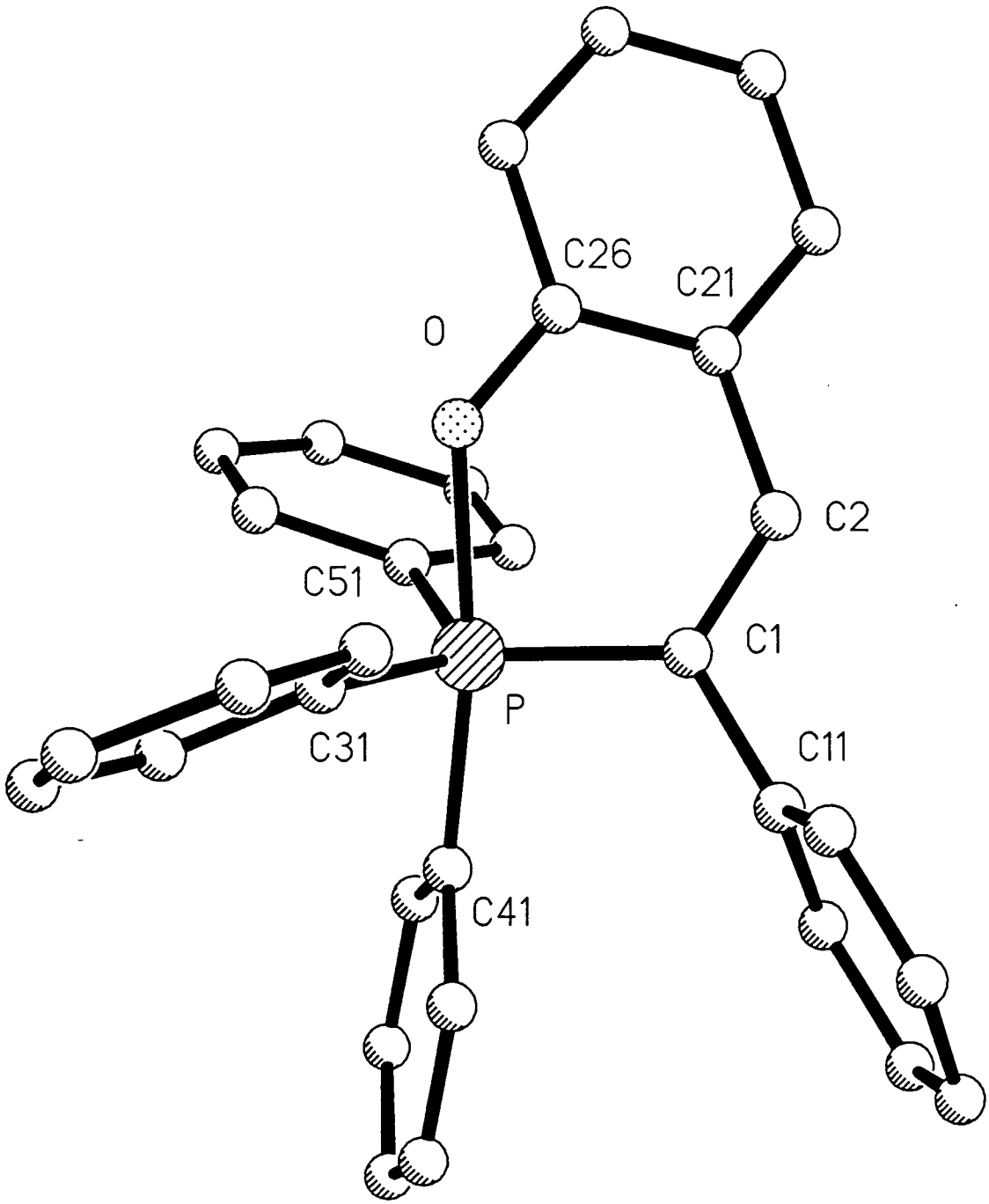

Figure 7.4 The molecular structure of $Ph_3P^+C(Ph)=C(H)C_6H_4O^-$, (25). All hydrogens have been omitted for clarity.

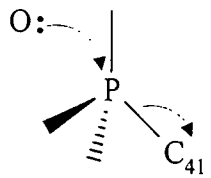

Figure 7.5

As pertained to earlier further reactions were undertaken with (24). Reacting (24) with NH_4Cl yielded a yellow crystalline solid. Characterisation, ultimately by X-ray diffraction, revealed the formation of the salt $(Ph_3PC(H)=C(H)C_6H_4OH)^+Cl^-$, (26). As expected this reaction involved the protonation of (24) at oxygen, with the loss of ammonia (readily detectable during synthesis), resulting in the formation of the chloride salt, (26).

In the solid-state structure of (26) there is one cation and one anion in the asymmetric unit (Figure 7.6). The Ph_3P group and the C_6H_4OH group are trans to one another as observed in (24). The molecular geometry of (26) differs most significantly from that of (24) in its deviation from planarity by rotation about C2 - C3. This makes the intramolecular C-H...O hydrogen bond no longer feasible. Instead the oxygen proton H01 is involved in a O-H...Cl hydrogen bond. All hydrogen bond parameters are given in Table 7.4.

Table 7.4 Hydrogen bond parameters of (26).

Interaction	X...X' distance (Å)	H...X' distance (Å)	X-H...X' angle (°)
O1-H01...Cl	3.005	1.929	173.5
C1A-H1A...ClA	3.642	2.612	155.9
C36A-H36A...ClA	3.587	2.523	168.1
C34B-H34B...O1A	3.437	2.472	148.2

On the supramolecular level (26) is aggregated via interactions between anions and cations of neighbouring units to form a polymeric structure with infinite chains of

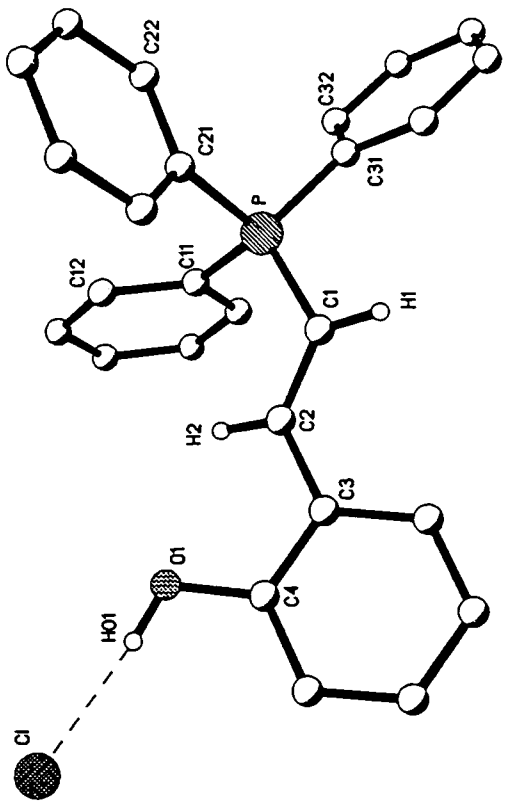

Figure 7.6 The asymmetric unit of $(Ph_3PC(H)=C(H)C_6H_4OH)^+Cl^-$, (26).

alternating anions and cations (Figure 7.7a). Each Cl anion is not only involved in O-H...Cl hydrogen bonding but is also chelated by an alkenyl hydrogen atom (H1A) and an ortho phenyl hydrogen atom from one of the groups on phosphorus (H36A) resulting in two C-H...Cl interactions (see Table 7.4). These are reminiscent of the motifs observed in the inorganic phosphonium salts (12) and (13) (Chapter 4), and as for the bromide anion in these inorganic phosphonium salts, the chloride anion has a spherical symmetry making it possible to be involved in these three interactions. On further examination these chains are also seen to be cross linked. Cations of one chain interact with cations in neighbouring chains via C-H...O hydrogen bonds. These involve para phenyl C-H groups from the same phenyl group involved in the C(aryl)H...Cl interactions (H34B) Figure 7.7b. Again, this emphasises the propensity of Ph_3P^+ groups to partake in C-H...X hydrogen bonding.

The crystal structure of (26) also allows comparisons to be drawn between its bond lengths and those of the parent zwitterion (24). In particular by studying the differences in bond lengths observed in the solid-state structures of (24) and (26) further insight into the proposed contribution of the substituted ylide resonance structure of (24), discussed earlier, can be gained. Table 7.5 lists the analogous bond lengths in (24) and (26) that will be discussed and Scheme 7.6 provides a schematic of the two structures and their proposed resonance structures.

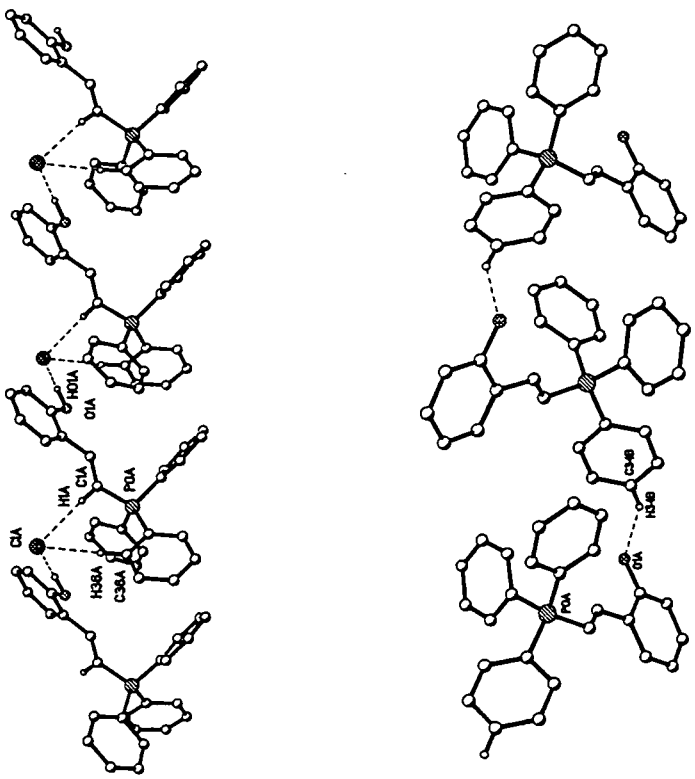

(a) (b)

Figure 7.7 The supramolecular structure of (26): (a) the infinite chains of anions and cations showing the two C-H...Cl hydrogen bonds; (b) association of neighbouring chains via C-H...O hydrogen bonds.

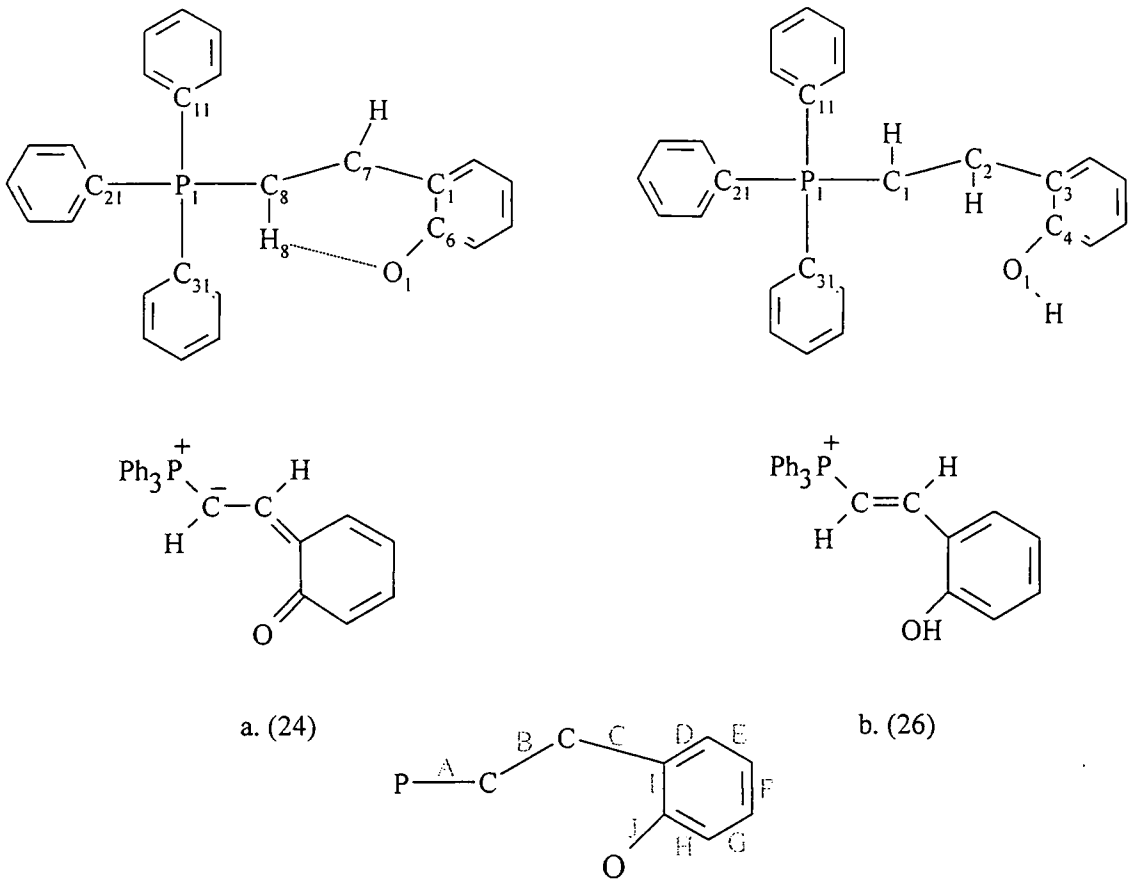

Scheme 7.6

Table 7.5 Comparison of analogous bonds in (24) and (26)

Struct.	Bond	Bond labels	Bond length Å	Bond	Bond labels	Bond length Å
(24)	A	P-C8	1.753(2)	F	C3-C4	1.406(4)
(26)		P-C1	1.780(1)		C7-C6	1.396(2)
(24)	B	C8-C7	1.356(3)	G	C4-C5	1.358(4)
(26)		C1-C2	1.345(2)		C6-C5	1.385(2)
(24)	C	C7-C1	1.439(3)	H	C5-C6	1.431(3)
(26)		C2-C3	1.469(2)		C5-C4	1.405(2)
(24)	D	C1-C2	1.409(3)	I	C6-C1	1.450(3)
(26)		C3-C87	1.404(2)		C4-C3	1.411(2)
(24)	E	C2-C3	1.375(3)	J	C6-O1	1.270(3)
(26)		C8-C7	1.388(2)		C4-O1	1.354(2)

Consider first Bond A. Unlike in (26), in (24) there is not only a positive charge localised on phosphorus but also a degree of negative charge on carbon, hence one would expect to observe an electrostatic shortening of this bond. Thus bond A in (24) should be shorter

than in (26) and this is indeed observed. Bond B is represented as a double bond in (26) but a single bond in (24) and as expected this bond is longer in (24) though perhaps not significantly. Conversely, bond C is a single bond in (24) and a double bond in (26). This again is supported by the data which reveals the shorter bond distance in (24). In examining the bond lengths within the rings (bonds D - I), if one assumes that the ring in (26) is fully delocalised, i.e. all its bonds have partial double bond character, and (24) is consistent with its proposed delocalisation, then the bonds in (26) should be shorter if a double bond is proposed but longer if a single bond is proposed. This is found to be the case, most obviously, as would be expected for the bonds adjacent to O, i.e. bonds H and I. Bond J is the carbon oxygen bond. In (24) this is proposed to be a double bond while in (26) it is a single bond. Again examination of the bond lengths upholds this interpretation. These observations, therefore, add weight to the proposal that the substituted ylide resonance form does indeed provide a contribution which is key to the bond lengths observed in (24).

The reaction of (24) with MeI in an acetonitrile solution was also carried out. Unfortunately no crystals could be grown, instead the product was a pale yellow powder. Analysis by ^{1}H NMR strongly pointed to the methylation of (24) at oxygen to form the iodide salt $(Ph_3PC(H)=C(H)C_6H_4OMe)^{+}I^{-}$, (27).

As stated earlier due to anomalies in ^{31}P NMR spectra of (24), namely the appearance of a second peak at - 50 ppm after several days, it was postulated that (24) could be undergoing some type of photochemical conversion. Preliminary investigations on (24) and subsequently (25) by UV/Vis spectroscopy revealed that both (24) and (25) are in fact photochromic. The following section will provide a brief outline of the background to this subject (a more detailed history is beyond the scope of this chapter[12]) and will report our results.

Photochromism was first reported in 1876 by Fritsche.[13] During the early stages of this field's development photochromism was observed simply as a reversible change in colour

---

[12]For a comprehensive discussion of photochromism see *'Photochromism: Molecules and Systems.'* H. Durr and H. Bouas-Laurent, Eds., Elsevier Science Publishers B. V., Amersterdam, 1990.
[13]H. Fritsche, *Comp. Rend.*, 1867, **69**, 1035.

initiated by sunlight and reversed at night. Since Fritsche's first observations, this field has received considerable attention and is still an active field of research today, mainly due to its actual and potential applications and its importance in biological reactions.[14] As a result of subsequent developments the definition of this phenomenon was extended to include not only solar radiation but all electromagnetic radiation and an accepted definition is now as follows.

> *"Photochromism is a reversible transformation of a single chemical species being induced in one or both directions by electromagnetic radiation between two states having different distinguishable absorption spectra."*[12]

These changes in radiation may be induced by UV, Visible, or IR radiation. Reversibility is an important criterion. The majority of photochromic systems are based on unimolecular reactions, (however bimolecular processes are known), for example, a starting material A undergoes formation of product P induced by electromagnetic radiation then the reverse reaction from P to A can occur either photochemically or thermally. Photochromic processes can involve for example, proton transfer reactions or reversible photoisomerisation i.e. cis-trans isomerisation.

An example of the former has been observed in N-salicylidene-4-bromoaniline which involves reversible proton transfer from oxygen to nitrogen Scheme 7.7.

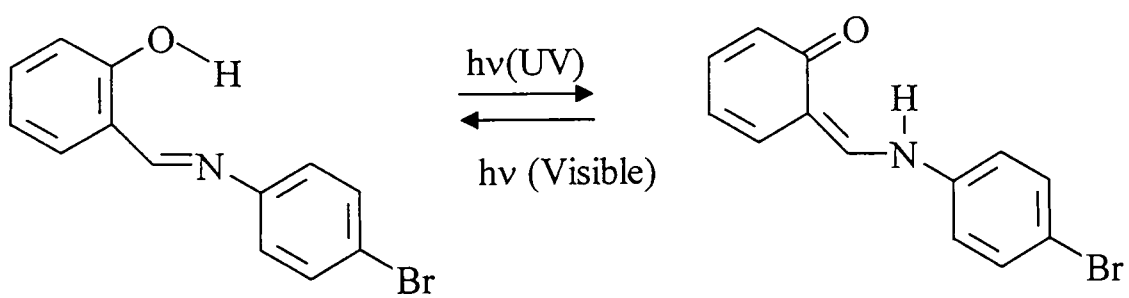

Scheme 7.7

[14]see for example I. Willner and S. Rubin, *Angew. Chem. Int. Ed. Eng.*, 1996, **35**, 367.

Many olefins[15] and azobenzenes[16] undergo cis-trans photoisomerisation about their C=C and N=N bonds respectively. Reversible photoisomerisation can also be exhibited by small molecules attached to polymers for example see Scheme 7.8.[17]

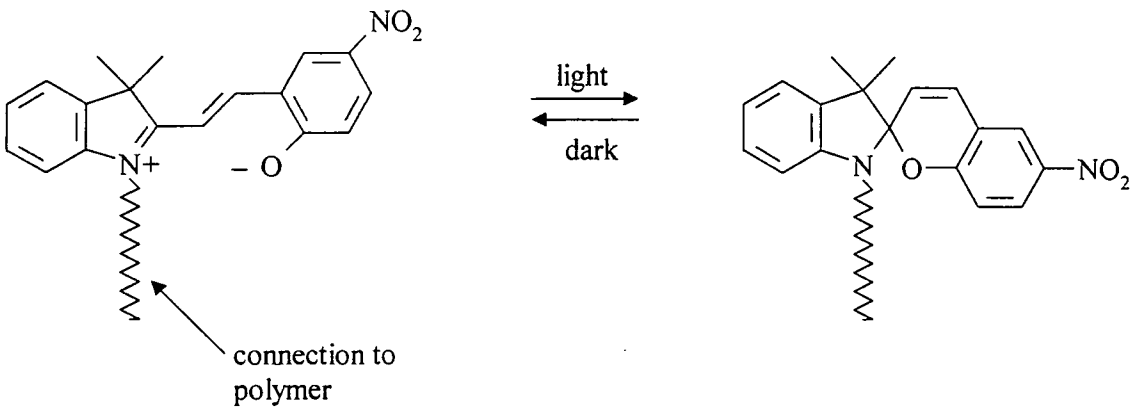

Scheme 7.8

The method of choice for investigating photochemical behaviour is UV/Vis absorption spectroscopy as it provides a quick and efficient way to monitor such reactions. When studying the photochemical properties of (24) by this method a number of factors had to be taken into consideration. Photochemical reactions can only occur if the reactant absorbs photons, therefore it was necessary to obtain an absorption spectrum of a fresh solution of (24) to establish the optimal wavelength for the incident radiation. In order to carry this out successfully other factors need to be addressed. Firstly, the choice of solvent is crucial. The solvent must be transparent (i.e. not absorb) at the wavelength of irradiation. Secondly, the concentration of the solution cannot be too high. If this were the case incident radiation would only be absorbed in a very small outer layer and inhomogeneities would arise.

Therefore, dilute solutions of (24) were prepared with the solvent systems preferred being toluene and benzene. The initial absorption spectrum obtained in toluene revealed a band

---

[15] '*Photochromism: Molecules and Systems.*' H. Durr and H. Bouas-Laurent, Eds., Elsevier Science Publishers B. V., Amersterdam, 1990, Chapter3.
[16] '*Photochromism: Molecules and Systems.*' H. Durr and H. Bouas-Laurent, Eds., Elsevier Science Publishers B. V., Amersterdam, 1990, Chapter 4.
[17] I. Willner and S. Rubin, *Angew. Chem. Int. Ed. Eng.*, 1996, **35**, 367.

which peaked at 470 nm. A series of experiments were then undertaken irradiating the sample at different wavelengths and observing the changes in the absorption spectrum.

In these preliminary experiments the light source employed was white light with filters being used to vary the wavelengths, namely a green filter which transmits only light of wavelength greater than 400 nm and a UV filter that only transmits light whose wavelength lies between 300 to 400 nm (Figure 7.8)

As the original spectrum revealed a peak at 470 nm the green filter was used for the initial experiment. On exposing the toluene solution of (24) to a flash of white light through this filter a band peaking at 370 nm was seen to emerge, meanwhile there was a simultaneous decrease in absorbance level of the original band (Figure 7.9).

This initial experiment revealed that (24) was photosensitive. This sort of behaviour was observed by Lequan et al,[18] in another zwitterionic species, namely, {4'-[methyl(diphenyl)phosphino]biphenyl-4-yl}triphenylborate, PBB (Figure 7.10). On irradiation of PBB the absorbance levels of the bands due to PBB decreased while a new band appeared at 300 nm. However, on further investigation this process was found to be irreversible.

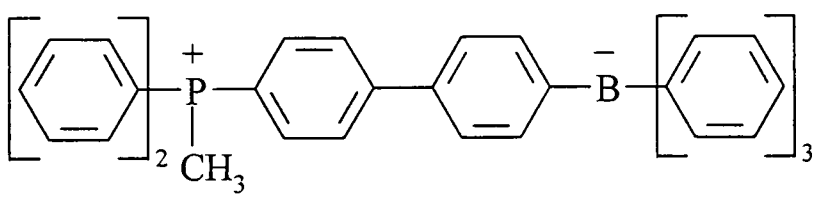

(PBB)

Figure 7.10

[18]K. C. Ching, M. Lequan and R-M. Lequan, *J. Chem. Soc., Faraday Trans.*, 1991, **87**, 2225.

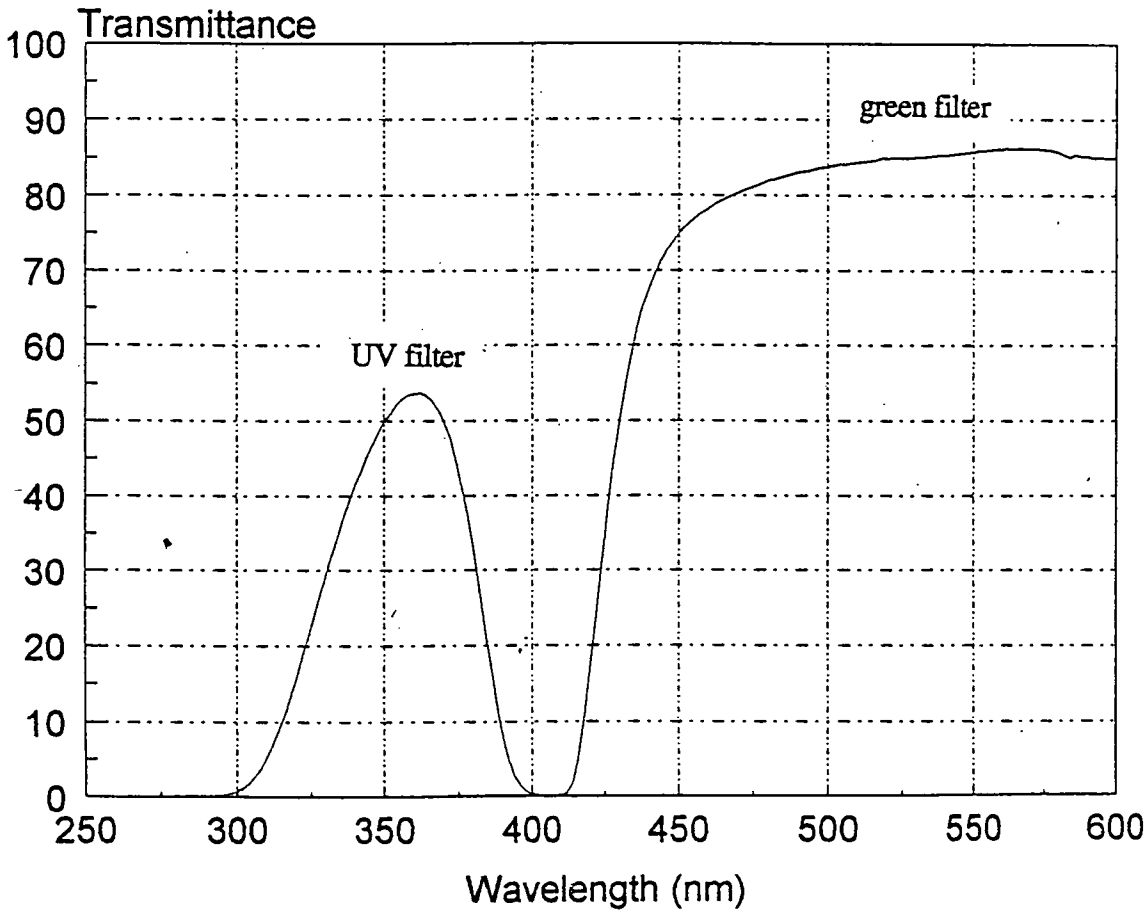

Figure 7.8 Transmittance spectrum of the UV and green filters.

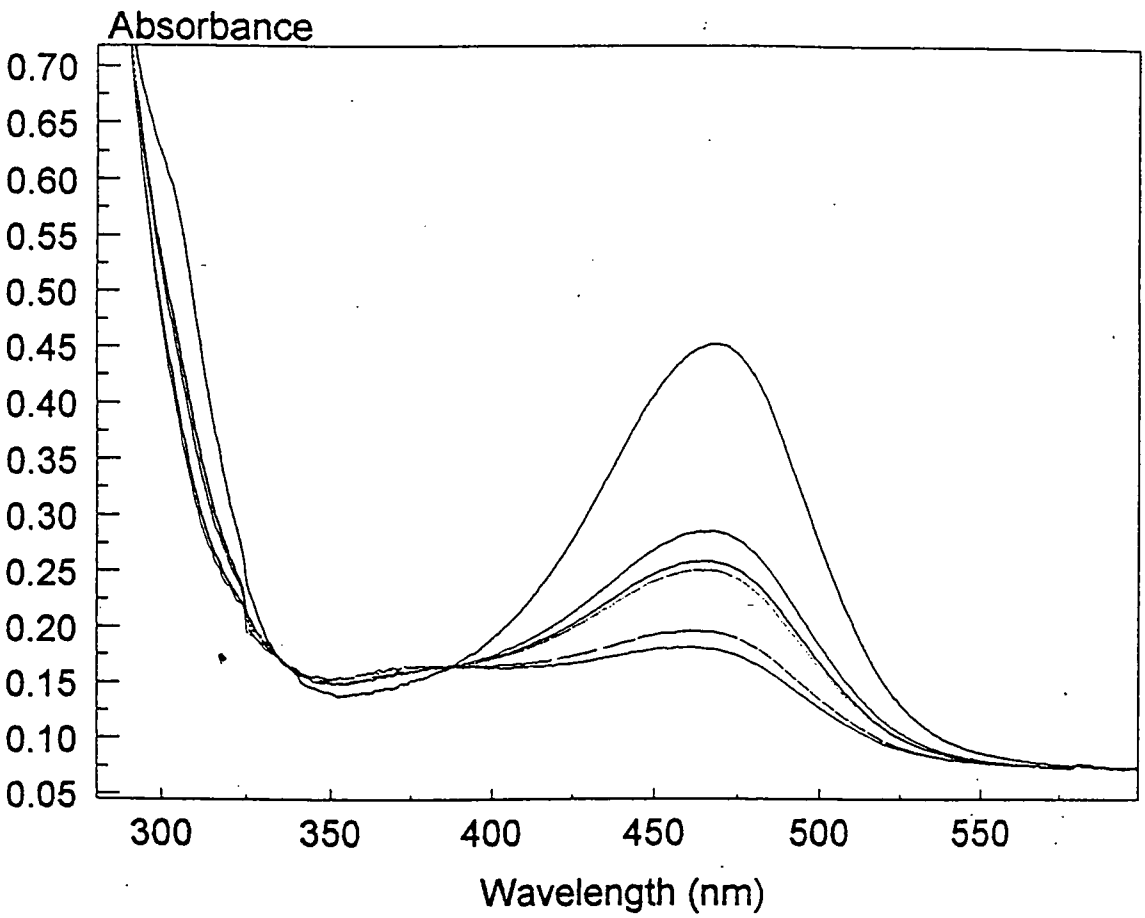

Figure 7.9 UV/Vis spectra of (24) in toluene showing the emergence of a band peaking at 370 nm and the decrease in the band at 470 nm.

In order to establish if the process occurring in (24) was reversible a second experiment was performed where the solution was exposed to the unfiltered white light. This resulted in an increase in the absorbance level of the original peak and a decrease in the band at 370 nm (Figure 7.9). These initial experiments revealed that unlike PBB, (24) was photochromic and further analysis was undertaken.

In the second batch of experiments the solvent used was benzene. Here the light source was a lamp which could emit light of different specific wavelengths. The sample was initially exposed to a wavelength of 450 nm for 50 minutes with spectra being recorded every 5 minutes. Once more, a gradual decrease in the absorbance level of the band peaking at 470 nm was observed while a second band peaking at about 375 nm emerged. Following this the sample was then irradiated with light of wavelength 340 nm for 20 minutes, again with spectra being recorded every 5 minutes. This revealed an increase in the original band and a decrease in the band at 375 nm (Figure 7.11). These results were consistent with the original set of experiments.

As mentioned previously the original reason for these investigations was the appearance of a second peak in the ^{31}P NMR. It was therefore felt prudent to try and see if on irradiation this second peak appeared in the NMR spectrum, This, however, proved difficult as the concentration required for a sufficiently 'noise free' ^{31}P NMR is much higher than that suitable for UV/Vis studies. Nevertheless it was possible to observe a second peak at -50 ppm emerging after exposure to radiation of 450 nm although due to the background noise this could not be detected without the solution being subject to a substantial period of irradiation.

Having established that (24) does exhibit photochromic properties the question that remained was what species was responsible for this second band. As mentioned earlier there are several processes that can be responsible for photochromic behaviour. In this case as the peak observed in the ^{31}P NMR was at -50 ppm, similar to that observed for (25) and typical of a five coordinate phosphorus, it seemed reasonable to hypothesise that the process occurring here was trans - cis photoisomerisation, that is a switch from the *E*

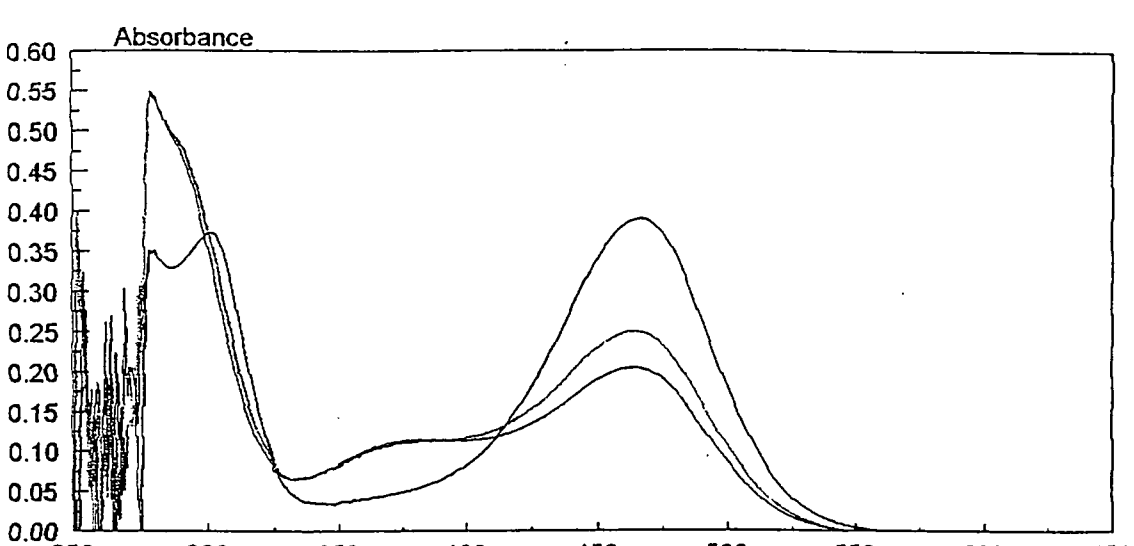

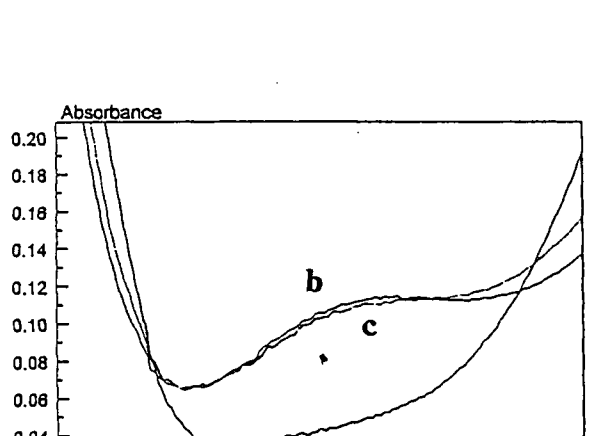

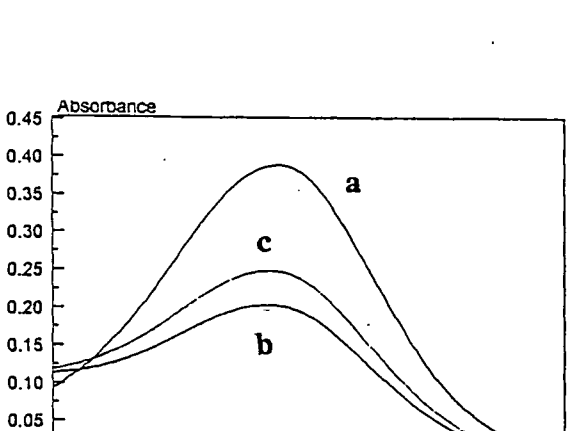

a - original spectrum

b - 50 minute exposure to light of wavelength 450nm

c - 20 minute exposure to light of wavelength 340 nm

Figure 7.11 UV/Vis spectra of (24) in benzene illustrating its photochromic nature.

to *Z* isomer with the formation of a five coordinated phosphorus species being responsible for the band peaking at 370 nm. The following mechanism is postulated, (Scheme 7.9).

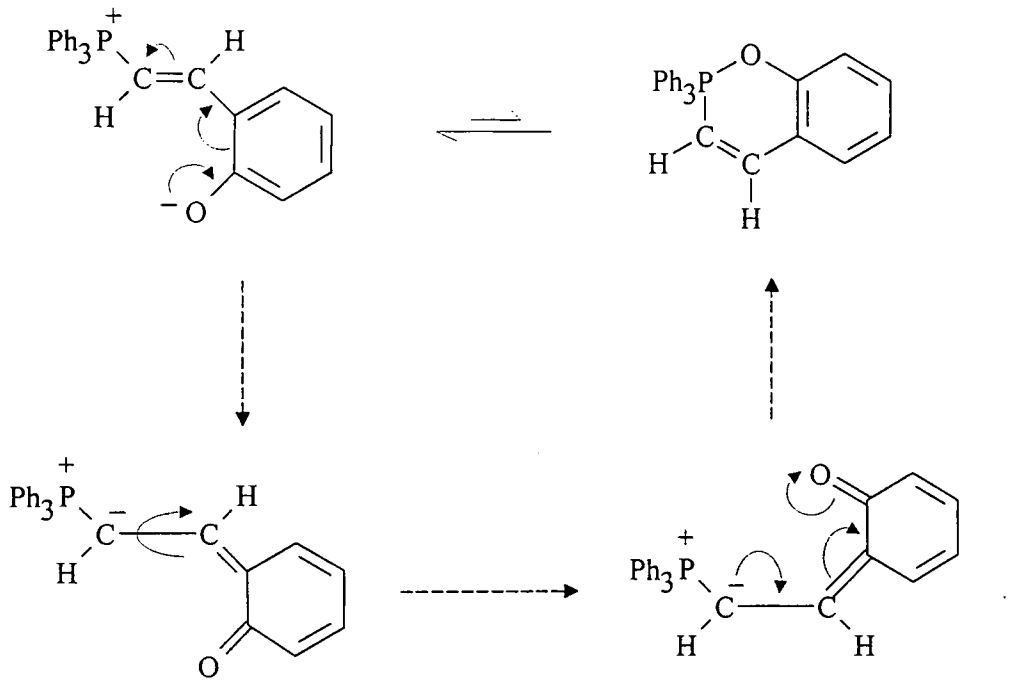

Scheme 7.9

The change of configuration is possible due to the C=C double bond becoming a C-C single bond, hence allowing rotation. It should be noted that 100 % conversion from one species to another is not observed, suggesting an equilibrium is set up.

The hypothesis for (24) attributed the second band to a five coordinate species similar to (25). It therefore seemed logical to investigate the absorption spectrum of (25) to see if it revealed a band peaking around 370 nm and if it also exhibited photochromism. Similar methods were employed and the original absorption spectrum of (25) revealed that there was indeed a band peaking at approximately 370 nm and no peak at 470 nm. In this case, when flashed with unfiltered white light the absorbance level of this peak decreased while a second band peaking at 500 nm was observed. A UV filter was then employed and on exposure the band at 500 nm decreased while that at 370 nm increased (Figure 7.12). This revealed that (25) was indeed photochromic, with the second peak presumably being due to a *E* isomeric form.

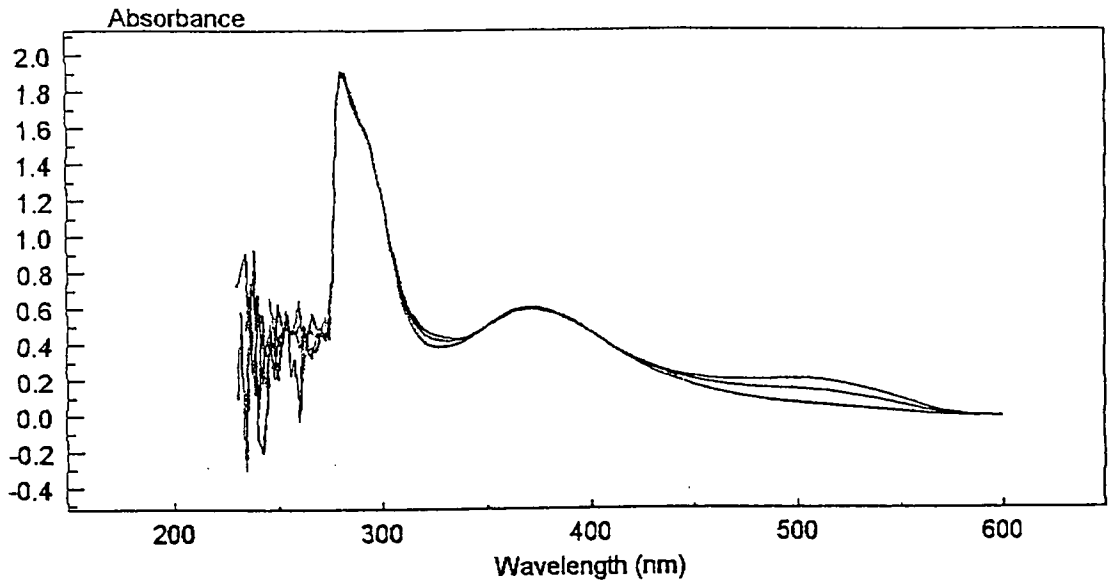

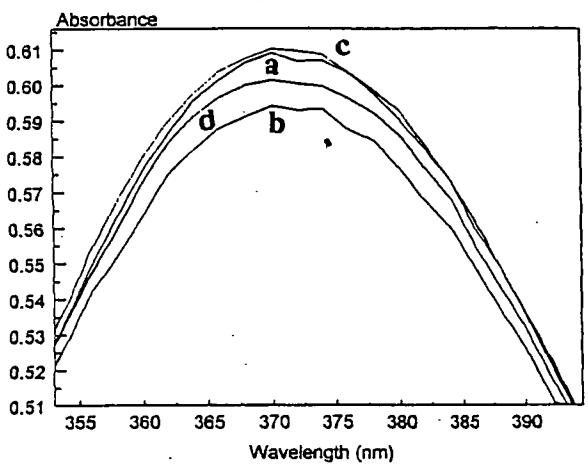

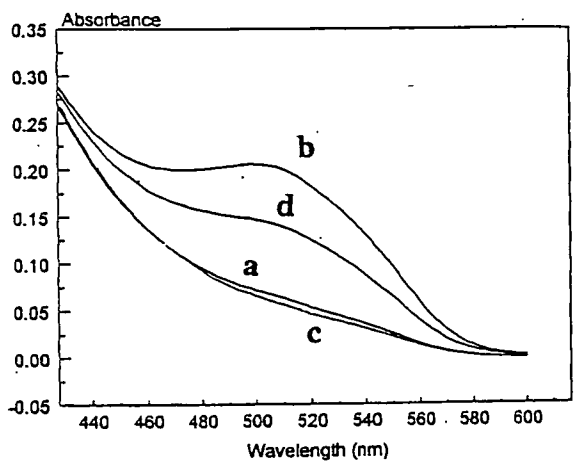

a - original spectrum c - flash with green filter

b - flash no filter d - flash with UV filter

Figure 7.12 UV/Vis spectra of (25) in benzene illustrating its photochromic nature.

Following on from work into the photochromic properties of (24), recent literature[19, 20] turned our attention to investigation, by UV/Vis absorption spectroscopy, of another physical property that (24) may exhibit, namely solvatochromism. The following section briefly outlines the background of this field and reports the results obtained for (24).

In recent years there has been much interest and research into organic molecules for application in non-linear optics, for example those capable of showing second order molecular polarisability (β) and hence of interest as second-harmonic generators (SHG) i.e. frequency doubling of laser radiation.[21] The types of structures that can have large β's are generally those with electron donating groups and electron withdrawing groups linked through some conjugated π-system. Consider the Mulliken resonance structures shown in Figure 7.13.

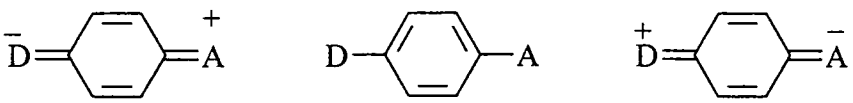

I II III

Figure 7.13

These represent the extreme situations where an electron has been transferred from the acceptor to the donor. Case I is highly unlikely, case II shows the neutral state while case III shows the maximal charge transfer or zwitterionic state. The actual ground and excited states are essentially a combination of II and III, and have dipole moments μg and μe respectively, where $\beta \propto \Delta\mu$. When an oscillating field is applied to the π electron of such a donor-acceptor molecule the flow of charge is inhibited in one direction and enhanced in the other (Figure 7.14).

---

[19]D. W, Allen and X. Li, *J. Chem. Soc., Perkin Trans. (2),* 1997, 1099.
[20]D. W. Allen, J. Hawkrigg, H. Adams, B. F. Taylor, D. E. Hibbs and M. B. Hursthouse, *J. Chem. Soc., Perkin Trans. (1),* 1998, 335.
[21]D. S. Chemla and J. Zyss, *'Nonlinear Optical Properties of Organic molecules and Crystals'* Academic Press, Orlando, Florida, 1987, Vol. 1.

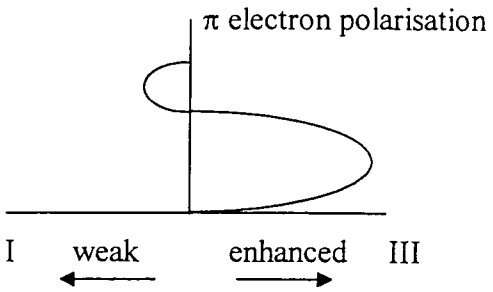

Figure 7.14

In other words, the charge - transfer molecule is acting as an 'optical diode' with an asymmetric response or a nonlinearity. Systems with large $\Delta\mu$ have large β and are hence of interest for SHG.

Molecules with these types of structures are often highly solvatochromic.[22, 23] The term solvatochromism relates to the pronounced change of an UV/Vis absorption band, accompanying a change in the polarity of the medium. Molecules that are solvatochromic are those whose UV/Vis absorption spectra are very sensitive to the solvent in which they are placed. The changes modified by the solvent are as a result of physical intermolecular solute-solvent interactions which tend to alter the energy differences between the ground state and excited state of the absorbing species containing the chromophore.[24] A hypsochromic (or blue) shift, (i.e. to longer wavelengths) with increasing solvent polarity, is known as negative solvatochromism, while a bathochromic (or red) shift (i.e. to shorter wavelengths) with increasing solvent polarity is known as positive solvatochromism. The extent and direction of solvatochromism depends on whether the zwitterionic structure is more important in the ground state or in the excited state. If the zwitterionic structure is more important in the ground state then a hypsochromic shift occurs (i.e. negative solvatochromism).

---

[22]W. Liptray, *Angew. Chem. Int. Ed. Engl.*, 1969, **8**, 177

[23]C. Reichardt, *'Solvents and Solvent Effects in Organic Chemistry' 2nd Edn.*, Verlag Chemie, Weinheim, 1990, Chapter 6.

[24]A chromophore is generally thought of as any group of organic molecules (sometimes the whole molecule) responsible for the light absorption under consideration.

A class of compounds investigated for their SHG properties were the pyridinium-N-phenoxide betaine dyes (Figure 7.15), first studied in depth by Reichardt and Dimroth in the 1960's.[25]

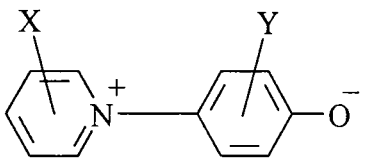

Figure 7.15

The electronic ground states of these compounds are dipolar ions, with the nitrogen atom bearing a positive charge and the oxygen atom bearing a negative charge. These dyes are highly negatively solvatochromic (i.e. exhibit a hypsochromic shift) with polar solvents shifting the longest wavelength UV/Vis absorption band [λ_{max} (nm)] to shorter wavelengths and non-polar solvents shifting them to longer wavelengths.

2,6-Diphenyl-4-(2,4,6-triphenyl-N-pyridinio)phenolate (Reichardt's dye Figure 7.16) is one of the most highly solvatochromic compounds known, displaying a 381 nm hypsochromic shift in λ_{max} on going from water to benzene (Table 7.6).[26]

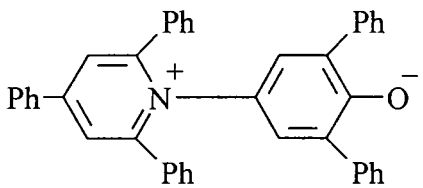

Figure 7.16

[25]K. Dimroth, C. Reichardt, T. Siepmann and F. Bohlmann, *Liebigs Ann. Chem.*, 1963, **661**, 1.
[26]C. Reichardt, *Angew. Chem. Int. Ed. Engl.*, 1965, **4**, 29.

Table 7.6 Solvatochromic behaviour of Reichardt's dye.

Solvent	λ_{max} (nm)	Solvent	λ_{max} (nm)
water	453	acetone	677
methanol	516	dichloromethane	702
ethanol	551	pyridine	706
2-propanol	591	chloroform	731
acetonitrile	625	chlorobenzene	777
dimethylsulphoxide	634	benzene	834

Only a few solvatochromic phosphonium betaines have been described. However work on such compounds reported by Allen et al involved a series of phosphonio-iminophenolate betaines (series a, Figure 7.17a) and a series of phosphonioimidazolide betaines, (series b, Figure 7.17b).

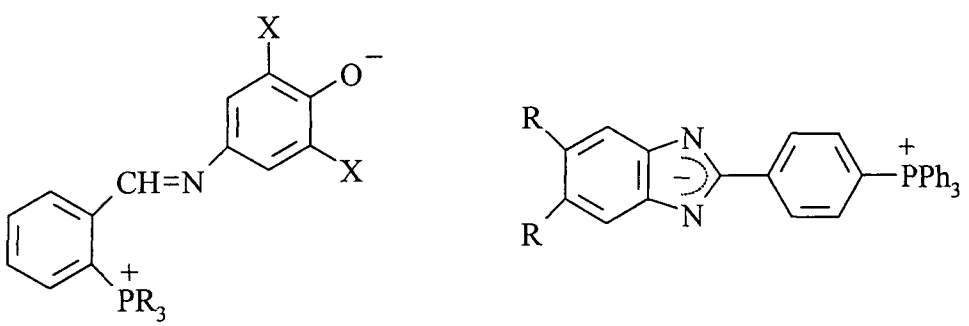

(a) (b)

Figure 7.17

The UV/Vis spectra of both these series of betaines revealed a shift in the absorption maximum to longer wavelengths as the polarity of the solvent decreased. That is, these too displayed negative solvatochromism, again consistent with a transition from the dipolar ground state to a less polar excited state in which the negative charge is displaced towards the cationic centre (Table 7.7).

Table 7.7 Sovatochromic behaviour of series a and b

Solvent	phosphonio-iminophenolates[19] range of λ_{max} (nm)	phosphonioimidazolides[20] range of λ_{max} (nm)
methanol	532 - 424	376 - 358
acetonitrile	598 - 460	432 - 434
acetone	628 - 502	446 - 452
dichloromethane	616 - 508	446 - 448

Another class of compounds that exhibit negative solvatochromism was investigated by Lequan et al. They suggested the use of charged donor or acceptor groups as another approach to the design of materials capable of SHG.[18] They studied the zwitterionic species of the type PBB, mentioned previously (Figure 7.10), for which the acceptor group was a phosphonium cation and the donor group a borate anion.

These were found to have a high dipole moment in the ground state (μg) and a considerably smaller one in the excited state (μe) and hence, when solvatochromic studies were carried out, they were found to exhibit a high dependency on solvent polarity with a hypsochromic shift clearly observed (Table 7.8).

Table 7.8 Solvatochromic behaviour of zwitterionic species of the type PBB.[18]

Solvent	λ_{max} (nm)	Solvent	λ_{max} (nm)
acetonitrile	318	thf	340
dimethylsulphoxide	320	trichloroethane[i]	340
N,N-dimethylformamide	322	hmpa	323
dichloromethane	337	dichloroethane	338
chloroform[i]	351		

i = poor solubility

These systems are somewhat reminiscent of our own zwitterionic compound (24) and it seemed prudent to carry out some preliminary investigations into the solvent dependency of its UV/Vis absorption spectrum.

For the solvatochromic determination all solvents were anhydrous (refluxed over Na/K or CaH). The choice of solvents was limited by the solubility of (24). The results obtained (Figure 7.18 and Table 7.9) showed a hypsochromic shift, i.e. there was a shift in λ_{max} to shorter wavelengths in more polar solvent and a shift to longer wavelengths in nonpolar solvents.

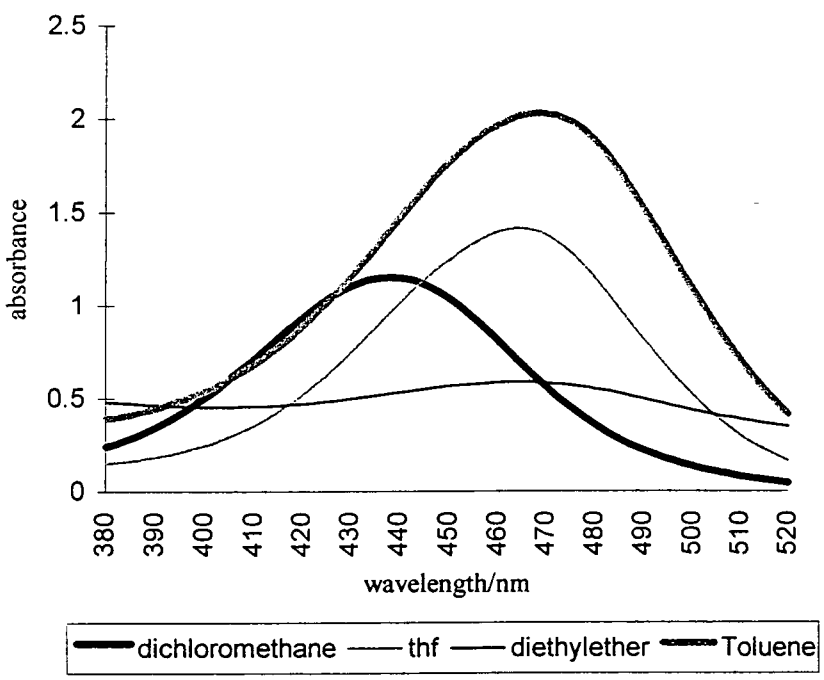

Figure 7.18 UV/Vis absorption spectra of (24), showing the hypsochromic shift.

Table 7.9 Solvatochromic behaviour of (24).

Solvent	λ_{max} (nm)
dichloromethane	438
thf	464
diethylether[i]	466
toluene	468

i = poor solubility

These results suggest that the zwitterionic form is the more stable in the ground state in solution as well as observed in the solid state.

To summarise, the work carried out in the reaction of H_2salen and the phosphonium ylides (1) and (3) has shown a different mode of reaction is encountered to that previously observed between (2) and H_2salen (Chapter 6). In the former case a zwitterionic compound (24) was observed, while in the latter the product was shown to be a five coordinate aryloxyphosphorane (25). Insight into the delocalisation of charge in (24) was gained from comparison of its bond lengths with those in related compounds including (25) and (26). Preliminary UV/Vis absorption spectroscopy has revealed that (24) and (25) are photochromic and further investigations revealed (24) to be solvatochromic.

Appendix A

Supplementary Crystallographic Data

Index of Tables in Appendix A

Table A.1b. Atomic coordinates (x 10^4) and equivalent isotropic displacement parameters (A^2 x 10^3) for (5). U(eq) is defined as one third of the trace of the orthogonalized Uij tensor.

	x	y	z	U(eq)
P(1A)	2630(1)	7683(1)	4428(1)	19(1)
C(1A)	3371(2)	9035(2)	4963(1)	24(1)
C(11A)	2930(2)	6640(1)	4965(1)	21(1)
C(12A)	1956(2)	5644(2)	4822(1)	27(1)
C(13A)	2146(2)	4864(2)	5259(1)	33(1)
C(14A)	3288(2)	5082(2)	5842(1)	37(1)
C(15A)	4262(2)	6064(2)	5982(1)	38(1)
C(16A)	4100(2)	6848(2)	5544(1)	29(1)
C(21A)	3482(2)	7399(2)	3611(1)	23(1)
C(22A)	3769(2)	6311(2)	3317(1)	31(1)
C(23A)	4301(2)	6096(2)	2650(1)	37(1)
C(24A)	4527(2)	6950(2)	2277(1)	39(1)
C(25A)	4244(2)	8027(2)	2569(1)	36(1)
C(26A)	3719(2)	8271(2)	3238(1)	28(1)
C(31A)	664(2)	7660(1)	4143(1)	19(1)
C(32A)	16(2)	7152(2)	3432(1)	24(1)
C(33A)	-1498(2)	7186(2)	3218(1)	28(1)
C(34A)	-2353(2)	7719(2)	3710(1)	24(1)
C(35A)	-1726(2)	8203(2)	4418(1)	25(1)
C(36A)	-215(2)	8180(2)	4640(1)	22(1)
O(1A)	3252(1)	10887(1)	3959(1)	28(1)
C(41A)	1930(2)	11179(2)	3793(1)	23(1)
C(42A)	1670(2)	12323(2)	3838(1)	27(1)
C(43A)	255(2)	12635(2)	3690(1)	30(1)
C(44A)	-997(2)	11839(2)	3486(1)	31(1)
C(45A)	-786(2)	10713(2)	3427(1)	30(1)
C(46A)	630(2)	10384(2)	3568(1)	26(1)
P(1B)	3997(1)	2499(1)	193(1)	20(1)
C(1B)	3561(2)	3912(2)	321(1)	27(1)
C(11B)	4116(2)	2057(2)	1050(1)	23(1)
C(12B)	2937(2)	2204(2)	1459(1)	30(1)
C(13B)	3018(3)	1891(2)	2129(1)	36(1)
C(14B)	4255(3)	1425(2)	2391(1)	37(1)
C(15B)	5426(3)	1280(2)	1987(1)	35(1)
C(16B)	5368(2)	1598(2)	1316(1)	26(1)
C(21B)	5739(2)	2391(1)	-161(1)	21(1)
C(22B)	6876(2)	3284(2)	49(1)	30(1)
C(23B)	8235(2)	3182(2)	-207(1)	40(1)
C(24B)	8463(2)	2204(2)	-671(1)	35(1)
C(25B)	7327(2)	1322(2)	-888(1)	28(1)
C(26B)	5968(2)	1409(2)	-631(1)	24(1)
C(31B)	2615(2)	1567(2)	-465(1)	21(1)
C(32B)	2300(2)	1823(2)	-1157(1)	23(1)
C(33B)	1359(2)	1064(2)	-1699(1)	29(1)
C(34B)	738(2)	54(2)	-1566(1)	32(1)
C(35B)	1034(2)	-192(2)	-880(1)	32(1)
C(36B)	1970(2)	561(2)	-329(1)	27(1)
O(1B)	3471(2)	4415(1)	-1234(1)	30(1)
C(41B)	2295(2)	4798(2)	-1519(1)	26(1)
C(42B)	2408(3)	5635(2)	-1941(1)	40(1)
C(43B)	1159(4)	6059(2)	-2221(1)	58(1)
C(44B)	-257(4)	5675(2)	-2114(2)	60(1)
C(45B)	-417(3)	4854(2)	-1706(1)	47(1)
C(46B)	826(2)	4429(2)	-1414(1)	33(1)

Table A.2a. Crystal data and structure refinement for (6)

Identification code	97srv111
Empirical formula	C26 H25 O P
Formula weight	384.43
Temperature	150(2) K
Wavelength	0.71073 A
Crystal system	Monoclinic
Space group	P2(1)/c
Unit cell dimensions	a = 10.578(1) A alpha = 90 deg. b = 18.344(1) A beta = 114.64(1) deg. c = 11.789(1) A gamma = 90 deg.
Volume	2079.3(3) A^3
Z	4
Density (calculated)	1.228 Mg/m^3
Absorption coefficient	0.146 mm^-1
F(000)	816
Crystal size	0.4 x 0.4 x 0.3 mm
Theta range for data collection	2.12 to 27.49 deg.
Index ranges	-13<=h<=13, -23<=k<=23, -15<=l<=14
Reflections collected	22545
Independent reflections	4774 [R(int) = 0.0323]
Absorption correction	None
Refinement method	Full-matrix least-squares on F^2
Data / restraints / parameters	4756 / 0 / 353
Goodness-of-fit on F^2	1.108
Final R indices [I>2sigma(I)]	R1 = 0.0347, wR2 = 0.0790
R indices (all data)	R1 = 0.0463, wR2 = 0.0917
Largest diff. peak and hole	0.302 and -0.285 e.A^-3

Table A.2b. Atomic coordinates (x 10^4) and equivalent isotropic displacement parameters (A^2 x 10^3) for (6). U(eq) is defined as one third of the trace of the orthogonalized Uij tensor.

	x	y	z	U(eq)
P	5747(1)	314(1)	2660(1)	20(1)
O	3197(1)	977(1)	3972(1)	37(1)
C(1)	2020(1)	1308(1)	3707(1)	25(1)
C(2)	1522(2)	1453(1)	4635(1)	28(1)
C(3)	301(2)	1829(1)	4378(2)	35(1)
C(4)	-523(2)	2069(1)	3172(2)	39(1)
C(5)	-89(2)	1921(1)	2236(2)	38(1)
C(6)	1142(2)	1551(1)	2482(2)	32(1)
C(7)	6186(2)	473(1)	4290(1)	26(1)
C(8)	7379(2)	1016(1)	4893(2)	38(1)
C(11)	4188(1)	-229(1)	2036(1)	22(1)
C(12)	3052(2)	-35(1)	934(1)	27(1)
C(13)	1888(2)	-490(1)	459(1)	32(1)
C(14)	1869(2)	-1135(1)	1063(2)	32(1)
C(15)	2993(2)	-1324(1)	2162(2)	32(1)
C(16)	4150(2)	-872(1)	2664(1)	28(1)
C(21)	7107(1)	-178(1)	2439(1)	22(1)
C(22)	6880(2)	-890(1)	1970(1)	24(1)
C(23)	7968(2)	-1290(1)	1905(1)	27(1)
C(24)	9278(2)	-979(1)	2301(1)	29(1)
C(25)	9508(2)	-265(1)	2737(2)	30(1)
C(26)	8433(2)	138(1)	2813(1)	26(1)
C(31)	5409(1)	1172(1)	1849(1)	22(1)
C(32)	5998(2)	1360(1)	1030(1)	25(1)
C(33)	5624(2)	2021(1)	379(1)	28(1)
C(34)	4668(2)	2480(1)	538(1)	31(1)
C(35)	4096(2)	2291(1)	1368(2)	33(1)
C(36)	4462(2)	1642(1)	2035(1)	28(1)

Table A.3a. Crystal data and structure refinement for (7)

Identification code	green
Empirical formula	C37 H31 O P
Formula weight	522.00
Temperature	293(2) K
Wavelength	1.31367 A
Crystal system	Triclinic
Space group	P-1
Unit cell dimensions	a = 13.42200(10) A alpha = 88.2990(10) deg. b = 13.7400(2) A beta = 70.1650(10) deg. c = 18.43300(10) A gamma = 62.5300(10) deg.
Volume	2804.22(5) A^3
Z	4
Density (calculated)	1.236 Mg/m^3
Absorption coefficient	0.000 mm^-1
F(000)	708
Crystal size	4.9 x 3.9 x 1.1 mm
Theta range for data collection	2.20 to 50.37 deg.
Index ranges	-14<=h<=15, -15<=k<=16, -21<=l<=21
Reflections collected	11427
Independent reflections	8291 [R(int) = 0.0310]
Refinement method	Full-matrix least-squares on F^2
Data / restraints / parameters	8291 / 0 / 1262
Goodness-of-fit on F^2	1.037
Final R indices [I>2sigma(I)]	R1 = 0.0429, wR2 = 0.1219
R indices (all data)	R1 = 0.0475, wR2 = 0.1265
Extinction coefficient	0.00085(9)
Largest diff. peak and hole	0.810 and -0.997 e.A^-3

Table A.3b. Atomic coordinates (x 10^4) and equivalent isotropic displacement parameters (A^2 x 10^3) for (7). U(eq) is defined as one third of the trace of the orthogonalized Uij tensor.

	x	y	z	U(eq)
P(11)	4416(2)	5700(2)	6910(1)	6(1)
O(11)	7130(2)	4390(2)	4586(1)	8(1)
C(11)	4688(2)	5881(2)	5912(1)	6(1)
H(11A)	3960(4)	5907(4)	5756(3)	24(1)
H(11B)	5578(4)	5216(4)	5527(3)	23(1)
H(11C)	4691(5)	6668(4)	5839(3)	26(1)
C(121)	3006(2)	6854(2)	7501(1)	7(1)
C(122)	2398(2)	6746(2)	8255(1)	8(1)
H(12A)	2764(4)	5970(4)	8481(2)	22(1)
C(123)	1281(2)	7626(2)	8713(1)	10(1)
H(12B)	794(5)	7533(4)	9296(3)	28(1)
C(124)	774(2)	8611(2)	8421(1)	10(1)
H(12C)	-90(5)	9287(4)	8777(3)	27(1)
C(125)	1377(2)	8718(2)	7665(1)	10(1)
H(12D)	978(5)	9477(4)	7432(3)	26(1)
C(126)	2487(2)	7840(2)	7201(1)	9(1)
H(12E)	2926(4)	7920(4)	6605(3)	21(1)
C(131)	5638(2)	5548(2)	7166(1)	6(1)
C(132)	5478(2)	5955(2)	7908(1)	8(1)
H(13A)	4580(4)	6475(4)	8338(3)	22(1)
C(133)	6486(2)	5693(2)	8098(1)	10(1)
H(13B)	6367(5)	5999(4)	8675(3)	28(1)
C(134)	7650(2)	5039(2)	7551(1)	10(1)
H(13C)	8426(4)	4843(4)	7708(3)	25(1)
C(135)	7812(2)	4641(2)	6809(1)	9(1)
H(13D)	8709(4)	4140(4)	6374(3)	25(1)
C(136)	6812(2)	4895(2)	6615(1)	8(1)
H(13E)	6948(4)	4573(4)	6038(3)	23(1)
C(141)	4312(2)	4451(2)	7079(1)	6(1)
C(142)	3638(2)	4207(2)	6754(1)	7(1)
H(14A)	3255(4)	4714(4)	6356(3)	21(1)
C(143)	3482(2)	3281(2)	6934(1)	8(1)
H(14B)	2962(5)	3091(4)	6687(3)	24(1)
C(144)	4013(2)	2599(2)	7418(1)	8(1)
H(14C)	3882(5)	1882(4)	7556(3)	27(1)
C(145)	4702(2)	2835(2)	7728(1)	8(1)
H(14D)	5106(4)	2303(4)	8106(3)	24(1)
C(146)	4847(2)	3768(2)	7563(1)	7(1)
H(14E)	5389(4)	3953(4)	7811(3)	22(1)
C(151)	8204(2)	3858(2)	4596(1)	6(1)
C(152)	8947(2)	4383(2)	4492(1)	6(1)
C(153)	10124(2)	3789(2)	4484(1)	8(1)
H(15A)	10650(4)	4209(4)	4415(3)	23(1)
C(154)	10610(2)	2674(2)	4589(1)	10(1)
H(15B)	11505(5)	2248(4)	4621(3)	24(1)
C(155)	9911(2)	2145(2)	4679(1)	8(1)
H(15C)	10289(4)	1279(3)	4770(3)	21(1)
C(156)	8741(2)	2698(2)	4672(1)	6(1)
C(161)	8085(2)	2062(2)	4704(1)	6(1)
C(162)	8728(2)	978(2)	4302(1)	8(1)
H(16A)	9687(5)	628(4)	3947(3)	23(1)
C(163)	8150(2)	333(2)	4345(1)	9(1)
H(16B)	8664(4)	-514(4)	4035(3)	25(1)
C(164)	6919(2)	776(2)	4790(1)	10(1)
H(16C)	6477(5)	278(4)	4828(3)	27(1)
C(165)	6275(2)	1855(2)	5188(1)	9(1)
H(16D)	5327(4)	2207(4)	5546(3)	24(1)
C(166)	6861(2)	2492(2)	5150(1)	8(1)
H(16E)	6335(4)	3329(4)	5468(3)	26(1)
C(171)	8487(2)	5552(2)	4356(1)	6(1)
C(172)	7345(2)	6403(2)	4834(1)	8(1)

H(17A)	6771(4)	6190(4)	5299(3)	23(1)
C(173)	6962(2)	7504(2)	4720(1)	9(1)
H(17B)	6076(4)	8148(4)	5102(3)	23(1)
C(174)	7704(2)	7792(2)	4118(1)	10(1)
H(17C)	7400(5)	8647(4)	4022(3)	26(1)
C(175)	8833(2)	6954(2)	3634(1)	10(1)
H(17D)	9418(5)	7167(4)	3167(3)	26(1)
C(176)	9211(2)	5853(2)	3754(1)	7(1)
H(17E)	10076(4)	5201(4)	3366(3)	24(1)
P(21)	7137(2)	9205(2)	8163(1)	5(1)
O(21)	3956(2)	11711(2)	9515(1)	7(1)
C(21)	6432(2)	9752(2)	9170(1)	6(1)
H(21A)	6238(4)	9155(4)	9523(2)	21(1)
H(21B)	5595(4)	10542(4)	9273(3)	24(1)
H(21C)	7053(4)	9912(4)	9346(3)	22(1)
C(221)	8443(2)	7888(2)	8009(1)	5(1)
C(222)	9546(2)	7606(2)	7403(1)	6(1)
H(22A)	9643(4)	8173(4)	7003(3)	22(1)
C(223)	10544(2)	6578(2)	7323(1)	7(1)
H(22B)	11395(4)	6354(4)	6852(3)	24(1)
C(224)	10436(2)	5832(2)	7836(1)	7(1)
H(22C)	11229(4)	5047(4)	7769(3)	24(1)
C(225)	9335(2)	6110(2)	8433(1)	8(1)
H(22D)	9234(4)	5543(4)	8837(3)	22(1)
C(226)	8332(2)	7137(2)	8521(1)	7(1)
H(22E)	7485(4)	7352(4)	8998(3)	26(1)
C(231)	7555(2)	10144(2)	7617(1)	6(1)
C(232)	7681(2)	10128(2)	6831(1)	8(1)
H(23A)	7533(5)	9554(4)	6558(3)	23(1)
C(233)	8018(2)	10845(2)	6399(1)	9(1)
H(23B)	8114(5)	10829(4)	5790(3)	25(1)
C(234)	8216(2)	11597(2)	6749(1)	10(1)
H(23C)	8457(5)	12161(4)	6401(3)	25(1)
C(235)	8085(2)	11617(2)	7530(1)	11(1)
H(23D)	8216(5)	12213(4)	7814(3)	29(1)
C(236)	7760(2)	10894(2)	7969(1)	8(1)
H(23E)	7628(5)	10948(4)	8584(3)	25(1)
C(241)	6122(2)	9031(2)	7816(1)	7(1)
C(242)	6586(2)	8161(2)	7221(1)	8(1)
H(24A)	7541(5)	7544(4)	7005(3)	24(1)
C(243)	5820(2)	8082(2)	6895(1)	9(1)
H(24B)	6185(5)	7408(4)	6434(3)	26(1)
C(244)	4597(2)	8881(2)	7170(1)	11(1)
H(24C)	4007(5)	8823(4)	6916(3)	29(1)
C(245)	4135(2)	9736(2)	7768(1)	9(1)
H(24D)	3186(5)	10350(4)	7988(3)	26(1)
C(246)	4895(2)	9824(2)	8097(1)	7(1)
H(24E)	4524(4)	10504(4)	8565(3)	22(1)
C(251)	3389(2)	12777(2)	9585(1)	6(1)
C(252)	2251(2)	13355(2)	9469(1)	7(1)
C(253)	1655(2)	14512(2)	9552(1)	8(1)
H(25A)	784(4)	14936(4)	9481(3)	21(1)
C(254)	2122(2)	15152(2)	9749(1)	8(1)
H(25B)	1602(5)	16045(4)	9849(3)	27(1)
C(255)	3235(2)	14608(2)	9835(1)	7(1)
H(25C)	3611(4)	15076(4)	9972(3)	24(1)
C(256)	3868(2)	13446(2)	9754(1)	6(1)
C(261)	5063(2)	12926(2)	9836(1)	7(1)
C(262)	5909(2)	13280(2)	9459(1)	9(1)
H(26A)	5702(4)	13925(4)	9093(3)	23(1)
C(263)	7027(2)	12824(2)	9547(1)	9(1)
H(26B)	7671(4)	13115(4)	9251(3)	24(1)
C(264)	7319(2)	12007(2)	10022(1)	9(1)
H(26C)	8181(5)	11656(4)	10096(3)	26(1)
C(265)	6475(2)	11655(2)	10409(1)	9(1)
H(26D)	6678(5)	11036(4)	10787(3)	24(1)
C(266)	5369(2)	12107(2)	10315(1)	7(1)
H(26E)	4725(4)	11817(4)	10613(3)	21(1)
C(271)	1703(2)	12733(2)	9263(1)	6(1)
C(272)	1729(2)	11794(2)	9595(1)	7(1)
H(27A)	2195(4)	11490(4)	9997(3)	23(1)

C(273)	1161(2)	11250(2)	9414(1)	9(1)
H(27B)	1192(5)	10529(4)	9680(3)	24(1)
C(274)	558(2)	11629(2)	8894(1)	11(1)
H(27C)	124(5)	11210(4)	8756(3)	24(1)
C(275)	535(2)	12556(2)	8558(1)	10(1)
H(27D)	62(5)	12875(4)	8153(3)	29(1)
C(276)	1103(2)	13091(2)	8735(1)	8(1)
H(27E)	1101(5)	13798(4)	8455(3)	26(1)

Table A.4a. Crystal data and structure refinement for (8)

Identification code	96srv118
Empirical formula	C39 H34.50 N0.50 O P
Formula weight	557.14
Temperature	150(2) K
Wavelength	0.71073 A
Crystal system	Monoclinic
Space group	P2(1)/n
Unit cell dimensions	a = 13.2060(2) A alpha = 90 deg. b = 17.7239(3) A beta = 103.7350(10) deg. c = 13.5396(2) A gamma = 90 deg.
Volume	3078.48(8) A^3
Z	4
Density (calculated)	1.202 Mg/m^3
Absorption coefficient	0.120 mm^-1
F(000)	1180
Crystal size	0.25 x 0.3 x 0.2 mm
Theta range for data collection	1.93 to 24.00 deg.
Index ranges	-15<=h<=15, -21<=k<=22, -16<=l<=15
Reflections collected	17405
Independent reflections	4836 [R(int) = 0.0989]
Refinement method	Full-matrix least-squares on F^2
Data / restraints / parameters	4776 / 0 / 390
Goodness-of-fit on F^2	1.211
Final R indices [I>2sigma(I)]	R1 = 0.0617, wR2 = 0.1093
R indices (all data)	R1 = 0.1193, wR2 = 0.1631
Largest diff. peak and hole	0.204 and -0.270 e.A^-3

Table A.4b. Atomic coordinates (x 10^4) and equivalent isotropic displacement parameters (A^2 x 10^3) for (8). U(eq) is defined as one third of the trace of the orthogonalized Uij tensor.

	x	y	z	U(eq)
P(1)	1294(1)	1651(1)	4591(1)	30(1)
O(1)	3334(2)	4235(1)	8210(2)	33(1)
C(2)	560(2)	2435(2)	3957(3)	27(1)
C(3)	1173(2)	1631(2)	5890(3)	27(1)
C(4)	1850(3)	4332(2)	6811(3)	31(1)
C(5)	2333(3)	4275(2)	7878(3)	29(1)
C(6)	1064(3)	2310(2)	6385(3)	32(1)
C(7)	1642(3)	4302(2)	8566(3)	30(1)
C(8)	1225(3)	949(2)	6426(3)	35(1)
C(9)	768(3)	4366(2)	6466(3)	35(1)
C(10)	3422(3)	1615(2)	5437(3)	38(1)
C(11)	1012(3)	2310(2)	7389(3)	36(1)
C(12)	814(3)	782(2)	3957(3)	38(1)
C(13)	564(3)	4345(2)	8172(3)	33(1)
C(14)	1165(3)	954(2)	7430(3)	39(1)
C(15)	2646(3)	1791(2)	4593(3)	31(1)
C(16)	1001(3)	3156(2)	4007(3)	33(1)
C(17)	2509(3)	4370(2)	6056(3)	32(1)
C(18)	1056(3)	1631(2)	7913(3)	38(1)
C(19)	-642(3)	3676(2)	3123(3)	36(1)
C(20)	2047(3)	4240(2)	9688(3)	34(1)
C(21)	402(3)	3764(2)	3591(3)	37(1)
C(22)	115(3)	4366(2)	7136(3)	36(1)
C(23)	-493(3)	2339(2)	3483(3)	31(1)
C(24)	1557(3)	4616(2)	10359(3)	39(1)
C(25)	4465(3)	1722(2)	5434(3)	44(1)
C(26)	3334(3)	3865(2)	6082(3)	41(1)
C(27)	2918(3)	2076(2)	3722(3)	42(1)
C(28)	1858(3)	4506(2)	11396(3)	50(1)
C(29)	-1083(3)	2963(2)	3070(3)	39(1)
C(30)	4724(3)	2009(2)	4579(3)	47(1)
C(31)	900(3)	763(2)	2846(3)	51(1)
C(32)	2930(3)	4957(3)	4583(3)	55(1)
C(33)	2316(3)	4913(2)	5289(3)	41(1)
C(34)	3948(3)	3924(3)	5382(3)	53(1)
C(35)	3751(3)	4465(3)	4633(3)	58(1)
C(36)	3959(3)	2180(2)	3727(3)	51(1)
C(37)	2881(3)	3779(3)	10125(3)	59(1)
C(38)	2670(3)	4030(3)	11813(3)	58(1)
C(39)	3191(4)	3675(3)	11169(3)	74(2)
C(40)	1718(8)	6904(6)	4624(8)	79(3)
C(41)	2626(9)	6958(6)	4196(7)	62(3)
N(1)	3336(7)	7007(6)	3854(7)	88(3)

Table A.5a. Crystal data and structure refinement for (9)

Identification code	96srv104
Empirical formula	C38 H49 O2 P
Formula weight	568.74
Temperature	150(2) K
Wavelength	0.71073 A
Crystal system	Orthorhombic
Space group	Pbca
Unit cell dimensions	a = 16.941(3) A alpha = 90 deg. b = 18.671(4) A beta = 90 deg. c = 21.294(4) A gamma = 90 deg.
Volume	6735(2) A^3
Z	8
Density (calculated)	1.122 Mg/m^3
Absorption coefficient	0.112 mm^-1
F(000)	2464
Crystal size	0.2 x 0.2 x 0.3 mm
Theta range for data collection	1.88 to 25.65 deg.
Index ranges	-15<=h<=19, -22<=k<=13, -25<=l<=25
Reflections collected	28263
Independent reflections	5983 [R(int) = 0.0352]
Refinement method	Full-matrix least-squares on F^2
Data / restraints / parameters	5893 / 0 / 406
Goodness-of-fit on F^2	1.109
Final R indices [I>2sigma(I)]	R1 = 0.0511, wR2 = 0.1187
R indices (all data)	R1 = 0.0709, wR2 = 0.1681
Largest diff. peak and hole	0.563 and -0.323 e.A^-3

Table A.5b. Atomic coordinates (x 10^4) and equivalent isotropic displacement parameters (A^2 x 10^3) for (9). U(eq) is defined as one third of the trace of the orthogonalized Uij tensor.

	x	y	z	U(eq)
P(1)	9521(1)	1747(1)	4965(1)	27(1)
C(1)	9996(1)	941(1)	4714(1)	32(1)
C(11)	10190(1)	2496(1)	4962(1)	31(1)
C(12)	10216(2)	2973(1)	5465(1)	45(1)
C(13)	10699(2)	3574(2)	5431(2)	58(1)
C(14)	11153(2)	3699(2)	4909(2)	54(1)
C(15)	11126(2)	3234(2)	4407(2)	49(1)
C(16)	10644(2)	2631(1)	4428(1)	41(1)
C(21)	9142(1)	1637(1)	5749(1)	30(1)
C(22)	9553(2)	1219(1)	6182(1)	37(1)
C(23)	9273(2)	1174(2)	6796(1)	46(1)
C(24)	8608(2)	1546(2)	6980(1)	46(1)
C(25)	8197(2)	1957(2)	6546(1)	49(1)
C(26)	8457(2)	2001(1)	5930(1)	41(1)
C(31)	8723(1)	1953(1)	4440(1)	28(1)
C(32)	8218(2)	1404(1)	4245(1)	37(1)
C(33)	7592(2)	1561(1)	3852(1)	47(1)
C(34)	7467(2)	2261(1)	3652(1)	45(1)
C(35)	7965(2)	2805(1)	3841(1)	38(1)
C(36)	8597(1)	2655(1)	4235(1)	32(1)
O(1)	11367(1)	505(1)	5712(1)	33(1)
C(41)	12107(1)	447(1)	5871(1)	27(1)
C(42)	12734(1)	507(1)	5411(1)	26(1)
C(43)	13523(1)	449(1)	5600(1)	29(1)
C(44)	13750(1)	338(1)	6223(1)	32(1)
C(45)	13148(1)	277(1)	6666(1)	31(1)
C(46)	12345(1)	329(1)	6518(1)	29(1)
C(47)	14616(2)	332(2)	6407(1)	46(1)
C(48)	11720(2)	331(1)	7047(1)	36(1)
C(49)	12064(2)	110(2)	7691(1)	52(1)
C(50)	11403(2)	1100(1)	7113(1)	42(1)
C(51)	11034(2)	-189(2)	6915(1)	44(1)
C(52)	12530(1)	678(1)	4718(1)	30(1)
C(53)	13271(2)	751(2)	4301(1)	40(1)
C(54)	12010(2)	83(1)	4432(1)	36(1)
C(55)	12094(2)	1401(1)	4691(1)	34(1)
O(2A)	10256(2)	1613(2)	3250(1)	70(1)
C(61)	9804(4)	2055(3)	2866(2)	73(1)
C(64)	10825(3)	1240(3)	2877(3)	74(1)
O(2B)	11224(7)	2272(5)	2924(5)	88(4)
C(71)	10489(11)	2410(8)	2669(11)	97(7)
C(74)	11372(11)	1589(7)	2830(5)	57(4)
C(62)	10043(5)	1902(4)	2233(2)	158(3)
C(63)	10737(4)	1497(4)	2272(3)	162(3)

Table A.6a. Crystal data and structure refinement for (10)

Identification code	rp3
Empirical formula	C35 H43 O P
Formula weight	80.00
Temperature	293(2) K
Wavelength	1.31367 A
Crystal system	Orthorhombic
Space group	Pbca
Unit cell dimensions	a = 18.574(4) A alpha = 90 deg. b = 17.224(3) A beta = 90 deg. c = 19.032(4) A gamma = 90 deg.
Volume	6089(2) A^3
Z	8
Density (calculated)	0.175 Mg/m^3
Absorption coefficient	0.000 mm^-1
F(000)	1016
Crystal size	3.5 x 3.5 x 2.4 mm
Theta range for data collection	3.58 to 50.71 deg.
Index ranges	-8<=h<=21, -6<=k<=20, -21<=l<=22
Reflections collected	9682
Independent reflections	4873 [R(int) = 0.0571]
Refinement method	Full-matrix least-squares on F^2
Data / restraints / parameters	4872 / 0 / 722
Goodness-of-fit on F^2	2.170
Final R indices [I>2sigma(I)]	R1 = 0.0474, wR2 = 0.0744
R indices (all data)	R1 = 0.0570, wR2 = 0.0759
Extinction coefficient	0.00027(2)
Largest diff. peak and hole	0.614 and -0.809 e.A^-3

Table A.6b. Atomic coordinates (x 10^4) and equivalent isotropic displacement parameters (A^2 x 10^3) for (10). U(eq) is defined as one third of the trace of the orthogonalized Uij tensor.

	x	y	z	U(eq)
P(1)	-4419(1)	4681(1)	3528(1)	6(1)
C(1)	-4063(1)	4472(1)	2664(1)	8(1)
H(1A)	-3536(2)	4200(2)	2761(2)	22(1)
H(1B)	-4421(2)	4036(2)	2438(2)	24(1)
C(2)	-3985(1)	5170(1)	2173(1)	13(1)
H(2A)	-3810(3)	4972(3)	1653(2)	35(1)
H(2B)	-3590(3)	5586(3)	2368(2)	36(1)
H(2C)	-4495(2)	5484(3)	2106(2)	36(1)
C(11)	-3878(1)	5383(1)	3976(1)	6(1)
C(12)	-3843(1)	6148(1)	3725(1)	6(1)
H(12A)	-4131(2)	6321(2)	3251(2)	21(1)
C(13)	-3446(1)	6707(1)	4087(1)	7(1)
H(13A)	-3424(2)	7297(2)	3893(2)	24(1)
C(14)	-3092(1)	6504(1)	4710(1)	7(1)
H(14A)	-2802(2)	6935(2)	5006(2)	23(1)
C(15)	-3125(1)	5739(1)	4959(1)	7(1)
H(15A)	-2853(2)	5582(2)	5440(2)	22(1)
C(16)	-3512(1)	5180(1)	4593(1)	6(1)
H(16A)	-3528(2)	4590(2)	4784(2)	21(1)
C(21)	-4427(1)	3770(1)	3991(1)	6(1)
C(22)	-3808(1)	3306(1)	3968(1)	6(1)
H(22A)	-3328(2)	3491(2)	3691(2)	20(1)
C(23)	-3811(1)	2589(1)	4315(1)	9(1)
H(23A)	-3340(2)	2224(2)	4290(2)	25(1)
C(24)	-4420(1)	2349(1)	4682(1)	9(1)
H(24A)	-4421(2)	1790(2)	4945(2)	27(1)
C(25)	-5036(1)	2812(1)	4703(1)	9(1)
H(25A)	-5510(2)	2618(2)	4994(2)	25(1)
C(26)	-5043(1)	3528(1)	4359(1)	7(1)
H(26A)	-5520(2)	3889(2)	4368(2)	23(1)
C(31)	-5318(1)	5059(1)	3480(1)	6(1)
C(32)	-5809(1)	4728(1)	3010(1)	7(1)
H(32A)	-5649(2)	4263(2)	2651(2)	23(1)
C(33)	-6521(1)	4985(1)	3002(1)	7(1)
H(33A)	-6898(2)	4725(2)	2637(2)	22(1)
C(34)	-6743(1)	5564(1)	3464(1)	7(1)
H(34A)	-7296(2)	5760(2)	3461(2)	23(1)
C(35)	-6248(1)	5901(1)	3929(1)	8(1)
H(35A)	-6419(2)	6363(2)	4280(2)	23(1)
C(36)	-5537(1)	5649(1)	3938(1)	7(1)
H(36A)	-5158(2)	5911(2)	4305(2)	22(1)
O(1)	-2443(1)	3805(1)	3160(1)	6(1)
C(41)	-1797(1)	3526(1)	3097(1)	5(1)
C(42)	-1226(1)	3748(1)	3573(1)	6(1)
C(43)	-536(1)	3428(1)	3496(1)	7(1)
H(43A)	-112(2)	3580(2)	3859(2)	21(1)
C(44)	-364(1)	2906(1)	2959(1)	7(1)
C(45)	-913(1)	2702(1)	2490(1)	6(1)
H(45A)	-775(2)	2295(2)	2069(2)	20(1)
C(46)	-1612(1)	2985(1)	2542(1)	5(1)
C(47)	375(1)	2547(1)	2896(1)	9(1)
H(47A)	598(2)	2602(3)	2373(2)	37(1)
H(47B)	371(2)	1926(3)	3001(3)	40(1)
H(47C)	756(2)	2816(3)	3251(3)	38(1)
C(48)	-1384(1)	4316(1)	4177(1)	6(1)
C(49)	-713(1)	4500(1)	4618(1)	12(1)
H(49A)	-287(2)	4769(3)	4304(2)	30(1)
H(49B)	-492(2)	3993(3)	4871(2)	30(1)
H(49C)	-857(2)	4914(3)	5031(2)	29(1)
C(50)	-1942(1)	3950(1)	4681(1)	9(1)
H(50A)	-1722(2)	3419(2)	4915(2)	28(1)
H(50B)	-2436(2)	3812(2)	4396(2)	26(1)
H(50C)	-2069(2)	4349(3)	5109(2)	28(1)
C(51)	-1662(1)	5096(1)	3888(1)	8(1)
H(51A)	-1263(2)	5359(2)	3538(2)	29(1)
H(51B)	-1759(2)	5504(2)	4321(2)	26(1)
H(51C)	-2161(2)	5021(2)	3597(2)	26(1)
C(52)	-2200(1)	2690(1)	2039(1)	4(1)
C(53)	-2753(1)	2224(1)	2468(1)	7(1)
H(53A)	-3193(2)	2015(2)	2136(2)	25(1)
H(53B)	-2977(2)	2578(2)	2887(2)	26(1)

H(53C)	-2503(2)	1715(2)	2706(2)	27(1)
C(54)	-1898(1)	2162(1)	1460(1)	7(1)
H(54A)	-2338(2)	1991(2)	1104(2)	24(1)
H(54B)	-1657(2)	1629(2)	1664(2)	25(1)
H(54C)	-1489(2)	2458(2)	1138(2)	23(1)
C(55)	-2578(1)	3367(1)	1659(1)	8(1)
H(55A)	-3003(2)	3142(2)	1304(2)	27(1)
H(55B)	-2188(2)	3682(2)	1335(2)	27(1)
H(55C)	-2815(2)	3772(2)	2032(2)	26(1)

Table A.7a. Crystal data and structure refinement for (11)

Identification code	97srv093
Empirical formula	C27 H25 Br N P
Formula weight	474.36
Temperature	150(2) K
Wavelength	0.71073 A
Crystal system	Monoclinic
Space group	P2(1)/c
Unit cell dimensions	a = 12.633(1) A alpha = 90 deg. b = 20.09(1) A beta = 108.08(1) deg. c = 9.618(1) A gamma = 90 deg.
Volume	2320.5(3) A^3
Z	4
Density (calculated)	1.358 Mg/m^3
Absorption coefficient	1.854 mm^-1
F(000)	976
Crystal size	0.25 x 0.15 x 0.10 mm
Theta range for data collection	1.70 to 25.00 deg.
Index ranges	-17<=h<=18, -26<=k<=28, -11<=l<=13
Reflections collected	13839
Independent reflections	4091 [R(int) = 0.0728]
Absorption correction	Semiempirical
Max. and min. transmission	0.9053 and 0.7144
Refinement method	Full-matrix least-squares on F^2
Data / restraints / parameters	4005 / 0 / 371
Goodness-of-fit on F^2	1.150
Final R indices [I>2sigma(I)]	R1 = 0.0439, wR2 = 0.0795
R indices (all data)	R1 = 0.0697, wR2 = 0.0963
Largest diff. peak and hole	0.370 and -0.350 e.A^-3

Table A.7b. Atomic coordinates (x 10^4) and equivalent isotropic displacement parameters (A^2 x 10^3) for (11). U(eq) is defined as one third of the trace of the orthogonalized Uij tensor.

	x	y	z	U(eq)
Br	5318(1)	3758(1)	7446(1)	25(1)
P	2317(1)	4817(1)	4345(1)	17(1)
C(1)	3626(3)	4684(2)	3989(4)	20(1)
C(11)	3586(3)	4180(2)	2796(4)	20(1)
C(12)	3450(3)	4389(2)	1368(4)	26(1)
C(13)	3494(3)	3929(2)	309(5)	33(1)
C(14)	3649(4)	3260(2)	649(5)	37(1)
C(15)	3766(4)	3044(2)	2065(5)	35(1)
C(16)	3746(3)	3505(2)	3142(5)	28(1)
C(21)	1771(3)	4032(2)	4723(4)	18(1)
C(22)	1232(3)	3595(2)	3595(4)	25(1)
C(23)	821(3)	2993(2)	3917(5)	26(1)
C(24)	970(4)	2821(2)	5352(5)	32(1)
C(25)	1518(5)	3242(2)	6476(5)	50(1)
C(26)	1912(4)	3851(2)	6159(5)	36(1)
C(31)	1305(3)	5216(2)	2835(4)	19(1)
C(32)	1616(4)	5736(2)	2089(4)	25(1)
C(33)	815(4)	6088(2)	1034(5)	33(1)
C(34)	-290(4)	5915(2)	693(5)	32(1)
C(35)	-616(4)	5395(2)	1408(5)	31(1)
C(36)	178(3)	5044(2)	2490(4)	26(1)
C(41)	2561(3)	5344(2)	5931(4)	17(1)
C(42)	1787(3)	5834(2)	5980(4)	22(1)
C(43)	1945(3)	6199(2)	7251(4)	27(1)
C(44)	2865(3)	6088(2)	8458(5)	28(1)
C(45)	3640(3)	5611(2)	8415(4)	25(1)
C(46)	3509(3)	5243(2)	7145(4)	22(1)
N	8523(3)	2429(2)	10914(5)	48(1)
C(2)	7610(4)	2304(2)	10369(5)	32(1)
C(3)	6434(4)	2148(3)	9679(7)	41(1)

Table A.8a. Crystal data and structure refinement for (12)

Identification code	96srv179
Empirical formula	C27 H25 As Br N
Formula weight	518.31
Temperature	150(2) K
Wavelength	0.71073 A
Crystal system	Monoclinic
Space group	P2(1)/c
Unit cell dimensions	a = 12.659(1) A alpha = 90 deg. b = 20.240(1) A beta = 107.58(1) deg. c = 9.658(1) A gamma = 90 deg.
Volume	2359.0(3) A^3
Z	4
Density (calculated)	1.459 Mg/m^3
Absorption coefficient	3.148 mm^-1
F(000)	1048
Crystal size	0.35 x 0.30 x 0.25 mm
Theta range for data collection	1.69 to 30.62 deg.
Index ranges	-17<=h<=17, -28<=k<=27, -12<=l<=13
Reflections collected	18976
Independent reflections	6519 [R(int) = 0.0232]
Absorption correction	Semi-empirical from psi-scans
Max. and min. transmission	0.6064 and 0.4446
Refinement method	Full-matrix least-squares on F^2
Data / restraints / parameters	6489 / 0 / 371
Goodness-of-fit on F^2	1.144
Final R indices [I>2sigma(I)]	R1 = 0.0250, wR2 = 0.0550
R indices (all data)	R1 = 0.0322, wR2 = 0.0625
Largest diff. peak and hole	0.367 and -0.360 e.A^-3

Table A.8b. Atomic coordinates (x 10^4) and equivalent isotropic displacement parameters (A^2 x 10^3) for (12). U(eq) is defined as one third of the trace of the orthogonalized Uij tensor.

	x	y	z	U(eq)
As	2683(1)	4808(1)	5678(1)	16(1)
C(1)	1381(1)	4152(1)	7262(2)	20(1)
C(2)	1509(2)	4357(1)	8685(2)	26(1)
C(3)	1498(2)	3893(1)	9745(2)	36(1)
C(4)	1384(2)	3229(1)	9405(2)	40(1)
C(5)	1273(2)	3018(1)	7999(3)	39(1)
C(6)	1263(2)	3478(1)	6925(2)	30(1)
C(7)	1293(1)	4654(1)	6082(2)	20(1)
C(11)	3284(1)	3986(1)	5275(2)	19(1)
C(12)	3124(2)	3814(1)	3839(2)	40(1)
C(13)	3535(3)	3216(1)	3511(3)	52(1)
C(14)	4109(2)	2798(1)	4613(2)	34(1)
C(15)	4265(2)	2967(1)	6046(2)	26(1)
C(16)	3841(2)	3560(1)	6384(2)	26(1)
C(21)	2421(1)	5356(1)	3988(2)	19(1)
C(22)	1492(2)	5236(1)	2789(2)	23(1)
C(23)	1349(2)	5606(1)	1530(2)	25(1)
C(24)	2115(2)	6089(1)	1470(2)	27(1)
C(25)	3023(2)	6210(1)	2673(2)	29(1)
C(26)	3188(1)	5844(1)	3943(2)	23(1)
C(31)	3755(1)	5238(1)	7251(2)	20(1)
C(32)	3427(2)	5759(1)	7973(2)	26(1)
C(33)	4239(2)	6104(1)	9031(2)	33(1)
C(34)	5344(2)	5927(1)	9359(2)	32(1)
C(35)	5660(2)	5402(1)	8651(2)	32(1)
C(36)	4867(2)	5058(1)	7581(2)	26(1)
Br	313(1)	6236(1)	7402(1)	25(1)
N	3452(2)	7424(1)	5900(3)	51(1)
C(8)	2548(2)	7302(1)	5329(3)	36(1)
C(9)	1385(2)	7155(1)	4602(3)	41(1)

Table A.9a. Crystal data and structure refinement for (13)

Identification code	dmb01
Empirical formula	C32 H30 N P
Formula weight	459.54
Temperature	153(2) K
Wavelength	0.71073 A
Crystal system	Monoclinic
Space group	P2(1)/c
Unit cell dimensions	a = 9.888(2) A alpha = 90 deg. b = 14.256(3) A beta = 98.75(3) deg. c = 17.815(4) A gamma = 90 deg.
Volume	2482.0(9) A^3
Z	4
Density (calculated)	1.230 Mg/m^3
Absorption coefficient	0.132 mm^-1
F(000)	976
Crystal size	0.5 x 0.4 x 0.3 mm
Theta range for data collection	2.64 to 27.54 deg.
Index ranges	-12<=h<=0, 0<=k<=18, 0<=l<=23
Reflections collected	3395
Independent reflections	3117 [R(int) = 0.0580]
Refinement method	Full-matrix least-squares on F^2
Data / restraints / parameters	3109 / 0 / 316
Goodness-of-fit on F^2	1.007
Final R indices [I>2sigma(I)]	R1 = 0.0403, wR2 = 0.1042
R indices (all data)	R1 = 0.0535, wR2 = 0.1214
Largest diff. peak and hole	0.157 and -0.176 e.A^-3

Table A.9b. Atomic coordinates (x 10^4) and equivalent isotropic displacement parameters (A^2 x 10^3) for (13). U(eq) is defined as one third of the trace of the orthogonalized Uij tensor.

	x	y	z	U(eq)
P(1)	3439(1)	10854(1)	-1776(1)	20(1)
N(1)	4380(3)	7951(1)	-965(2)	26(1)
C(1)	2985(3)	10238(2)	-960(2)	24(1)
C(2)	1449(3)	10003(2)	-1034(2)	31(1)
C(11)	5772(3)	7925(2)	-722(2)	27(1)
C(12)	6595(4)	8568(2)	-1063(2)	33(1)
C(13)	7993(4)	8623(2)	-848(2)	41(1)
C(14)	8656(4)	8057(2)	-283(2)	41(1)
C(15)	7885(4)	7440(2)	89(2)	36(1)
C(16)	6476(4)	7386(2)	-125(2)	31(1)
C(21)	3576(3)	7181(2)	-921(2)	26(1)
C(22)	3998(3)	6229(2)	-812(2)	29(1)
C(23)	3074(4)	5508(2)	-809(2)	34(1)
C(24)	1658(4)	5664(2)	-925(2)	38(1)
C(25)	1215(4)	6582(2)	-1039(2)	34(1)
C(26)	2130(4)	7312(2)	-1044(2)	30(1)
C(31)	3032(3)	10157(2)	-2613(2)	23(1)
C(32)	3236(3)	9185(2)	-2560(2)	25(1)
C(33)	3005(3)	8654(2)	-3217(2)	31(1)
C(34)	2576(4)	9070(2)	-3920(2)	32(1)
C(35)	2377(4)	10028(2)	-3968(2)	33(1)
C(36)	2614(3)	10576(2)	-3318(2)	29(1)
C(41)	5257(3)	11051(2)	-1596(2)	21(1)
C(42)	6005(3)	10963(2)	-2203(2)	24(1)
C(43)	7426(3)	11117(2)	-2056(2)	28(1)
C(44)	8047(3)	11359(2)	-1347(2)	31(1)
C(45)	7298(3)	11456(2)	-748(2)	25(1)
C(46)	5891(3)	11298(2)	-880(2)	25(1)
C(51)	2568(3)	11951(2)	-1949(2)	23(1)
C(52)	1153(3)	11970(2)	-2164(2)	27(1)
C(53)	468(4)	12815(2)	-2284(2)	36(1)
C(54)	1195(4)	13646(2)	-2209(2)	37(1)
C(55)	2607(4)	13635(2)	-2021(2)	35(1)
C(56)	3297(3)	12793(2)	-1887(2)	28(1)

Table A.10a. Crystal data and structure refinement for (14)

Identification code	97srv186
Empirical formula	C32 H28 N P
Formula weight	445.51
Temperature	150(2) K
Wavelength	0.71073 A
Crystal system	Monoclinic
Space group	'P(2)1/n'
Unit cell dimensions	a = 18.9883(2) A alpha = 90 deg. b = 13.422 A beta = 95.3080(10) deg. c = 19.4539(2) A gamma = 90 deg.
Volume	4936.89(7) A^3
Z	8
Density (calculated)	1.199 Mg/m^3
Absorption coefficient	0.130 mm^-1
F(000)	1888
Crystal size	0.4 x 0.2 x 0.2 mm
Theta range for data collection	1.43 to 27.49 deg.
Index ranges	-24<=h<=24, -17<=k<=17, -24<=l<=24
Reflections collected	53667
Independent reflections	11282 [R(int) = 0.0337]
Refinement method	Full-matrix least-squares on F^2
Data / restraints / parameters	11230 / 0 / 653
Goodness-of-fit on F^2	1.093
Final R indices [I>2sigma(I)]	R1 = 0.0386, wR2 = 0.0893
R indices (all data)	R1 = 0.0520, wR2 = 0.1052
Largest diff. peak and hole	0.337 and -0.341 e.A^-3

Table A.10b. Atomic coordinates (x 10^4) and equivalent isotropic displacement parameters (A^2 x 10^3) for (14). U(eq) is defined as one third of the trace of the orthogonalized Uij tensor.

	x	y	z	U(eq)
N(1')	2235(1)	2862(1)	5154(1)	32(1)
C(1)	3171(1)	3893(1)	3762(1)	30(1)
P(1)	3003(1)	3193(1)	2972(1)	23(1)
N(1)	3268(1)	5749(1)	4896(1)	30(1)
P(1')	3063(1)	4922(1)	7035(1)	24(1)
C(1')	3341(1)	4375(1)	6260(1)	29(1)
C(2)	3955(1)	4172(2)	3906(1)	38(1)
C(2')	4131(1)	4119(2)	6313(1)	39(1)
C(11)	2075(1)	2943(1)	2790(1)	25(1)
C(11')	3547(1)	6064(1)	7219(1)	26(1)
C(12)	1816(1)	2619(1)	2130(1)	31(1)
C(12')	3812(1)	6591(1)	6677(1)	32(1)
C(13)	1109(1)	2348(1)	2002(1)	35(1)
C(13')	4171(1)	7482(1)	6809(1)	37(1)
C(14)	664(1)	2396(1)	2530(1)	34(1)
C(14')	4267(1)	7854(1)	7479(1)	37(1)
C(15)	921(1)	2713(1)	3183(1)	33(1)
C(15')	4003(1)	7338(1)	8019(1)	34(1)
C(16)	1626(1)	2987(1)	3321(1)	28(1)
C(16')	3643(1)	6444(1)	7892(1)	30(1)
C(21)	3463(1)	2018(1)	3045(1)	27(1)
C(21')	2127(1)	5174(1)	6936(1)	27(1)
C(22)	3578(1)	1474(1)	2453(1)	32(1)
C(22')	1705(1)	4842(1)	6355(1)	33(1)
C(23)	3915(1)	554(1)	2520(1)	40(1)
C(23')	982(1)	5048(1)	6300(1)	39(1)
C(24)	4135(1)	180(1)	3169(1)	48(1)
C(24')	685(1)	5566(1)	6814(1)	39(1)
C(25)	4007(1)	713(1)	3754(1)	49(1)
C(25')	1103(1)	5889(1)	7393(1)	38(1)
C(26)	3671(1)	1629(1)	3696(1)	37(1)
C(26')	1823(1)	5699(1)	7457(1)	33(1)
C(31)	3325(1)	3909(1)	2285(1)	25(1)
C(31')	3242(1)	4092(1)	7757(1)	26(1)
C(32)	4029(1)	3807(1)	2135(1)	28(1)
C(32')	3936(1)	4013(1)	8070(1)	31(1)
C(33)	4291(1)	4427(1)	1644(1)	33(1)
C(33')	4085(1)	3360(1)	8617(1)	34(1)
C(34)	3861(1)	5144(1)	1312(1)	37(1)
C(34')	3548(1)	2789(1)	8859(1)	34(1)
C(35)	3163(1)	5249(1)	1458(1)	38(1)
C(35')	2863(1)	2861(1)	8550(1)	34(1)
C(36)	2892(1)	4635(1)	1948(1)	31(1)
C(36')	2707(1)	3505(1)	7997(1)	29(1)
C(41')	1543(1)	2553(1)	5134(1)	27(1)
C(41)	2594(1)	6085(1)	4707(1)	26(1)
C(42')	928(1)	3127(1)	4969(1)	31(1)
C(42)	1969(1)	5510(1)	4622(1)	32(1)
C(43')	271(1)	2691(1)	4990(1)	34(1)
C(43)	1338(1)	5979(1)	4410(1)	34(1)
C(44')	201(1)	1680(1)	5169(1)	36(1)
C(44)	1306(1)	7013(1)	4279(1)	33(1)
C(45')	793(1)	1099(1)	5327(1)	34(1)
C(45)	1911(1)	7593(1)	4365(1)	30(1)
C(46')	1468(1)	1522(1)	5310(1)	28(1)
C(46)	2561(1)	7138(1)	4575(1)	25(1)
C(51')	2618(1)	2021(1)	5355(1)	31(1)
C(51)	3681(1)	6585(1)	4873(1)	26(1)
C(52')	3356(1)	1924(1)	5476(1)	39(1)
C(52)	4422(1)	6648(1)	5007(1)	31(1)
C(53')	3642(1)	1013(2)	5683(1)	47(1)

C(53)	4747(1)	7566(1)	4967(1)	34(1)
C(54')	3211(1)	179(2)	5771(1)	49(1)
C(54)	4356(1)	8434(1)	4794(1)	36(1)
C(55')	2483(1)	251(1)	5653(1)	41(1)
C(55)	3627(1)	8391(1)	4653(1)	31(1)
C(56')	2179(1)	1169(1)	5452(1)	30(1)
C(56)	3282(1)	7473(1)	4691(1)	25(1)

Table A.11a. Crystal data and structure refinement for (15)

Identification code	97srv047
Empirical formula	C37 H22 F18 P2
Formula weight	870.49
Temperature	153(2) K
Wavelength	0.71073 A
Crystal system	Triclinic
Space group	P-1
Unit cell dimensions	a = 11.5320(10) A alpha = 110.210(10) deg. b = 12.6250(10) A beta = 102.850(10) deg. c = 13.5790(10) A gamma = 96.960(10) deg.
Volume	1765.9(2) A^3
Z	2
Density (calculated)	1.637 Mg/m^3
Absorption coefficient	0.248 mm^-1
F(000)	872
Crystal size	0.20 x 0.20 x 0.08 mm
Theta range for data collection	1.67 to 30.09 deg.
Index ranges	-14<=h<=16, -17<=k<=12, -10<=l<=18
Reflections collected	12640
Independent reflections	9054 [R(int) = 0.0290]
Reflections observed	4709 [I>2sigma(I)]
Refinement method	Full-matrix least-squares on F^2
Data / restraints / parameters	9044 / 0 / 630
Goodness-of-fit on F^2	0.930
Final R indices [I>2sigma(I)]	R1 = 0.0455, wR2 = 0.0738
R indices (all data)	R1 = 0.1178, wR2 = 0.0976
Largest diff. peak and hole	0.365 and -0.309 e.A^-3

Table A.11b. Atomic coordinates (x 10^4) and equivalent isotropic displacement parameters (A^2 x 10^3) for (15). U(eq) is defined as one third of the trace of the orthogonalized Uij tensor.

	x	y	z	U(eq)
P(1)	7796(1)	7494(1)	2572(1)	24(1)
C(1)	6834(2)	6318(2)	2653(2)	26(1)
C(2)	7324(3)	5586(2)	3119(2)	34(1)
C(3)	6580(3)	4634(3)	3103(2)	40(1)
C(4)	5351(3)	4400(3)	2630(2)	44(1)
C(5)	4840(3)	5115(3)	2175(3)	54(1)
C(6)	5579(3)	6076(3)	2181(3)	43(1)
C(7)	8391(2)	6931(2)	1424(2)	21(1)
C(8)	7929(3)	5808(2)	655(2)	33(1)
C(9)	8392(3)	5403(3)	-228(2)	39(1)
C(10)	9308(3)	6114(2)	-352(2)	33(1)
C(11)	9768(2)	7229(2)	406(2)	30(1)
C(21)	9322(2)	7644(2)	1301(2)	28(1)
C(13)	6937(2)	8535(2)	2386(2)	22(1)
C(14A)	6582(2)	8622(2)	1373(2)	26(1)
C(15)	5962(2)	9460(2)	1248(2)	30(1)
C(16)	5684(2)	10211(2)	2150(2)	32(1)
C(17)	6015(2)	10124(2)	3154(2)	32(1)
C(18)	6650(2)	9289(2)	3285(2)	28(1)
C(19)	9030(3)	8189(3)	3793(2)	31(1)
P(2)	8488(1)	9427(1)	6606(1)	24(1)
C(20)	8466(2)	7916(2)	6449(2)	19(1)
C(21)	9562(2)	7506(2)	6568(2)	23(1)
C(22)	9570(2)	6366(2)	6451(2)	27(1)
C(23)	8494(2)	5580(2)	6187(2)	26(1)
C(24)	7393(2)	5917(2)	5971(2)	24(1)
C(25)	7369(2)	7047(2)	6068(2)	20(1)
C(26)	10784(2)	8286(2)	6837(2)	28(1)
C(27)	8507(3)	4372(2)	6113(3)	38(1)
C(28)	6133(2)	7294(2)	5704(2)	28(1)
C(29)	7797(2)	10091(2)	7667(2)	21(1)
C(30)	7831(2)	9940(2)	8681(2)	22(1)
C(31)	7514(2)	10729(2)	9528(2)	24(1)
C(32)	7114(2)	11691(2)	9440(2)	24(1)
C(33)	6993(2)	11844(2)	8464(2)	23(1)
C(34)	7294(2)	11069(2)	7596(2)	21(1)
C(35)	8278(2)	8970(2)	8939(2)	26(1)
C(36)	6881(3)	12562(2)	10401(2)	31(1)
C(37)	7019(2)	11284(2)	6552(2)	29(1)
F(11)	6283(1)	10372(1)	5692(1)	38(1)
F(12)	8030(1)	11563(1)	6259(1)	37(1)
F(13)	6453(2)	12171(1)	6628(1)	43(1)
F(14)	6159(1)	13237(1)	10117(1)	39(1)
F(15)	6343(2)	12083(1)	10974(1)	43(1)
F(16)	7916(1)	13301(1)	11126(1)	44(1)
F(17)	9372(1)	8849(1)	8788(1)	35(1)
F(18)	8387(1)	9103(1)	9985(1)	36(1)
F(19)	7510(1)	7924(1)	8335(1)	36(1)
F(21)	5796(1)	8044(1)	6518(1)	36(1)
F(22)	5240(1)	6325(1)	5293(1)	39(1)
F(23)	6041(1)	7708(1)	4921(1)	39(1)
F(24)	7514(3)	3603(4)	5418(4)	51(1)
F(25)	8661(6)	4252(3)	7033(3)	85(2)
F(26)	9421(3)	3970(3)	5696(4)	64(1)
F(24')	8060(28)	3615(14)	5254(13)	179(14)
F(25')	7866(15)	4185(14)	6823(16)	100(7)
F(26')	9579(9)	4287(10)	6660(18)	92(5)
F(27)	10834(1)	8749(1)	6083(1)	36(1)
F(28)	11097(1)	9176(1)	7807(1)	40(1)
F(29)	11696(1)	7718(1)	6865(1)	43(1)

Table A.12a. Crystal data and structure refinement for (Bisphenol)

Identification code	98srv014
Empirical formula	C29 H44 O2
Formula weight	424.64
Temperature	150(2) K
Wavelength	0.71073 A
Crystal system	Tetragonal
Space group	I4(1)/a
Unit cell dimensions	a = 21.0591(12) A alpha = 90 deg. b = 21.0591(12) A beta = 90 deg. c = 23.800(2) A gamma = 90 deg.
Volume	10555.0(12) A^3
Z	16
Density (calculated)	1.069 Mg/m^3
Absorption coefficient	0.065 mm^-1
F(000)	3744
Crystal size	0.4 x 0.3 x 0.25 mm
Theta range for data collection	1.29 to 27.48 deg.
Index ranges	-27<=h<=27, -27<=k<=27, -30<=l<=29
Reflections collected	59144
Independent reflections	6056 [R(int) = 0.0995]
Refinement method	Full-matrix least-squares on F^2
Data / restraints / parameters	5942 / 0 / 461
Goodness-of-fit on F^2	1.317
Final R indices [I>2sigma(I)]	R1 = 0.0447, wR2 = 0.0893
R indices (all data)	R1 = 0.1312, wR2 = 0.1729
Extinction coefficient	0.00044(6)
Largest diff. peak and hole	0.220 and -0.217 e.A^-3

Table A.12b. Atomic coordinates (x 10^4) and equivalent isotropic displacement parameters (A^2 x 10^3) for (Bisphenol). U(eq) is defined as one third of the trace of the orthogonalized Uij tensor.

	x	y	z	U(eq)
C(1)	5852(1)	6067(1)	637(1)	26(1)
O(1)	9736(1)	3633(1)	-535(1)	46(1)
O(2)	6898(1)	6832(1)	947(1)	37(1)
C(2)	5384(1)	5577(1)	402(1)	34(1)
C(3)	5588(1)	6728(1)	488(1)	38(1)
C(4)	5873(1)	5977(2)	1279(1)	35(1)
C(5)	8199(1)	6747(1)	509(1)	28(1)
C(6)	8061(2)	7460(1)	417(2)	43(1)
C(7)	8352(2)	6615(2)	1131(1)	44(1)
C(8)	8807(1)	6606(2)	177(1)	42(1)
C(9)	9155(1)	4001(1)	517(1)	36(1)
C(10)	8729(2)	4257(3)	990(1)	64(1)
C(11)	9790(2)	4359(2)	569(1)	47(1)
C(12)	9260(2)	3286(2)	625(2)	57(1)
C(13)	9265(1)	3904(1)	-1651(1)	32(1)
C(14)	9338(2)	3179(2)	-1696(1)	47(1)
C(15)	9922(2)	4229(2)	-1678(1)	46(1)
C(16)	8900(2)	4120(2)	-2172(1)	46(1)
C(17)	7362(1)	4906(1)	-675(1)	31(1)
C(21)	9159(1)	3948(1)	-570(1)	28(1)
C(22)	8911(1)	4084(1)	-1105(1)	26(1)
C(23)	8326(1)	4398(1)	-1121(1)	26(1)
C(24)	7998(1)	4570(1)	-635(1)	27(1)
C(25)	8271(1)	4425(1)	-118(1)	29(1)
C(26)	8855(1)	4121(1)	-66(1)	28(1)
C(31)	7030(1)	6377(1)	544(1)	25(1)
C(32)	7645(1)	6319(1)	315(1)	24(1)
C(33)	7737(1)	5840(1)	-82(1)	27(1)
C(34)	7252(1)	5427(1)	-244(1)	26(1)
C(35)	6654(1)	5508(1)	-5(1)	25(1)
C(36)	6521(1)	5981(1)	387(1)	23(1)

Table A.13a. Crystal data and structure refinement for (16)

Identification code	98srv004
Empirical formula	C73 H88 N2 O2 P2
Formula weight	1087.39
Temperature	100(2) K
Wavelength	0.71073 A
Crystal system	Orthorhombic
Space group	P2(1)2(1)2(1)
Unit cell dimensions	a = 18.0475(2) A alpha = 90 deg. b = 18.7762(2) A beta = 90 deg. c = 19.1060(2) A gamma = 90 deg.
Volume, Z	6474.33(12) A^3, 4
Density (calculated)	1.116 Mg/m^3
Absorption coefficient	0.112 mm^-1
F(000)	2344
Crystal size	0.70 x 0.60 x 0.20 mm
Theta range for data collection	1.52 to 27.60 deg.
Limiting indices	-22<=h<=23, -24<=k<=24, -24<=l<=24
Reflections collected	65843
Independent reflections	14952 [R(int) = 0.0882]
Absorption correction	None
Refinement method	Full-matrix least-squares on F^2
Data / restraints / parameters	14932 / 0 / 1042
Goodness-of-fit on F^2	1.064
Final R indices [I>2sigma(I)]	R1 = 0.0341, wR2 = 0.0819
R indices (all data)	R1 = 0.0413, wR2 = 0.0909
Absolute structure parameter	-0.05(4)
Largest diff. peak and hole	0.281 and -0.231 e.A^-3

Table A.13b. Atomic coordinates (x 10^4) and equivalent isotropic displacement parameters (A^2 x 10^3) for (16). U(eq) is defined as one third of the trace of the orthogonalized Uij tensor.

	x	y	z	U(eq)
N(1)	-2732(1)	-3198(1)	-4697(1)	50(1)
C(1N)	-3972(2)	-3878(3)	-4650(2)	113(2)
P(1)	-5975(1)	-4564(1)	-1768(1)	18(1)
C(1)	-6861(1)	-4127(1)	-1844(1)	21(1)
O(1)	-6199(1)	-1635(1)	-2192(1)	33(1)
N(2)	-2664(2)	-5001(2)	-5758(2)	89(1)
P(2)	-8698(1)	-8439(1)	-1957(1)	18(1)
C(2N)	-3273(1)	-3487(1)	-4683(1)	45(1)
C(2)	-7219(1)	-4001(1)	-1130(1)	25(1)
O(2)	-8261(1)	-6389(1)	-2292(1)	24(1)
C(3N)	-3009(2)	-4021(2)	-6661(2)	78(1)
C(3)	-8877(1)	-7702(1)	-1374(1)	23(1)
C(4N)	-2816(2)	-4569(2)	-6158(1)	61(1)
C(4)	-9663(1)	-7715(1)	-1055(1)	28(1)
C(5)	-8534(1)	-3460(1)	-3086(1)	20(1)
C(6)	-6061(1)	-2232(1)	-3577(1)	24(1)
C(7)	-7439(1)	-1788(1)	-1247(1)	24(1)
C(8)	-7681(1)	-5992(1)	-3662(1)	20(1)
C(9)	-9037(1)	-5439(1)	-1334(1)	24(1)
C(11)	-6070(1)	-5313(1)	-1183(1)	20(1)
C(12)	-6459(1)	-5916(1)	-1413(1)	27(1)
C(13)	-6595(1)	-6473(1)	-948(1)	29(1)
C(14)	-6348(1)	-6430(1)	-259(1)	28(1)
C(15)	-5970(1)	-5829(1)	-26(1)	26(1)
C(16)	-5834(1)	-5268(1)	-487(1)	22(1)
C(21)	-5278(1)	-3967(1)	-1428(1)	21(1)
C(22)	-5393(1)	-3232(1)	-1429(1)	26(1)
C(23)	-4831(1)	-2777(1)	-1196(1)	33(1)
C(24)	-4162(1)	-3057(1)	-965(1)	35(1)
C(25)	-4039(1)	-3787(1)	-977(1)	31(1)
C(26)	-4590(1)	-4248(1)	-1211(1)	25(1)
C(31)	-5682(1)	-4863(1)	-2617(1)	19(1)
C(32)	-5934(1)	-4507(1)	-3219(1)	23(1)
C(33)	-5675(1)	-4716(1)	-3873(1)	26(1)
C(34)	-5164(1)	-5270(1)	-3933(1)	27(1)
C(35)	-4909(1)	-5621(1)	-3340(1)	25(1)
C(36)	-5167(1)	-5421(1)	-2681(1)	22(1)
C(41)	-9088(1)	-8293(1)	-2813(1)	24(1)
C(42)	-8819(1)	-8711(1)	-3367(1)	32(1)
C(43)	-9078(1)	-8598(1)	-4043(1)	43(1)
C(44)	-9597(1)	-8071(1)	-4168(1)	48(1)
C(45)	-9866(1)	-7663(1)	-3626(1)	46(1)
C(46)	-9612(1)	-7765(1)	-2939(1)	33(1)
C(51)	-7713(1)	-8532(1)	-2068(1)	20(1)
C(52)	-7378(1)	-9204(1)	-2054(1)	27(1)
C(53)	-6613(1)	-9258(1)	-2148(1)	32(1)
C(54)	-6195(1)	-8647(1)	-2255(1)	30(1)
C(55)	-6532(1)	-7980(1)	-2275(1)	27(1)
C(56)	-7295(1)	-7915(1)	-2187(1)	23(1)
C(61)	-9061(1)	-9241(1)	-1571(1)	20(1)
C(62)	-9633(1)	-9627(1)	-1883(1)	24(1)
C(63)	-9923(1)	-10225(1)	-1545(1)	28(1)
C(64)	-9637(1)	-10434(1)	-901(1)	29(1)
C(65)	-9070(1)	-10047(1)	-585(1)	29(1)
C(66)	-8781(1)	-9446(1)	-912(1)	25(1)
C(67)	-6120(1)	-2646(1)	-4270(1)	32(1)
C(68)	-6056(1)	-1429(1)	-3763(1)	32(1)
C(69)	-5318(1)	-2440(1)	-3233(1)	32(1)
C(71)	-6728(1)	-2052(1)	-2394(1)	21(1)
C(72)	-6712(1)	-2395(1)	-3075(1)	20(1)
C(73)	-7300(1)	-2836(1)	-3280(1)	19(1)
C(74)	-7920(1)	-2961(1)	-2854(1)	18(1)
C(75)	-7942(1)	-2619(1)	-2204(1)	19(1)
C(76)	-7373(1)	-2178(1)	-1957(1)	19(1)
C(77)	-7451(1)	-977(1)	-1374(1)	33(1)
C(78)	-6784(1)	-1972(1)	-759(1)	33(1)
C(79)	-8153(1)	-1977(1)	-850(1)	35(1)
C(81)	-8303(1)	-5718(1)	-2467(1)	18(1)
C(82)	-8024(1)	-5459(1)	-3133(1)	18(1)
C(83)	-8100(1)	-4740(1)	-3312(1)	18(1)
C(84)	-8442(1)	-4239(1)	-2872(1)	17(1)

C(85)	-8708(1)	-4483(1)	-2229(1)	19(1)
C(86)	-8653(1)	-5195(1)	-2014(1)	19(1)
C(87)	-6989(1)	-6343(1)	-3343(1)	24(1)
C(88)	-8257(1)	-6569(1)	-3850(1)	30(1)
C(89)	-7442(1)	-5629(1)	-4349(1)	26(1)
C(97)	-8502(1)	-5855(1)	-851(1)	28(1)
C(98)	-9701(1)	-5913(1)	-1548(1)	30(1)
C(99)	-9346(1)	-4817(1)	-902(1)	37(1)

Table A.14a. Crystal data and structure refinement for (17)

Identification code	98srv019
Empirical formula	C65 H76 N2 O2 P2
Formula weight	979.22
Temperature	150(2) K
Wavelength	0.71073 A
Crystal system	Triclinic
Space group	P-1
Unit cell dimensions	a = 10.8909(4) A alpha = 103.643(2) deg. b = 14.3109(6) A beta = 95.5520(10) deg. c = 19.4658(8) A gamma = 102.318(2) deg.
Volume	2845.7(2) A^3
Z	2
Density (calculated)	1.143 Mg/m^3
Absorption coefficient	0.121 mm^-1
F(000)	1052
Crystal size	0.50 x 0.25 x 0.2 mm
Theta range for data collection	1.09 to 25.00 deg.
Index ranges	-13<=h<=14, -18<=k<=15, -25<=l<=22
Reflections collected	15409
Independent reflections	9934 [R(int) = 0.0259]
Refinement method	Full-matrix least-squares on F^2
Data / restraints / parameters	9794 / 0 / 663
Goodness-of-fit on F^2	1.083
Final R indices [I>2sigma(I)]	R1 = 0.0520, wR2 = 0.1028
R indices (all data)	R1 = 0.0839, wR2 = 0.1305
Largest diff. peak and hole	0.234 and -0.342 e.A^-3

Table A.14b. Atomic coordinates (x 10^4) and equivalent isotropic displacement parameters (A^2 x 10^3) for (17). U(eq) is defined as one third of the trace of the orthogonalized Uij tensor.

	x	y	z	U(eq)
P(1)	4901(1)	3278(1)	4110(1)	25(1)
O(1)	4588(2)	1859(1)	5629(1)	32(1)
N(1)	4518(2)	3228(2)	4864(1)	32(1)
P(2)	10307(1)	8826(1)	8011(1)	28(1)
O(2)	9460(2)	7011(1)	9229(1)	33(1)
N(2)	9715(2)	7766(2)	8098(1)	36(1)
C(11)	4625(2)	2034(2)	3540(1)	28(1)
C(12)	5070(3)	1332(2)	3814(2)	43(1)
H(12)	5462(3)	1501(2)	4299(2)	51
C(13)	4941(3)	386(2)	3380(2)	53(1)
H(13)	5251(3)	-90(2)	3567(2)	64
C(14)	4360(3)	130(2)	2673(2)	53(1)
H(14)	4270(3)	-519(2)	2378(2)	64
C(15)	3913(3)	825(2)	2399(2)	48(1)
H(15)	3508(3)	650(2)	1916(2)	58
C(16)	4054(3)	1778(2)	2829(1)	36(1)
H(16)	3759(3)	2256(2)	2636(1)	43
C(21)	6557(2)	3856(2)	4106(1)	28(1)
C(22)	7170(3)	4686(2)	4654(2)	39(1)
H(22)	6743(3)	4910(2)	5040(2)	46
C(23)	8400(3)	5192(2)	4643(2)	46(1)
H(23)	8805(3)	5770(2)	5015(2)	56
C(24)	9040(3)	4857(2)	4092(2)	48(1)
H(24)	9884(3)	5204(2)	4084(2)	58
C(25)	8450(3)	4017(3)	3552(2)	48(1)
H(25)	8894(3)	3778(3)	3177(2)	58
C(26)	7209(2)	3519(2)	3555(1)	38(1)
H(26)	6803(2)	2947(2)	3179(1)	46
C(31)	4022(2)	3934(2)	3628(1)	26(1)
C(32)	2707(2)	3735(2)	3595(1)	33(1)
H(32)	2292(2)	3280(2)	3834(1)	40
C(33)	1997(3)	4202(2)	3213(2)	41(1)
H(33)	1099(3)	4059(2)	3189(2)	49
C(34)	2589(3)	4870(2)	2869(2)	42(1)
H(34)	2099(3)	5181(2)	2605(2)	50
C(35)	3888(3)	5086(2)	2908(2)	43(1)
H(35)	4296(3)	5556(2)	2679(2)	52
C(36)	4612(3)	4620(2)	3282(1)	35(1)
H(36)	5510(3)	4768(2)	3302(1)	41
C(41)	11959(2)	9195(2)	8418(1)	32(1)
C(42)	12692(3)	10155(2)	8520(2)	46(1)
H(42)	12324(3)	10633(2)	8371(2)	55
C(43)	13956(3)	10418(3)	8839(2)	57(1)
H(43)	14452(3)	11073(3)	8902(2)	68
C(44)	14492(3)	9732(3)	9064(2)	60(1)
H(44)	15355(3)	9913(3)	9285(2)	72
C(45)	13775(3)	8788(3)	8968(2)	70(1)
H(45)	14145(3)	8315(3)	9125(2)	84
C(46)	12515(3)	8514(3)	8645(2)	54(1)
H(46)	12030(3)	7854(3)	8579(2)	64
C(51)	9623(2)	9810(2)	8455(1)	31(1)
C(52)	9111(3)	9702(2)	9074(1)	39(1)
H(52)	9099(3)	9119(2)	9229(1)	47
C(53)	8622(3)	10446(3)	9459(2)	57(1)
H(53)	8281(3)	10373(3)	9880(2)	68
C(54)	8628(3)	11288(3)	9235(2)	66(1)
H(54)	8285(3)	11792(3)	9499(2)	79
C(55)	9130(3)	11405(2)	8627(2)	60(1)
H(55)	9136(3)	11992(2)	8478(2)	72
C(56)	9629(3)	10669(2)	8231(2)	43(1)

H(56)	9969(3)	10750(2)	7811(2)	51
C(61)	10244(2)	8848(2)	7084(1)	31(1)
C(62)	11225(3)	8624(2)	6722(1)	41(1)
H(62)	11983(3)	8573(2)	6979(1)	50
C(63)	11102(3)	8475(2)	5984(2)	54(1)
H(63)	11777(3)	8324(2)	5739(2)	65
C(64)	10004(3)	8546(2)	5608(2)	56(1)
H(64)	9919(3)	8435(2)	5103(2)	67
C(65)	9028(3)	8779(2)	5962(2)	53(1)
H(65)	8277(3)	8836(2)	5701(2)	64
C(66)	9140(3)	8929(2)	6696(2)	43(1)
H(66)	8464(3)	9088(2)	6937(2)	52
C(70)	6439(2)	3049(2)	8626(1)	27(1)
C(71)	5921(2)	2686(2)	7829(1)	24(1)
C(72)	6735(2)	2503(2)	7333(1)	26(1)
C(73)	6331(2)	2230(2)	6597(1)	26(1)
C(74)	5031(2)	2153(2)	6356(1)	25(1)
C(75)	4168(2)	2295(2)	6845(1)	25(1)
C(76)	4649(2)	2569(2)	7579(1)	26(1)
C(77)	2731(2)	2151(2)	6598(1)	32(1)
C(78)	2153(3)	1093(2)	6136(2)	55(1)
H(78A)	2300(17)	621(2)	6407(4)	82
H(78B)	2553(14)	980(5)	5703(6)	82
H(78C)	1237(4)	1002(5)	6000(9)	82
C(79)	2007(3)	2311(3)	7242(2)	62(1)
H(79A)	2326(15)	2994(6)	7539(7)	93
H(79B)	2137(18)	1849(12)	7526(7)	93
H(79C)	1097(4)	2191(17)	7069(2)	93
C(80)	2506(2)	2904(2)	6183(2)	37(1)
H(80A)	2902(14)	3578(2)	6479(4)	56
H(80B)	1590(2)	2830(9)	6061(8)	56
H(80C)	2883(15)	2785(8)	5743(5)	56
C(81)	7289(2)	2042(2)	6076(1)	32(1)
C(82)	7465(3)	2841(2)	5661(1)	36(1)
H(82A)	6656(5)	2785(8)	5366(7)	53
H(82B)	8111(12)	2746(8)	5351(7)	53
H(82C)	7738(16)	3499(2)	5999(1)	53
C(83)	8614(3)	2116(3)	6478(2)	52(1)
H(83A)	8538(4)	1646(11)	6775(9)	77
H(83B)	8963(9)	2791(5)	6784(8)	77
H(83C)	9184(6)	1958(15)	6132(2)	77
C(84)	6845(3)	988(2)	5561(2)	41(1)
H(84A)	5988(7)	898(5)	5309(7)	61
H(84B)	6835(16)	494(2)	5836(2)	61
H(84C)	7432(10)	904(5)	5213(6)	61
C(91)	7260(2)	4099(2)	8828(1)	25(1)
C(92)	6734(2)	4906(2)	9040(1)	26(1)
C(93)	7446(2)	5885(2)	9187(1)	26(1)
C(94)	8746(2)	6046(2)	9098(1)	25(1)
C(95)	9332(2)	5246(2)	8923(1)	25(1)
C(96)	8553(2)	4289(2)	8785(1)	25(1)
H(96)	8925(2)	3742(2)	8657(1)	22(6)
C(97)	6812(2)	6752(2)	9424(1)	34(1)
C(98)	5443(3)	6386(2)	9557(2)	51(1)
H(98A)	4926(5)	5946(12)	9112(3)	76
H(98B)	5080(7)	6956(2)	9717(11)	76
H(98C)	5452(3)	6025(13)	9926(8)	76
C(99)	7552(3)	7486(2)	10128(2)	51(1)
H(99A)	7141(11)	8035(8)	10260(6)	76
H(99B)	8429(6)	7747(11)	10063(3)	76
H(99C)	7557(16)	7143(4)	10508(3)	76
C(100)	6721(3)	7284(2)	8824(2)	43(1)
H(10A)	6218(15)	6812(4)	8387(3)	65
H(10B)	7577(3)	7550(12)	8731(7)	65
H(10C)	6309(16)	7829(9)	8973(4)	65
C(101)	10757(2)	5381(2)	8850(1)	30(1)
C(102)	11214(3)	4439(2)	8876(2)	52(1)
H(10D)	11034(18)	4257(9)	9317(5)	78
H(10E)	12131(4)	4567(5)	8865(11)	78
H(10F)	10766(14)	3894(5)	8462(5)	78
C(104)	10944(2)	5594(2)	8122(1)	35(1)
H(10G)	11847(3)	5695(13)	8072(4)	52

H(10H)	10663(15)	6193(7)	8096(4)	52
H(10I)	10443(13)	5031(6)	7736(1)	52
C(103)	11628(2)	6228(2)	9457(1)	41(1)
H(10J)	11453(6)	6121(4)	9921(1)	62
H(10K)	11465(6)	6863(2)	9421(3)	62
H(10L)	12520(2)	6237(5)	9416(3)	62
H(70B)	5784(4)	2996(4)	8925(2)	34(7)
H(72)	7585(6)	2549(4)	7531(1)	27(6)
H(92A)	5779(2)	4750(4)	9044(3)	29(7)
H(70A)	6986(5)	2645(4)	8762(1)	36(7)
H(76)	3978(3)	2669(4)	7939(2)	38(7)
H(02)	9569(6)	7259(2)	8782(3)	104(14)
H(01)	4378(5)	2384(3)	5384(3)	101(13)
HN2	8975(6)	7438(2)	7725(3)	65(10)
HN1	4573(6)	3886(2)	5171(3)	105(14)

Table A.15a. Crystal data and structure refinement for (19)

Identification code	98srv009
Empirical formula	C26 H23 O2 P
Formula weight	398.41
Temperature	150(2) K
Wavelength	0.71073 A
Crystal system	Triclinic
Space group	P-1
Unit cell dimensions	a = 9.6129(2) A alpha = 90.4510(10) deg. b = 13.3172(3) A beta = 92.8880(10) deg. c = 16.3966(3) A gamma = 93.6170(10) deg.
Volume	2092.07(7) A^3
Z	4
Density (calculated)	1.265 Mg/m^3
Absorption coefficient	0.151 mm^-1
F(000)	840
Crystal size	0.4 x 0.4 x 0.3 mm
Theta range for data collection	1.24 to 27.54 deg.
Index ranges	-12<=h<=10, -16<=k<=17, -21<=l<=21
Reflections collected	19008
Independent reflections	9558 [R(int) = 0.0240]
Refinement method	Full-matrix least-squares on F^2
Data / restraints / parameters	9541 / 0 / 571
Goodness-of-fit on F^2	1.028
Final R indices [I>2sigma(I)]	R1 = 0.0403, wR2 = 0.1216
R indices (all data)	R1 = 0.0583, wR2 = 0.1450
Largest diff. peak and hole	0.302 and -0.356 e.A^-3

Table A.15b. Atomic coordinates (x 10^4) and equivalent isotropic displacement parameters (A^2 x 10^3) for (19). U(eq) is defined as one third of the trace of the orthogonalized Uij tensor.

	x	y	z	U(eq)
P(1)	7036(1)	8631(1)	1799(1)	17(1)
C(01)	7750(2)	9408(1)	1009(1)	23(1)
H(1B)	8161(25)	10051(19)	1301(15)	46(7)
H(1A)	8550(23)	9071(17)	801(14)	36(6)
P(1')	7800(1)	13494(1)	3248(1)	17(1)
C(01')	7169(2)	14042(1)	4150(1)	22(1)
H(1'B)	6626(21)	14606(16)	4004(12)	26(5)
H(1'A)	6451(23)	13548(16)	4356(13)	33(6)
O(1')	880(1)	9209(1)	560(1)	24(1)
C(1')	800(2)	8308(1)	231(1)	21(1)
O(1)	4670(1)	5526(1)	4120(1)	26(1)
C(1)	4874(2)	6478(1)	4312(1)	21(1)
C(02)	6651(2)	9651(2)	343(1)	29(1)
H(2C)	5899(23)	10049(17)	555(13)	34(6)
H(2B)	7123(23)	10058(18)	-68(14)	39(6)
H(2A)	6233(28)	9046(22)	113(17)	56(8)
C(02')	8361(2)	14347(2)	4778(1)	27(1)
H(2'C)	7983(23)	14478(17)	5285(15)	37(6)
H(2'B)	8886(24)	14979(18)	4602(14)	39(6)
H(2'A)	9016(23)	13796(17)	4828(13)	34(6)
O(2')	-736(2)	8839(1)	-886(1)	33(1)
H(2')	-572(29)	9443(23)	-636(18)	66(9)
C(2')	-52(2)	8088(1)	-502(1)	23(1)
O(2)	6572(1)	6142(1)	5416(1)	30(1)
H(2)	6071(27)	5529(22)	5428(16)	54(8)
C(2)	5855(2)	6820(1)	4965(1)	22(1)
C(3')	-221(2)	7120(2)	-826(1)	28(1)
H(3')	-810(2)	6994(2)	-1303(1)	34
C(3)	6108(2)	7833(1)	5149(1)	26(1)
H(3)	6775(2)	8035(1)	5575(1)	31
C(4')	459(2)	6327(2)	-463(1)	33(1)
H(4')	328(2)	5665(2)	-685(1)	40
C(4)	5396(2)	8569(1)	4717(1)	29(1)
H(4)	5590(2)	9264(1)	4841(1)	35
C(5')	1329(2)	6526(2)	228(1)	34(1)
H(5')	1818(2)	5998(2)	473(1)	41
C(5)	4406(2)	8263(1)	4105(1)	27(1)
H(5)	3899(2)	8750(1)	3817(1)	33
C(6')	1493(2)	7490(1)	567(1)	27(1)
H(6')	2094(2)	7602(1)	1041(1)	33
C(6)	4151(2)	7243(1)	3911(1)	24(1)
H(6)	3463(2)	7054(1)	3492(1)	28
C(11)	6382(2)	7419(1)	1404(1)	21(1)
C(11')	8510(2)	12308(1)	3504(1)	20(1)
C(12)	7058(2)	6978(1)	768(1)	26(1)
H(12)	7760(2)	7354(1)	492(1)	31
C(12')	9411(2)	11875(1)	2973(1)	28(1)
H(12')	9674(2)	12218(1)	2493(1)	34
C(13)	6689(2)	5981(2)	545(1)	33(1)
H(13)	7138(2)	5678(2)	111(1)	40
C(13')	9917(2)	10942(2)	3152(2)	36(1)
H(13')	10520(2)	10644(2)	2791(2)	43
C(14)	5675(2)	5428(2)	949(1)	35(1)
H(14)	5436(2)	4747(2)	796(1)	41
C(14')	9541(2)	10446(2)	3856(1)	38(1)
H(14')	9901(2)	9814(2)	3982(1)	45
C(15)	5009(2)	5865(2)	1577(1)	34(1)
H(15)	4310(2)	5483(2)	1850(1)	41
C(15')	8640(2)	10869(2)	4381(1)	36(1)
H(15')	8384(2)	10523(2)	4861(1)	43
C(16)	5356(2)	6860(1)	1809(1)	28(1)
H(16)	4897(2)	7157(1)	2241(1)	34
C(16')	8111(2)	11797(1)	4205(1)	25(1)
H(16')	7484(2)	12082(1)	4558(1)	30
C(21)	5664(2)	9303(1)	2209(1)	18(1)
C(21')	6387(2)	13259(1)	2495(1)	20(1)
C(22)	6000(2)	10004(1)	2839(1)	22(1)
H(22)	6903(2)	10037(1)	3105(1)	26
C(22')	5018(2)	13418(1)	2692(1)	24(1)
H(22')	4838(2)	13717(1)	3200(1)	29
C(23)	5015(2)	10651(1)	3073(1)	26(1)

H(23)	5237(2)	11123(1)	3505(1)	31
C(23')	3925(2)	13131(2)	2132(1)	28(1)
H(23')	2992(2)	13236(2)	2261(1)	33
C(24)	3696(2)	10608(1)	2675(1)	27(1)
H(24)	3024(2)	11055(1)	2835(1)	32
C(24')	4184(2)	12693(2)	1388(1)	29(1)
H(24')	3428(2)	12487(2)	1017(1)	35
C(25)	3354(2)	9914(1)	2043(1)	25(1)
H(25)	2454(2)	9889(1)	1772(1)	30
C(25')	5543(2)	12557(2)	1186(1)	30(1)
H(25')	5717(2)	12274(2)	670(1)	36
C(26)	4335(2)	9260(1)	1812(1)	22(1)
H(26)	4106(2)	8783(1)	1385(1)	26
C(26')	6651(2)	12834(1)	1736(1)	26(1)
H(26')	7582(2)	12736(1)	1599(1)	32
C(31)	8365(2)	8372(1)	2564(1)	18(1)
C(31')	9168(2)	14316(1)	2865(1)	19(1)
C(32)	9776(2)	8503(1)	2385(1)	19(1)
H(32)	10039(2)	8803(1)	1887(1)	23
C(32')	10545(2)	14286(1)	3188(1)	21(1)
H(32')	10780(2)	13785(1)	3571(1)	26
C(33)	10785(2)	8187(1)	2947(1)	22(1)
H(33)	11744(2)	8276(1)	2834(1)	27
C(33')	11566(2)	14994(1)	2944(1)	23(1)
H(33')	12500(2)	14980(1)	3161(1)	28
C(34)	10400(2)	7740(1)	3674(1)	25(1)
H(34)	11098(2)	7523(1)	4052(1)	30
C(34')	11210(2)	15722(1)	2380(1)	24(1)
H(34')	11909(2)	16199(1)	2208(1)	29
C(35)	8998(2)	7610(1)	3850(1)	26(1)
H(35)	8742(2)	7307(1)	4348(1)	31
C(35')	9840(2)	15760(1)	2064(1)	26(1)
H(35')	9609(2)	16263(1)	1682(1)	32
C(36)	7974(2)	7923(1)	3301(1)	23(1)
H(36)	7017(2)	7835(1)	3419(1)	28
C(36')	8816(2)	15062(1)	2309(1)	23(1)
H(36')	7879(2)	15091(1)	2101(1)	27

Table A.16a. Crystal data and structure refinement for (20)

Identification code	97srv003
Empirical formula	C38 H38 N3 O2 P
Formula weight	599.68
Temperature	150(2) K
Wavelength	0.71073 A
Crystal system	Orthorhombic
Space group	P2(1)2(1)2(1)
Unit cell dimensions	a = 12.695(4) A alpha = 90 deg. b = 13.044(5) A beta = 90 deg. c = 19.312(5) A gamma = 90 deg.
Volume	3197.9(1) A^3
Z	4
Density (calculated)	1.246 Mg/m^3
Absorption coefficient	0.124 mm^-1
F(000)	1272
Crystal size	0.50 x 0.25 x 0.25 mm
Theta range for data collection	1.88 to 25.00 deg.
Index ranges	-16<=h<=14, -16<=k<=16, -24<=l<=25
Reflections collected	19234
Independent reflections	5626 [R(int) = 0.0764]
Absorption correction	SADABS
Max. and min. transmission	0.956 and 0.530
Refinement method	Full-matrix least-squares on F^2
Data / restraints / parameters	5321 / 0 / 384
Goodness-of-fit on F^2	1.083
Final R indices [I>2sigma(I)]	R1 = 0.0643, wR2 = 0.1618
R indices (all data)	R1 = 0.1092, wR2 = 0.1995
Absolute structure parameter	-0.1(2)
Extinction coefficient	none
Largest diff. peak and hole	0.317 and -0.451 e.A^-3

Table A.16b. Atomic coordinates (x 10^4) and equivalent isotropic displacement parameters (A^2 x 10^3) for (20). U(eq) is defined as one third of the trace of the orthogonalized Uij tensor.

	x	y	z	U(eq)
P(1)	5825(1)	9183(1)	2289(1)	42(1)
O(1)	1604(3)	12871(3)	938(2)	54(1)
O(2)	1961(3)	4719(2)	820(2)	46(1)
N(1)	1253(3)	9826(3)	1300(2)	41(1)
N(2)	2875(3)	7697(3)	561(2)	45(1)
C(1)	997(3)	12616(3)	1477(2)	37(1)
C(2)	870(3)	11570(3)	1642(2)	33(1)
C(3)	270(3)	11297(3)	2226(2)	37(1)
C(4)	-196(4)	12031(4)	2635(2)	45(1)
C(5)	-82(4)	13066(4)	2469(3)	47(1)
C(6)	509(4)	13351(4)	1896(3)	45(1)
C(7)	1312(3)	10787(3)	1177(2)	36(1)
C(8)	1662(4)	9139(4)	769(2)	45(1)
C(9)	2475(4)	8425(3)	1072(2)	42(1)
C(10)	2514(3)	6793(3)	585(2)	38(1)
C(11)	2812(3)	5956(3)	103(2)	35(1)
C(12)	2514(3)	4935(3)	254(2)	35(1)
C(13)	2841(3)	4168(4)	-208(2)	40(1)
C(14)	3416(4)	4397(4)	-791(2)	44(1)
C(15)	3697(4)	5411(4)	-937(2)	44(1)
C(16)	3390(4)	6166(3)	-492(2)	40(1)
C(21)	5134(3)	10002(3)	1702(2)	40(1)
C(22)	5533(4)	10103(4)	1028(3)	63(2)
C(23)	5077(5)	10803(5)	580(3)	77(2)
C(24)	4225(4)	11387(4)	790(3)	60(1)
C(25)	3853(4)	11312(4)	1455(3)	55(1)
C(26)	4307(4)	10634(4)	1911(2)	45(1)
C(31)	5009(4)	8915(3)	3031(2)	43(1)
C(32)	4005(4)	8519(4)	2934(3)	54(1)
C(33)	3375(5)	8262(4)	3499(3)	62(2)
C(34)	3767(5)	8404(4)	4162(3)	55(1)
C(35)	4746(4)	8800(4)	4258(3)	53(1)
C(36)	5385(4)	9057(4)	3703(2)	48(1)
C(41)	6148(3)	8005(3)	1846(2)	39(1)
C(42)	7100(4)	7502(4)	1985(2)	44(1)
C(43)	7309(4)	6590(4)	1653(3)	52(1)
C(44)	6596(4)	6176(4)	1190(2)	49(1)
C(45)	5674(4)	6664(4)	1056(2)	48(1)
C(46)	5437(3)	7577(4)	1381(2)	41(1)
C(51)	7035(4)	9816(4)	2543(3)	49(1)
C(52)	6875(4)	10933(4)	2726(3)	64(2)
C(3S)	4654(9)	8950(8)	-541(5)	147(4)
C(2S)	4055(9)	9854(9)	-709(6)	137(3)
N(1S)	3564(9)	10625(9)	-790(6)	182(4)

Table A.17a. Crystal data and structure refinement for (21)

Identification code	98srv035
Empirical formula	C67 H79 N2 O4 P
Formula weight	1007.29
Temperature	150(2) K
Wavelength	0.71073 A
Crystal system	Monoclinic
Space group	P2(1)/c
Unit cell dimensions	a = 18.3934(3) A alpha = 90 deg. b = 12.6138(2) A beta = 90.4220(10) deg. c = 25.3686(4) A gamma = 90 deg.
Volume	5885.6(2) A^3
Z	4
Density (calculated)	1.137 Mg/m^3
Absorption coefficient	0.095 mm^-1
F(000)	2168
Crystal size	0.4 x 0.4 x 0.3 mm
Theta range for data collection	1.11 to 27.50 deg.
Index ranges	-23<=h<=23, -16<=k<=14, -32<=l<=32
Reflections collected	48067
Independent reflections	13478 [R(int) = 0.1002]
Refinement method	Full-matrix-block least-squares on F^2
Data / restraints / parameters	13313 / 6 / 746
Goodness-of-fit on F^2	1.202
Final R indices [I>2sigma(I)]	R1 = 0.0716, wR2 = 0.1202
R indices (all data)	R1 = 0.1452, wR2 = 0.1883
Largest diff. peak and hole	0.283 and -0.328 e.A^-3

Table A.17b. Atomic coordinates (x 10^4) and equivalent isotropic displacement parameters (A^2 x 10^3) for (21). U(eq) is defined as one third of the trace of the orthogonalized Uij tensor.

	x	y	z	U(eq)
O(1)	6320(1)	2259(2)	1206(1)	25(1)
C(1)	6863(2)	3765(2)	1980(1)	28(1)
H(1B)	6331(2)	3756(2)	1919(1)	34
H(1C)	7002(2)	4486(2)	2098(1)	34
P(1)	4396(1)	2805(1)	658(1)	24(1)
N(1X)	9671(3)	832(4)	1726(3)	113(2)
O(2)	6035(1)	1868(2)	2169(1)	32(1)
H(2A)	6146(24)	2041(35)	1826(18)	74(15)
C(2)	6432(2)	245(2)	2904(1)	27(1)
H(2B)	6433(2)	15(2)	3277(1)	33
H(2C)	5920(2)	350(2)	2792(1)	33
N(2X)	4291(2)	784(3)	3662(2)	60(1)
O(3)	5867(1)	-388(2)	1895(1)	32(1)
H(3A)	5883(27)	-197(40)	1571(19)	94(19)
C(3)	6620(2)	-1786(2)	1171(1)	26(1)
H(3B)	6698(2)	-2542(2)	1083(1)	31
H(3C)	6093(2)	-1636(2)	1139(1)	31
O(4)	6211(1)	351(2)	921(1)	30(1)
H(4A)	6216(28)	1162(44)	1032(20)	111(19)
C(4)	7046(2)	1744(2)	245(1)	23(1)
H(4B)	6510(2)	1806(2)	239(1)	27
H(4C)	7226(2)	1940(2)	-108(1)	27
C(8)	4868(2)	3585(3)	1141(2)	35(1)
H(8C)	5332(21)	3222(30)	1240(15)	54(11)
H(8B)	4968(19)	4280(30)	998(14)	45(11)
H(8A)	4569(21)	3632(30)	1477(16)	55(12)
C(10)	9110(2)	4177(2)	863(1)	32(1)
C(11)	6962(2)	2753(2)	1110(1)	22(1)
C(11X)	9053(3)	813(3)	1715(2)	57(1)
C(12)	7250(2)	3507(2)	1468(1)	24(1)
C(12X)	8262(2)	798(3)	1704(2)	54(1)
H(1XA)	8093(2)	331(17)	1420(7)	80
H(1XB)	8080(2)	1518(5)	1642(11)	80
H(1XC)	8082(2)	536(20)	2042(4)	80
C(13)	7930(2)	3948(2)	1370(1)	26(1)
H(13A)	8118(2)	4452(2)	1614(1)	31
C(14)	8352(2)	3691(2)	932(1)	26(1)
C(15)	8041(2)	2968(2)	575(1)	24(1)
H(15A)	8308(2)	2777(2)	271(1)	29
C(16)	7353(2)	2517(2)	649(1)	23(1)
C(17)	9591(2)	3862(3)	1337(2)	59(1)
H(17A)	9371(8)	4122(19)	1663(2)	88
H(17B)	10075(5)	4176(19)	1298(6)	88
H(17C)	9634(13)	3088(4)	1353(7)	88
C(18)	9476(2)	3801(3)	356(2)	47(1)
H(18A)	9963(6)	4113(16)	333(5)	70
H(18B)	9185(7)	4024(17)	51(2)	70
H(18C)	9516(12)	3027(3)	359(5)	70
C(19)	9056(2)	5398(3)	845(1)	38(1)
H(19A)	8850(11)	5658(3)	1176(4)	56
H(19B)	8742(10)	5611(3)	550(6)	56
H(19C)	9542(2)	5700(3)	798(9)	56
C(20)	8590(2)	2517(3)	3441(1)	32(1)
C(21)	6641(2)	2047(2)	2474(1)	25(1)
C(21X)	4424(2)	1311(3)	3311(2)	42(1)
C(22)	6843(2)	1295(2)	2857(1)	24(1)
C(22X)	4594(2)	2018(4)	2872(2)	59(1)
H(2XA)	5008(10)	1733(12)	2677(7)	89
H(2XB)	4718(15)	2723(7)	3009(2)	89
H(2XC)	4171(6)	2073(18)	2637(6)	89
C(23)	7459(2)	1491(2)	3165(1)	27(1)
H(23A)	7585(2)	993(2)	3432(1)	32
C(24)	7900(2)	2384(2)	3102(1)	26(1)
C(25)	7679(2)	3112(2)	2719(1)	25(1)
H(25A)	7963(2)	3732(2)	2668(1)	30
C(26)	7059(2)	2966(2)	2407(1)	23(1)
C(27)	9100(2)	1570(3)	3348(2)	58(1)
H(27A)	9541(7)	1654(12)	3563(9)	88
H(27B)	9231(13)	1539(14)	2975(3)	88
H(27C)	8852(6)	912(4)	3447(11)	88
C(28)	9004(2)	3541(3)	3308(2)	53(1)

H(28A)	9436(8)	3597(11)	3534(8)	80
H(28B)	8688(5)	4154(3)	3366(10)	80
H(28C)	9153(13)	3523(10)	2938(3)	80
C(29)	8384(2)	2568(4)	4025(1)	53(1)
H(29A)	8825(3)	2647(22)	4240(2)	80
H(29B)	8133(14)	1913(10)	4124(3)	80
H(29C)	8062(12)	3175(13)	4084(2)	80
C(30)	8431(2)	-2517(3)	2646(1)	32(1)
C(31)	6509	-851	2061	23
C(32)	6868	-1583	1737	23
C(33)	7481	-2104	1935	26
H(33A)	7720	-2604	1717	31
C(34)	7755	-1920	2440	25
C(35)	7396	-1159	2744	25
H(35A)	7580	-1004	3086	29
C(36)	6777	-617	2565	24
C(37)	8318	-3720	2570	68
H(37A)	8228	-3871	2196	103
H(37B)	7899	-3953	2777	103
H(37C)	8754	-4100	2688	103
C(37D)	8700	-3387	2281	62
H(37E)	8319	-3923	2236	133
H(37F)	9134	-3718	2435	16
H(37G)	8820	-3081	1938	76
C(38)	9096	-2163	2338	81
H(38A)	9176	-1403	2394	121
H(38B)	9015	-2298	1961	121
H(38C)	9523	-2559	2459	121
C(38D)	9071	-1683	2675	95
H(38E)	8957	-1142	2938	65
H(38F)	9128	-1347	2329	197
H(38G)	9523	-2044	2774	83
C(39)	8558	-2339	3230	63
H(39A)	8640	-1582	3296	94
H(39B)	8986	-2742	3345	94
H(39C)	8132	-2577	3427	94
C(39D)	8304	-3009	3189	144
H(39E)	8768	-3259	3336	40
H(39F)	7967	-3608	3155	176
H(39G)	8095	-2476	3425	24
C(40)	8806	-1334	-1	27
C(41)	6829	-36	688	22
C(42)	7252	601	360	21
C(43)	7886	179	142	23
H(43A)	8178	621	-73	27
C(44)	8107	-864	228	23
C(45)	7659	-1485	550	24
H(45A)	7790	-2204	611	29
C(46)	7035	-1095	784	23
C(47)	9181	-566	-385	40
H(47A)	9617	-903	-528	60
H(47B)	9318	84	-197	60
H(47C)	8846	-392	-674	60
C(48)	9335	-1594	455	36
H(48A)	9779	-1907	312	55
H(48B)	9105	-2098	696	55
H(48C)	9456	-942	646	55
C(49)	8619	-2357	-308	37
H(49A)	9062	-2640	-469	55
H(49B)	8261	-2195	-585	55
H(49C)	8417	-2883	-66	55
C(51)	4075	1607	964	25
C(52)	4434	1206	1410	31
H(52A)	4873	1524	1531	38
C(53)	4146	345	1676	36
H(53A)	4390	71	1978	44
C(54)	3507	-117	1504	38
H(54A)	3305	-693	1694	46
C(55)	3157	256	1054	35
H(55A)	2723	-75	932	42
C(56)	3442	1119	779	30
H(56A)	3207	1372	469	36
C(61)	3620	3558	441	23
C(62)	3071	3756	810	26
H(62A)	3093	3436	1149	31
C(63)	2496	4423	677	28
H(63A)	2122	4557	925	34
C(64)	2469	4890	184	31
H(64A)	2083	5361	99	37
C(65)	3000	4680	-188	32
H(65A)	2970	4994	-527	38

C(66)	3578	4007	-62	29
H(66A)	3940	3856	-316	34
C(71)	4967	2574	101	26
C(72)	5441	3378	-65	36
H(72A)	5490	4008	138	44
C(73)	5837	3257	-523	40
H(73A)	6155	3805	-635	48
C(74)	5769	2337	-817	40
H(74A)	6036	2257	-1134	48
C(75)	5311	1531	-651	38
H(75A)	5274	896	-851	45
C(76)	4907	1647	-195	31
H(76A)	4590	1096	-84	37

Table A.18a. Crystal data and structure refinement for (22)

Identification code	98srv036
Empirical formula	C63 H73 N2 O4 P
Formula weight	953.20
Temperature	150(2) K
Wavelength	0.71073 A
Crystal system	Monoclinic
Space group	P2(1)/n
Unit cell dimensions	a = 12.8544(2) A alpha = 90 deg. b = 21.84100(10) A beta = 90.2100(10) deg. c = 21.02710(10) A gamma = 90 deg.
Volume	5903.38(10) A^3
Z	4
Density (calculated)	1.072 Mg/m^3
Absorption coefficient	0.091 mm^-1
F(000)	2048
Crystal size	0.5 x 0.5 x 0.3 mm
Theta range for data collection	1.34 to 25.00 deg.
Index ranges	-16<=h<=16, -28<=k<=28, -27<=l<=27
Reflections collected	50318
Independent reflections	10386 [R(int) = 0.1179]
Refinement method	Full-matrix least-squares on F^2
Data / restraints / parameters	10198 / 0 / 738
Goodness-of-fit on F^2	1.146
Final R indices [I>2sigma(I)]	R1 = 0.0753, wR2 = 0.1795
R indices (all data)	R1 = 0.1126, wR2 = 0.2212
Largest diff. peak and hole	1.039 and -0.420 e.A^-3

Table A.18b. Atomic coordinates (x 10^4) and equivalent isotropic displacement parameters (A^2 x 10^3) for (22). U(eq) is defined as one third of the trace of the orthogonalized Uij tensor.

	x	y	z	U(eq)
P(1)	8092(1)	393(1)	638(1)	22(1)
O(1)	5000(2)	-2348(1)	-169(1)	32(1)
C(1)	8881(3)	1018(2)	355(2)	29(1)
C(01)	337(4)	2153(2)	3315(2)	42(1)
H(01A)	-113(17)	2069(7)	3680(6)	62
H(01B)	139(22)	2546(3)	3124(4)	62
H(01C)	1063(6)	2172(9)	3458(10)	62
N(1)	142(6)	1293(3)	2484(3)	109(2)
O(2)	2973(2)	-2587(1)	-173(1)	36(1)
C(2)	9390(4)	1425(2)	853(2)	44(1)
C(02)	221(4)	1672(2)	2852(2)	55(1)
N(2)	9615(5)	-2822(3)	-125(3)	96(2)
O(3)	2906(2)	-1465(1)	619(1)	31(1)
C(03)	10028(6)	-3296(4)	-228(3)	83(2)
O(4)	4909(2)	-1390(1)	472(1)	28(1)
C(4)	6930(3)	-1947(2)	403(2)	32(1)
H(4A)	7699(3)	-1919(2)	408(2)	39
H(4B)	6673(3)	-1716(2)	29(2)	39
C(04)	10538(6)	-3876(3)	-356(3)	95(2)
H(04A)	10190(25)	-4081(11)	-713(16)	143
H(04B)	10499(35)	-4137(9)	23(9)	143
H(04C)	11268(12)	-3803(4)	-463(23)	143
C(5)	4388(3)	-3608(2)	-287(2)	33(1)
H(5A)	4469(3)	-4030(2)	-453(2)	40
H(5B)	4228(3)	-3336(2)	-651(2)	40
C(6)	1494(3)	-2459(2)	833(2)	29(1)
H(6A)	769(3)	-2558(2)	952(2)	35
H(6B)	1476(3)	-2209(2)	441(2)	35
C(7)	4060(3)	-848(2)	1605(2)	26(1)
H(7A)	4049(3)	-533(2)	1943(2)	32
H(7B)	3907(3)	-644(2)	1195(2)	32
C(11)	8876(3)	-129(2)	1097(2)	25(1)
C(12)	9329(3)	77(2)	1664(2)	31(1)
H(12)	9176(3)	474(2)	1822(2)	37
C(13)	10005(3)	-304(2)	1996(2)	40(1)
H(13)	10316(3)	-165(2)	2380(2)	48
C(14)	10231(3)	-888(2)	1769(2)	39(1)
H(14)	10711(3)	-1142(2)	1991(2)	46
C(15)	9753(3)	-1097(2)	1221(2)	34(1)
H(15)	9887(3)	-1501(2)	1076(2)	41
C(16)	9079(3)	-723(2)	880(2)	28(1)
H(16)	8759(3)	-869(2)	501(2)	33
C(21)	7067(3)	679(2)	1131(2)	23(1)
C(22)	6663(3)	311(2)	1618(2)	29(1)
H(22)	6923(3)	-91(2)	1685(2)	34
C(23)	5880(3)	540(2)	2001(2)	35(1)
H(23)	5596(3)	293(2)	2329(2)	42
C(24)	5509(3)	1130(2)	1908(2)	36(1)
H(24)	4990(3)	1290(2)	2182(2)	43
C(25)	5891(3)	1489(2)	1414(2)	35(1)
H(25)	5615(3)	1887(2)	1344(2)	42
C(26)	6673(3)	1266(2)	1025(2)	30(1)
H(26)	6937(3)	1510(2)	688(2)	36
C(31)	7561(3)	-7(2)	-38(2)	23(1)
C(32)	8187(3)	-99(2)	-573(2)	33(1)
H(32)	8870(3)	67(2)	-588(2)	40
C(33)	7800(3)	-433(2)	-1083(2)	36(1)
H(33)	8226(3)	-507(2)	-1443(2)	43
C(34)	6799(3)	-660(2)	-1068(2)	31(1)
H(34)	6533(3)	-879(2)	-1423(2)	37
C(35)	6181(3)	-568(2)	-539(2)	30(1)
H(35)	5495(3)	-730(2)	-530(2)	36
C(36)	6560(3)	-242(2)	-21(2)	26(1)
H(36)	6136(3)	-180(2)	342(2)	31
C(40)	5660(3)	-2780(2)	62(2)	28(1)
C(41)	6607(3)	-2613(2)	344(2)	32(1)
C(42)	7236(4)	-3065(2)	615(2)	43(1)
H(42)	7877(4)	-2948(2)	806(2)	52
C(43)	6956(4)	-3684(2)	615(2)	51(1)
C(44)	6052(4)	-3838(2)	291(2)	44(1)
H(44)	5873(4)	-4259(2)	256(2)	53

C(45)	5396(3)	-3407(2)	16(2)	32(1)
C(46)	7578(5)	-4174(3)	974(3)	75(2)
C(47)	6904(7)	-4429(5)	1542(4)	147(4)
H(47A)	6597(52)	-4086(5)	1775(23)	221
H(47B)	7348(15)	-4668(32)	1828(22)	221
H(47C)	6348(40)	-4691(30)	1373(5)	221
C(48)	7872(7)	-4693(3)	570(3)	103(3)
H(48A)	8286(38)	-4984(13)	819(8)	155
H(48B)	8283(36)	-4546(5)	210(15)	155
H(48C)	7243(7)	-4897(15)	412(21)	155
C(49)	8512(5)	-3912(3)	1333(3)	81(2)
H(49A)	8270(6)	-3613(15)	1647(15)	121
H(49B)	8982(18)	-3711(18)	1032(4)	121
H(49C)	8882(21)	-4244(4)	1551(18)	121
C(50)	2856(3)	-3077(2)	235(2)	28(1)
C(51)	3484(3)	-3594(2)	178(2)	31(1)
C(52)	3321(3)	-4088(2)	588(2)	31(1)
H(52)	3757(3)	-4438(2)	552(2)	37
C(53)	2539(3)	-4087(2)	1049(2)	28(1)
C(54)	1940(3)	-3558(2)	1095(2)	28(1)
H(54)	1406(3)	-3545(2)	1406(2)	33
C(55)	2085(3)	-3047(2)	707(2)	26(1)
C(56)	2352(3)	-4637(2)	1493(2)	32(1)
C(57)	3233(4)	-5106(2)	1460(2)	47(1)
H(57A)	3897(5)	-4903(3)	1551(14)	71
H(57B)	3254(16)	-5285(10)	1033(5)	71
H(57C)	3112(13)	-5430(8)	1773(10)	71
C(58)	2274(5)	-4418(2)	2187(2)	61(2)
H(58A)	1676(17)	-4143(13)	2230(4)	91
H(58B)	2912(12)	-4200(14)	2304(6)	91
H(58C)	2183(29)	-4772(2)	2467(3)	91
C(59)	1336(4)	-4950(2)	1304(2)	49(1)
H(59A)	763(5)	-4656(4)	1336(14)	74
H(59B)	1207(13)	-5296(9)	1589(10)	74
H(59C)	1387(9)	-5098(13)	865(6)	74
C(60)	2718(3)	-1625(2)	1238(2)	24(1)
C(61)	2007(3)	-2095(2)	1367(2)	25(1)
C(62)	1822(3)	-2250(2)	1999(2)	27(1)
H(62)	1328(3)	-2562(2)	2087(2)	32
C(63)	2326(3)	-1969(2)	2511(2)	24(1)
C(64)	3029(3)	-1503(2)	2365(2)	24(1)
H(64)	3382(3)	-1300(2)	2702(2)	29
C(65)	3232(3)	-1323(2)	1738(2)	24(1)
C(66)	2099(3)	-2166(2)	3197(2)	33(1)
C(67)	2747(4)	-1826(2)	3686(2)	46(1)
H(67A)	2616(18)	-1385(2)	3648(10)	69
H(67B)	3487(4)	-1908(11)	3612(9)	69
H(67C)	2558(17)	-1964(10)	4113(2)	69
C(68)	2280(5)	-2850(2)	3267(2)	69(2)
H(68A)	1870(24)	-3070(2)	2947(12)	103
H(68B)	2065(29)	-2981(4)	3693(7)	103
H(68C)	3020(7)	-2940(3)	3208(18)	103
C(69)	935(4)	-2019(3)	3334(2)	62(2)
H(69A)	827(7)	-1575(3)	3318(17)	93
H(69B)	751(9)	-2171(15)	3758(8)	93
H(69C)	495(4)	-2218(14)	3014(11)	93
C(70)	5509(3)	-1391(2)	1006(2)	25(1)
C(71)	5131(3)	-1137(2)	1577(2)	25(1)
C(72)	5716(3)	-1207(2)	2134(2)	29(1)
H(72)	5452(3)	-1038(2)	2517(2)	34
C(73)	6669(3)	-1514(2)	2155(2)	31(1)
C(74)	7056(3)	-1721(2)	1574(2)	33(1)
H(74)	7722(3)	-1909(2)	1566(2)	39
C(75)	6501(3)	-1662(2)	1004(2)	29(1)
C(76)	7221(3)	-1636(2)	2796(2)	40(1)
C(77)	6512(5)	-2027(3)	3207(3)	60(2)
H(77A)	5863(15)	-1805(8)	3287(17)	90
H(77B)	6859(14)	-2116(17)	3612(9)	90
H(77C)	6356(27)	-2411(9)	2986(9)	90
C(78)	8234(5)	-2008(3)	2705(3)	61(2)
H(78A)	8561(19)	-2080(18)	3119(3)	91
H(78B)	8713(15)	-1777(10)	2433(18)	91
H(78C)	8070(6)	-2401(9)	2503(20)	91
C(79)	7458(7)	-1039(3)	3121(3)	66(2)
H(79A)	6806(7)	-834(11)	3233(21)	99
H(79B)	7860(34)	-777(9)	2835(9)	99
H(79C)	7863(34)	-1117(4)	3509(13)	99
C(77')	7352(29)	-2290(16)	2929(17)	58(11)
H(77D)	7662(188)	-2491(27)	2559(49)	88
H(77E)	6672(37)	-2473(29)	3018(122)	88
H(77F)	7809(163)	-2342(16)	3299(76)	88

C(78')	8046(85)	-1082(47)	2879(52)	166(47)
H(78D)	8618(295)	-1214(115)	3155(268)	249
H(78E)	7697(161)	-728(118)	3069(318)	249
H(78F)	8322(411)	-967(221)	2461(61)	249
C(79')	8332(33)	-1327(20)	2784(21)	61(11)
H(79D)	8254(33)	-880(21)	2769(134)	91
H(79E)	8712(88)	-1466(100)	2407(70)	91
H(79F)	8719(84)	-1441(101)	3168(63)	91
H(1B)	9385(32)	815(19)	107(19)	33(11)
H(1A)	8411(35)	1237(21)	92(21)	46(12)
H(2C)	9710(37)	1758(23)	641(22)	52(13)
H(2B)	9914(39)	1234(23)	1141(24)	58(14)
H(3O)	3524(43)	-1409(25)	569(25)	63(17)
H(2A)	8916(39)	1604(23)	1165(24)	58(15)
H(2O)	3759(47)	-2525(26)	-192(26)	80(18)
H(1O)	5045(44)	-1862(28)	138(27)	87(18)

Table A.19a. Crystal data and structure refinement for (23)

Identification code	98srv064
Empirical formula	C52.80 H62.40 N2.40 O3.20 P0.80
Formula weight	806.63
Temperature	150(2) K
Wavelength	0.71073 A
Crystal system	Monoclinic
Space group	P2(1)/n
Unit cell dimensions	a = 18.161(4) A alpha = 90 deg. b = 12.592(3) A beta = 90.63(3) deg. c = 25.652(5) A gamma = 90 deg.
Volume	5866(2) A^3
Z	5
Density (calculated)	1.142 Mg/m^3
Absorption coefficient	0.096 mm^-1
F(000)	2168
Crystal size	0.65 x 0.15 x 0.15 mm
Theta range for data collection	1.12 to 27.46 deg.
Index ranges	-21<=h<=23, -15<=k<=16, -19<=l<=33
Reflections collected	41742
Independent reflections	13400 [R(int) = 0.1332]
Refinement method	Full-matrix least-squares on F^2
Data / restraints / parameters	13302 / 0 / 707
Goodness-of-fit on F^2	1.272
Final R indices [I>2sigma(I)]	R1 = 0.0939, wR2 = 0.1714
R indices (all data)	R1 = 0.1679, wR2 = 0.2235
Extinction coefficient	not refined
Largest diff. peak and hole	0.464 and -0.565 e.A^-3

Table A.19b. Atomic coordinates (x 10^4) and equivalent isotropic displacement parameters (A^2 x 10^3) for (23). U(eq) is defined as one third of the trace of the orthogonalized Uij tensor.

	x	y	z	U(eq)
O(1)	6284(1)	2345(2)	1199(1)	22(1)
O(3)	5827(1)	-381(2)	1908(1)	27(1)
H(3)	5922(28)	-191(41)	1584(21)	59(16)
O(2)	6030(1)	1893(2)	2158(1)	28(1)
H(2)	6133(27)	2051(38)	1819(20)	54(15)
O(4)	6201(1)	382(2)	951(1)	25(1)
H(4)	6186(32)	1104(49)	1008(22)	81(20)
C(1)	6859(2)	3813(3)	1978(1)	24(1)
H(1C)	6320(2)	3813(3)	1915(1)	29
H(1D)	7005(2)	4534(3)	2093(1)	29
C(11)	6950(2)	2807(3)	1116(1)	20(1)
C(12)	7252(2)	3542(3)	1475(1)	22(1)
C(13)	7941(2)	3976(3)	1381(2)	25(1)
H(13)	8133(2)	4482(3)	1621(2)	30
C(14)	8365(2)	3702(3)	949(2)	24(1)
C(15)	8055(2)	2978(3)	599(2)	23(1)
H(15)	8328(2)	2774(3)	301(2)	27
C(16)	7355(2)	2542(3)	671(1)	20(1)
C(10)	9131(2)	4206(3)	879(2)	31(1)
C(17)	9623(3)	3936(4)	1349(2)	57(2)
H(17A)	9393(10)	4193(25)	1669(3)	86
H(17B)	10104(7)	4277(24)	1309(7)	86
H(17C)	9688(16)	3164(5)	1371(8)	86
C(18)	9507(2)	3803(4)	383(2)	47(1)
H(18A)	9203(9)	3984(23)	78(2)	71
H(18B)	9566(16)	3030(5)	404(6)	71
H(18C)	9992(8)	4137(20)	352(7)	71
C(19)	9060(2)	5422(3)	837(2)	37(1)
H(19A)	8749(13)	5603(3)	535(7)	55
H(19B)	9550(3)	5735(4)	794(11)	55
H(19C)	8837(15)	5701(4)	1155(5)	55
C(2)	6408(2)	295(3)	2894(1)	24(1)
H(2A)	5893(2)	403(3)	2776(1)	29
H(2B)	6400(2)	67(3)	3263(1)	29
C(21)	6633(2)	2094(3)	2465(1)	23(1)
C(22)	6825(2)	1340(3)	2852(1)	23(1)
C(23)	7436(2)	1546(3)	3165(1)	25(1)
H(23A)	7559(2)	1052(3)	3432(1)	30
C(24)	7882(2)	2449(3)	3108(1)	25(1)
C(25)	7668(2)	3171(3)	2722(1)	25(1)
H(25A)	7955(2)	3793(3)	2675(1)	30
C(26)	7048(2)	3016(3)	2403(1)	22(1)
C(20)	8574(2)	2597(3)	3456(2)	32(1)
C(27)	9099(3)	1659(4)	3373(2)	58(2)
H(27A)	8858(8)	999(6)	3480(14)	87
H(27B)	9548(9)	1765(15)	3583(11)	87
H(27C)	9227(16)	1615(18)	3004(3)	87
C(28)	8985(3)	3635(4)	3332(2)	47(1)
H(28A)	9158(16)	3613(11)	2971(4)	70
H(28B)	9408(11)	3713(13)	3569(9)	70
H(28C)	8651(6)	4240(4)	3375(12)	70
C(29)	8339(3)	2635(4)	4029(2)	49(1)
H(29A)	8107(17)	1959(11)	4123(4)	73
H(29B)	7986(14)	3215(17)	4078(3)	73
H(29C)	8772(4)	2754(27)	4252(2)	73
C(3)	6602(2)	-1761(3)	1196(1)	23(1)
H(3A)	6069(2)	-1607(3)	1165(1)	27
H(3B)	6678(2)	-2520(3)	1112(1)	27
C(31)	6489(2)	-824(3)	2070(1)	21(1)
C(32)	6862(2)	-1546(3)	1750(1)	20(1)
C(33)	7485(2)	-2057(3)	1947(1)	22(1)

H(33A)	7735(2)	-2548(3)	1731(1)	27
C(34)	7754(2)	-1873(3)	2451(2)	24(1)
C(35)	7389(2)	-1119(3)	2749(1)	23(1)
H(35A)	7571(2)	-967(3)	3090(1)	27
C(36)	6761(2)	-572(3)	2565(1)	22(1)
C(30)	8441(2)	-2463(3)	2657(2)	28(1)
C(37)	9122(3)	-1963(7)	2435(3)	107(3)
H(37A)	9103(16)	-2007(42)	2054(3)	160
H(37B)	9559(3)	-2339(31)	2565(19)	160
H(37C)	9148(17)	-1216(15)	2541(19)	160
C(38)	8505(3)	-2427(6)	3249(2)	75(2)
H(38A)	8052(10)	-2705(32)	3402(2)	112
H(38B)	8580(24)	-1692(7)	3363(2)	112
H(38C)	8924(15)	-2861(29)	3364(2)	112
C(39)	8411(4)	-3628(5)	2506(3)	114(3)
H(39A)	8477(35)	-3697(6)	2128(5)	171
H(39B)	7933(14)	-3926(13)	2602(22)	171
H(39C)	8805(23)	-4014(11)	2688(20)	171
C(4)	7042(2)	1763(3)	271(1)	21(1)
H(4A)	7224(2)	1959(3)	-78(1)	25
H(4B)	6499(2)	1829(3)	263(1)	25
C(41)	6819(2)	-18(3)	713(1)	19(1)
C(42)	7246(2)	608(3)	382(1)	19(1)
C(43)	7872(2)	175(3)	157(1)	20(1)
H(43A)	8163(2)	610(3)	-62(1)	24
C(44)	8086(2)	-871(3)	241(1)	20(1)
C(45)	7640(2)	-1482(3)	566(1)	20(1)
H(45A)	7768(2)	-2205(3)	624(1)	24
C(46)	7019(2)	-1081(3)	809(1)	18(1)
C(40)	8782(2)	-1360(3)	1(2)	26(1)
C(47)	8563(2)	-2376(3)	-300(2)	33(1)
H(47A)	9001(3)	-2682(12)	-463(9)	49
H(47B)	8199(11)	-2199(5)	-571(7)	49
H(47C)	8352(14)	-2893(9)	-58(2)	49
C(48)	9332(2)	-1639(3)	444(2)	34(1)
H(48A)	9472(11)	-991(4)	632(7)	50
H(48B)	9772(7)	-1967(20)	296(2)	50
H(48C)	9101(6)	-2137(17)	686(6)	50
C(49)	9154(2)	-605(3)	-384(2)	37(1)
H(49A)	9319(14)	35(11)	-200(3)	55
H(49B)	8802(5)	-408(18)	-660(6)	55
H(49C)	9579(10)	-960(9)	-539(9)	55
P(1)	4491(1)	2839(1)	603(1)	21(1)
N(1)	5028(2)	3489(3)	992(2)	33(1)
H(1A)	4967(28)	4128(43)	1053(19)	55(16)
H(1B)	5456(25)	3170(35)	1059(16)	35(12)
C(51)	3723(2)	3665(3)	425(1)	22(1)
C(52)	3648(2)	4118(3)	-70(2)	26(1)
H(52A)	4004(2)	3973(3)	-329(2)	31
C(53)	3057(2)	4775(3)	-183(2)	29(1)
H(53A)	3008(2)	5089(3)	-519(2)	35
C(54)	2532(2)	4976(3)	199(2)	28(1)
H(54A)	2132(2)	5438(3)	123(2)	34
C(55)	2590(2)	4509(3)	683(2)	27(1)
H(55A)	2222(2)	4634(3)	937(2)	33
C(56)	3184(2)	3857(3)	802(2)	26(1)
H(56A)	3226(2)	3541(3)	1138(2)	31
C(61)	4110(2)	1701(3)	930(2)	22(1)
C(62)	4417(2)	1371(3)	1403(2)	28(1)
H(62A)	4851(2)	1700(3)	1535(2)	34
C(63)	4085(2)	557(3)	1682(2)	34(1)
H(63A)	4295(2)	326(3)	2003(2)	41
C(64)	3448(2)	82(3)	1491(2)	32(1)
H(64A)	3214(2)	-459(3)	1687(2)	39
C(65)	3152(2)	395(3)	1016(2)	32(1)
H(65A)	2719(2)	59(3)	886(2)	38
C(66)	3481(2)	1195(3)	728(2)	26(1)
H(66A)	3283(2)	1397(3)	399(2)	31
C(71)	4977(2)	2478(3)	27(2)	23(1)
C(72)	5453(2)	3250(3)	-183(2)	30(1)
H(72A)	5510(2)	3915(3)	-13(2)	35

C(73)	5836(2)	3046(3)	-634(2)	36(1)
H(73A)	6155(2)	3569(3)	-774(2)	43
C(74)	5754(2)	2067(4)	-884(2)	35(1)
H(74A)	6010(2)	1928(4)	-1198(2)	42
C(75)	5297(2)	1297(3)	-674(2)	32(1)
H(75A)	5252(2)	627(3)	-842(2)	38
C(76)	4906(2)	1498(3)	-222(2)	25(1)
H(76A)	4591(2)	969(3)	-83(2)	30
N(1X)	9682(3)	887(5)	1706(3)	118(3)
C(11X)	9054(3)	868(4)	1714(2)	59(2)
C(12X)	8253(3)	829(5)	1727(2)	50(1)
H(1AX)	8096(3)	521(39)	2059(9)	131(29)
H(1BX)	8069(3)	390(34)	1439(12)	185(42)
H(1CX)	8054(3)	1550(6)	1693(21)	140(31)
N(2X)	5459(3)	-4351(3)	1374(2)	62(1)
C(21X)	5430(2)	-3740(4)	1700(2)	39(1)
C(22X)	5383(3)	-2945(4)	2111(2)	44(1)
H(2AX)	4995(12)	-3146(13)	2355(7)	56(15)
H(2BX)	5267(17)	-2252(6)	1957(2)	82(20)
H(2CX)	5855(6)	-2904(18)	2299(8)	62(16)

Table A.20a. Crystal data and structure refinement for (24)

Identification code	phos033
Empirical formula	C66 H42 N0 O2 P2
Formula weight	928.94
Temperature	153(2) K
Wavelength	0.71073 A
Crystal system	Monoclinic
Space group	C2/c
Unit cell dimensions	a = 25.015(5) A alpha = 90 deg. b = 8.882(2) A beta = 113.87(3) deg. c = 25.444(5) A gamma = 90 deg.
Volume	5170(2) A^3
Z	4
Density (calculated)	1.194 Mg/m^3
Absorption coefficient	0.129 mm^-1
F(000)	1936
Crystal size	0.5 x 0.5 x 0.3 mm
Theta range for data collection	2.73 to 22.50 deg.
Index ranges	-26<=h<=26, -9<=k<=9, -15<=l<=27
Reflections collected	6873
Independent reflections	3383 [R(int) = 0.0461]
Refinement method	Full-matrix least-squares on F^2
Data / restraints / parameters	3381 / 15 / 340
Goodness-of-fit on F^2	1.057
Final R indices [I>2sigma(I)]	R1 = 0.0456, wR2 = 0.1277
R indices (all data)	R1 = 0.0726, wR2 = 0.1480
Largest diff. peak and hole	0.429 and -0.278 e.A^-3

Table A.20b. Atomic coordinates (x 10^4) and equivalent isotropic displacement parameters (A^2 x 10^3) for (24). U(eq) is defined as one third of the trace of the orthogonalized Uij tensor.

	x	y	z	U(eq)
P(1)	9299(1)	827(1)	5708(1)	20(1)
C(11)	9363(1)	-1127(3)	5561(1)	19(1)
C(12)	9221(1)	-1635(3)	5004(1)	23(1)
H(12A)	9054(1)	-964(3)	4688(1)	27
C(13)	9323(1)	-3131(4)	4909(1)	26(1)
H(13A)	9223(1)	-3487(4)	4529(1)	32
C(14)	9572(1)	-4095(4)	5371(1)	26(1)
H(14A)	9649(1)	-5110(4)	5306(1)	32
C(15)	9709(1)	-3602(4)	5925(1)	29(1)
H(15A)	9877(1)	-4278(4)	6239(1)	35
C(16)	9601(1)	-2125(4)	6023(1)	27(1)
H(16A)	9688(1)	-1788(4)	6403(1)	32
C(21)	8862(1)	1776(3)	5045(1)	21(1)
C(22)	8261(1)	1891(4)	4861(1)	33(1)
H(22A)	8073(1)	1470(4)	5084(1)	40
C(23)	7937(1)	2619(5)	4351(1)	41(1)
H(23A)	7524(1)	2681(5)	4221(1)	50
C(24)	8211(1)	3260(4)	4031(1)	35(1)
H(24A)	7985(1)	3784(4)	3686(1)	42
C(25)	8808(1)	3146(4)	4205(1)	29(1)
H(25A)	8994(1)	3579(4)	3981(1)	35
C(26)	9133(1)	2389(3)	4710(1)	24(1)
H(26A)	9544(1)	2288(3)	4830(1)	29
C(31)	8925(1)	975(3)	6179(1)	22(1)
C(32)	9049(2)	2179(4)	6565(1)	35(1)
H(32A)	9328(2)	2918(4)	6576(1)	42
C(33)	8763(2)	2289(4)	6932(1)	41(1)
H(33A)	8846(2)	3106(4)	7193(1)	50
C(34)	8360(1)	1222(4)	6917(1)	35(1)
H(34A)	8171(1)	1296(4)	7173(1)	41
C(35)	8227(1)	34(4)	6528(1)	29(1)
H(35A)	7945(1)	-696(4)	6516(1)	35
C(36)	8509(1)	-83(4)	6158(1)	24(1)
H(36A)	8416(1)	-888(4)	5890(1)	29
C(1)	11079(1)	1543(4)	6485(1)	23(1)
C(2)	11557(1)	565(4)	6603(1)	28(1)
H(2A)	11483(1)	-459(4)	6489(1)	34
C(3)	12129(1)	1038(4)	6879(1)	35(1)
H(3A)	12444(1)	359(4)	6952(1)	42
C(4)	12231(1)	2560(4)	7049(1)	35(1)
H(4A)	12621(1)	2906(4)	7242(1)	41
C(5)	11783(1)	3536(4)	6941(1)	31(1)
H(5A)	11872(1)	4549(4)	7066(1)	37
C(6)	11182(1)	3114(4)	6649(1)	25(1)
C(7)	10499(1)	929(4)	6200(1)	23(1)
H(7A)	10501(1)	-263(4)	6096(1)	28
C(8)	9987(1)	1685(4)	6026(1)	23(1)
H(8A)	10003(1)	2697(4)	6118(1)	27
O(1)	10773(1)	4068(3)	6542(1)	34(1)
C(40)	10444(3)	-2643(9)	7505(5)	46(2)
C(41)	10101(3)	-3837(6)	7541(5)	52(2)
C(42)	9566(3)	-3559(8)	7569(4)	65(3)
C(43)	9374(4)	-2087(10)	7559(4)	62(3)
C(44)	9716(6)	-893(6)	7523(3)	53(3)
C(45)	10251(6)	-1171(7)	7495(8)	42(3)
C(46)	11030(4)	-2949(11)	7454(4)	60(2)
C(50)	6997(4)	-582(14)	4142(4)	81(3)
C(51)	7251(2)	-1471(7)	4569(3)	83(2)
C(52)	7288(2)	-2606(8)	5435(3)	83(2)
C(53)	7046(2)	-1595(7)	5007(3)	80(2)

Table A.21a. Crystal data and structure refinement for (25)

Identification code	97srv164
Empirical formula	C32 H25 O P
Formula weight	456.49
Temperature	150(2) K
Wavelength	0.71073 A
Crystal system	Triclinic
Space group	P-1
Unit cell dimensions	a = 8.13670(10) A alpha = 99.5230(10) deg. b = 10.5476(2) A beta = 90.7240(10) deg. c = 14.3050(3) A gamma = 98.8220(10) deg.
Volume	1195.54(4) A^3
Z	2
Density (calculated)	1.268 Mg/m^3
Absorption coefficient	0.138 mm^-1
F(000)	480
Crystal size	0.30 x 0.25 x 0.20 mm
Theta range for data collection	1.98 to 25.82 deg.
Index ranges	-9<=h<=9, -12<=k<=12, -17<=l<=16
Reflections collected	7694
Independent reflections	3884 [R(int) = 0.0388]
Refinement method	Full-matrix least-squares on F^2
Data / restraints / parameters	3849 / 0 / 407
Goodness-of-fit on F^2	1.155
Final R indices [I>2sigma(I)]	R1 = 0.0478, wR2 = 0.1011
R indices (all data)	R1 = 0.0642, wR2 = 0.1284
Largest diff. peak and hole	0.218 and -0.322 e.A^-3

Table A.21b. Atomic coordinates (x 10^4) and equivalent isotropic displacement parameters (A^2 x 10^3) for (25). U(eq) is defined as one third of the trace of the orthogonalized Uij tensor.

	x	y	z	U(eq)
P(1)	4212(1)	6155(1)	2822(1)	24(1)
O(1)	2756(2)	4749(2)	3315(1)	29(1)
C(1)	2590(3)	3226(2)	1883(2)	29(1)
C(2)	2363(3)	1912(3)	1436(2)	34(1)
C(3)	2184(3)	916(3)	1960(2)	35(1)
C(4)	2197(3)	1214(3)	2951(2)	36(1)
C(5)	2391(3)	2489(3)	3408(2)	32(1)
C(6)	2604(3)	3518(2)	2882(2)	29(1)
C(7)	2661(3)	4291(3)	1350(2)	30(1)
C(8)	3159(3)	5576(2)	1664(2)	28(1)
C(11)	2839(3)	6506(2)	1018(2)	29(1)
C(12)	4033(4)	7016(3)	433(2)	40(1)
C(13)	3634(5)	7859(3)	-159(2)	50(1)
C(14)	2070(5)	8205(3)	-174(2)	48(1)
C(15)	871(4)	7695(3)	394(2)	42(1)
C(16)	1249(4)	6846(3)	987(2)	35(1)
C(31)	3186(3)	7134(2)	3742(2)	25(1)
C(32)	1455(3)	7056(3)	3712(2)	29(1)
C(33)	691(4)	7859(3)	4389(2)	36(1)
C(34)	1624(4)	8697(3)	5119(2)	38(1)
C(35)	3337(4)	8755(3)	5163(2)	37(1)
C(36)	4128(3)	8003(2)	4467(2)	31(1)
C(41)	5653(3)	7626(2)	2529(2)	26(1)
C(42)	7372(3)	7693(3)	2485(2)	32(1)
C(43)	8407(4)	8834(3)	2361(2)	36(1)
C(44)	7733(4)	9940(3)	2276(2)	34(1)
C(45)	6021(3)	9897(3)	2299(2)	31(1)
C(46)	5005(3)	8765(3)	2432(2)	29(1)
C(51)	5862(3)	5277(2)	3111(2)	25(1)
C(52)	6367(3)	5317(3)	4053(2)	29(1)
C(53)	7662(3)	4676(3)	4266(2)	35(1)
C(54)	8447(3)	3983(3)	3540(2)	36(1)
C(55)	7935(3)	3921(3)	2603(2)	35(1)
C(56)	6637(3)	4561(2)	2383(2)	30(1)

Table A.22b. Crystal data and structure refinement for (26)

Identification code	slylidm
Empirical formula	C26 H22 Cl O P
Formula weight	416.86
Temperature	150(2) K
Wavelength	0.71073 A
Crystal system	monoclinic
Space group	P2(1)/C
Unit cell dimensions	a = 9.1964(2) A alpha = 90 deg. b = 15.3911(3) A beta = 103.1900(10) deg. c = 15.2888(3) A gamma = 90 deg.
Volume, Z	2106.93(7) A^3, 4
Density (calculated)	1.314 Mg/m^3
Absorption coefficient	0.272 mm^-1
F(000)	872
Crystal size	0.4 x 0.4 x 0.25 mm
Theta range for data collection	1.90 to 27.48 deg.
Limiting indices	-11<=h<=10, -18<=k<=19, -19<=l<=19
Reflections collected	16579
Independent reflections	4813 [R(int) = 0.0316]
Refinement method	Full-matrix least-squares on F^2
Data / restraints / parameters	4793 / 0 / 350
Goodness-of-fit on F^2	1.092
Final R indices [I>2sigma(I)]	R1 = 0.0319, wR2 = 0.0753
R indices (all data)	R1 = 0.0387, wR2 = 0.0857
Largest diff. peak and hole	0.393 and -0.286 e.A^-3

Table A.22b. Atomic coordinates (x 10^4) and equivalent isotropic displacement parameters (A^2 x 10^3) for (26). U(eq) is defined as one third of the trace of the orthogonalized Uij tensor.

	x	y	z	U(eq)
P	749(1)	2045(1)	7348(1)	16(1)
Cl	-3518(1)	4268(1)	2698(1)	26(1)
O(1)	-2341(1)	3115(1)	4287(1)	28(1)
C(1)	-867(2)	1688(1)	6551(1)	19(1)
C(2)	-1203(2)	2021(1)	5715(1)	19(1)
C(3)	-2482(1)	1761(1)	4997(1)	18(1)
C(4)	-2988(2)	2322(1)	4260(1)	20(1)
C(5)	-4129(2)	2048(1)	3537(1)	24(1)
C(6)	-4742(2)	1227(1)	3544(1)	26(1)
C(7)	-4262(2)	669(1)	4272(1)	25(1)
C(8)	-3150(2)	941(1)	4995(1)	21(1)
C(11)	2130(1)	2417(1)	6765(1)	18(1)
C(12)	2312(2)	3306(1)	6642(1)	23(1)
C(13)	3325(2)	3592(1)	6152(1)	31(1)
C(14)	4158(2)	2992(1)	5795(1)	32(1)
C(15)	3993(2)	2108(1)	5921(1)	29(1)
C(16)	2970(2)	1814(1)	6398(1)	24(1)
C(21)	278(2)	2947(1)	7979(1)	19(1)
C(22)	1292(2)	3203(1)	8767(1)	26(1)
C(23)	1019(2)	3953(1)	9202(1)	32(1)
C(24)	-249(2)	4447(1)	8862(1)	31(1)
C(25)	-1273(2)	4184(1)	8095(1)	27(1)
C(26)	-1013(2)	3433(1)	7649(1)	23(1)
C(31)	1479(2)	1177(1)	8111(1)	18(1)
C(32)	3016(2)	1011(1)	8372(1)	22(1)
C(33)	3529(2)	333(1)	8967(1)	26(1)
C(34)	2534(2)	-165(1)	9310(1)	27(1)
C(35)	1005(2)	8(1)	9057(1)	25(1)
C(36)	470(2)	674(1)	8460(1)	22(1)

Appendix B

Colloquia, Lectures and Conferences Attended

Research Colloquia, lectures and Seminars

Only those attended by the author are shown

1995 - 1996 (August 1 - July 31)

October 13 Professor R. Schmutzler, University of Braunschweig, Germany
Calixarene-Phosphorus Chemistry: A New Dimension in Phosphorus Chemistry

November 29 Professor Dennis Tuck, University of Windsor, Ontario, Canada
New Indium Coordination Chemistry

December 8 Professor M. T. Reetz, Max Planck Institut, Mulheim
Perkin Regional Meeting

January 17 Professor J. W. Emsley, University of Southampton
Liquid Crystals: More than Meets the Eye

February 12 Dr Paul Pringle, University of Bristol
Catalytic Self-Replication of Phosphines on Platinum(0)

February 21 Dr C. R. Pulham, University of Edinburgh
Heavy Metal Hydrides - an exploration of the chemistry of stannanes and plumbanes

March 7 Dr D. S. Wright, University of Cambridge
Synthetic Applications of Me_2N-p-Block Metal Reagents

March 13 Professor Dave Garner, Manchester University
Mushrooming in Chemistry

1996 - 1997 (August 1 - July 31)

October 22 Professor Lutz Gade, University of Wurzburg, Germany
Organic transformations with Early-Late Heterobimetallics: Synergism and Selectivity

October 22 Professor B. J. Tighe, Department of Molecular Sciences and Chemistry, University of Aston
Making Polymers for Biomedical Application - can we meet Nature's Challenge?
Joint lecture with the Institute of Materials

October 23 Professor H. Ringsdorf (Perkin Centenary Lecture), Johannes Gutenberg-Universität, Mainz, Germany
Function Based on Organisation

October 29 Professor D. M. Knight, Department of Philosophy, University of Durham
The Purpose of Experiment - A Look at Davy and Faraday

October 30 Dr Phillip Mountford, Nottingham University
Recent Developments in Group IV Imido Chemistry

November 12 Professor R. J. Young, Manchester Materials Centre, UMIST
New Materials - Fact or Fantasy?
Joint Lecture with Zeneca & RSC

November 18 Professor G. A. Olah, University of Southern California, USA
Crossing Conventional Lines in my Chemistry of the Elements

November 19 Professor R. E. Grigg, University of Leeds
Assembly of Complex Molecules by Palladium-Catalysed Queueing Processes

January 16 Dr Sally Brooker, University of Otago, New Zealand
Macrocycles: Exciting yet Controlled Thiolate Coordination Chemistry

January 21 Mr D. Rudge, Zeneca Pharmaceuticals
High Speed Automation of Chemical Reactions

February 12 Dr Geert-Jan Boons, University of Birmingham
New Developments in Carbohydrate Chemistry

February 18 Professor Sir James Black, Foundation, King's College London
My Dialogues with Medicinal Chemists

February 19 Professor Brian Hayden, University of Southampton
The Dynamics of Dissociation at Surfaces and Fuel Cell Catalysts

February 25 Professor A. G. Sykes, University of Newcastle
The Synthesis, Structures and Properties of Blue Copper Proteins

March 4 Professor C. W. Rees, Imperial College
Some Very Heterocyclic Chemistry

March 11 Dr A. D. Taylor, ISIS Facility, Rutherford Appleton Laboratory
Expanding the Frontiers of Neutron Scattering

1997 - 1998 (August 1 - July 31)

October 15 Dr. R. Mark Ormerod, Department of Chemistry, Keele University
Studying catalysts in action

October 21 Professor A. F. Johnson, IRC, Leeds
Reactive processing of polymers: science and technology

October 28 Professor A. P. de Silva, The Queen's University, Belfast
Luminescent signalling systems

November 5 Dr Mimi Hii, Oxford University
Studies of the Heck reaction

November 11 Professor V. Gibson, Imperial College, London
Metallocene polymerisation

November 25 Dr R. Withnall, University of Greenwich
Illuminated molecules and manuscripts

November 26 Professor R. W. Richards, University of Durham, Inaugural Lecture
A random walk in polymer science

December 2 Dr C. J. Ludman, University of Durham
Explosions

January 20 Professor J. Brooke, University of Lancaster
What's in a formula? Some chemical controversies of the 19th century

February 3 Dr J. Beacham, ICI Technology
The chemical industry in the 21st century

February 25 Dr C. Jones, Swansea University
Low coordination arsenic and antimony chemistry

Conferences and Symposia Attended

Fourth Anglo/German Inorganic Chemistry meeting, September 14-17, 1997, Marburg, Germany.[i]

Second International Conference on the Chemistry of the Alkali and Alkaline Earth Metals, September 17-20, 1997, Erlangen,
Germany.[i]

1998 National Congress and Young Researchers' Meeting, April 6-9, University of Durham.[i]

Main Group Symposium in Honour of Dr. Arthur Banister and Professors. Evelyn Ebsworth and Ken Wade, June 29, University of Durham.

i Posters presented.